# Agrociencia

eISSN: 2521-9766

VOLUMEN 57, NÚMERO 8 | 16 DE NOVIEMBRE - 31 DE DICIEMBRE, 2023 | MÉXICO

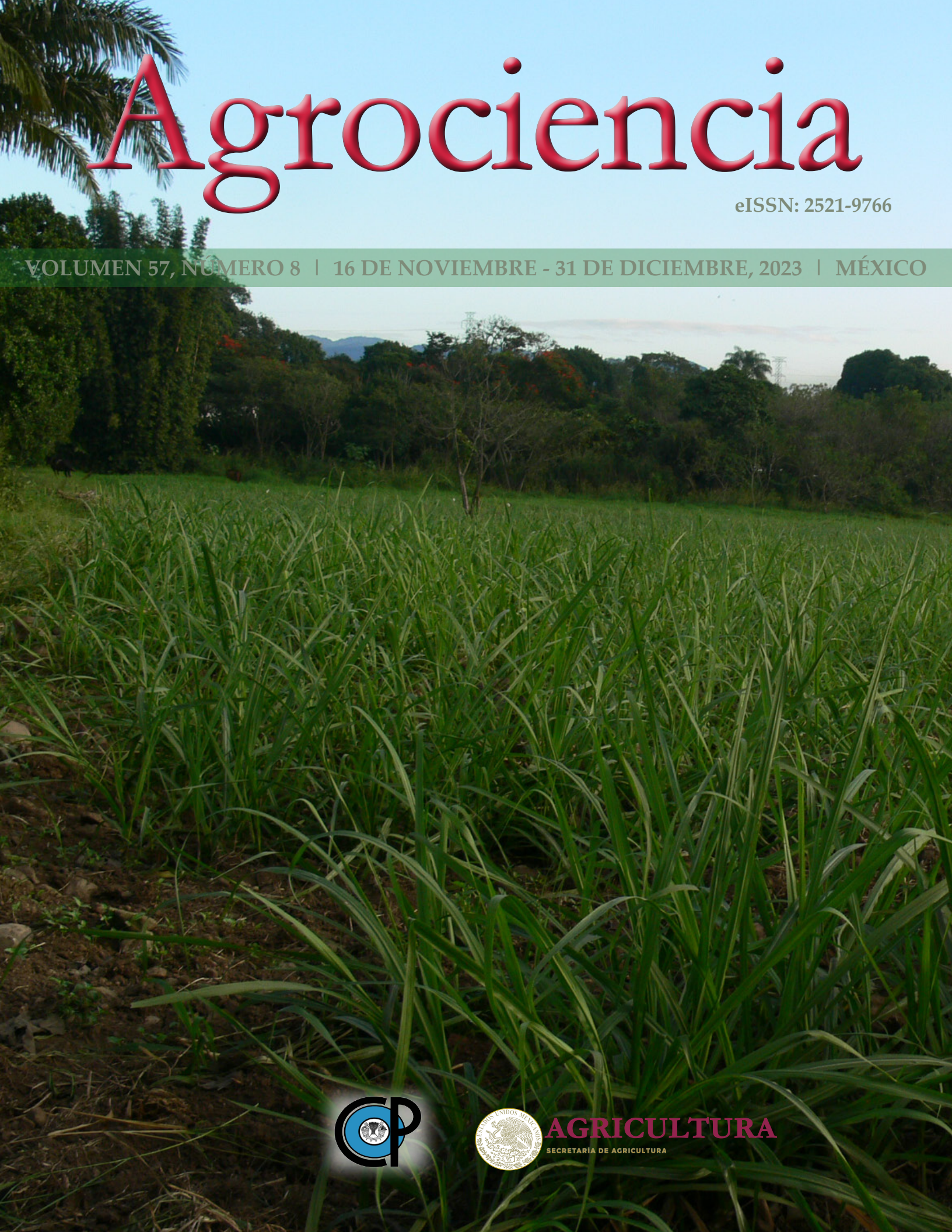

AGRICULTURA
SECRETARÍA DE AGRICULTURA

DERECHOS DE AUTOR Y DERECHOS CONEXOS, **Volumen 57, Número 8, 16 de noviembre - 31 de diciembre, 2023**, Agrociencia es una publicación sesquimensual editada por el Colegio de Postgraduados. Carretera México-Texcoco, Km 36.5, Montecillo, Texcoco, Estado de México. CP 56264. Tel. 5959284427. www.colpos.mx. Editor responsable: **Dr. Fernando Carlos Gómez Merino**. Reservas de Derechos al Uso Exclusivo 04-2021-031913431800-203. eISSN: 2521-9766, otorgados por el Instituto Nacional del Derecho de Autor. Fecha de última modificación, **31 de diciembre del 2023**.





Toda correspondencia (información de suscripciones, ventas, publicidad, contribuciones de autores, etc.) deberá dirigirse a:

Oficinas Centrales:

**Agrociencia**
Guerrero #9, Esquina Avenida Hidalgo.
56220. San Luis Huexotla. Texcoco,
Estado de México

Teléfono: 595 92 84427

https://agrociencia-colpos.org/index.php/agrociencia




**Portada:** Cultivo de caña de azúcar
**Fotografía y créditos:** Colegio de Postgraduados


AGRICULTURA
SECRETARÍA DE AGRICULTURA Y DESARROLLO RURAL

# Contents ❊ Contenido

Volumen 57, Número 8 | 16 de noviembre - 31 de diciembre, 2023

## Animal Science ❊ Ciencia Pecuaria



## Applied Mathematics-Statistics-Computer Science ❊ Matemáticas Aplicadas, Estadística y Computación



❊



## Crop Science ❊ Fitociencia



❊

## Natural Renewable Resources * Recursos Naturales Renovables

Agrociencia

# YIELD AND CHEMICAL QUALITY OF CHEPIL (*Crotalaria longirostrata* Hook. & Arn) FORAGE AT DIFFERENT SEEDING DENSITIES AND CUTTING FREQUENCY

María de los Á. **Maldonado-Peralta**[1], Adelaido R. **Rojas-García**[1*], Oswar **Cristobal-Santiago**[1]

[1] Universidad Autónoma de Guerrero. Maestría en Ciencias Agropecuaria y Gestión Local. Iguala de la Independencia, Guerrero, Mexico. C. P. 40101.
* Author for correspondence: rogarcia@uagro.mx

**Citation:** Maldonado-Peralta M de los Á, Rojas-García AR, Cristobal-Santiago O. 2023. Yield and chemical quality of chepil (*Crotalaria longirostrata* Hook. & Arn) forage at different sowing densities and cutting frequency. **Agrociencia** 57(8): 1634-1645. doi.org/ 10.47163/agrociencia.v57i8.2695

**Editor in Chief:**
Dr. Fernando C. Gómez Merino

Received: January 28, 2023.
Approved: July 26, 2023.
**Published in Agrociencia:** December 18, 2023.



## ABSTRACT

Ruminant grazing in the tropics requires supplementation given the nutritional characteristics of pastures to cover protein needs. The objective of this research was to evaluate the yield and chemical quality of chepil (*Crotalaria longirostrata* Hook. & Arn) forage at different seeding densities and cutting frequencies to obtain the optimum harvest time. The experiment was set up in a completely randomized design with three replications. The treatments were planting densities T1: 200 000; T2: 100 000; and T3: 50 000 plants ha$^{-1}$. The variables evaluated were: dry matter yield, morphological composition, growth rate, leaf:stem ratio, intercepted radiation, plant height, crude protein, neutral detergent fiber, acid detergent fiber, dry matter, and ash. For the 64-day cutting frequency, the three densities presented the highest yield with 3406, 3500, and 4200 kg MS ha$^{-1}$, for 200 000, 100 000 and 50 000 plants ha$^{-1}$, respectively ($p < 0.05$). PC decreased ($p < 0.05$) in T2 and T3 (23 %) in comparison to T1 (24 %). The planting density with the highest percentage of crude protein was 200 000 plants ha$^{-1}$ with 24 %. The densities of 100 000 and 50 000 plants ha$^{-1}$ presented a lower crude protein percentage, with 23 % ($p < 0.05$). It is concluded that the optimum cutting time is at 36 days of regrowth, when the chepil is planted at a density of 100 000 plants ha$^{-1}$, and harvested at the frequency of 36 days of regrowth, since 95 % of intercepted radiation and better quality between yield and chemical characteristics, mainly crude protein, are obtained.

**Keywords:** Fabaceae, fodder legumes, chipilin, thresher.

## INTRODUCTION

In Mexico, the search for different unconventional protein sources is necessary (Galindo *et al*., 2005; Sosa-Pérez *et al*., 2017). In underdeveloped countries, tropical fabaceae are an accessible and economically viable alternative for human and animal feed (Renté-Martí *et al*., 2020; Pincay-Ganchozo *et al*., 2021). Legumes in animal feed contain nutritional compounds that supplement the needs of ruminants and non-ruminants at different times of the year; they are also used as mulch, for phytoremediation, and as agroecological transition in sustainable agriculture (Voisin *et al*., 2013; Ruiz *et al*., 2015; Almeida-Santos *et al*., 2019).

In the tropics and subtropics of the Americas, approximately 89 species of the genus *Crotalaria* have been reported, most of which are important for food, bioenergy, medicine, and ornamentals (Avendaño, 2011). Some of these species are characterized by rapid biomass production (Parenti *et al*., 2021), being drought-tolerant, resistant to nematodes and other pests, and high germination rates, which in turn influence the yield and quality of dry matter produced (Wang *et al*., 2002; Kamireddy *et al*., 2013). Studies conducted on *C. juncea* show that, between 40 and 60 days of development, it presents 7 Mg $ha^{-1}$ of dry matter per cutting, contributing up to 176.37 kg N $ha^{-1}$ (Ríos-Hilario *et al*., 2022); in addition, the leaf contains 27 % protein (Almeida-Santos *et al*., 2019).

Chepil, chipil, chipile, or chipilín (*Crotalaria longirostrata* Hook. & Arn.) is endemic to Central America, where it is consumed as a green leafy vegetable (Camarillo-Castillo and Mangan, 2020). In southern Mexico, it is used in traditional cooking (Chávez-Quiñones *et al*., 2009). It is an herbaceous species that develops annually during the rainy season and is collected wild; sometimes it is associated with the milpa or is semi-cultivated as a shrub. With agronomic management, it can be biannual or perennial. Chepil seeds have low germination rates ranging from 12.3 to 80 % (Rojas-García *et al*., 2021). Its leaves have a high protein content ranging from 30.6 to 38.3 % (Arias *et al*., 2003; Jiménez-Aguilar and Grusak, 2015), making it as high in quality as alfalfa; however, there are few studies on dry matter yield, physical and chemical quality (Pérez-Cornelio *et al*., 2016).

The chepil could be considered the alfalfa of the tropics, and it could be used in animal feed, added mainly in the diet in the form of meal, green, or silage. It is drought tolerant, provides organic matter in poor soils, and its seeds are resistant to fire (Rojas-García *et al*., 2021), which makes it an alternative species for the dry season. The objective of this research was to evaluate the yield and chemical quality of chepil (*Crotalaria longirostrata* Hook. & Arn) at different planting densities and cutting frequencies to obtain the optimum harvest time.

## MATERIALS AND METHODS

The research was carried out in experimental plots and in the Animal Nutrition laboratory of the Faculty of Veterinary Medicine No. 2 of the Autonomous University of Guerrero, located in Cuajinicuilapa, Guerrero, Mexico (16° 28′ 28′′ N, 98° 25′ 11.27′′ W, at 46 m altitude). The climate of the region is classified as Aw and is known as dry tropic (García, 2004). Temperature and precipitation data were obtained from the Conagua agro-meteorological station, which was located 2 km from the experimental plots. During the study period, the average annual temperature was 27.5 °C, and the total precipitation was 668 mm.

Mature chepil (*C. longirostrata*) pods were collected from wild plants from January to May 2020. Planting took place on June 1st of the same year in 3 L polystyrene (unicel) trays. A 50:50 v/v mixture of composted manure and river soil was used as substrate; 2 kg of substrate were placed in each tray, then 60 g of seeds were sprinkled,

covered approximately 0.2 cm with the same substrate, and irrigated to field capacity, repeating the irrigations every two days. A total of 10 trays were sown. Thirty days after planting, when the plants were 15 to 20 cm tall, they were transplanted into the field. On June 29, the experimental plots were delimited and transplanted, with the treatments being: 200 000, 100 000, and 50 000 plants $ha^{-1}$.

Each plot measured 3 x 3 m, and one plot was established for each week of evaluation (10 plots), in a completely randomized design with three replications. To obtain each density, the spacing between plants was 10, 20, and 30 cm, and 50 cm between rows. Weed control was done with the help of a hoe whenever the crop required it. No fertilizers or agrochemicals were used, and drip irrigation was used every third day. A uniformity cut was made 50 days after transplanting, leaving a height of 40 cm. The variables were evaluated from 15 days after the uniformity cut, with intervals of one week until week 10 or the beginning of flowering, with sampling for forage yield at 15, 22, 29, 36, 43, 50, 57, 64, 71, and 79 days after cutting; while for bromatological composition, sampling was carried out every two weeks: 15, 29, 43, 57, and 71 days after cutting.

## Variables evaluated

### Total dry matter, leaf and stem yields

Two random destructive samplings were carried out in one linear meter. For this purpose, the forage was cut, leaving a remaining height of 40 cm in each experimental plot. Of the total yield sample, 20 % was obtained by separating its morphological components (leaf and stem). These were placed in paper bags, labeled, and placed in an electric oven (Faithfull, WGLL-230BE, Cangzhou, China) at a temperature of 55 °C, until constant weight.

### Plant height

In each experimental plot, twenty heights were measured with a ruler graduated in centimeters, using the highest morphological component as a reference.

### Intercepted radiation

Five measurements of intercepted radiation were taken randomly one day before each cutting, using the wood ruler method, by placing a graduated ruler (100 cm) on the ground in the middle of the experimental plots, from furrow to furrow, below the plant canopy (Maldonado-Peralta *et al*., 2019).

### Growth rate

It was calculated using the data obtained in the total dry matter yield variable for each of the treatments evaluated, using the following formula:

$$TC = R / T$$

where TC = seasonal average growth rate (kg DM $ha^{-1}$ $d^{-1}$); R = seasonal yield (kg DM $ha^{-1}$), and T = days elapsed from one cutting to another.

### Leaf:stem ratio

It was obtained from the morphological composition, by dividing the dry leaf component by the stem.

### Chemical composition

It was determined using the AOAC (2005) methods: MS (method 930.15), ash (method 942.05), and crude protein (PC; method 984.13). Neutral detergent fiber (FDN) and acid detergent fiber (FDA) were evaluated with the ANKOM Technology methodology according to van Soest *et al.* (1991).

### Statistical analysis

The experimental design was completely randomized with three replications. Data were analyzed using PROC GLM (SAS, 2011), with the effects of planting density and cutting frequency held constant. Treatments means were compared using Tukey's test ($\alpha = p < 0.05$).

## RESULTS AND DISCUSSION

Chepil total dry matter yield showed statistical differences between planting density and cutting stages ($p < 0.05$) (Figure 1). For the 64-day cutting frequency, the three densities produced the highest yield, with 3406, 3500, and 4200 kg MS $ha^{-1}$ for 200 000, 100 000, and 50 000 plants $ha^{-1}$, respectively ($p < 0.05$). Subsequently, due to the loss of the lower leaves of the plant canopy caused by senescence or the onset of flowering, they tended to decrease. Another trend in yield behavior is that chepil develops stem bifurcation on day 34 after planting, and there is inter-specific competition for water, light, and nutrient resources.

Alonzo-Griffith and Paniagua-Alcaraz (2010) reported lower averages of 1401 kg MS $ha^{-1}$ at 128 days after sowing in alfalfa when evaluating different calcareous doses. In turn, Godoy-Espinoza *et al.* (2012) obtained higher values than those of this research in *Arachis pintoi*, with 7084 and 12 480 kg MS $ha^{-1}$ at 60 and 75 days of regrowth age, respectively. Other researchers, such as Romero *et al*. (2013), report lower values for the legume clitoria (*Clitoria ternatea*) with 1800 kg MS $ha^{-1}$. Rojas-García *et al.* (2017) reported higher yields of alfalfa (*Medicago sativa L.*) varieties in the summer season, with annual average of 6246 kg MS $ha^{-1}$. Lagunes-Rivera *et al*. (2019) report an average value similar to this research, with 2668 kg MS $ha^{-1}$ in different legumes.

For the leaf component yield, it was observed that the density with the highest percentage of leaves was 50 000 plants $ha^{-1}$ with 38.13 %, followed by 100 000 and 200 000 plants $ha^{-1}$ with 37.76 and 37.19 %. From days 15 to 36, the three densities had the highest leaf percentage, with values ranging between 60 and 40 % ($p < 0.05$). The opposite occurred in the stem component, with higher yields after a cutting frequency

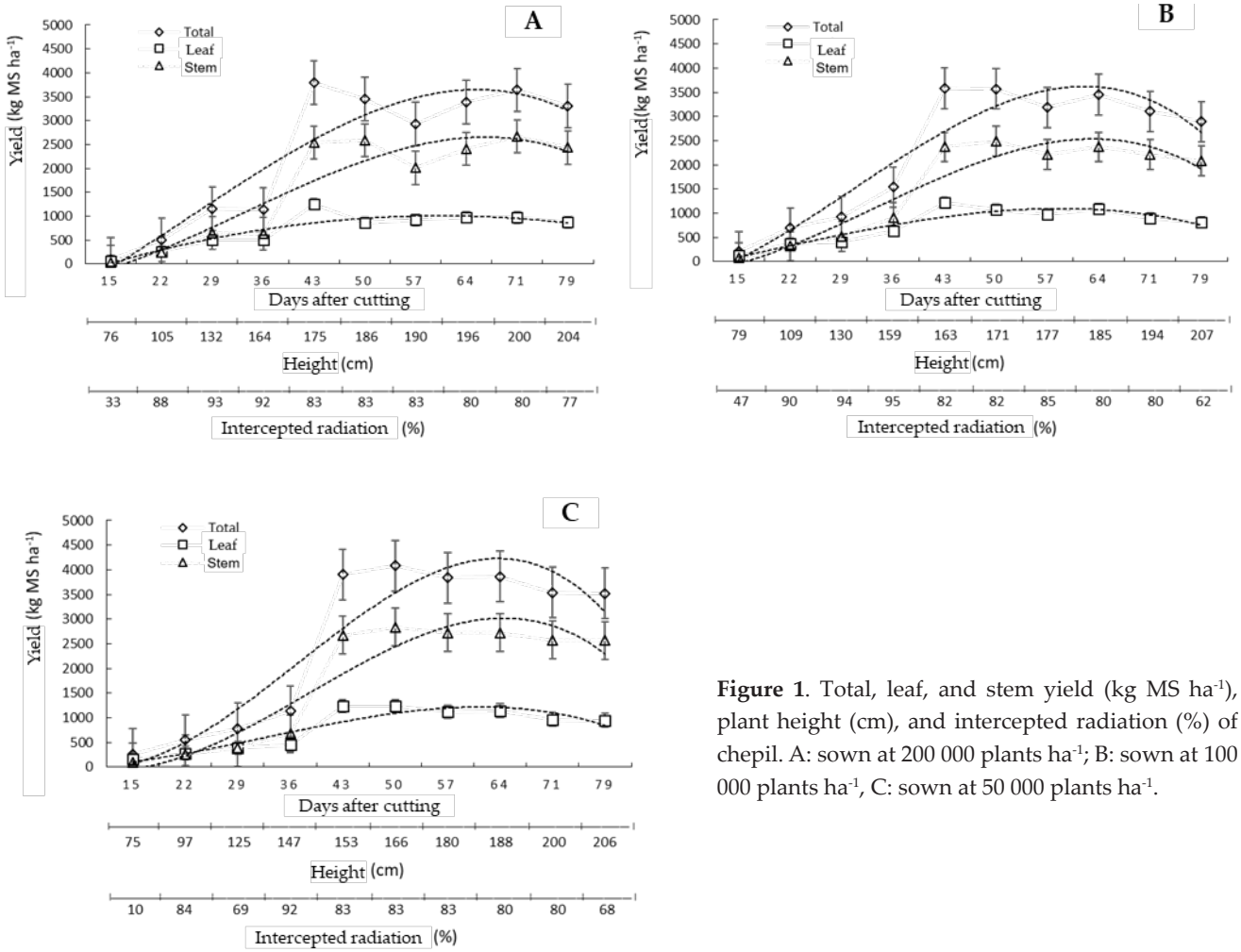


**Figure 1**. Total, leaf, and stem yield (kg MS ha$^{-1}$), plant height (cm), and intercepted radiation (%) of chepil. A: sown at 200 000 plants ha$^{-1}$; B: sown at 100 000 plants ha$^{-1}$, C: sown at 50 000 plants ha$^{-1}$.

of 64 days, with an average of 73 % stem in the three planting densities ($p < 0.05$). In turn, Rojas-García *et al.* (2017) reported alfalfa (*Medicago sativa* L.) yield and obtained an average of 45 % leaves at the 29-day cutting frequency, which is comparable to the values obtained in this study.

Regarding the height of the chepil grassland at different sowing densities and cutting stages (Figure 1), at the 43 to the 79-day cutting frequencies, the plants presented greater height (163 to 203 cm) independently of the sowing density ($p < 0.05$); however, at a density of 200 000 plants ha$^{-1}$, it was observed that the greatest average height was 163 cm, while at a sowing density of 50 000 plants ha$^{-1}$, the lowest was 154 cm ($p < 0.05$). The higher plant growth at these densities can be attributed to interspecific competition for light, which increased plant height at the densest planting density. On the other hand, Pincay-Ganchozo *et al.* (2021) used different scarification methods on *Clitoria ternatea* and reported plants with a height of 79 cm when cut at 75 days. Sosa-

Rubio *et al*. (2008) reported, in tropical legumes, a relationship between plant height and dry matter yield as observed in this trial.

The intercepted radiation is observed as plant density and cutting stages vary (Figure 1). The planting density of 100 000 plants $ha^{-1}$ intercepted 95 % of incident radiation at the 36-day mowing frequency and subsequently decreased to 62 % at the 79-day mowing frequency ($p < 0.05$). The planting densities with the highest average intercepted radiation were 100 000 and 200 000 plants $ha^{-1}$, with 80 and 79 %, respectively. The density of 50 000 plants $ha^{-1}$ was the one with the lowest average intercepted radiation percentage, with a value of 73 %. This behavior is possibly due to the loss of lower leaves from the plant canopy, plant maturity, and competition with other plants (Maldonado-Peralta *et al*., 2019). Several researchers report an optimum intercepted radiation of 95 %, indicating that this is when the best structural characteristics of legume grassland are found (Rojas-García *et al*., 2017). On the other hand, Alonzo-Griffith and Paniagua-Alcaraz (2010) report similar values of legume intercepted radiation, with an average of 90 %.

Chepil growth rates vary depending on planting density and cutting stage (Table 1). Statistical differences were found in plant densities ($p < 0.05$). The density of 50 000 plants $ha^{-1}$ produced 65 kg MS $ha^{-1}$ $d^{-1}$, while the densities of 200 000 and 100 000 plants $ha^{-1}$ showed a lower growth rate with 59 kg MS $ha^{-1}$ $d^{-1}$. From the 15 to the 36-day mowing frequencies, all three planting densities showed slow growth, which increased at the 43-day mowing frequency and then decreased as the experimental period continued. This behavior is possibly due to the recovery process when performing the uniformization cutting, which leaves a remaining plant height of

**Table 1.** Growth rate (kg MS $ha^{-1}$ $d^{-1}$) in chepil (*Crotalaria longirostrata*), grown at different planting densities and cutting frequencies.

| | Planting density (plants $ha^{-1}$) | | | |
|---|---|---|---|---|
| Age of plants | T1: 200 000 | T2: 100 000 | T3: 50 000 | Average |
| 15 | 6 F c | 14 E b | 17 F a | 12 F |
| 22 | 29 E b | 32 DE a | 25 E c | 29 E |
| 29 | 40 CD a | 32 DE b | 27 E c | 33 DE |
| 36 | 32 DE a | 43 D a | 31 E a | 35 D |
| 43 | 88 A ab | 83 A b | 91 A a | 87 A |
| 50 | 69 B b | 71 B b | 82 B a | 74 B |
| 57 | 51 C b | 56 C b | 67 C a | 58 C |
| 64 | 53 C b | 54 C b | 60 C a | 56 C |
| 71 | 52 C a | 44 D b | 50 D a | 49 CD |
| 79 | 42 D ab | 37 DE b | 45 D a | 41 D |
| Average | 59 b | 59 b | 65a | |

ABC: Means with the same uppercase literal in the same column are not statistically different ($p > 0.05$); abc: means with the same lowercase literal in the same row are not statistically different ($p > 0.05$).

40 cm. On the other hand, the highest growth rate was observed at the 43-day cutting frequency at a planting density of 50 000 plants $ha^{-1}$ with 91 kg MS $ha^{-1}$ ($p < 0.05$). Sánchez-Santillán *et al*. (2019) reported a growth rate of 25 kg MS $ha^{-1}$ $d^{-1}$ in winter and 70 kg MS $ha^{-1}$ $d^{-1}$ in summer in alfalfa at 45 days of regrowth; which is similar to the results reported in this study.

Regarding the leaf:stem ratio of chepil when varying planting density and cutting frequency (Table 2), statistical differences were found between cutting frequency and planting density ($p < 0.05$). The leaf:stem ratio was higher in 50 000 and 100 000 plants $ha^{-1}$ with a value of 0.70; the density of 200 000 plants $ha^{-1}$ had the lowest percentage, with a value of 0.68 ($p < 0.05$). For both the 15 and 22-day cutting frequencies, the three densities presented the highest leaf:stem ratios, with 1.61 and 1.18, respectively, while the density of 50 000 plants $ha^{-1}$ at frequency 15 had the highest leaf:stem ratio, with 1.67 ($p < 0.05$), and the 71 and 79-day cutting stages presented the lowest leaf:stem ratios. This is possibly due to the loss of lower leaves from the plant canopy caused by senescence or the onset of flowering. Rojas-García *et al.* (2017) reported similar values for the leaf:stem ratio of alfalfa varieties in the summer and autumn seasons (0.92 and 1.46, respectively). Other researchers, such as Lagunes-Rivera *et al*. (2019), observed values of 1.36 leaf:stem ratio at the 15 and 22-day cutting stages.

**Table 2.** Leaf:stem ratio in cultivated chepil (*Crotalaria longirostrata*) at different planting densities and cutting frequencies.

| | Planting density (plants $ha^{-1}$) | | | |
|---|---|---|---|---|
| Age of plants | T1: 200 000 | T2: 100 000 | T3: 50 000 | Average |
| 15 | 1.58 A b | 1.57 A b | 1.67 A a | 1.61 A |
| 22 | 1.17 A b | 1.20 A a | 1.16 A b | 1.18 B |
| 29 | 0.79 B b | 0.82 B b | 1.04 B a | 0.88 C |
| 36 | 0.80 B a | 0.69 C b | 0.67 C b | 0.72 C |
| 43 | 0.49 C b | 0.52 C a | 0.47 D b | 0.49 D |
| 50 | 0.34 C b | 0.44 D a | 0.44 D a | 0.41 D |
| 57 | 0.46 C a | 0.45 E a | 0.41 D b | 0.44 D |
| 64 | 0.41 C b | 0.46 E a | 0.42 D b | 0.43 D |
| 71 | 0.37 C b | 0.41 E a | 0.38 E b | 0.39 E |
| 79 | 0.36 C c | 0.39 F a | 0.37 E b | 0.37 E |
| Average | 0.68 b | 0.70a | 0.70a | |

ABC: Means with the same uppercase literal in the same column are not statistically different ($p > 0.05$); abc: means with the same lowercase literal in the same row are not statistically different ($p > 0.05$).

For the percentage of crude protein, acid detergent fiber, and neutral detergent fiber (Table 3), the planting density with the highest average crude protein was 200 000 plants $ha^{-1}$, with 24 %, while the densities of 100 000 and 50 000 plants $ha^{-1}$ had the lowest percentage, with 23 % ($p < 0.05$). Regardless of plant density, crude protein

**Table 3.** Percentage of crude protein, neutral detergent fiber, and acid detergent fiber of chepil (*Crotalaria longirostrata*) grown at different planting densities and cutting frequencies.

| | Planting density (plants ha$^{-1}$) | | | |
|---|---|---|---|---|
| | Crude protein (%) | | | |
| Age of plant | T1: 200 000 | T2: 100 000 | T3: 50 000 | Average |
| 15 | 30 A a | 29 A a | 29 A a | 29 A |
| 29 | 28 A a | 28 A a | 26 AB b | 27AB |
| 43 | 25 B a | 21 B b | 20 B b | 22 B |
| 57 | 20 C a | 19 B b | 20 B a | 20 B |
| 71 | 19 C a | 19 B a | 19 B a | 19 B |
| Average | 24 a | 23 b | 23 b | |
| | Neutral detergent fiber (%) | | | |
| 15 | 41 B b | 42 B a | 41 B b | 41 C |
| 29 | 48 B a | 42 B b | 48 B a | 46 B |
| 43 | 53 AB b | 59 A a | 62 A a | 58 A |
| 57 | 57 A ab | 61 A a | 62 A a | 60 A |
| 71 | 60 A a | 60 A a | 60 A a | 60 A |
| Average | 52 b | 53 b | 55 a | |
| | Acid detergent fiber (%) | | | |
| 15 | 35 B a | 36 AB ab | 35 B a | 35 B |
| 29 | 38AB a | 30 B b | 29 C a | 32 C |
| 43 | 33 B a | 37 AB a | 41 AB a | 37 AB |
| 57 | 38 AB a | 40 A a | 42 A a | 40 [a] |
| 71 | 40 A a | 39 A a | 44 A a | 41 [a] |
| Average | 37 b | 37 b | 38 a | |

ABC: Means with the same uppercase literal in the same column are not statistically different ($p > 0.05$); abc: means with the same lowercase literal in the same row are not statistically different ($p > 0.05$).

was highest at the youngest cutting frequencies of 15 and 22 days, averaging 29 to 27 %, respectively, while at the 71-day cutting frequency, the lowest percentage was observed at 17 % ($p < 0.05$). This could be due to the loss of lower canopy leaves and the increase of stems, which have a higher percentage of cellulose, hemicellulose, and lignin, reducing the quality of the plant. Several researchers (Alonzo-Griffith and Paniagua-Alcaraz, 2010; Godoy-Espinoza *et al*., 2012; Romero *et al*., 2013; Portillo-López *et al*., 2019; Lagunes-Rivera *et al*., 2019) reported similar values in legumes, with protein percentages ranging from 28 to 14 % in the cutting stages from 30 to 75 days of age, respectively, with a behavior similar to that of this research; however, Balseca *et al*. (2015) reported an average of 8.26 % PC in legumes, a lower result than this study. On the other hand, the planting density with the highest percentage of neutral detergent fiber (Table 3) was 50 000 plants ha$^{-1}$ with 55 % ($p < 0.05$); the density with the lowest percentage was 200 000 plants ha$^{-1}$ with 52 %. Regarding cutting stages, days 43, 57, and 71 presented the highest percentage of FDN, with 58, 60, and 60,

respectively ($p < 0.05$). Romero *et al.* (2013) and Portillo-López *et al.* (2019) conducted research on *Clitoria ternatea* and found lower percentages than this research, but with the same behavior of increasing as the time of FDN regrowth passes, of 25 and 40 %, at 30 and 60 days from sowing, respectively. Valles-de la Mora *et al.* (2014), in a study on *Cratylia argentea*, found an average value of 57.48 % FDN, while Lagunes-Rivera *et al.* (2019) reported 64.25 % FDN; however, Balseca *et al.* (2015) obtained a higher average of 71 %.

Similar behavior was observed in the acid detergent fiber (Table 3), where the planting density with the highest percentage was 50 000 plants ha$^{-1}$, with 38 % ($p < 0.05$), and the densities of 100 000 and 200 000 plants ha$^{-1}$ had the lowest percentage, with an average of 37 %. The cutting stages with the highest and lowest percentages of acid detergent fiber were at 71 and 15 days, with 41 and 35 %, respectively. Romero *et al.* (2013) conducted research on *Clitoria ternatea* and found lower FDA percentages of 18, 25, and 25 % at 30, 60, and 75 days of plant age, respectively, which is similar to the behavior observed in this study. Valles-de la Mora *et al.* (2014), in their research on *Cratylia argentea* conducted during rainy season, found an average value of 37.35 % FDA, similar to this research. Portillo-López *et al.* (2019) found similar percentages of FDA, ranging from 30.1 to 38.2 % in white clover (*Trifolium repens* L.), red clover (*Trifolium pratense* L.), and vicia (*Vicia sativa* L.) during the low rainfall season; however, Lagunes-Rivera *et al.* (2019) reported higher average values of 42.25 %.

For the percentage of dry matter and ash (Table 4), in general, the planting density of 100 000 plants ha$^{-1}$ obtained the highest average percentage of dry matter, with

**Table 4.** Percentage dry matter and ash of chepil (*Crotalaria longirostrata*) grown at different planting densities and cutting frequencies.

| | Plant density (plants ha$^{-1}$) Dry matter (%) | | | |
|---|---|---|---|---|
| Age of plant | T1: 200 000 | T2: 100 000 | T3: 50 000 | Average |
| 15 | 17 B | 18 B | 17C | 17 B |
| 29 | 18 B | 18 B | 19 B | 18 B |
| 43 | 22 AB | 24 A | 23 A | 23 A |
| 57 | 22 AB | 24 A | 21 AB | 22 AB |
| 71 | 24 A | 25 A | 24 A | 24 A |
| Average | 21 b | 22 a | 21 b | |
| | | Ash (%) | | |
| 15 | 6 AB b | 6 AB a | 6 A a | 6 AB |
| 29 | 7 A a | 7 A a | 6 A b | 7[a] |
| 43 | 4 B b | 7 A a | 6 AB b | 6 B |
| 57 | 7 A a | 5 B c | 5 B b | 6 B |
| 71 | 5 AB a | 5 B b | 5 AB b | 5 C |
| Average | 6 a | 6 a | 6 a | |

ABC: Means with the same uppercase literal in the same column are not statistically different ($p > 0.05$); abc: means with the same lowercase literal in the same row are not statistically different ($p > 0.05$).

22 %; while the densities of 200 000 and 50 000 plants $ha^{-1}$ obtained lower values, with 21 % ($p < 0.05$). The highest percentage of MS was obtained at the 71-day cut-off frequency, while the 15-day cut-off frequency had the lowest value with 24 and 17 %, respectively ($p < 0.05$). In terms of ash content, statistical differences were found in cutting frequencies. A decrease was observed as cutting frequency increased, with the highest percentage on day 29 (7 %) and the lowest on day 71, with 5 %; however, no statistical differences were found in planting densities, with an average of 6 % ash ($p < 0.05$). Similar averages were reported by Fernández-Valeriano and Sánchez-Chávez (2017) in beans, with a value of 8 %.

## CONCLUSIONS

The optimum cutting time for forage is when chepil is sown at a density of 100 000 plants $ha^{-1}$ and harvested at a frequency of 36 days after the uniformity cut, with 95 % intercepted radiation. At this stage it presents better quality, yield, and protein characteristics. It is recommended that further research be conducted using different remaining heights, evaluating them at different times of the year and with more harvesting time, as well as analyzing weight gain in domestic animals.

## REFERENCES

Almeida-Santos LE, Obrador-Olán JJ, García-López E, Castelán-Estrada M, Carrillo-Ávila E. 2019. Cultivo e incorporación de *Crotalaria juncea* L. en un suelo cañero de la Chontalpa, Tabasco, México. Agro Productividad 12 (7): 87–93. https://doi.org/10.32854/agrop.v0i0.1475

Alonzo-Griffith LA, Paniagua-Alcaraz PL. 2010. Efectos de dosis de calcáreo sobre el comportamiento productivo y calidad de la alfalfa. Investigación Agraria 12 (1): 35–39.

AOAC (Association of Official Analytic Chemists). 2005. Official methods of analysis (18th edition). Association of Official Analytic Chemists: Washington, DC, USA. 1094 p.

Arias L, Losada H, Rendón A, Grande D, Vieyra J, Soriano R, Rivera J, Cortés J. 2003. Evaluation of Chipilín (*Crotalaria longirostrata*) as a forage resource for ruminant feeding in the tropical areas of Mexico. Livestock Research for Rural Development 15 (4): 1–9.

Avendaño N. 2011. Revisión taxonómica del género *Crotalaria* L. (Faboideae-Crotalarieae) en Venezuela. Acta Botanica Venezuelica 34 (1): 13–78.

Balseca DG, Cienfuegos EG, López HB, Guevara HP, Martínez JC. 2015. Valor nutricional de Brachiarias y leguminosas forrajeras en el trópico húmedo del Ecuador. Ciencia e Investigación Agraria 42 (1): 57–63. https://doi.org/10.4067/s0718-16202015000100006

Camarillo-Castillo F, Mangan FX. 2020. Biological nitrogen fixation in chipilín (*Crotalaria longirostrata* Hook. & Arn), a sustainable nitrogen source for commercial production. Revista Chapingo Serie Horticultura 26 (2): 125–141. https://doi.org/10.5154/r.rchsh.2020.01.002

Chávez-Quiñones E, Roldan-Toriz J, Sotelo-Ortiz BE, Ballinas-Díaz J, López-Zúñiga EJ. 2009. Plantas comestibles no convencionales en Chiapas, México. Revista Salud Pública y Nutrición 10 (2): 1–11.

Fernández-Valeriano AF, Sánchez-Chávez E. 2017. Estudio de las propiedades fisicoquímicas y calidad nutricional en distintas variedades de frijol consumidas en México. Nova Scientia 9 (18): 133–148. https://doi.org/10.21640/ns.v9i18.763

Galindo J, Delgado D, Pedraza R, García DE. 2005. Impacto de los árboles, los arbustos y otras leguminosas en la ecología ruminal de animales que consumen dietas fibrosas. Pastos y Forrajes 28 (1): 59–68.

García E. 2004. Modificaciones al sistema de clasificación climática de Köppen (Cuarta edición). Universidad Nacional Autónoma de México: Ciudad de México, México. 217 p.

Godoy-Espinoza V, Barrera-Álvarez A, Vivas-Moreira R, Quintana-Zamora J, Peña-Galeas M, Villota-González L, Casanova-Ferrín L, Avellaneda-Cevallos J. 2012. Evaluación fenológica y digestibilidad *in vivo* de la leguminosa forrajera (*Arachis pintoi*) en diferentes edades de corte. Ciencia y Tecnología 5 (2): 7–16. https://doi.org/10.18779/cyt.v5i2.82

Jiménez-Aguilar DM, Grusak MA. 2015. Evaluation of minerals, phytochemical compounds and antioxidant activity of Mexican, Central American, and African green leafy vegetables. Plant Foods for Human Nutrition 70 (4): 357–364. https://doi.org/10.1007/s11130-015-0512-7

Kamireddy SR, Li J, Abbina S, Berti M, Tucker M, Ji Y. 2013. Converting forage sorghum and sunn hemp into biofuels through dilute acid pretreatment. Industrial Crops and Products 49: 598–609. https://doi.org/10.1016/j.indcrop.2013.06.018

Lagunes-Rivera SA, Guerrero-Rodríguez JDD, Hernández-Velez JO, Ramírez-González J de JM, García-Bonilla DV, Alatorre-Hernández A. 2019. Rendimiento de materia seca y valor nutritivo de cuatro leguminosas herbáceas en la zona tropical de Hueytamalco, Puebla, México. Revista Mexicana de Ciencias Pecuarias 10 (4): 1042–1053. https://doi.org/10.22319/rmcp.v10i4.4660

Maldonado-Peralta M de los Á, Rojas-García AR, Sánchez-Santillán P, Bottini-Luzardo MB, Torres-Salado N, Ventura-Ríos J, Joaquín-Cancino S, Luna-Guerrero MJ. 2019. Growth analysis of Cuba grass OM-22 (*Pennisetum purpureum* x *Pennisetum glaucum*) in the dry tropics. Agro Productividad 12 (8): 17–22. https://doi.org/10.32854/agrop.v0i0.1445

Parenti A, Cappelli G, Zegada-Lizarazu W, Martín-Sastre C, Christou M, Monti A, Ginaldi F. 2021. SunnGro: A new crop model for the simulation of sunn hemp (*Crotalaria juncea* L.) grown under alternative management practices. Biomass and Bioenergy 146: 105975. https://doi.org/10.1016/j.biombioe.2021.105975

Pérez-Cornelio BA, Lagunes-Espinoza LC, Villarreal-Ibarra EC, Bolio GI, Bolaños-Aguilar ED, Hernández-Villegas M. 2016. Acumulación de biomasa, concentración de proteína y alcaloides totales en chipilín durante su crecimiento. *In* Martínez JH, Ramírez-Guillermo MA, Cámara-Córdova J. (eds.), Innovación Tecnológica para la seguridad. Universidad Juárez Autónoma de Tabasco, Instituto Nacional de Investigaciones forestales, Agrícolas y Pecuarias: Villahermosa, México. 13 p.

Pincay-Ganchozo RA, Luna-Murillo RA, Espinosa-Cunuhay KA, Espinales-Suárez HO. 2021. Escarificación química y biológica en la emergencia y crecimiento de *Clitoria ternatea*. Centro Agropecuario 48 (3): 53–59.

Portillo-López PA, Meneses-Buitrago DH, Morales-Montero SP, Cadena-Guerrero MM, Castro-Rincón E. 2019. Evaluación y selección de especies forrajeras de gramíneas y leguminosas en Nariño, Colombia. Pastos y Forrajes 42 (2): 93–103.

Renté-Martí O, Reyes PP, Corrales-Vila Y, Cuevas-Rodríguez M, Nápoles-García MC. 2020. *Canavalia ensiformis* (L): en propiedades químicas de un suelo fluvisol diferenciado. Revista Científica del Amazonas 3 (6): 65–75. https://doi.org/10.34069/RA/2020.6.05

Ríos-Hilario JJ, Maldonado-Peralta M de los Á, Rojas-García AR, Hernández-Castro E, Sabino-López JE, Segura-Pacheco H. 2022. Yield, intercepted radiation, and morphology of

crotalaria (*Crotalaria juncea* L.) at different densities. Agroproductividad 15: 177–185. https://doi.org/10.32854/agrop.v15i7.2316

Rojas-García AR, Maldonado-Peralta M de los Á, Sánchez-Santillán P, Ayala-Monter MA, Álvarez-Vázquez P, Ramírez-Reynoso O. 2021. Scarification treatments in chepil seeds (*Crotalaria longirostrata* Jook. & Arn.) used to improved their germination. Agroproductividad 14: 67–72. https://doi.org/10.32854/agrop.v14i2.1966

Rojas-García AR, Torres-Salado N, Joaquín-Cancino S, Hernández-Garay A, Maldonado-Peralta M de los Á, Sánchez-Santillán P. 2017. Componentes del rendimiento en variedades de alfalfa *(Medicago sativa L.).* Agrociencia 51 (7): 697–708.

Romero N, Leonard I, Ramírez JL, Córdova A. 2013. Rendimiento y calidad de la *Clitoria ternatea* en un suelo arcilloso del estado Falcón, Venezuela. Revista Electrónica de Veterinaria 14 (10): 1–10.

Ruiz TE, Febles G, Alonso J. 2015. Estudios con leguminosas, un informe a la ciencia durante los cincuenta años del Instituto de Ciencia Animal. Revista Cubana de Ciencia Agrícola 49 (2): 433–241.

Sánchez-Santillán P, Maldonado-Peralta M de los Á, Rojas-García AR, Torres-Salado N, Herrera-Pérez J, Bottini-Luzardo MB, Wilson-García CY, Quero-Carrillo AR. 2019. Productividad de variedades de alfalfa en el valle de México. Acta Universitaria 29: 1–11. https://doi.org/10.15174/au.2019.2202

SAS Institute, Inc. 2011. Statistical Analysis Software (SAS/STAT). Version 9.33 Ed. Cary, NC, USA. 528 pp.

Sosa-Rubio EE, Cabrera-Torres E, Pérez-Rodríguez D, Ortega-Reyes L. 2008. Producción estacional de materia seca de gramíneas y leguminosas forrajeras con corte en el estado de Quintana Roo, México. Técnica Pecuaria en México 46 (4): 413–426.

Sosa-Pérez G, López-Ortiz S, Pérez-Hernández P, Cortez-Romero C, Gallegos-Sánchez J. 2017. Uso de frutos tropicales (Fabaceae) completo alimenticio de pequeños rumiantes. Agroproductividad 10 (2): 37–41.

Valles-de la Mora B, Castillo-Gallegos E, Ocaña-Zavaleta E, Jarillo-Rodríguez J. 2014. *Cratylia argentea*: un arbusto forrajero potencial en sistemas silvopastoriles. Rendimiento y calidad de accesiones según las edades de rebrote y estaciones climáticas. Revista Chapingo Serie Ciencias Forestales y del Ambiente 20 (2): 277–293. https://doi.org/10.5154/r.rchscfa.2013.11.040

van Soest PJ, Robertson JB, Lewis BA. 1991. Methods for dietary fiber, neutral detergent fiber, and nonstarch polysaccharides in relation to animal nutrition. Journal of Dairy Science 74 (10): 3583–3597. https://doi.org/10.3168/jds.S0022-0302(91)78551-2

Voisin AS, Guéguen J, Huyghe C, Jeuffroy MH, Magrini MB, Meynard JM, Mougel C, Pellerin S, Pelzer E. 2013. Legumes for feed, food, biomaterials and bioenergy in Europe: a review. Agronomy for Sustainable Development 34 (2): 361–380. https://doi.org/10.1007/s13593-013-0189-y

Wang KH, Sipes BS, Schmitt DP. 2002. Crotalaria as a cover crop for nematode management: a review. Nematropica 32 (1): 35–57.

Agrociencia

# TRACES OF GLYPHOSATE IN CORN (*Zea mays* L.) AND AVOCADO (*Persea americana* Mill.) WEEDS SUPPORTED BY VANT AND RAMAN SPECTROSCOPY

María Guadalupe **Galindo-Mendoza**[1], Rita **Schwentensius-Rindermann**[2*], Valter Armando **Barrera-López**[1], Hugo Ricardo **Navarro-Contreras**[3], Benjamín **Hernández-Vázquez**[2], Geovanni **Saldierna-Salas**[1]

[1] Universidad Autónoma de San Luis Potosí. Laboratorio Nacional de Geoprocesamiento de Información Fitosanitaria. Av. Sierra Leona No. 550, Lomas 2ª Sección, San Luis Potosí, San Luis Potosí, Mexico. C. P. 78210.
[2] Universidad Autónoma Chapingo. Centro de Investigaciones Interdisciplinarias para el Desarrollo Rural Integral. Carretera México-Texcoco km 38.5, Chapingo, Texcoco, State of Mexico, Mexico. C. P. 56230.
[3] Universidad Autónoma de San Luis Potosí. Laboratorio Nacional de Análisis Físicos, Químicos y Biológicos. Av. Sierra Leona No. 550, Lomas 2ª Sección, San Luis Potosí, San Luis Potosí, Mexico. C. P. 78210.
* Author for correspondence: rschwentesiuss@chapingo.mx

**Citation:** Galindo-Mendoza MG, Schwentensius-Rindermann R, Barrera-López VA, Navarro-Contreras HR, Hernández-Vázquez B, Saldierna-Salas G. 2023. Traces of glyphosate in corn (*Zea mays* l.) and avocado (*Persea americana* Mill.) weeds supported by vant and raman spectroscopy. **Agrociencia** 57(8): 1646-1660. doi.org/ 10.47163/agrociencia.v57i8.2911

**Editor in Chief:**
Dr. Fernando C. Gómez Merino

Received: November 14, 2022.
Approved: September 13, 2023.
**Published in Agrociencia:** December 22, 2023.



## ABSTRACT

Since the 1990s, radiometric and biophotonic sensor applications have provided reliable alternatives and rapid non-invasive diagnostics for the detection and delimitation of pests and diseases, as well as pesticide traces. Active sensors have been shown to be more accurate in detecting the heterogeneity of environmental factors based on thermal and infrared characteristics, chlorophyll fluorescence, and plant reflectance. Unmanned Aerial Vehicles (UAVs) equipped with infrared cameras locate and delimit weed abundance and diversity using Normalized Difference Vegetation Index (NDVI) algorithms, which highlight heterogeneous chlorophyll activity and herbicide-limited photosynthesis in crops. The resulting map serves as the foundation for collecting plant samples. In this study, the technology of these sensors was applied to determine glyphosate traces using Raman spectroscopy, which allowed a quick, low-cost, simple, and practical diagnosis with immediate results. These are essential characteristics for surveillance and monitoring activities, as well as the basis for a geo-referenced inventory of pesticides in production units. Of the 44 weed samples collected, eight were positive for glyphosate traces: two in corn and six in avocado. Weeds are identified as positive to glyphosate traces in Raman spectroscopy in the carotenoid and phenylpropanoid reduction ranges (1186 and 1213 $cm^{-1}$) as a result of a decrease in the immune response. The vibrations presented by the amines in glyphosate and the C-OH of the carboxyl group are detected in the range of 1565 and 1567 $cm^{-1}$.

**Keywords:** Pesticides, biochemical signatures, crops.

## INTRODUCTION

Weeds (endemic and invasive) are a fierce competitor for cash and subsistence crops, causing significant losses due to a decrease in yield of up to 50 % in harvesting efficiency and approximately 20 % in productivity, as well as competition for light, water, and nutrients (Radosevich *et al.*, 2007). Some weeds can produce toxic substances that are transferred to the final agricultural product, resulting in the loss of certified seed, and they can also serve as hosts for pests and diseases (de Pardo *et al.*, 2010).

The crops most affected in yield and productivity worldwide by the presence of weeds are corn (*Zea mays* L.), soybean (*Glycine max* L. Merril), and bean (*Phaseolus vulgaris* L.), with up to 50 % yield losses, followed by sunflower (*Helianthus annuus* L.) with up to 40 % losses; canola (*Brassica napus* subsp. *napus*), up to 25 %; and sugarcane (*Saccharum* spp.) and winter oats (*Avena sativa* L.), up to 10 % (Wall and Smith, 2000; Page *et al.*, 2017). In this regard, a typology known as "*aggressive weeds*" was created, which are weeds that have developed herbicide resistance, causing agrochemicals to be less effective, to be applied in greater volume, and to be used in combination with several herbicides.

Mexico has 36 % of the cases of herbicide resistant weeds, and 1.7 % of these are resistant to glyphosate (Heap, 2022). Since 1996, this country increased by 1500 % the preferential application of glyphosate for the planting of genetically modified corn, cotton, and soybeans (CONACyT, 2020). There is also evidence of the increase of this pesticide in Mexican agriculture, both conventional and subsistence, in corn production units (35 %), followed by citrus (14 %), pasture (12 %), sorghum (*Sorghum bicolor* (L.) Moench) (11 %), and avocado (*Persea amaricana* Mill.) (3 %) (Alcántara-de la Cruz *et al.*, 2021). The most concerning example is avocado, which has increased 251 % in the last 20 years (from 96 000 ha in 2000 to 241 000 ha in 2021) (SIAP, 2021), and whose production system includes the use of five herbicides: carfentrazone ethyl, diquat, glyphosate, oxyfluren, and simazine. Glyphosate is the most widely used of these as it has an extremely broad spectrum of action, combating 81 of the 86 species listed for avocado (Rodríguez-Campos *et al*., 2017).

Glyphosate is an organophosphate herbicide with a simple chemical structure, but its four highly polar groups make it difficult to analyze using conventional methods. The so-called "gold standard" for trace detection techniques are gas chromatography (GC) and high-performance liquid chromatography (HPLC) (Dias *et al.*, 2019). Despite their remarkable advantages of high sensitivity and precision in quantitative detection, these techniques still require sample pretreatment and well-trained laboratory personnel, as well as hours or even days to complete the entire analysis process.

Since the 1990s, radiometric and biophotonic sensor applications have provided reliable alternatives and rapid non-invasive diagnostics for the detection and delimitation of pests and diseases, as well as pesticide traces (Mahlein *et al*., 2012; Martinelli *et al*., 2015). Precision agriculture, also known as digital agriculture or 4.0, involves the detection, quantification, and mapping of plant stress through monitoring and data collection, information processing, and decision support for the temporal and spatial

allocation of inputs for crop production (Pedersen and Lind, 2017; Bongiovanni and Lowenberg, 2017).

Active sensors are the most accurate at detecting the heterogeneity of environmental factors (Chaerle and van der Straeten, 2001). Symptoms (non-visible and early stage) of pests and diseases, as well as traces of pesticides, are determined using measurements based on thermal and infrared characteristics (Jones and Schofield, 2008), chlorophyll fluorescence (Chaerle and van der Straeten, 2001), and plant reflectance (Galieni *et al*., 2021). Unmanned aerial vehicles (UAVs) equipped with infrared cameras are used to detect and delimit glyphosate impact on crops (Huang *et al*., 2014; Daouk *et al*., 2015). Multispectral images determine weed abundance and diversity using NDVI algorithms (Castaldi, 2017), and the resulting map serves as the basis for sample collection for the detection and impact of glyphosate and other herbicides (Esposito *et al*., 2021). Once the plant sample is obtained, weed identification is carried out, and Raman spectroscopy (RS) is used for the determination of glyphosate traces and residues (Sato-Berrú *et al*., 2004; Singh *et al*., 2021, Farber *et al*., 2019).

RS measures the inelastic scattering of light from a monochromatic source, providing information on the chemical composition by recording the molecular vibrations of the constituent components; the "biochemical signature" or "molecular fingerprint" is then obtained (Vallejo-Pérez *et al*., 2016). Both infrared and Raman spectroscopy provide a characteristic spectrum of the specific vibrations of a molecule and are valuable in identifying a substance, as Raman spectra contain vibrational bands that can be assigned to carbohydrates, carotenoids, proteins, and phenylpropanoids affected by glyphosate (Singh *et al*., 2021).

Based on this knowledge, we propose the hypothesis of using high spectroscopic and radiometric resolution sensors to detect glyphosate traces in weeds and map its distribution in agricultural lands in real time. This is a pioneer study in corn and avocado crops in Mexico, whose objective is to reveal the structural biochemical changes of weeds containing traces of glyphosate in the reduction of carotenoids and phenylpropanoids (1186 and 1213 $cm^{-1}$) resulting from a decrease in the defense response, when compared to the spectra obtained from the concentrations of applied pesticides specified positive to glyphosate traces in RS in the ranges of 1081 and 1082 $cm^{-1}$, in the vibrations of phosphonate molecules in glyphosate. While mapping their distribution in agricultural premises, vibrations in the C-N bonds in the amino group part and those in the C-OH of the carboxyl group are detected between 1565 and 1567 $cm^{-1}$ (Singh *et al*., 2021; Balafoutis *et al*., 2017).

For this purpose, the precision agriculture (PA) methodology is utilized, which consists of a cyclical data collection system used for crop management and decision evaluation through smart farming technologies (SFT) such as infrared cameras mounted on UAVs, active biophotonic sensors to obtain geo-referenced spectral information of plant physiological parameters, as well as the characterization of environmental parameters of productive units processed in spatial information software such as Geographic Information Systems (GIS) and, later, through Principal Component Analysis (PCA).

## MATERIALS AND METHODS

### Study area

The experimental production units were determined by the consensus of both producers (who lent land) and researchers from the project "Evaluation and validation of agronomic practices for the agroecological management of weeds in corn and avocado crops" (UACH-CONACyT, 321134; 2022). In the municipality of Texcoco, State of Mexico, Mexico, four corn production units are rainfed, with only one property having auxiliary irrigation (two peri-urban and two in rural landscapes). It was also agreed to work on two avocado production units with an irrigated agroforestry landscape in Tetela del Volcán, Morelos, Mexico (Figure 1).

### Sampling

The multidisciplinary field work took place from June 13 to July 18, 2022, and consisted of sampling weeds in the early stages of growth (11 days after emergence) before weeding activities in the case of corn and in the ripening stage in the case of avocado, as well as the definition of treatment application and flight missions with the DJI Phantom 3 unmanned aerial vehicle (UAV) and onboard the Mapir Survey RGN camera (visible and near infrared-NIR) covering an area of 9 ha.

A total of 44 samples collected throughout the study area were processed. Thirteen weeds were collected for corn and 31 for avocado (Table 1). The PA cyclic production process can be achieved through data acquisition, data processing, analysis and evaluation (decision making), and accurate application of operations (implementation,

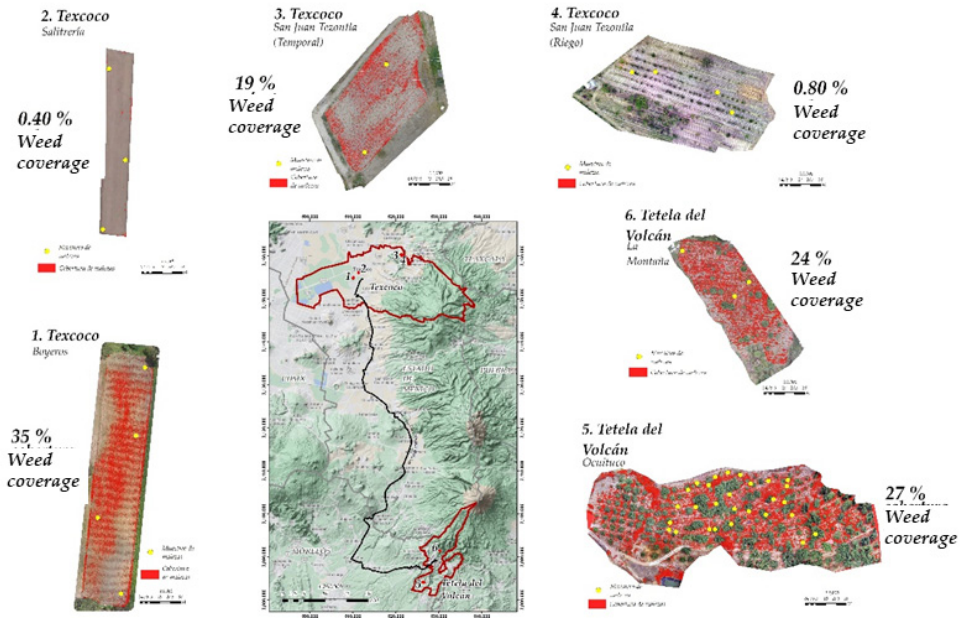


**Figure 1.** Location of the study area and identification of weed cover with the UAV.

**Table 1.** Characterization of the experimental and sampling production units of corn (*Zea mays* L.) and avocado (*Persea americana* Mill.).

| State | Municipality | Plots | Lot | Variety | Area (ha) | Samples analyzed | Weed density ($m^2$) |
|---|---|---|---|---|---|---|---|
| State of Mexico | Texcoco | Boyeros | Corn | Yellow | 1 | 4 | 374 |
| State of Mexico | Texcoco | Salitrería | Corn | Yellow | 0.5 | 3 | 3 |
| State of Mexico | Texcoco | San Juan Tezontla (Temporary) | Corn | Yellow and blue | 1 | 2 | 6 |
| State of Mexico | Texcoco | San Juan Tezontla (Irrigation) | Corn | Yellow and white | 1.5 | 4 | 128 |
| Morelos | Tetela del Volcán | Ocuituco | Avocado | Hass | 4 | 28 | 550 |
| Morelos | Tetela del Volcán | La Montaña | Avocado | Hass | 1 | 3 | 498 |

classification, or typing). These three components define, in this case, risk management specific to weed density and the determination of glyphosate positives (Pedersen and Lind, 2017).

## Data acquisition

### Spatialization

To determine the percentage of weed coverage, six photogrammetric missions were planned with Pix4D Capture, which delimited the UAV flight lines at 25 m, obtaining an 80 % overlap between aerial images with a GSD of 1 cm pixel. The aerial images were obtained using a 12-megapixel MAPIR Survey3 (550–850 nm) multispectral camera mounted to the UAV Phantom 3 Professional and processed in Agisoft Metashape Professional v1.5.2, resulting in six georeferenced orthomosaics. The NDVI algorithm (Castaldi *et al*., 2017) was calculated to each orthomosaic and spectral information extraction was applied for the determination of percent weed coverage.

### Weed collection

To measure weed population density in the field, the "W" method (SENASICA, 2013) was used, using a metallic quadrant (0.5 x 0.5 m), where the weeds remaining within the quadrant were counted and multiplied by four to obtain population per square meter ($m^2$). The collected samples were stored in self-sealing plastic bags to maintain the cold chain but without freezing the samples, so they were placed in unicel coolers containing refrigerant gels.

### Raman diagnosis

For the determination of biochemical signatures of glyphosate traces in the collected weed samples, two high-purity pesticides (from eight commercial brands of glyphosate) were used and analyzed at the Center for the Application of Infrared Radiation, Alternative Energies and Materials (CARIEM) of CIACyT-UASLP. The Xplora Plus Raman Microscope was used, with the green laser at 100 % power and 785 nm excitation in a 20/2 second acquisition time that incorporates unique and powerful features in a reliable, high-performance system. These systems feature an enhanced range of options to measure with at least one other laser wavelength in the infrared, including EMCCD detection, combined Raman polarization, and Raman-AFM. Being a multisample Raman microscope, the observation technique of using microscope objectives with a typical spatial resolution of 2-4 μm is improved. To obtain the reference spectra of glyphosate, a drop of both pesticides was taken with a glass pipette and placed on an aluminum slide for liquids.

The biochemical signature of the Raman Spectra of the two pesticides (Takle 360 and Faena Fuerte) shows changes in the intensity level in comparison to the ranges 1081–1082 and 1565–1567 $cm^{-1}$, where the vibrations of phosphonate molecules in glyphosate are found, as well as the vibration in the C-N bonds in the amino group and C-OH part of the carboxyl group (Table 2).

**Table 2.** Raman band assignment for glyphosate-positive weeds according to the literature.

| Raman | Assignment | Interpretation |
|---|---|---|
| 477–484 | $\delta(OH)+\varrho(CH_2)+(PO_2)$ | Vibration present in phosphonate molecules in glyphosate. |
| 915 | v (C-O-O) in plane, symmetrical | Cellulose, phenylpropanoids |
| 870–895 | $\varrho(CH_2)+\delta(NH)+v(C-C)$ | Vibration in bonded molecules of the phosphonate-carboxyl group bonding |
| 989–992 | $\varrho(CH_2)+\delta(OH)$ | Methylene molecule balancing vibrations and bending of OH |
| 1081–1082 | v(C-N)+v(C-OH) | Vibration in the C-N bonds in the amino group part and C-OH of the carboxyl group. |
| 1145–1157 | β-carotene | β-carotene, which is a strong orange-red organic pigment. |
| 1156 | C-C stretching; v (C-O-C), v (C-C) in glycosidic bonds, asymmetric ring respiration | Carotenoid, organic pigments present in plants |
| 1186 | v (C-O-H) next to the aromatic ring+ δ(CH) | Carotenoid, organic pigments present in plants |
| 1213 | δ(C–C–H) | Carotenoid, organic pigments present in plants |
| 1325–1337 | $\varrho(CH_2)+v(C-C)$ | Stretch vibration of C-C bonds in glyphosate. |
| 1425–1427 | $\delta(CH_2)$ | Flexural vibration of the methylene molecule |
| 1525 | -C=C-(in plane) | Carotenoid, organic pigments present in plants. |
| 1565–1567 | $\delta(NH_2)$, $\delta(NH_2^+)$ | Types of vibration exhibited by amines in glyphosate |
| 1607 | v(C-C) aromatic ring +δ(CH) | Phenylpropanoids |

Source: Sato-Berrú *et al.* (2004), Farber *et al.* (2019).

### Glyphosate trace quantification

The Raman device was calibrated and configured for use. The laser power used on the Xplora Plus was 532 nm, with an acquisition time of 3 s in five accumulations and at 1 % of the laser power (mW). To avoid oxidative processes in the plant samples, they were analyzed no later than 48 hours after collection (Vallejo-Pérez *et al*., 2016). Leaf samples were extracted from the corresponding bags and placed on a 76 mm x 26 mm glass slide. The leaves analyzed were carefully collected to avoid physical damage from improper handling, and there were no signs or symptoms of disease-causing agents or other residues. The selected samples were recorded in the logbook with label information and Raman device information to ensure traceability and trackability.

Each leaf sample was placed on the sample holder at the focal point of the Xplora Plus, allowing the laser pass through the leaf beam for 3 s. The areas to be analyzed corresponded to the 0.5 and 0.75 portions of the leaf blade in longitudinal orientation to avoid hitting the central rib of the leaf. Once the portion of the plant tissue of interest was located, the sample was covered with cardboard material to prevent light from entering the sensor, and the Raman spectrum was obtained. The data obtained were analyzed using the Origin 2018 software, which removed the fluorescence from the Raman spectra.

After obtaining the biochemical signatures, a multivariate statistical method, such as Principal Component Analysis (PCA), can be used to reduce the number of variables or, in this case, group the main characteristics of the Raman spectra. This technique is widely used for one or more data sets without any prior knowledge about their nature. Component analysis reduces the dimension of the data set by finding an alternative set of coordinates known as principal components, which are orthogonal linear combinations of the original variables that explain a given and acceptable amount of variance. Considering that there is a sample with $n$ individuals, each with $p$ variables ($X_1$, $X_2$,...$Xp$), the sample space has $p$ dimensions. PCA allows finding a number of underlying factors ($Z<p$) that explain approximately the same as the original $p$ variables. Whereas previously p values were required to characterize each individual, this analysis assumes that Z values, also known as principal components, are now sufficient.

Each principal component ($Zi$) is obtained by linear combination of the original variables. The first principal component of a group of variables ($X_1$, $X_2$, ..., Xp) is the normalized linear combination of these variables that has the highest variance:

$$Z1 = \phi 11\, X_1 + \phi 21\, X_2 + \ldots + \phi p1\, X_p$$

The normalized linear combination implies that:

$$\sum_{j=1}^{p} \phi^2_{j1} = 1$$

where the terms ϕ11, ..., ϕ1p define the component and can be interpreted as the contribution or weight/importance that each variable has in each component, therefore, they help to know what type of information each component collects (James *et al*., 2021).

## RESULTS AND DISCUSSION

Eight of the 44 samples tested positive for glyphosate: two in corn and six in avocado (Table 3). The lot with the highest concentration of glyphosate traces was the Ocuituco avocado lot in Tetela del Volcán, and the second was the Salitrería corn lot in the urban area of Texcoco. According to an interview with the farmers in charge of the production units, in the first case, they stated that they "had a health problem due to a weed that caused hives and skin rashes to the workers and that they applied glyphosate to eradicate it in the north area of their property three years ago". In the second case, the producer stated that she just "rents the lot and does not know the type of management and application of poisons" (CONACyT project fieldwork logs, 321134/2022).

Although the percentage of glyphosate-positive weeds per plot is relatively low in avocado (0.3 %), leaves from trees adjacent and close to these weeds were also positive (five trees). In the case of positive corn plots, there is a distribution of 2 % in San Juan Tezontla, where the stubble leaf and corn also tested positive for glyphosate traces

**Table 3.** Weed glyphosate trace identification and weed cover percentage in corn and avocado production units.

| Plots | Weed Positive | Weed Negative | Total weed coverage (%) | Glyphosate-positive weed coverage (%) |
|---|---|---|---|---|
| Texcoco (Boyeros) Corn | 0 | *Ricinus communis* (4) | 35 | 0 |
| Texcoco (Salitrería) Corn | *Chenopodium album* (1) | *Rumex crispus* (2) | 0.40 | 10 |
| San Juan Tezontla (Temporary) Corn | *Baccharis linearis* (1) | *Baccharis linearis* (1) | 19 | 15 |
| San Juan Tezontla (Irrigation) Corn | 0 | *Brachiaria plantaginea* (4) | 0.80 | 0 |
| Tetela del Volcán (Ocuituco) Avocado | *Amaranthus palmeri* (6) | *Solanum americanum* (8), *Malva sylvestris (10)*, *Artemisia dracunculus* (4) | 27 | 20 |
| Tetela del Volcán (La Montaña) Avocado | 0 | *Rumex crispus* (2), *Tithonia tubiformis* (1) | 24 | 0 |

Source: Heap (2022), Syngenta (2022), CENGICAÑA (2013).

using Raman applications. The spectral analysis was carried out in two stages: (1) preprocessing of the spectra and (b) principal component analysis (PCA).

Trace glyphosate-positive weeds displayed bands at the positions of ranges 1081–1082 and 1565–1567 $cm^{-1}$ where the vibrations of phosphonate molecules in glyphosate (equivalent to the chemical fingerprint of the herbicides selected for this study) are found. The sample with the highest intensity in avocado was #32, while the sample with the highest intensity in corn was #25. Some herbicides interfere with chlorophyll biosynthesis and functional changes in chloroplasts. It can also affect the formation of other pigments, such as xanthophylls and carotenoids, causing interference in electron flow and a reduction in ATP production by inhibiting ATP-synthase activity in the photophosphorylation process (Corrêa *et al*., 2018). In fact, glyphosate inhibits photosynthesis and stimulates stomatal closure. It also produces oxidative stress, inhibits aromatic amino acid synthesis, and decreases protein synthesis (Meloni *et al*., 2019). The beta-carotene vibrations in the 1145-1156-1523 $cm^{-1}$ records of very low intensity in the glyphosate positives compared to the three highest peaks in the glyphosate-free weeds (Figure 2), where there is a low intensity portion of 3.31 % in comparison to the glyphosate-free ones.

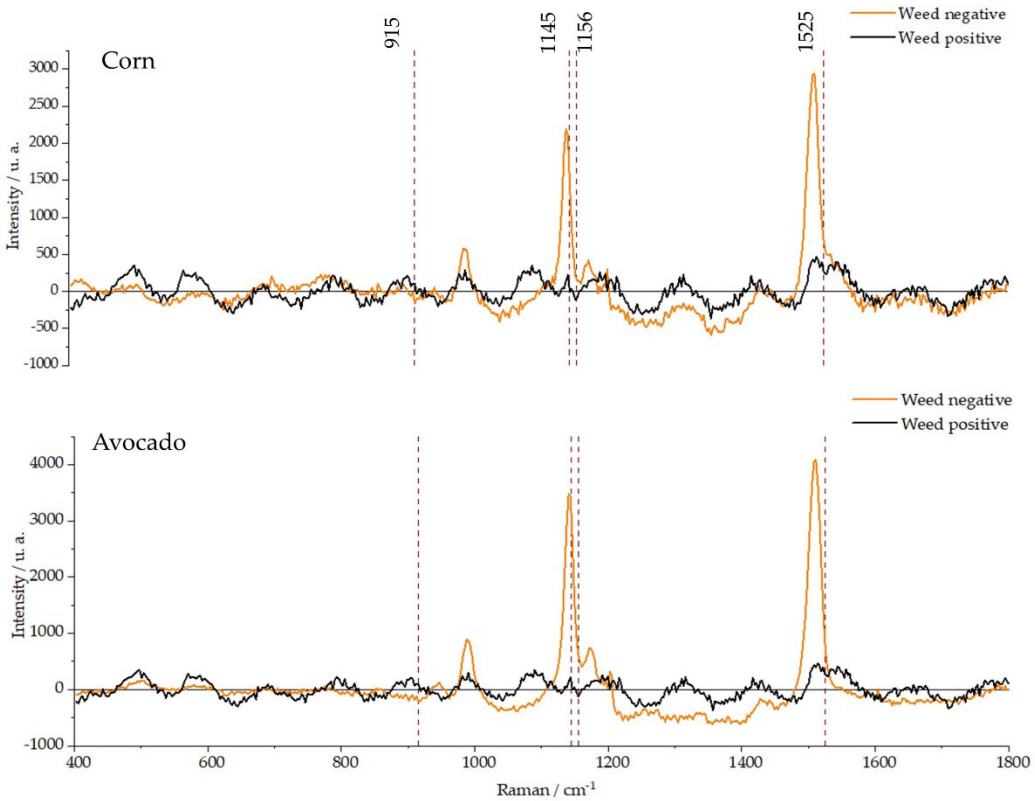


**Figure 2.** Comparison of Raman spectra of glyphosate positive and negative weeds in experimental units of corn and avocado.

After obtaining the biochemical signatures, the PCA method was used to reduce the complexity of the Raman spectra and reduce their behavior to two variables, allowing for measuring, explaining, and predicting the degree of relationship and variation between the spectra obtained in positive-negative to glyphosate. Samples below 0 on the y-axis have positive values because they are close to the samples of the base herbicides of the study and show less variation (T, Ff). On the other hand, the samples that tested negative for glyphosate are above 0 on the same axis. Similarly, the positive samples show positive intensity values in both representative bands (1156 and 1525 $cm^{-1}$) (Table 4).

There were seven negative samples that shared some spectral signature characteristics with the positive samples. The PCA technique was used to distinguish any trace of glyphosate, resulting in a pattern of separation of negative and positive weeds (Figure 3). The PCA technique allowed the interpretation of complex data matrices, as well as the improvement of understanding of the state of the system under study and the identification of the factors influencing the system. All of this made it possible to differentiate the data according to positive and negative (Figure 3), to detect traces of glyphosate with a high degree of reliability, and to use this technique in later stages to classify new samples as "positive" or "free" (negative) of glyphosate (Vallejo-Pérez *et al.*, 2016). Therefore, this methodology proves to be reliable for sample identification.

To carry out the following studies, it is necessary to consider the type of matrix or state of the sample to be evaluated, as well as the type of radiation or irradiation beam at which the experiments will be carried out. Radiometry and spectroscopy technologies are an accurate and cost-effective approach to early and geo-referenced search and detection of glyphosate traces in any agricultural production lot, in addition to an alternative for pre-diagnosis and sample selection for HPCL analysis in certified laboratories.

## CONCLUSIONS

Raman spectroscopy combined with Principal Component Analysis (PCA) demonstrated 86.9 % sensitivity and 89.2 % accuracy in distinguishing between glyphosate-positive weeds and healthy plants. The spatiality of plant sample collection in the field is determined by the 0.5 Normalized Difference Vegetation Index of the orthomosaics obtained by the Unmanned Aerial Vehicles and infrared photographs of weeds. Therefore, it is proposed that this protocol serve as the basis for a geo-referenced inventory of pesticides with the support of a catalog of spectral signatures and the use of Raman in real time (supported by intelligent mobile technologies), as well as part of the protocols for organic certification inventories. The intelligent algorithm is expected to make pesticide residue detection more instrumented and programmatic. Finally, the establishment of a Raman database of pesticides and the standardization of instruments should attract more attention in the field of rapid *in situ* detection in the future.

**Table 4.** Raman wave assignment values for weeds with glyphosate residues.

| Sample number | (1156) $cm^{-1}$ | (1525) $cm^{-1}$ | Qualitative assignment | Lot |
|---|---|---|---|---|
| 1 | -100 | 409 | Low | Avocado |
| 2 | 334 | 894 | | Avocado |
| 3 | 413 | 1067 | | Avocado |
| 4 | 201 | 633 | | Avocado |
| 5 | 143 | 492 | | Avocado |
| 6 | 347 | 684 | | Avocado |
| 7 | 130 | 388 | | Avocado |
| 8 | 137 | 378 | Low | Avocado |
| 9 | 158 | 520 | | Avocado |
| 10 | 53 | 265 | Low | Avocado |
| 11 | 164 | 460 | | Avocado |
| 12 | 199 | 582 | | Avocado |
| 13 | 180 | 541 | | Avocado |
| 14 | 324 | 772 | | Avocado |
| 15 | 187 | 518 | | Avocado |
| 16 | 241 | 671 | | Avocado |
| 17 | 234 | 626 | | Avocado |
| 18 | 204 | 454 | | Avocado |
| 19 | 277 | 727 | | Avocado |
| 20 | 223 | 721 | | Avocado |
| 21 | 184 | 422 | | Avocado |
| 22 | 134 | 414 | | Avocado |
| 23 | 271 | 685 | | Avocado |
| 24 | 293 | 801 | | Avocado |
| 25 | 232 | 532 | | Avocado |
| 26 | 231 | 526 | | Avocado |
| 27 | 285 | 711 | | Avocado |
| 28 | 212 | 678 | | Avocado |
| 29 | 19 | 91 | Mean | Avocado |
| 30 | 34 | 95 | Mean | Avocado |
| 31 | 568 | 1160 | | Corn |
| 32 | -97 | 402 | Very high | Avocado |
| 33 | 130 | 234 | Mean | Corn |
| 34 | 1089 | 1237 | | Corn |
| 35 | 105 | 408 | Very high | Corn |
| 36 | 235 | 267 | | Corn |
| 37 | 169 | 174 | | Corn |
| 38 | 1074 | 1517 | | Corn |
| 39 | 346 | 499 | | Corn |
| 40 | 499 | 832 | | Corn |
| 41 | 203 | 593 | | Corn |
| 42 | 189 | 604 | | Corn |
| 43 | 168 | 533 | | Corn |
| 44 | 196 | 573 | | Corn |

Source: Farber *et al.* (2019).

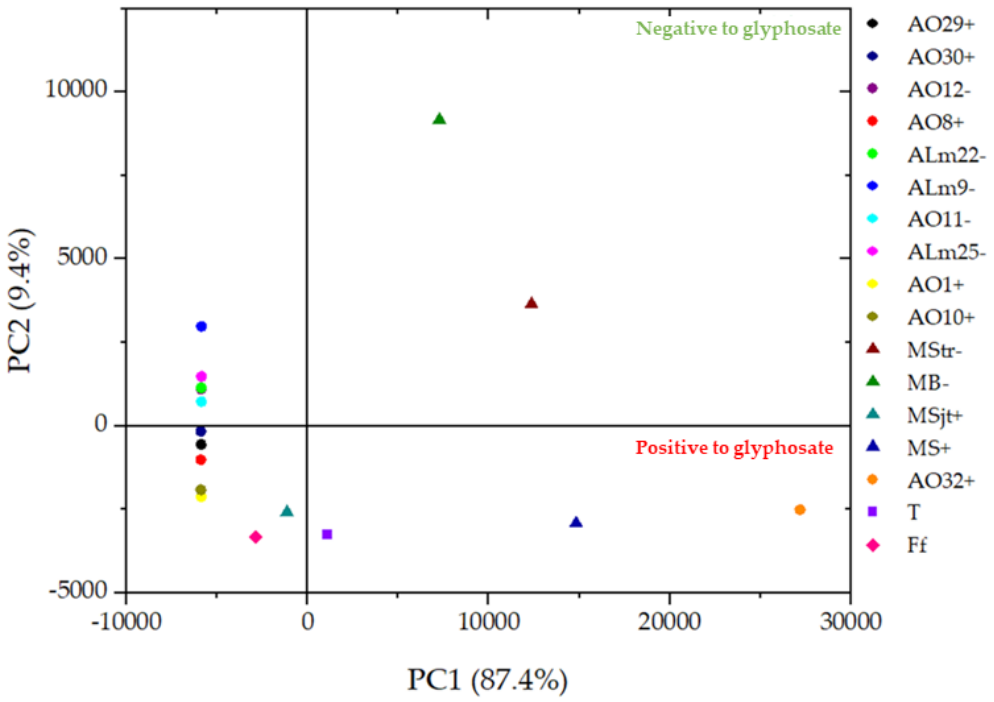


**Figure 3**. Principal component analysis of samples collected from corn and avocado lots. Lots: Corn (M), avocado (A); Plots: Boyeros (B), Salitrería (S), San Juan Tezontla-Temporal (Sjt), San Juan Tezontla-Riego (Str), Ocuituco (O), La Montaña (Lm); Pesticides: Takle 360 (T), Faena Fuerte (Ff); Positive (+) and Negative (-) result.

## ACKNOWLEDGMENTS

This study was financed by Project 2022 "Evaluation and validation of agronomic practices for the agroecological management of weeds in corn and avocado crops" funded by the Universidad Autónoma Chapingo with resources from CONACyT. (321134). F003 "National Strategic Science, Technology and Linkage Programs with the social, public and private sectors". To CARIEM-CIACyT-UASLP for the support provided by the Raman equipment.

## REFERENCES

Alcántara-de la Cruz R, Cruz-Hipolito HE, Domínguez-Valenzuela JA, de Prado R. 2021. Glyphosate ban in Mexico: potential impacts on agriculture and weed management. Pest Management Science 77 (9): 3820–3831. https://doi.org/10.1002/ps.6362

Balafoutis AT, Beck B, Fountas S, Tsiropoulos Z, Vangeyte J, van der Wal T, Soto-Embodas I, Gómez-Barbero M, Pedersen SM. 2017. Smart Farming Technologies– Description, Taxonomy and Economic Impact. *In* Pedersen M, Martin K. (eds.), Precision Agriculture:

Technology and Economic Perspectives. Springer: Cham, Switzerland, pp: 21–77. https://doi.org/10.1007/978-3-319-68715-5_2

Bongiovanni R, Lowenberg-Deboer J. 2004. Precision agriculture and sustainability. Precision Agriculture 5 (4): 359–387. https://doi.org/10.1023/B:PRAG.0000040806.39604.aa

Castaldi F, Pelosi F, Pascucci S, Casa R. 2017. Assessing the potential of images from unmanned aerial vehicles (UAV) to support herbicide patch spraying in Corn. Precision Agriculture 18 (1): 76–94. https://doi.org/10.1007/s11119-016-9468-3

CENGICAÑA (Centro Guatemalteco de Investigación y Capacitación de la Caña de Azúcar). 2013. Manual de malezas y catálogo de herbicidas para cultivo de caña de azúcar en Guatemala. Ciudad de Guatemala, Guatemala. 97 p. https://cengicana.org/files/20150902101640359.pdf (Retrieved: September 2022).

Chaerle L, Van Der Straeten D. 2001. Seeing is believing: imaging techniques to monitor plant health. Biochimica et Biophysica Acta 1519 (3): 153–166. https://doi.org/10.1016/s0167-4781(01)00238-x

CONACyT (Consejo Nacional de Ciencia y Tecnología). 2020. Expediente científico sobre glifosato y los GM. Ciudad de México, México. 31 p. https://conacyt.mx/wp-content/uploads/documentos/glifosato/Dossier_formato_glifosato.pdf (Retrieved: May 2022).

Corrêa JM, Ferreira EA, Pereira GAM, Piratoba ARA, dos Santos JB, de Oliveira CH, Silva CT. 2018. Fluorescencia de la clorofila *a* en plantas de piña sometidas a aplicación de herbicidas. Revista Colombiana de Ciencias Hortícolas 12 (1): 50–58.

Daouk S, Frege C, Blanc N, Mounier S, Redon R, Merdy P, Lucas Y, Pfeifer HR. 2015. Fluorescence spectroscopy to study dissolved organic matter interactions with agrochemicals applied in Swiss vineyards. Environmental Science and Pollution Ressearch 22 (12): 9284–9292. https://doi.org/10.1007/s11356-015-4086-6

de Pardo R, Cruz-Hipólito H, Rosario-Socorro JM. 2010. Mecanismos de resistencia de las plantas a los herbicidas. Departamento de Química Agrícola y Edafología: Córdoba, España. 14 p.

Dias LAF, Jussiani EI, Appoloni C. 2019. Reference Raman Spectral Database of Commercial Pesticides. Journal of Applied Spectroscopy 86 (1): 166–175. https://doi.org/10.1007/s10812-019-00798-1

Esposito M, Crimaldi M, Cirillo M, Sarghini F, Maggio A. 2021. Drone and sensor technology for sustainable weed management: a review. Chemical and Biological Technologies in Agriculture 8 (18). https://doi.org/10.1186/s40538-021-00217-8

Farber C, Shires M, Ong K, Byrne D, Kurouski D. 2019. Raman spectroscopy as an early detection tool for rose rosette infection. Planta 250 (4): 1247–1254. https://doi.org/10.1007/s00425-019-03216-0

Galieni A, D'Ascenzo N, Stagnari F, Pagnani G, Xie G, Pisante M. 2021. Past and future of plant stress detection: An overview from remote sensing to positron emission tomography. Frontiers in Plant Science 11: 609155. https://doi.org/10.3389/fpls.2020.609155

Heap I. 2022. The international survey of herbicide-resistant weed database. Global Herbicide Resistance Action Committee. CropLife International. https://www.weedscience.org (Retrieved: September 2022).

Huang Y, Reddy KN, Thomson SJ, Yao H. 2014. Assessment of soybean injury from glyphosate using airborne multispectral remote sensing. Pest Management Science 71 (4): 525–552. https://doi.org/10.1002/ps.3839

James G, Witten D, Hastie T, Tibshirani R. 2021. An introduction to statistical learning with applications in R. Springer: New York, NY, USA. 607 p. https://doi.org/10.1007/978-1-0716-1418-1

Jones HG, Schofield P. 2008. Thermal and other remote sensing of plant stress. General and Applied Plant Physiology 34 (1–2): 19–32.

Mahlein AK, Oerke EC, Steiner U, Dehne HW. 2012. Recent advances in sensing plant diseases for precision crop protection. European Journal of Plant Pathology 133 (1): 197–209. https://doi.org/10.1007/s10658-011-9878-z

Martinelli F, Scalenghe R, Davino S, Panno S, Scuderi G, Ruisi P, Villa P, Stroppiana D, Boschetti M, Goulart LR, Davis CE, Dandekar AM. 2015. Advanced methods of plant disease detection. Agronomy for Sustainable Development 35 (1): 1–25. https://doi.org/10.1007/s13593-014-0246-1

Meloni DA, Targa G, Fraño A, Ledesma R, Silva MC, Catán EA, Ledesma R. 2019. La deriva de glifosato inhibe la fotosíntesis y produce estrés oxidativo en *Eucalyptuscamaldulensis*. Quebracho Revista de Ciencias Forestales 27 (1): 5–12.

Page ER, Cerrudo D, Westra P, Loux M, Smith K, Foresman C, Wright H, Swanton CJ. 2017. Why early season weed control is important in maize. Weed Science 60 (3): 423–430. https://doi.org/10.1614/WS-D-11-00183.1

Pedersen MS, Lind KM. 2017. Precision Agriculture: Technology and Economic Perspectives. *In* Pedersen SM, Lind KM. (eds.), Progress in Precision Agriculture. Springer: Cham, Switzerland. 276 p. https://doi.org/10.1007/978-3-319-68715-5

Radosevich SR, Holt JS, Ghersa CM. 2007. Ecology of weeds and invasive plants: Relationship to agricultural and natural resource management. Wiley: Hoboken, NJ, USA. 454 p. https://doi.org/10.1002/9780470168943

Rodríguez-Campos J, Escobedo-Reyes A, Lugo-Melchor OY. 2017. Inocuidad del aguacate. *In* Lugo-Melchor OY, Alvarado-Osuna C, Ramírez-Cerda EL. (eds.), Inocuidad y trazabilidad de los alimentos mexicanos. CIATEJ: Guadalajara, Jalisco, pp: 165–186.

Sato-Berrú RY, Medina-Gutiérrez C, Medina-Valtierra J, Frausto-Reyes C. 2004. Aplicación de la espectroscopía Raman para la caracterización de pesticidas orgánicos. Revista Internacional de Contaminación Ambiental 20 (1): 17–24.

SENASICA (Servicio Nacional de Sanidad, Inocuidad y Calidad Agroalimentaria). 2013. Manual operativo de la campaña contra malezas reglamentadas. Secretaría de Agricultura, Ganadería, Desarrollo Rural, Pesca y Alimentación. Servicio Nacional de Sanidad, Inocuidad y Calidad Agroalimentaria. Ciudad de México, México. 30 p. https://www.gob.mx/cms/uploads/attachment/file/108116/Manual_Operativo.pdf (Retrieved: May 2022)

SIAP (Servicio de Información Agroalimentaria y Pesquera). 2021. Anuario estadístico de la producción agrícola. Servicio de Información Agroalimentaria y Pesquera. Ciudad de México, México. https://nube.siap.gob.mx/cierreagricola/ (Retrieved: May 2022).

Singh V, Dou T, Krimmer M, Singh S, Humpal D, Payne WZ, Sanchez L, Veronine DV, Prosvirin A, Scully M *et al*. 2021. Raman spectroscopy can distinguish glyphosate susceptible and resistant palmer amaranth (*Amaranthus palmeri*). Frontiers in Plant Science 12: 657963. https://doi.org/10.3389/fpls.2021.657963

Syngenta. 2022. Manual de identificación de malezas. Syngenta Agro S.A.: Buenos Aires, Argentina. 334 p. https://www.cadia.com.ar/2023/01/21/manual-de-identificacion-de-malezas-edicion-2022/ (Retrieved: September 2022).

Vallejo-Pérez MR, Galindo-Mendoza MG, Ramírez-Elías MG, González FJ, Navarro-Contrearas HR, Contreras C. 2016. Raman spectroscopy an option for the early detection of citrus Huanglongbing. Applied Spectroscopy 70 (5): 829–839. https://doi.org/10.1177/0003702816638229

Wall DA, Smith MAH. 2000. Quackgrass (*Elytrigia repens*) management in flax (*Linum usitatissimum*). Canadian Journal of Plant Science 80 (2): 411–417. https://doi.org/10.4141/P99-027

Agrociencia

# FUNCTIONAL STABILITY OF THE INVERTED PENDULUM AND ITS RELATION TO UNCREWED AERIAL VEHICLE WINGS THROUGH SYSTEM MATHEMATICAL MODELING AND SIMULATION

Naji Mordi Naji **Al-Dosary**[1*], Alex Greg **Zolotorevskiy**[2], Cassidy Paul **Schram**[2]

[1] King Saud University. College of Food and Agriculture Sciences. Department of Agricultural Engineering. Riyadh, Saudi Arabia.
[2] University of Florida. Department of Mechanical and Aerospace Engineering. Gainesville, FL, USA.
* Author for correspondence: nalsawiyan@ksu.edu.sa

**Citation:** Al-Dosary NMN, Zolotorevskiy AG, Schram CP. 2023. Functional stability of the inverted pendulum system and its relation to uncrewed aerial vehicle wings through mathematical modeling and simulation of the system. **Agrociencia** 57(8): 1661-1681. doi.org/ 10.47163/agrociencia.v57i8.2956

**Editor in Chief:**
Dr. Fernando C. Gómez Merino

Received: January 28, 2023.
Approved: July 26, 2023.
**Published in Agrociencia:** December 13, 2023.



## ABSTRACT

The flight instability of an uncrewed aerial vehicle (UAV) can be considered critical, and investigations of stability can be compared to the study of the stabilization of an inverted pendulum. This study investigated the stability of two dynamic systems, represented by an inverted pendulum and a simple approximation of an aircraft wing surface exposed to aerodynamic forces. This study illustrates the advantages of time-domain simulation for solving the differential equation of motion. The simulation used the Euler integration approach for various system parameters. Essentially, an aircraft in flight must constantly maintain pitch stability, which, in practical considerations, can be compared to the mechanism of a rotary motion represented by the up-swinging motion of an inverted pendulum. The pendulum may conserve the same concept as an aircraft's acceleration, as both are affected by the same gravity and acceleration forces, in which the longitudinal stability of the aircraft must be ensured immediately upon takeoff. An inverted pendulum and a UAV aircraft system simulation were developed with basic MATLAB software. The inverted pendulum simulation showed that as the value of the spring's stiffness at the limit of stability ($k_{lim}$) increased, the system became more convergent and, as a result, more stable. The stiffness of the spring at the limit of stability, $k_{lim}$ = 32.69 N $m^{-1}$ (i.e., equivalent to an initial angular rotation $\theta = 5$ °), and the system's stability were observed up to the value of $k_{lim}$ = 179.79 N $m^{-1}$, which resulted in an unstable short initial period. In addition, for the aircraft's wing, the damping coefficient ($c_{lim}$) value was in the range of $c_{lim} \geq$ 10,000 N s $m^{-1}$. Therefore, with the damping ratio $\zeta$ being equal to zero, the system vibrated consistently at its natural frequency ($w_n$), never deviating drastically to become unstable.

**Keywords:** Aerodynamic forces, aircraft wings, damping coefficient, Euler integration, limiting spring stiffness.

## INTRODUCTION

### An overview of the scientific pendulum scheme

A pendulum rotating around a pivot point, whether suspended or inverted, includes a long rigid arm that ends with a mass affected by gravity at various time intervals and rotation angles. Studying the time period that the pendulum takes to become stable is one of the most important variables to be taken into consideration when analyzing the effects of vibration in numerous mechanical applications, including agricultural machinery. In the agricultural field, it is also possible to compare the effect of forces on the movement and acceleration of a pendulum with the effect of forces and acceleration on the stability of the center of gravity (CG) of a farm tractor to predict and prevent the tractor rolling over. An oscillation methodology for tractors is easily applied to find the height of the center of gravity (CG) of agricultural tractors, where a vertical plane containing the center of gravity is obtained by measuring the relative height levels of the tractor's wheels (Fabbri and Molari, 2004; Khorsandi *et al*., 2018; Bietresato and Mazzetto, 2019).

The concept of a simple pendulum can be illustrated by the seat's shock absorbers and the longitudinal (x) and lateral (y) axis of the driver's seat of a self-propelled agricultural machine (e.g., tractors, combines, lawn mowers, etc.), as well as the flight stability of an uncrewed aerial vehicle (UAV) with or without an associated load during field operations, which means that the dynamic model is with or without change of parameters, as they are all expected to behave in the same way. The pendulum also appears in the design of robotic arm and leg motions (i.e., to increase the walking efficiency of robots and the associated control of robotic manipulators) or a tree trunk and a canopy shaker machine, where the systems can monitor the inverted pendulum's trajectory in order to stabilize their movements. These agricultural applications widely apply the concept of the equilibrium of the pendulum and mass-spring-damper systems (MSD). Recently, modern agricultural practices, especially in the field of control and precision farming methods, have quickly advanced through the application of various technologies, electronic tools, and programming systems, such as LabVIEW, MATLAB, Arduino Uno, Raspberry Pi, etc. These approaches have become key factors contributing to the increased efficiency of agricultural operations, especially regarding machines that are subjected to high levels of vibrations during only the machines that are not cushioned by the soil or the harvested mass (e.g., potato harvesters).

Moreover, a simulation study of the effectiveness of some proposed pendulum models in stabilizing a robot's walk for agricultural machines was performed by Li *et al.* (2021). They established a trajectory-planning method that achieved flexible, stable, and periodic walking independently for bipedal robots in different virtual circumstances that could be realized in real time using linear and inverted pendulum models. The stability of any mechanical system with respect to vibration depends on several different parameters. For example, the mechanical system of an inverted

pendulum attached to a cart shows that the pendulum can be steady in an inverted position if the cart is stationary or if the cart has a displacement moving at a constant velocity, i.e., it has no further acceleration (University of Michigan, 1997). The inverted pendulum is a common application used in several mechanical systems. When the center of gravity (CG) is higher than its pivot point, an inverted pendulum becomes unstable (Hanada *et al.*, 2019). Also, the pendulum's stability is affected by several parameters, as proposed in this study, such as the mass of the pendulum ($m$), the length to the pendulum's center of mass ($l$), and the pendulum's angle from vertical ($\theta$).

## Simplifying the concept of the relationship between the inverted pendulum scheme and the stability of uncrewed aircraft

In agricultural applications, an UAV flying at low altitudes may encounter unfavorable winds, which will affect the required flight altitude of the aircraft during field operations. Wind may cause the GPS antenna on top of the UAV to fluctuate, affecting its stability, and it may disable the aircraft or affect its operational systems. Therefore, the vibration of the GPS antenna on the fuselage in such a situation is similar to the vibration of an inverted pendulum.

Sharma *et al.* (2021) noted the many current uses of hybrid uncrewed aircraft with both helicopter and fixed-wing technology in civilian life and analyzed their aerodynamic properties, including enhanced payload capacity. The load capacity (empty weight plus added cargo load weight) and position of the center of gravity (CG) are the important factors influencing flight stability that determine the appropriateness of certain applications of the UAV in agricultural field operations, for example, aerial agricultural spraying operations with agrochemicals. Assuming that the UAV aircraft is acting in a consistent rotation, during a turn, the aircraft might act as a pendulum affected by an external force (i.e., an aerial vehicle can swing, similar to a torsional pendulum). Due to the aircraft's shape, especially the design of the wings, which may be affected by external aerodynamic forces, the displacement of the center of gravity will create a significant rolling motion of the wings around the center of the aircraft's lift. If an aircraft is disturbed, resulting in one wing being in a high position and the other wing in a lower position relative to the neutral point of the lateral axis, the weight of the aircraft's main body acts as a pendulum, bringing the aircraft back to its equilibrium level (FAA, 2016). Aerodynamic variables affecting the aircraft's wing systems can help us predict an optimized design of the airframe and the wing structure.

Estevez *et al.* (2021) proposed a control technique utilized for carrying a pendulum with the lowest possible oscillations for a system consisting of a multi-rotor aircraft that transmits a double pendulum. They indicated that the transmission of a multi-pendulum using an aerial vehicle is perfectly adequate to the latest technology in order to study the transportation of UAV-borne payloads using complicated dynamics

considering the estimation and tuning of UAV dynamic parameters. The stability of an inverted pendulum can be used to model the application in flight conditions of an aircraft subject to various aerodynamic forces, such as spraying crop and soil nutrients and applying pesticides and insecticides for pest and weed control in agriculture, with the objective of determining the system's ability to achieve stability, especially in the initial inflight stabilization period. The controlling parameters of the rotary inverted pendulum can be specified in two vibration modes that result in a wide frequency domain with partly large amplitude vibrations. These conditions of large amplitude should be avoided when setting a time-varying set point (Dolatabad *et al.*, 2022). Gunawan *et al.* (2018) developed a four-engine flight system (flying quadrotor) that stabilized an inverted pendulum. The results showed the optimum response of the output roll angle of the inverted pendulum and demonstrated the ability to control a short period of autonomous flight (5.40 s) with a settling time of 0.80 s and an overshoot of the roll angle of 17 °.

Moreover, Sowjanya and Ramesh (2015) and Jibril *et al.* (2021) indicated that the inverted pendulum system is a typical nonlinear, multivariate, and naturally unstable system. The problem of controlling an inverted pendulum is the fluttering of conventional control systems; since the pendulum system is inherently unstable, the pendulum will not remain upright without external forces (i.e., it is unstable without control). This concept can be applied to the longitudinal stability of an aircraft's fuselage as it relates to wing stability. The aircraft's wings are designed to accomplish safe and balanced flight. When the wings of an aircraft move through the air, the position of the center of the aerodynamic lift force remains at the same point regardless of the change in the attack angle of the airfoil blade, with or without vibration. Gatto (2009) investigated a longitudinal stability information technique derived from a wind tunnel test model, which was set up as a pendulum support rig. A test model was inverted and suspended inside the wind tunnel's roof by a supporting strut with a degree of freedom, which allowed the model to move. An additional gimbal attaching the model to the strut was used to allow the model to freely rotate in pitch, thus simulating a device (pendulum) oriented horizontally in a moving body (the wind tunnel).

Since longitudinal stability denotes stability along the plane's latitudinal axis, the effectiveness of the elevator provides aerodynamic control of the aircraft's pitch angle. Technically, the results for the system's sensitivity and the input parameters showed that the length of the pendulum's rod and the pendulum's velocity, mass, inertia, rod angle, and angle of attack had the greatest influence on the estimated values of the magnitude of the pendulum's movement. These parameters can be adjusted to achieve the aircraft's optimum flight performance. As a result, the pendulum model, which has only one degree of freedom, can be referred to as the angular displacement. This angular displacement might act as an unbalanced force, which may cause the stability or instability of the pendulum (Tulapurkara, 2012).

When evaluating the performance of any dynamic model of an UAV, an issue arises concerning the system's control inputs and output states, which can be measured.

However, to take these measurements, an observer is required to estimate the state feedback of the UAV under the influence of an incidental external circumstance. In this simulation study, the stability of two systems was investigated. For example, simulations of an inverted pendulum and a simple approximation of an UAV aircraft's wing were tested for a stable flight of the UAV with a short duration. The study included the development of a time-domain simulation to solve the differential equation of motion. The simulation used the Euler integration approach for various system parameters. The Euler integration approach is a numerical method that gives a value for the displacement, velocity, and acceleration with the time steps for the inverted pendulum and aircraft wing systems. In particular, this is important for cases of interaction between the agricultural apparatus and the material to be processed.

The two systems were investigated by using the simulation program in MATLAB software (The MathWorks Inc., 2022a). Thus, the main objectives of the simulation study were to analyze the motion of a system that included a damper, a spring, and an inverted pendulum. The system needed to be able to maintain the pendulum's stability when it stayed vertical and respond to disturbances to the pendulum's angle and, similarly, disturbances of the angle of attack of the aircraft wing (airfoil) by an aerodynamic force. Thus, to demonstrate the aircraft's flight stability, the simulation should perform in the same way as a stable set of wings symmetrically designed around the center of the longitudinal axis to achieve a suitable attack angle of the aircraft's wings (airfoils) along the lateral axis to obtain an appropriate flight lift level. There is a gap between studies of the concept of a pendulum vibration and the vibration of an UAV aircraft that needs to be adressed. Hence, the motive for this work was to investigate the factors causing vibration problems in an inverted pendulum and an UAV (spring and damper coefficients) using Newton's fundamental analysis of motion (Euler equation). Therefore, this study expects to provide investigators with more information for proper comparison and methods for evaluating UAV's vibration and performance, as well as encouraging aeronautical engineers and academic investigators who are interested in studying vibrations, dynamic behaviors, and stabilization systems to consider all the missions to better understand the UAV's stability, which can be generalized in agricultural applications for the use of UAVs in agriculture spraying and crop aerial images to support precision farming.

## MODELING METHODOLOGY AND PROCEDURES

### Simulation methodology of the two systems

The two systems that were analyzed in this study are as follows: (1) an inverted pendulum (linearized only for small rotation angles, so that the system equation could be linear) and (2) a simple approximation of an aircraft wing subject to aerodynamic forces. Initially, the system used to carry out the simulation was the inverted pendulum system. The proposed model of an inverted pendulum was pivoted at one end, with double springs and viscous dampers attached at the halfway point of the pendulum rod (Figure 1).

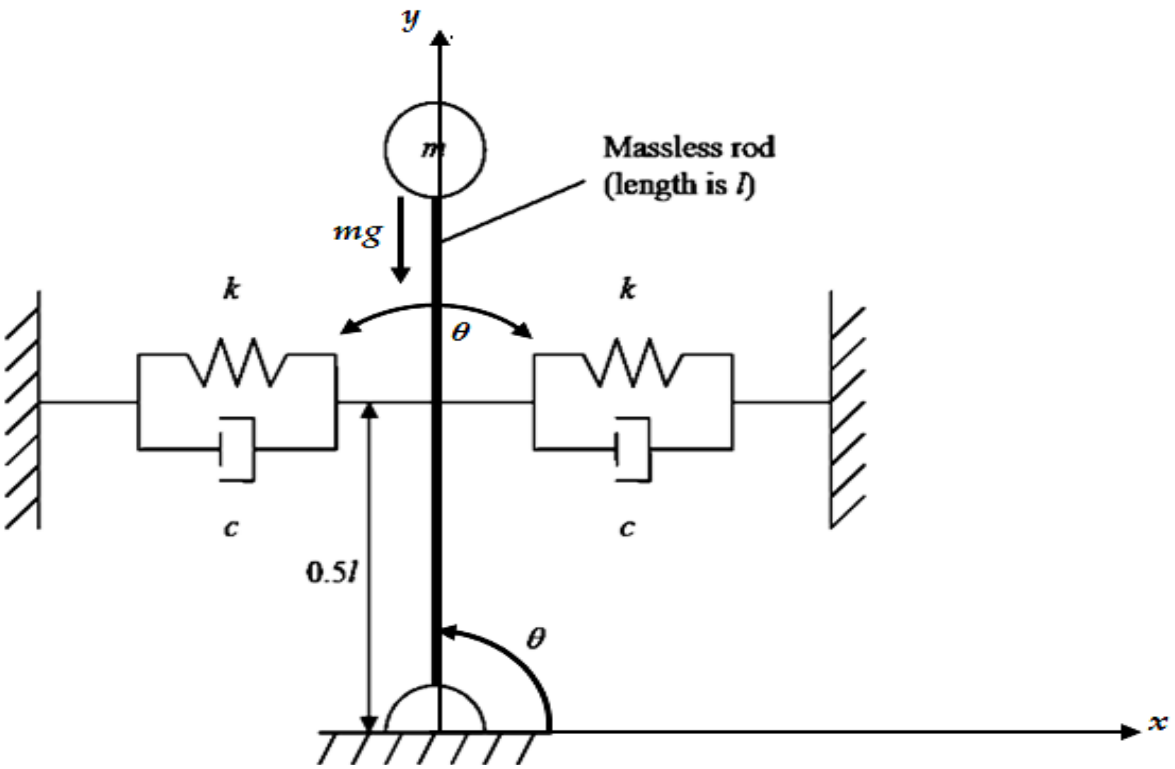


**Figure 1.** Diagram of the proposed dynamic model of an inverted pendulum with coupled springs and viscous dampers.

For the system of an inverted pendulum subject to aerodynamic forces, where the spring and damping combinations were located at the halfway point of the massless rod holding a small spherical mass m (0.5 kg), k is the spring's stiffness constant (32.69 N $m^{-1}$), c is the damping coefficient (1 N s $m^{-1}$), and θ is the angle through which the pendulum rotates (i.e., theta is the pendulum's angle from its vertical position (upward)). Proposed angular displacement (angle of the pendulum's rotation) θ = array of 2001 elements initialized to zero, and *l* is the length of the pendulum's rod (0.3 m) (Figure 1). Springs and viscous dampers are the mechanism of the pendulum pivoting rod for keeping the inverted pendulum moving horizontally until it reaches the vertical stability state.

The explanation of the UAV dynamic model parameters of the fuselage and wings is proposed to be the same as that of the dynamic model of the inverted pendulum machine with center pivot (Figure 1). The derivation of the motion equation and the natural frequency of the system were based on the mass of the pendulum, the length of the inverted pendulum. the stiffness of the springs, the damping coefficient required for the oscillations, with the oscillation reducing over time to zero, mass of the pendulum rod, and the initial angular displacement (in degrees). The acceleration of

the rod along its swing can be computed as the acceleration (motion) of the pendulum due to gravity, the direction, and the location of its head sphere, which is equal to some constant multiplied by the sine function. Consequently, Euler integration was used to carry out the project's time-domain simulation (Kelly, 2012; Russell, 2018; Garcia-Nieto *et al.*, 2019; The MathWorks Inc., 2022b). If a system with a generic single degree of freedom (SDOF) under free vibration is considered and Newton's law of motion is applied, the corresponding equation of motion is:

$$m\ddot{x} + c\dot{x} + kx = 0 \tag{1}$$

where $\ddot{x}$ is the system's acceleration (m $s^{-2}$), $\dot{x}$ is the velocity (m $s^{-1}$), x is the displacement (m) (i.e., the distance traveled by the mass), m is the pendulum's mass (kg), c is the damping coefficient (equivalent to the damping coefficient from combination of the two dampers, N s $m^{-1}$), and k is the spring's stiffness (equivalent to the stiffness from a combination of the two springs, N $m^{-1}$). The Euler integration was constructed from small time steps, *dt*. The acceleration of the current time step was determined by rearranging Equation (1) to yield the following expression for acceleration:

$$\ddot{x} = \frac{- c\dot{x} - kx}{m} \tag{2}$$

where the velocity and position can be obtained from the previous step; the initial conditions are used for the first step. The velocity for the current time step is determined by numerical Euler integration as:

$$\dot{x} = \dot{x} + \ddot{x}\, dt$$

where the velocity on the right-hand side of the equation is retained from the previous time step and is used to update the current value, and the acceleration multiplied by the time step *dt* is used to account for the increase in the velocity due to the acceleration of the system. The velocity from the left-hand side of the equation is then applied to determine the current displacement:

$$x = x + \dot{x}\, dt$$

The displacement on the right-hand side of the equation is retained from the previous time step, and the velocity multiplied by the time step *dt* is used to account for the increase in displacement due to the velocity of the dynamical system.
The value of the current acceleration is calculated in the following expression, which comes from the rearranged differential equation of motion of the inverted pendulum for θ, where θ is the pendulum angle (i.e., a second-order ordinary differential equation):

$$ml^2\ddot{\theta} + \frac{cl^2}{2}\dot{\theta} + \left(\frac{kl^2}{2} - mgl\right)\theta = 0 \quad (3)$$

The second part of the simulation was for the aircraft's wing. This process was based on a dynamic model derived by using the Euler approach, where Euler integration was used to estimate the response of an aircraft's wing section to aerodynamic forces. The behavior of the wing can be modeled by a single degree of freedom differential equation. The aerodynamic forces acting on the wings depend on the velocity. It is being assumed that this system did not have a constant velocity, so the acceleration occurred because of the variation in the aircraft's direction. This means that the equation of motion for the forcing term is:

$$m\ddot{x} + c\dot{x} + kx = \gamma\dot{x}$$

where $\gamma$ (gamma) is the damping coefficient (N s m$^{-1}$) and $\gamma\dot{x}$ is the velocity-dependent effect of the aerodynamic forces on the wings (N) (i.e., a periodic propulsive force).

**Intended procedures of the two systems**

The two systems that needed to be activated were the inverted pendulum and a simple aircraft wing subject to aerodynamic forces, where the spring and damping combinations were located at the midpoint of the massless rod holding a small spherical mass m, k was the spring's stiffness constant, c the damping coefficient, θ the angle through which the pendulum rotated (i.e., theta was the pendulum angle from its vertical position (upwards)), $l$ the length of the pendulum rod, and g was the constant gravitational acceleration (9.80665 m s$^{-2}$) (Figure 1). Therefore, an overall description of the MATLAB simulations for each system implemented in this study is presented in the following sections.

**The inverted pendulum simulation process**

MATLAB is widely used to implement simulations of various application models, such as simulating the behavior of a dynamic system. The unique advantage of using MATLAB is that this software can handle the time in milliseconds to develop and confirm the results of the algorithms. In the simulation of the inverted pendulum system, the user is first asked to input the simulation system they wish to run, as follows: 1 for the inverted pendulum system, and 2 for the aircraft wing system. If the choice is 1, several variables are initiated. The gravitational constant g is set to a value of 9.80665 m s$^{-2}$. The mass of the pendulum is set to 0.5 kg, the damping coefficient is set to 1 N s m$^{-1}$, and the length of the pendulum rod is set to 0.3 m.

Initially, the simulation calculates the value of the limiting spring's stiffness at the limit of stability (k_lim = 2 m g $l^{-1}$). The system displays the value of the calculated limiting stiffness, and the user is asked for the value of the multiplier of k_lim to be used as the

final variable. The k_value (spring stiffness) is the product of the multiplier and the calculated limiting spring's stiffness (k_lim). The final stiffness of the spring (k_value) is then displayed in units of N $m^{-1}$. Certain selected time steps were too large to carry out the simulation and were not considered in this study. Thus, the step size (*dt*), i.e., the step size in seconds, is then set to a value of 5 ms and the time is set to run from 0 s to 2000 step sizes, or 10 s, in steps of 5 ms. The variable theta (θ) is set as an array of 2001 elements initialized to zero. Theta_dot ($\dot{\theta}$), which is a variable representing the velocity of the center of mass (m) from the vertical position, is set to an array of 2001 elements initialized to zero. Theta_dbl_dot ($\ddot{\theta}$) is set to an array of 2001 elements initialized to zero, and this variable represents the acceleration of the center of mass (m) of the inverted pendulum as it swings. The following expression was used:

$(\theta_1)$ *theta* (1) = 5 * (*pi* / 180) + *theta* (1)

which is where the initial conditions of theta are set; the theta (θ, angle) on the left side is the current value of theta (angle) and is set to 5 ° in terms of radians plus the value of the first element in the theta array, which is zero.

The next expression is:

$(\dot{\theta}_1)$ *theta_dot* (1) = 0 + *theta_dot* (1)

which is where the initial conditions of velocity theta_dot are set; the velocity (theta_dot) on the left-hand side is the current value of velocity and is set to 0 (rad $s^{-1}$) plus the value of the first element in the velocity array, which is zero. Thus, the programming loop can start calculating the value of theta (*θ*, angular displacement) with respect to time, θ(t). The counter-variable, n, was set to run from 2 to 2001 in steps of 1. The value of the current acceleration ($\ddot{\theta}_n$) theta_dbl_dot(n) is calculated by the following expression (as written in MATLAB):

$(\ddot{\theta}_n)$ *theta_dbl_dot* (*n*) = - (((*c* * ($l^2$)/2) * *theta_dot* (*n*-1)) + (((*k_value* * ($l^2$)/2) - (*m* * *g* * *l*)) * *theta* (*n*-1))) / (*m* * ($l^2$))

which comes from the rearranged differential equation of motion of the inverted pendulum as shown in Equation 3.

The theta_dot(n-1) is the value of the velocity ($\dot{\theta}_{n-1}$) from the previous step, and theta(n-1) is the value of the theta for angular displacement ($\theta_{n-1}$) from the previous step. The proposed equation assumes small angles (*θ*) (i.e., theta is varied between +5 and -5 °), so the system's equation is linear. The expression used to calculate the current value of velocity ($\dot{\theta}_n$) *theta_dot*(*n*) as written in MATLAB is: *theta_dot*(*n*) = *theta_dot*(*n*-1) + *theta_dbl_dot*(*n*) * *dt*, where *theta_dot*(*n*-1) is the value of the velocity from the previous step plus the current value of acceleration multiplied by the time step.

The expression used to calculate the current angular displacement ($\theta_n$) theta($n$) as written in MATLAB is:

*theta*($n$) = *theta*($n$-1) + *theta_dot*($n$) * *dt*,

where theta(n-1) is the value of the pendulum's swing angle from the previous step plus the value of the current velocity multiplied by the time step. This is so the programming loop ends and the angle's theta ($\theta$) is converted back to degrees. A plot of theta (angular displacement, $\theta$) versus time is established with the time as the horizontal axis and the theta ($\theta$, angular displacement) as the vertical axis. The boundaries of the plot are set as follows: the horizontal axis is set between 0 and 10 s and the vertical axis is set between -15 and 15 °. Finally, the simulation can be terminated by writing "End", and the inverted pendulum simulation ends.

**The aircraft wing simulation process**

In MATLAB, if the user selects Choice 2, the user wants to run the aircraft wing simulation, the aircraft wing simulation starts immediately. Several variables are initiated: the system's mass (m) is set to 500 kg, the spring's stiffness (k) is set to $1\times10^7$ N m$^{-1}$, and the aerodynamic effect on the system (i.e., gamma ($\gamma$)) is set to $1\times10^4$ N s m$^{-1}$. The damping coefficient at the limit of stability (c_lim) is set to equal to the value of gamma ($\gamma$), the calculated value of c_lim is then displayed in N s m$^{-1}$. The user is then asked to enter the desired multiplier value for the damping coefficient at the limit of stability (c_lim). The final value for the damping coefficient at the limit of stability is then set to c_value and is equal to the damping multiplier (c_multiplier) multiplied by the c_lim. The final calculated value of c_value (damping coefficient) is displayed in N s m$^{-1}$. The time step ($dt$) is set to 0.002 s and the time is initially set to be between 0 and 2500 step sizes, or 5 s. The displacement ($x$), velocity x_dot ($\dot{x}$), and acceleration x_dbl_dot ($\ddot{x}$) are each set to an array of 2501 elements initialized at zero.

The expression ($x_1$), $x(1) = 1 + x(1)$ is where the initial conditions of the displacement ($x$) are set, where the x on the left side is the current value of x and is set to 1 mm plus the value of the first element in the x array, which is zero. The next expression as written in MATLAB is ($\dot{x}_1$), $x\_dot(1) = 0 + x\_dot(1)$, which is where the initial conditions of the velocity $\dot{x}$ (x_dot) are set; the x_dot on the left-hand side is the current value of x_dot and is set to 0 mms$^{-1}$ plus the value of the first element in the x_dot array, which is zero. Thus, the programming loop can be started to calculate the value of the displacement ($x$) with respect to time, $x(t)$. The counter-variable, n, is set to run from 2 to 2501 in steps of 1.

The mathematical expression used to calculate the acceleration ($\ddot{x}$), x_dbl_dot, as written in MATLAB is:

*x_dbl_dot* ($n$) = - (((*c_value - gamma)* * (*x_dot* ($n$-1)) + ((*k*) * *x* ($n$ - 1))) / *m*)

which is derived from the rearranged equation of motion of the aircraft wing (Equation 2). The expression used to calculate the current value of velocity ($\dot{x}_n$ ), x_dot(n), as written in MATLAB is:

$$x\_dot\ (n) = x\_dot\ (n\text{-}1) + x\_dbl\_dot\ (n) * dt$$

where ($\dot{x}_{n\text{-}1}$) x_dot(n-1) is the value of velocity from the previous step plus the current value of acceleration multiplied by the time step. Likewise, the expression used to calculate the current value of displacement, x(n) as written in MATLAB is:

$$x(n) = x\ (n\text{-}1) + x\_dot\ (n) * dt$$

where $x(n\text{-}1)$ is the value of displacement from the previous step plus the current value of velocity multiplied by the time step. The loop of the programming circuit ends, and the plot of displacement x versus time is established. The boundaries of the plot are set as follows: the horizontal axis limit is set between 0 and 5 s and the vertical axis limit is set between -5 and +5 mm. Finally, the simulation can be terminated by writing "End", so the aircraft wing simulator ends.

## RESULTS AND DISCUSSION

To clarify the performance of the proposed inverted pendulum, a numerical simulation was carried out using MATLAB software based on the physical parameters of the pendulum system, which were set. In the inverted pendulum simulation system, the initial results found the spring's stiffness at the limit of stability $k_{lim}$ = 32.69 N $m^{-1}$, then the time-domain simulation was programmed to determine the angular displacement (rotation ($\theta$)) as a function of time.

Before running the time domain simulations for the two systems, the limiting coefficients of the springs and viscous dampers of the two systems (spring's stiffness $k_{lim}$ and damping coefficient $c_{lim}$) need to be manually calculated. The limiting factor for the inverted pendulum was considered to be the spring's stiffness at the limit of stability, $k_{lim}$. The calculation was as follows:

$$k\left(\frac{2mg}{l}\right)\text{lim} = k\left(\frac{2(0.5\ kg)\ (9.807\ ms^{-2}}{0.3\ m}\right)\text{lim} = 32.69\ N\ m^{-1}$$

When the value of $k_{lim}$ (32.69 N $m^{-1}$) was used, the time-domain simulation for the inverted pendulum could be run for various values of stiffness (k) to obtain the rotation angle ($\theta$). An inverted pendulum with an affected force (mechanical energy) has an initial position of theta > 0 ° at t = 0 s (Figure 2).

The behavior of an inverted pendulum (Figures 2-4) showed its response is evident at different values of stiffness ($k_{lim}$) when the simulation was run at 0.1, 0.5, 0.9, 0.99, 1, 5, and 10 $k_{lim}$. The angular displacement of the moving inverted pendulum mass

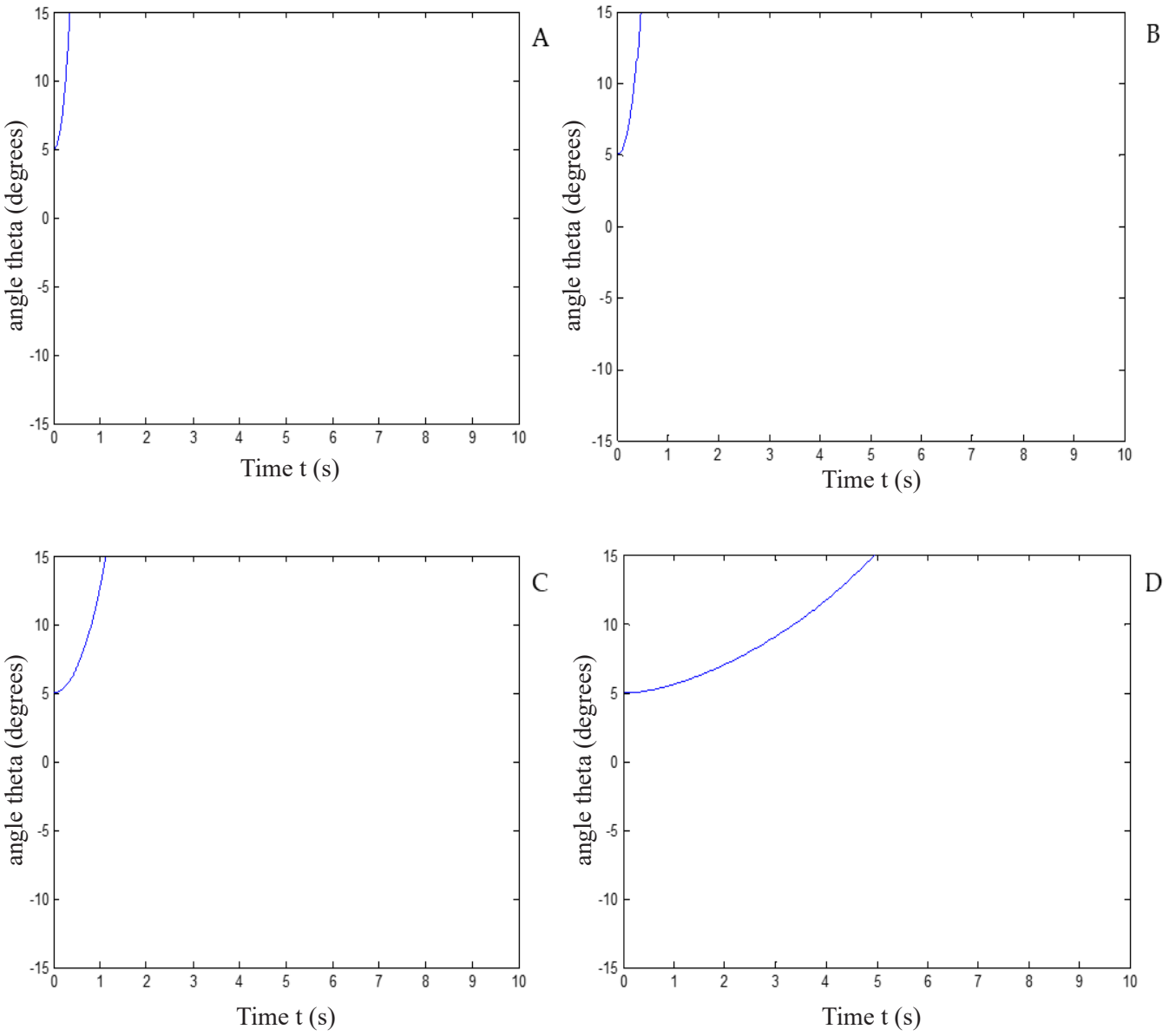


**Figure 2.** Angular displacement θ, with rotation at different levels of spring's stiffness $k_{lim}$ (nonideal step response). A: rotation at 0.1 $k_{lim}$; B: rotation at 0.5 $k_{lim}$; C: rotation at 0.9 $k_{lim}$; D: rotation at 0.99 $k_{lim}$.

was considered to be a function of time. The response of the pendulum model (Figure 2) clearly depicts the instability of the system with different levels of stiffness ($k_{lim}$), namely 0.1, 0.5, 0.9, and 0.99 $k_{lim}$. With the proper optimal spring stiffness (k), the system's state stabilized within a few seconds. The same responses were studied with different initial conditions (0.087 rad (≈ 0.1 rad) for angle) (Figures 2 and 3). Further

simulations were run with a step disturbance (Figure 4), and the proposed optimal controller was able to stabilize the system successfully.

As seen in the figures, the function describing the rotation angle varied greatly when the value of k was changed. Unfortunately, for values of k less than $k_{lim}$, the system displayed divergent instability and immediately deviated sharply from the mean without stabilizing. In the model, this would represent the case where the inverted pendulum moved all the way to one side and stayed there without being able to stabilize itself about the mean angle.

The output of the pendulum's vibration was where the system was able to stabilize the pendulum in 7 s (Figure 4B). The swinging stabilization system had a number of decreasing swings before the pendulum reached a vertical position. The angular displacement of the pendulum deviated to a maximum of 5 ° when the vibration was introduced, but the swinging stabilization system was able to reduce the oscillation in less than 8 s, which made the pendulum maintain its upright position. For values of k greater than $k_{lim}$, the system displayed asymptotic stability. The rotation angle approached an equilibrium position of $\theta$ = 0 °, with the magnitude of vibrations decreasing over time. This means that the pendulum could reach the vertical position ($\theta$ = 0 °); however, with parameters set (at the ideal step response of 10 $k_{lim}$), the time the system takes to reach stability is important (in 7 s).

In the particular case where the stiffness was equal to the limiting stiffness ($k = k_{lim}$), the system displayed stable behavior. The rotation angle in this case remained at the initial value without deviation over time. This could be seen when $k_{lim}$ was entered as the value of k in the original differential equation (with an initial displacement ($\theta$) of 5 ° and an initial velocity ($\dot{\theta}$) of zero), as in the following formulae:

$$k = k\left(\frac{2mg}{l}\right)\lim$$

$$ml^2\ddot{\theta} + \frac{cl^2}{2}\dot{\theta} + \left(\frac{kl^2}{2} - mgl\right)\theta = 0$$

$$ml^2\ddot{\theta} + \frac{cl^2}{2}\dot{\theta} + \left(\frac{\frac{2mg}{l}l^2}{2} - (mgl)\right)\theta = 0$$

$$ml^2\ddot{\theta} + \frac{cl^2}{2}\dot{\theta} + (0)\theta = 0$$

$$ml^2\ddot{\theta} + \frac{cl^2}{2}(0) + (0)(5°) = 0$$

$$ml^2\ddot{\theta} = 0$$

$$So, \ddot{\theta} = 0$$

In this case, no vibratory motion occurred, and the system remained at the initial displacement angle. This makes sense because of the small angle assumption made at the start of the process (Sin (0) ≈ 0 and Cos (0) ≈ 1). In general, the figures illustrate that the angle and position of the pendulum system can provide an acceptable response since the initial condition of $\theta$ = 5 ° was not large. The initial displacement angle at time $t$ = 0 s for this system was 5 °. The pendulum's response shows that for a unit step actuated by a force, the system was unstable, and a settling time of 7 s was achieved

by increasing the value of the spring's stiffness, k. In the beginning, with a small value of stiffness k, there was a small amount of oscillation, but it took an unacceptably long time to reach the steady state. The result of theta rotation ($\theta$) versus time (t) at different levels of limiting the spring's stiffness (5 and 10 $k_{lim}$) is shown (Figure 4). It is clear that for 10 $k_{lim}$, the pendulum's position became almost stable in a short settling time (7 s). In addition, for the second system, to clarify the performance of the proposed simple aircraft wing subject to aerodynamic forces, a numerical simulation was carried out using MATLAB software based on the parameters of the wing system that were set. Furthermore, as shown in the simulation figures, the displacement of the moving system's mass was considered to be a function of time. For the system analysis, in the case of self-excited vibration (flutter), the factor limiting the motion was the damping coefficient at the limit of stability ($c_{lim}$). This is because the aerodynamic forces on the wing are velocity-dependent (similar to the damping force), feeding back into the differential equation of motion and thus affecting the stability of the system.

The limit of stability occurs when the damping ratio ($\zeta$, dimensionless) reaches zero ($\zeta = 0$), meaning the damping coefficient at the limit of stability ($c_{lim}$) can be calculated as follows:

$$\zeta = \frac{(c - \gamma)}{2\sqrt{km}} = 0$$

$$c_{\lim} = \gamma$$

$$S_o,\ c_{\lim} = 1 \times 10^4\ N\ s\ m^{-1}$$

Using this value for $c_{lim}$ (10 000 N s $m^{-1}$), the simulation for the aircraft wing was run for various values of the damping coefficient (c) to determine the wing's position (displacement x) as a function of time (t) and implemented by using the Euler Method. Therefore, the simulation's output results for different values of the damping coefficient (c), namely 0.5, 0.9, 0.99, 1, 1.1, and 2 $c_{lim}$, show the displacement response of the moving system's mass (x) versus time (t) (Figure 5).

The model's response shows that for the 0.5 and 0.9 $c_{lim}$ damping coefficients, the instability of the system showed a clear periodic oscillation (Figure 5). Moreover, the displacement amplitude of the system's oscillations and the period of oscillations increased with time. Furthermore, a negative dynamic stability (dynamically unstable, with divergent oscillation) at damping coefficients at limits of stability ($c_{lim}$) of 0.5, 0.9, and 0.99 $c_{lim}$ (i.e., the disturbance caused a magnification of the amplitude over time) was found (Figures 5A, 5B, and 5C). An undamped oscillation (a neutral dynamic system) was obtained at 1 $c_{lim}$ (Figure 5D). The results also show that as the damping coefficient increased with time, the displacement amplitude of the oscillations decreased, but the period of the oscillations was still at the increasing limit (Figures 5A–5D). The system was under damped oscillation (dynamically stable, called a positive dynamic system in a stable equilibrium position) when the damping coefficient at the limit of stability ($c_{lim}$) was 1.1 and 2 $c_{lim}$ (Figures 5E and 5F). In general, as only applied

to this study, for the flight of an aircraft to be stable, the results of the oscillation must be damped immediately, and this can be achieved by increasing the value of the damping coefficient (c).

Moreover, as seen from the simulation figures, the stability of the aircraft wing was dramatically affected by changes in the damping coefficient (which relate to a change in the damping ratio ζ of the system). For values of c less than $c_{lim}$, the damping ratio, ζ, will be negative. In these cases, the system will be unstable and will show an exponential rise due to underdamping (i.e., disturbance over time). This can be seen in the first four cases (Figures 5A–5D), where the damping coefficient (c) was less than the damping coefficient at the limit of stability ($c_{lim}$). However, for the cases where c was greater than $c_{lim}$, the system (Figures 5E and 5F) exhibited stable behavior (or asymptotically stable behavior, as ζ < 1 for the given cases). The displacement rapidly approached the equilibrium position of 0 mm as time (t) increased. In addition, in the particular case where c = $c_{lim}$ (Figure 5E), the airplane wing displays what is known as marginal stability (in 3.5 s). This is because the damping ratio ζ of the system was equal to zero, as shown by:

$$c = c_{\text{lim}} = \gamma$$
$$\zeta = \frac{(c - \gamma)}{2\sqrt{km}} = \frac{(\gamma - \gamma)}{2\sqrt{km}} = 0$$
$$S_o, \zeta = 0$$

According to this result, if the damping ratio (ζ) is equal to zero, the system will vibrate consistently at its natural frequency of oscillation ($w_n$), i.e., for a zero-damping effect, it will never deviate so drastically as to become unstable, but it will never stabilize at a final value. Significantly, one can observe in the figures that the displacement of the moving system mass and the position of the aircraft wing system as simulated in the MATLAB experiment showed a satisfactory response.

For the inverted pendulum (Figures 2–4), the critical angular displacement (θ) versus time (t) measured by simulation of the pendulum's vibration for different levels of the spring's stiffness $k_{lim}$, demonstrated that the system contained the positive characteristics of the equation of motion and that its step response to the inputs could also increase to infinity (i.e., an unbounded response), and thus the angle θ could increase infinitely (Figure 2). In this case, the $k_{lim}$ command can be utilized to simulate the response of the angular displacement $\theta$ of the pendulum model to random inputs. The result confirmed that the response of the pendulum system to a step input with slow oscillation was unstable around the vertical position (Monir, 2018); however, the pendulum could become stable in its inverted position (i.e., the inverted pendulum can eventually reach the vertical equilibrium position) if the pendulum oscillates at a constant velocity, or the inverted pendulum will stabilize at an angle (the stability angle of the inverted position). It can be seen that the pendulum swung until it settled at $\theta$ = 5 ° (the angle of stability) (Figure 3). Additionally, the pendulum remained in

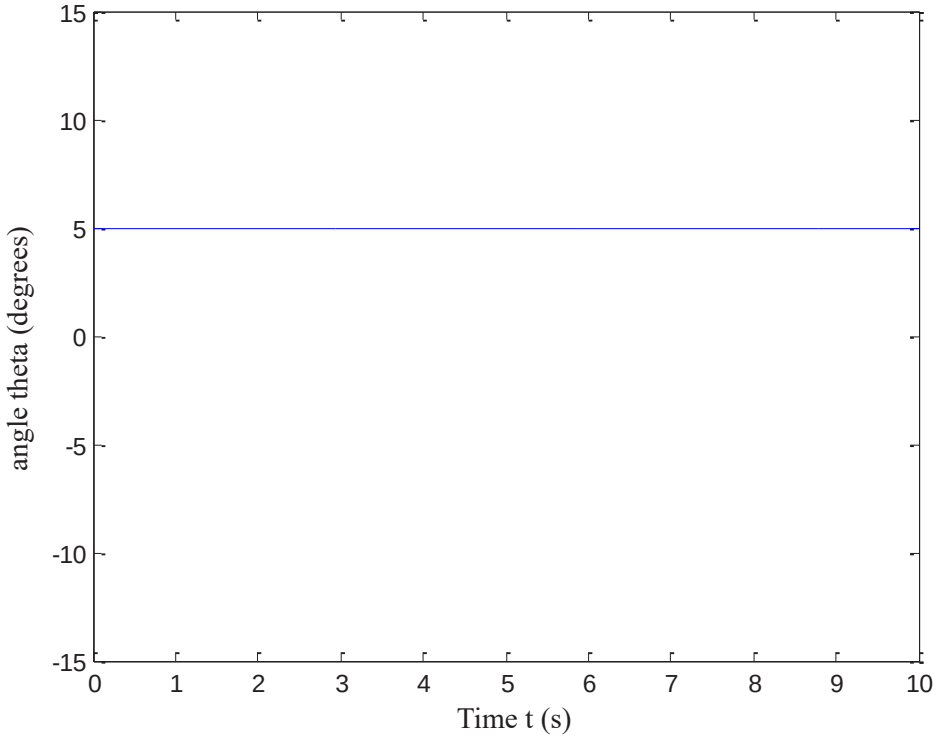


**Figure 3.** Angular displacement $\theta$, with rotation at spring's stiffness 1 $k_{lim}$ (neutral position).

an upright position with rapid oscillation, and the pendulum's oscillation around the vertical position remained small. Thus, with fast oscillation, in which the initial oscillation amplitude of the inverted pendulum was 5 °, the pendulum could be kept stable around its vertical position (Figures 4A and 4B), and the pendulum swung at θ = 5 ° until it settled at $\theta$ = 0 ° in 7 s.

Over time, the angular amplitude of the oscillations decreased, but the period of the oscillations was still at the increasing limit (Figure 4A). Fluttering was dampened in about 7 s (Figure 4B), when the value of the spring's stiffness was about 10 $k_{lim}$. In general, the results show that the inverted pendulum can be kept vertical within 5 ° when controlled by using different spring displacements k, and that when the pendulum is in the vertical position ($\theta$ = 0 °), the springs do not extend. In these figures, it is obvious that the amplitude of vibration decayed over time. The simulation results demonstrated that the lateral angular (angular rotation) response of the inverted pendulum, which showed a normal vibration with different values of the spring coefficient (k), had a very small settling time with increased spring coefficient (k) values, which efficiently brought the pendulum to the inverted position (i.e., upswing). The method of analyzing the aerodynamics that affect the aircraft can be used to analyze the stability and flight control of UAVs. This can be accomplished by comparing

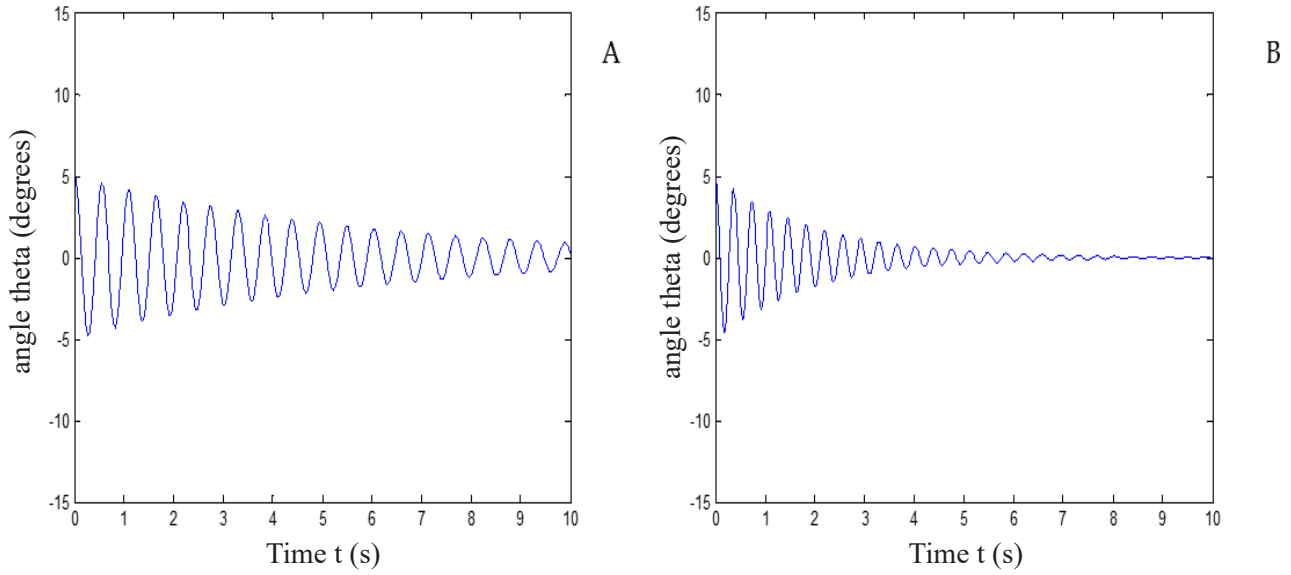


**Figure 4.** Angular displacement $\theta$, with rotation at different levels of spring's stiffness $k_{lim}$ (ideal step response). A: rotation at 5 $k_{lim}$; B: rotation at 10 $k_{lim}$.

the stability of an inverted pendulum system to the wings of an uncrewed aircraft. Accordingly, there are some noticeable aerodynamic forces that affect a UAVs' flight: thrust, drag, lift, weight, and the coefficients of pitch moment and attack angle (FAA, 2016). Furthermore, from the perspective of an aircraft wing subject to aerodynamic forces, the displacement of the moving system's mass (mm) versus time (seconds) when the simulated values of the damping coefficient c increased, namely 0.5, 0.9, 0.99, 1, 1.1, and 2 $c_{lim}$, reflected a stable system (Figures 5A–5F).

For the aircraft wing (Figure 5), the initial displacement at time t = 0 s for this system was 1 mm. The initial displacement response of the moving system's mass (x) varied between +5 and -5 mm at the lowest damping coefficients (c) at the limit of stability. With increasingly higher coefficients, the displacement decreased to the initial displacement limit between +1 and -1 mm. The time-domain responses in displacement of the moving system's mass for the two highest values of the damping coefficient c (the damping coefficient at the limit of stability), namely 1.1 and 2 $c_{lim}$, showed the minimum amplitude of the mass displacement of this system and the least time required for the system to reach stability (Figures 5E and 5F). This illustrated greater responsiveness to relatively rapid changes in state and thus represented the most efficient flight path.

In addition, the results showed that with time, the displacement amplitude of the oscillations decreased and the period of the oscillations also decreased (Figures 5E and 5F). Therefore, to stabilize the flight, the oscillation was completely damped after a certain time period. Finally, the originally proposed equivalent viscous damping ratio

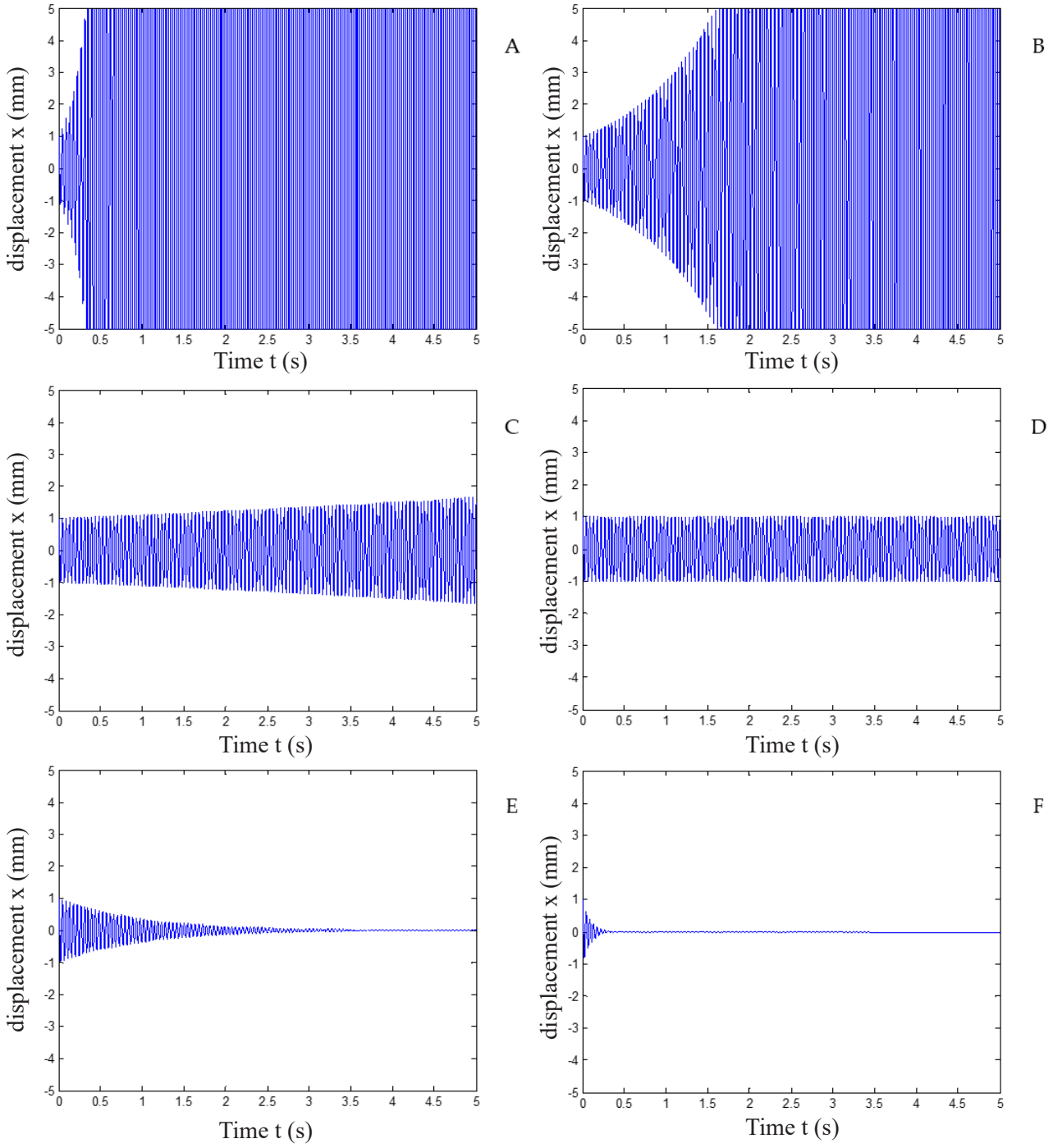


**Figure 5.** Displacement response of the moving system's mass at different values of damping coefficient $c_{lim}$. A: response at 0.5 $c_{lim}$; B: response at 0.9 $c_{lim}$; C: response at 0.99 $c_{lim}$; D: response at 1 $c_{lim}$; E: response at 1.1 $c_{lim}$; F: response at 2 $c_{lim}$.

was 0 % ($\zeta < 1$), with the displacement amplitude ranging from less than 1 to 5 mm, according to the Euler method. The time taken to reduce the displacement amplitude from 5 mm to less than 1 mm was reduced from about 5 s to 400 ms. The results show that a damping coefficient of more than 10,000 N s $m^{-1}$ was more effective. The aircraft took a very short time to return to its reference condition and was kept at a certain rotation angle (i.e., the aircraft took off in an accurate and stable position).

This system gave an actual time response with a relatively small magnitude of oscillation, since the figures clearly show that the amplitude of oscillation decayed over time more quickly, thus achieving the objective of designing effective aircraft wings. There was only a small degree of oscillation for 400 ms (Figure 5F). For a system controlled by the damping coefficient, the system's model is more responsive to relatively fast alterations in its state induced by aerodynamic forces, and so the model of a dynamic system will therefore be faster to reach a steady-state position and to respond to disturbances than a system with a poorly-tuned damping coefficient or one in which the dynamic system has not achieved damping control. In addition, these results also show that the flight instability of UAV aircraft during the turbulence associated with takeoff and the subsequently delayed flight stability were more pronounced than that of flight at higher airspeeds, and significant stability disturbances could be caused by the action of small external forces on the aircraft's propellers or the aircraft itself. Inefficiencies in the flight control systems can also be a problem for stable operations.

Recently, UAVs have been widely applied in agriculture, especially for operations in precision agriculture (PA) (Radoglou-Grammatikis *et al.*, 2020; Wang *et al.*, 2021), which require a highly efficient aircraft control system. Therefore, modern automated control systems have been applied in many areas, but are of particular importance in flight operations. The elements of the control system need to be clearly understood, and the basic concepts of controllers need to be developed to maintain stability while reacting to external forces, such as unexpected vibration on the uncrewed aircraft's structure or the multirotor aircraft arms (rotary wings) that operate almost autonomously, which may indicate the presence of external noise entering the UAV's control systems, typically caused by sequential excitation of aerodynamic or atmospheric air turbulence (i.e., external sources) (Al-Mashhadani, 2018, 2019; Ghazali and Rahiman, 2022).

## CONCLUSIONS

This research indicated that for the establishment of flight stability, the first dynamic moments of flight in an uncrewed aerial vehicle (UAV) and its response to any surrounding disturbances are the most significant. The findings from the simulation of the inverted pendulum showed that as the value of the spring's stiffness at the limit of stability, $k_{lim}$, increased, the system became more convergent and, as a result, more stable. The system vibrated consistently at its natural frequency ($w_n$), never deviating drastically to become unstable, but also never stabilizing at a final value. The simulated inverted pendulum's displacement versus time showed that the inverted pendulum could become stable despite the slightly periodic oscillation with an increase in the

value of the spring coefficient. The aircraft system displayed stable behavior with an increase in the value of the damping coefficient. The displacement amplitude of the system's oscillations, as well as the period of the oscillations, increased with time when the damping coefficient was below a certain value. These results would significantly help in creating a clear and understandable path for improving the implementation of UAVs in agricultural field operations, especially with an additional payload, which may affect the center of gravity of the UAV and its flight stability.

## ACKNOWLEDGEMENTS

The authors of this study would like to express their appreciation to the University of Florida, and the Deanship of Scientific Research, Researchers Support Services Unit, Agriculture Research Center, and College of Food and Agriculture Sciences at the King Saud University for their support and encouragement.

## REFERENCES

Al-Mashhadani MA. 2018. Random vibrations in unmanned aerial vehicles, mathematical analysis and control based on expectation and probability. Journal of Low Frequency Noise, Vibration and Active Control 38 (1): 143–153. https://doi.org/10.1177/1461348418813031

Al-Mashhadani MA. 2019. Optimal control and state estimation for unmanned aerial vehicle under random vibration and uncertainty. Measurement and Control 52 (9–10): 1264–1271. https://doi.org/10.1177/0020294019866860

Bietresato M, Mazzetto F. 2019. Definition of the layout for a new facility to test the static and dynamic stability of agricultural vehicles operating on sloping grounds. Applied Sciences 9 (19): 4135. https://doi.org/10.3390/app9194135

Dolatabad MR, Pasharavesh A, Khayyat AAA. 2022. Analytical and experimental analyses of nonlinear vibrations in a rotary inverted pendulum. Nonlinear Dynamics 107 (3): 1887–1902. https://doi.org/10.1007/s11071-021-06969-0

Estevez J, Lopez-Guede JM, Garate G, Graña M. 2021. A hybrid control approach for the swing free transportation of a double pendulum with a quadrotor. Applied Sciences 11 (12): 5487. https://doi.org/10.3390/app11125487

FAA (Federal Aviation Administration). 2016. Pilot's handbook of aeronautical knowledge, Chapter 5: Aerodynamics of Flight. Oklahoma City, OK, USA. https://www.faa.gov/regulations_policies/handbooks_manuals/aviation/phak (Retrieved: June 2022).

Fabbri A, Molari G. 2004. Static measurement of the centre of gravity height on narrow-track agricultural tractors. Biosystems Engineering 87 (3): 299–304. https://doi.org/10.1016/j.biosystemseng.2003.12.008

Garcia-Nieto S, Velasco-Carrau J, Paredes-Valles F, Salcedo JV, Simarro R. 2019. Motion equations and attitude control in the vertical flight of a VTOL bi-rotor UAV. Electronics 8 (2): 208. https://doi.org/10.3390/electronics8020208

Gatto A. 2009. Application of a pendulum support test rig for aircraft stability derivative estimation. Journal of Aircraft 46 (3): 927–934. https://doi.org/10.2514/1.38916

Ghazali MHM, Rahiman W. 2022. Vibration-based fault detection in drone using artificial intelligence. IEEE Sensors Journal 22 (9): 8439–8448. https://doi.org/10.1109/jsen.2022.3163401

Gunawan WW, Likafia A, Joelianto E, Widyotriatmo A. 2018. Inverted pendulum stabilization with flying quadrotor. Internetworking Indonesia Journal 10 (2): 29–35.

Hanada H, Asari K, Tsuruta S, Araki H, Funazaki K, Satoh A, Taniguchi H, Kikuchi M. 2019. Experiments of inverted pendulum as a vertical reference of a telescope. Journal of Physics: Conference Series 1301 (1): 012013. https://doi.org/10.1088/1742-6596/1301/1/012013

Jibril M, Tadese M, Tadese EA. 2021. Stability control of a rotational inverted pendulum using augmentations with weighting functions based robust control system. Researcher 13 (1): 17–21. https://doi.org/10.7537/marsrsj130121.03

Kelly SG. 2012. Mechanical vibrations: Theory and applications. Cengage Learning: Stamford, CT, USA. 898 p.

Khorsandi F, Ayers PD, Freeland RS, Wang X. 2018. Modeling the effect of liquid movement on the center of gravity calculation of agricultural vehicles. Journal of Terramechanics 75: 37–48. https://doi.org/10.1016/j.jterra.2017.09.005

Li L, Xie Z, Luo X, Li J. 2021. Trajectory planning of flexible walking for biped robots using linear inverted pendulum model and linear pendulum model. Sensors 21 (4): 1082. https://doi.org/10.3390/s21041082

The MathWorks Inc. 2022a. MATLAB version: 9.13.0 (R2022b). The MathWorks Inc. Natick, MA, USA. https://www.mathworks.com

The MathWorks Inc. 2022b. Help center: Simulate the motion of the periodic swing of a pendulum. The MathWorks Inc. Natick, MA, USA. https://www.mathworks.com

Monir M. 2018. Analyzing and designing control system for an inverted pendulum on a cart. European Scientific Journal 14 (6): 387–398. https://doi.org/10.19044/esj.2018.v14n6p387

Radoglou-Grammatikis P, Sarigiannidis P, Lagkas T, Moscholios I. 2020. A compilation of UAV applications for precision agriculture. Computer Netwworks 172: 107148. https://doi.org/10.1016/j.comnet.2020.107148

Russell DA. 2018. Acoustics and vibration animations: Oscillation of a simple pendulum. The Pennsylvania State University: University Park, PA, USA. https://www.acs.psu.edu/drussell/Demos/Pendulum/Pendulum.html (Retrieved: June, 2022).

Sharma S, Sharma R, Kumar V, Chandel S. 2021. Analysis of a tiltrotor vertical take-off and landing unmanned aerial vehicle: CFD approach. IOP conference series: Materials Science and Engineering 1116 (1): 012096. https://doi.org/10.1088/1757-899x/1116/1/012096

Sowjanya R, Ramesh G. 2015. Design of optimal controller for double inverted pendulum. International Journal of Emerging Engineering Science and Technology 1 (5): 261–265.

Tulapurkara EG. 2012. Flight dynamics II - Airplane stability and control, IIT Madras. National Programme on Technology Enhanced Learning: Chennai, India. https://nptel.ac.in/courses/101106043 (Retrieved: July, 2022).

University of Michigan. 1997. Control tutorials for matlab. Ann Arbor, MI, USA. https://www3.diism.unisi.it/~control/ctm/examples/pend/invSS.html (Retrieved: July, 2022).

Wang X, Zhang X, Gong H, Jiang J, Rai HM. 2021. A flight control method for unmanned aerial vehicles based on vibration suppression. IET Collaborative Intelligent Manufacturing 3 (3): 252–261. https://doi.org/10.1049/cim2.12027

Agrociencia

# ASSESSMENT OF THE GENETIC DIVERSITY OF NEW SUGARCANE HYBRIDS USING PRINCIPAL COMPONENT AND CLUSTER ANALYSES

Gustavo **Ramírez-Madero**[1], Fernando Carlos **Gómez-Merino**[1,2], Jericó Jabín **Bello-Bello**[3], Libia Iris **Trejo-Téllez**[2], Juan Valente **Hidalgo-Contreras**[1*]

[1] Colegio de Postgraduados Campus Córdoba. Carretera Córdoba-Veracruz km 348, Manuel León, Amatlán de los Reyes, Veracruz, Mexico. C. P. 94953.
[2] Colegio de Postgraduados Campus Montecillo. Carretera México-Texcoco km 36.5, Montecillo, Texcoco, State of Mexico, Mexico. C. P. 56264.
[3] CONACYT-Colegio de Postgraduados Campus Córdoba. Carretera Córdoba-Veracruz km 348, Manuel León, Amatlán de los Reyes, Veracruz, Mexico. C. P. 94953.
* Author for correspondence: jvhidalgo@colpos.mx

**Citation:** Ramírez-Madero G, Gómez-Merino FC, Bello-Bello JJ, Trejo-Téllez LI, Hidalgo-Contreras JV. 2023. Assessment of the genetic diversity of new sugarcane hybrids using principal component and cluster analyses. **Agrociencia** 57(8): 1682-1695. doi.org/ 10.47163/agrociencia.v57i8.2847

**Editor in Chief:**
Dr. Fernando C. Gómez Merino

Received: July 14, 2022.
Approved: September 11, 2022.
**Published in Agrociencia:** October 26, 2023.



## ABSTRACT

With a cultivated area of approximately 800 thousand hectares distributed in 15 states, sugarcane (*Saccharum* spp.) is one of the main crops in Mexico. Despite its socioeconomic importance, the genetic base of this crop has been reduced in recent decades, making the production system vulnerable to both biotic and abiotic stresses. For this reason, the Colegio de Postgraduados Campus Córdoba initiated a varietal selection program in 2009. In this study, morphological and agronomic attributes of 20 advanced hybrids were analyzed during the 2020-2021 and 2021-2022 growing seasons to determine genetic variability based on principal component analysis (PCA) and cluster analysis. Commercial cultivars widely planted in the area of influence of the Córdoba Campus (CP 72-2086, Mex 79-431, Mex 69-290 and Mex 05-204) were used as reference samples. In terms of agronomic indicators, most of the new hybrids showed higher averages than the commercial control cultivars. The hybrids COLPOSCCMex 09-50 and COLPOSCCMex 09-66 showed better germination capacity. The average height of the tallest milling stems was presented by the hybrids COLPOSCCMex 09-341 (318.1 cm) and COLPOSCCMex 09-93 (311.85 cm). The hybrid COLPOSCCMex 09-289 showed outstanding values for five variables: diameter (36.43 mm), °Brix (21.89 %), stem height (149.33 cm), leaf width (5.36 cm) and number of leaves (11.15). Morphological characterization was carried out according to 54 descriptors, combining categorical and continuous traits that were easy to observe, with a high degree of differentiation and low environmental influence. Principal component and cluster analyses showed the distribution of hybrids into five groups. These results show promising sugarcane lines with high yields, which can contribute to genetic diversity in agroecological zones where they can be adapted.

**Keywords:** Poaceae, genetic variability, promising lines, descriptors, agroecological zones.

## INTRODUCTION

Sugarcane (*Saccharum* spp.) is the largest plant source of table sugar and one of the most important crops for the generation of green energy worldwide. Currently, 80 % of the sugar consumed in the world comes from this grass (FAO, 2023). The sugar industry has positioned itself as one of Mexico's main economic activities, generating income through agricultural, processing and marketing activities. The total area of Mexico is 198 million hectares, of which only 27.5 million hectares are used for agriculture (INEGI, 2014; Torres-Torres and Rojas-Martínez, 2018). Of these, about 800,000 hectares are planted with sugarcane annually (CONADESUCA, 2021).

Increasing agricultural productivity in the sugar industry has become more important in recent years, aiming for a more competitive level in global markets. In the 2020-2021 growing season, the national average yield was 64.92 Mg $ha^{-1}$, which was considered low compared to previous harvests. The highest national yield was recorded in the 2012-2013 harvest, with a value that reached 78.74 Mg $ha^{-1}$ (CONADESUCA, 2021). These variations are closely related to the need for innovation in sugarcane production, since adaptation to climate change, efficient use of water, fertilizers, biofertilizers and manures, resistance and tolerance to biotic and abiotic stress factors, increased yields and the generation of cultivars for different uses are among the main demands to be considered to improve the primary sector of this agribusiness (Gómez-Merino *et al*., 2014; 2017).

With respect to genetic variability, the sugar industry in Mexico mainly relies on four commercial cultivars: CP 72-2086, Mex 69-290, Mex 79-431 and ITV 92-1424, with percentages of land planted of 31, 26, 8 and 6 %, respectively (CONADESUCA, 2016). This highlights the need to increase the genetic base of the crop, as it is exposed to the severe effects of climate change and the attack of new pests and diseases. Prioritizing the main problems of the sugar industry in Mexico, in 2009 the Colegio de Postgraduados implemented a program for the selection and exchange of sugarcane cultivars (Lavín-Castañeda *et al*., 2020). The main objective of this program has been to increase the productivity and profitability of the sugar agroindustry through the selection of new outstanding sugarcane genotypes. Among other elements requiring improvement, there is a need for a greater ability to adapt to the different agroecological zones where sugarcane is grown in Mexico, higher sucrose yields than current commercial cultivars, greater resistance to pests and diseases, and agronomic characteristics that facilitate its cultivation and management.

The correct selection of a new genotype to be planted in one of Mexico's six agroecological zones is a fundamental requirement to exploit its maximum productivity. This is why the analysis of genetic diversity has become one of the main tools for studying the relationships that exist among sugarcane genotypes. Biotechnology has provided breeders with a large number of DNA-based markers to analyze the genetic diversity of sugarcane (Junior *et al*., 2020; Emegha *et al*., 2021). Phenotypic traits to estimate this type of diversity are now widely used because, compared to molecular markers, they are simple, easy to identify and collect, inexpensive, effective and practical (Wu *et al*., 2021).

Among the different characteristics that define a genotype, morphological, agronomic and agro-industrial traits are used to identify a new sugarcane cultivar. Several statistical approaches are used to study genetic diversity, depending on the amount and nature of data collected. Multivariate data analysis techniques and the use of morphological data are frequently employed for the understanding of genetic diversity. Cluster analysis and principal component analysis (PCA) use agronomic and quality characteristics to investigate the nature of genetic divergence among different genotypes (Seema *et al*., 2017). These analyses also help to quantify the variability available in the gene pool, as well as to identify groups of genetically similar or different plants (Baloch *et al*., 2017).

The objective of this study was to analyze the genetic diversity of a group of 20 hybrids in advanced selection processes and four commercial cultivars (controls) based on analysis of variance (ANOVA), multivariate cluster analysis and principal component analysis of morphological and agronomic variables. The multivariate analysis was based on the clustering technique to form groups of observations (hybrids) with common characteristics through Euclidean distance. On the other hand, the principal component analysis showed the formation of small groups of uncorrelated variables (morphological and agronomic) that can facilitate the interpretation of the genetic diversity of the hybrids through small groups based on the original variables.

## MATERIALS AND METHODS

### Plant material and experimental design

The study involved 20 new sugarcane hybrids (Table 1) selected on the basis of their performance during previous phases, compared to three control cultivars with the largest area planted in Mexico: CP 72-2086 of early maturity, Mex 79-431 of intermediate maturity and Mex 69-290 of late maturity. As an additional control, an outstanding cultivar selected by the Colegio de Postgraduados Campus Tabasco was evaluated: COLPOSCTMEX 05-204 (Mex 05-204), also early maturing.

Genotypes were evaluated in experimental plots at the Colegio de Postgraduados Campus Córdoba, located in the municipality of Amatlán de los Reyes, Veracruz, Mexico (18° 51′ N, 96° 51′ E; 650 m elevation), during the 2020-2021 and 2021-2022 growing seasons. The climate of the area is tropical humid, with rainfall in summer and an average annual temperature of 20 °C, a maximum temperature of 35 °C and a minimum of 10 °C. Average annual precipitation is 1807 mm (Soto-Esparza and García, 1989). The main soil types of this experimental center are vertisols and feozems (CONABIO, 2011).

The 24 genotypes (20 hybrids and four commercial controls) were planted in a randomized block design in plots with dimensions of 6 m long x 6 m wide and 2 m between each plot, with 1.2 m row spacing. For the characterization of the genotypes, nine traits of interest were recorded 2 m linearly from the center of each plot: stem height (cm); stem diameter (mm); leaf number, length (cm) and width (cm); SPAD indirect chlorophyll index (ICC); °Brix and sprouting of the sown buds (%). The entries

**Table 1.** Sugarcane genotypes (*Saccharum* spp.) evaluated during the Semi-commercial Stage of the genetic improvement program of the Colegio de Postgraduados Campus Córdoba.

| No. | Cross | Parents | | | Genotype |
|---|---|---|---|---|---|
| | | Female | | Male | |
| 01 | 222 | LCP 81-10 | × | Gloria 57 | COLPOSCCMex 09-29 |
| 02 | 255 | CP 52-68 | × | CP 70-1527 | COLPOSCCMex 09-50 |
| 03 | 257 | CP 92-1401 | × | CP 81-1384 | COLPOSCCMex 09-66 |
| 04 | 258 | CP 81-10 | × | CP 70-133 | COLPOSCCMex 09-93 |
| 05 | 258 | CP 81-10 | × | CP 70-133 | COLPOSCCMex 09-95 |
| 06 | 264 | Tue 72-9 | × | CP 80-1827 | COLPOSCCMex 09-97 |
| 07 | 264 | Tue 72-9 | × | CP 80-1827 | COLPOSCCMex 09-125 |
| 08 | 294 | CC 93-3826 | × | CP 62-378 | COLPOSCCMex 09-132 |
| 09 | CMI V | LTMex 92-52 | × | ¿? | COLPOSCCMex 09-208 |
| 10 | CMI V | LTMex 92-52 | × | ¿? | COLPOSCCMex 09-212 |
| 11 | CMI V | LTMex 92-52 | × | ¿? | COLPOSCCMex 09-217 |
| 12 | CMI V | LTMex 92-52 | × | ¿? | COLPOSCCMex 09-222 |
| 13 | 774 | PR 62-632 | × | CP 80-1743 | COLPOSCCMex 09-273 |
| 14 | 707 | Mex 79-431 | × | CP 89-2377 | COLPOSCCMex 09-289 |
| 15 | 707 | Mex 79-431 | × | CP 89-2377 | COLPOSCCMex 09-290 |
| 16 | 529 | ITV 92-1424 | × | B 45-181 | COLPOSCCMex 09-312 |
| 17 | 529 | ITV 92-1424 | × | B 45-181 | COLPOSCCMex 09-321 |
| 18 | 527 | ITV 92-1424 | × | CP 81-1384 | COLPOSCCMex 09-333 |
| 19 | 523 | CP 87-1490 | × | Mex 79-341 | COLPOSCCMex 09-341 |
| 20 | 523 | CP 87-1490 | × | Mex 79-341 | COLPOSCCMex 09-348 |
| 21 | Control 1 | CP 62-374 | × | CP 63-588 | CP 72-2086 |
| 22 | Control 2 | Co 421 | × | Mex 57-473 | Mex 79-431 |
| 23 | Control 3 | Mex 56-476 | × | Mex 53-142 | Mex 69-290 |
| 24 | Control 4 | CC 92-2198 | × | CC 93-4206 | Mex 05-204 |

were made every month throughout the crop cycle, except for °Brix, which was not evaluated until cane maturity, i.e., 12 months after planting.

The hybrids were characterized by 50 descriptors, using morphological and agronomic characteritics based on the methodologies described in the UPOV (2005) and Gómez-Merino and Sentíes-Herrera (2015). The traits were identified in fully developed sugarcane plants from the useful section of each experimental plot in the 24 genotypes. The descriptors evaluated were: growth habit, stem diameter, stem height, internode arrangement, longitudinal aspect of internodes, internode length, color of sun-exposed internodes, color of non-sun-exposed internodes, wax on internodes, bud canal, length of bud canal, narrow fissures or grooves, stem cracks, root band shape, bud position at node, bud shape and color, pubescence and bud position, node color, bud size and type, bud lala width, leaf width, leaf blade conformation, leaf blade color, leaf edge pubescence, amount of sheath wax, sheath color, sheath pubescence, length of sheath hairs, auricle shape, ligule shape, ligule width, collar color, collar shape, sheath adherence, crown conformation, crown size, inflorescence, presence of

lalas, number of water suckers, spreading, pith, hollowness, °Brix, number of milling stems, and growth ring thickness on bud side and opposite bud side.

### Statistical analyses

The data obtained were processed using Minitab statistical software version 19.2020 (Minitab; State College, PA, USA). An analysis of variance (ANOVA) was performed for each agronomic variable studied and a comparison of means was applied using Tukey's test ($p \leq 0.05$). Multivariate analyses were carried out considering agronomic and morphological variables, using cluster analysis by similarity of observations with the complete linkage method, with which a dendrogram was constructed. A principal component analysis was also performed for the same group of variables.

## RESULTS AND DISCUSSION

Some of the hybrids evaluated showed a faster emergence than the controls. At 13 days after planting, up to six shoots were found on some hybrids, compared to controls that showed three shoots on average (data not shown). The results revealed differences in the development of the hybrids (Figure 1). One month after planting, the hybrids

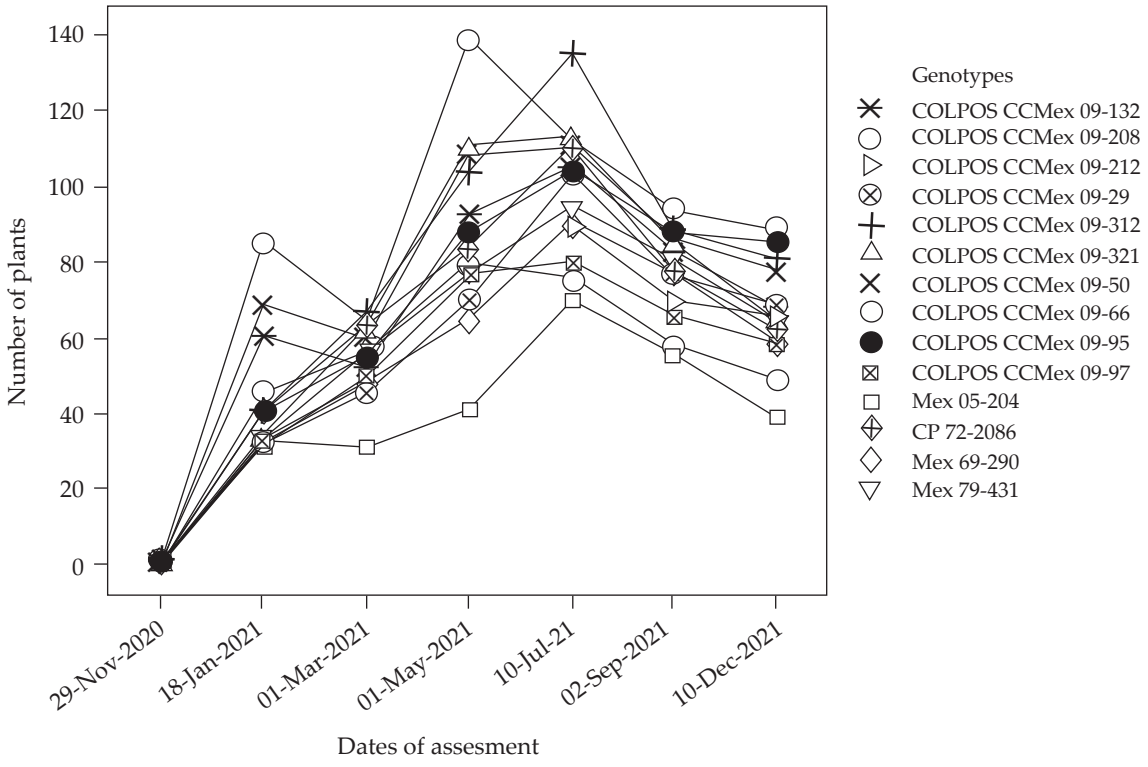


**Figure 1.** Comparison of the number of plants in hybrids under selection and commercial control cultivars of sugarcane (*Saccharum* spp.) in the Semi-commercial Stage, grown at the Experimental Field of the Colegio de Postgraduados Campus Córdoba, 2020-2021 and 2021-2022 growing seasons.

that showed the best development were COLPOSCCMex 09-66 and COLPOSCCMex 09-50, with average values of 85.33 and 68.67 shoots emitted, respectively, higher than those observed in the control cultivars. Just recently, Lesmes-Vesga *et al*. (2023) demonstrated that lalas may produce more tillers and higher shoot dry biomass than pop-eyes and ungerminated buds, while both lalas and pop-eyes produced higher root dry biomass than ungerminated buds.

This greater initial development was maintained throughout the crop cycle since these same hybrids presented the highest number of milling stems in May and June of the first cycle, which coincides with the tillering phase, with means of 138.83 and 108.50 stems, respectively. At this evaluation stage, COLPOSCCMex 09-312 outperformed the aforementioned hybrids with an average of 162.3 shoots in June, followed by COLPOSCCMex 09-321 with an average of 120.7 shoots (data not shown in the graph). Others such as COLPOSCCMex 09-29, COLPOSCCMex 09-95, COLPOSCCMex 09-132 and COLPOSCCMex 09-212 reached their highest value during this same month, with averages of 98.8, 93.3, 89.0 and 92.2 stems emitted, respectively.

During the high growth phase, from June to September, the hybrids exhibited a significant decrease in the number of milling stems, a negative characteristic that should be avoided in new commercial cultivars, since the number of stems is closely related to the final yields obtained in the field. Finally, the hybrids that presented the highest number of stems at the final stage of the harvest cycle were COLPOSCCMex 09-66, COLPOSCCMex 09-29 and COLPOSCCMex 09-312, with averages of 88, 84.8 and 80.8 stems, respectively.

The germination percentage is a critical characteristic that determines the productive potential of the cultivars to be established (Ganapathy and Purushothaman, 2017). The first factor determining germination percentage is genetic (Patil and Patel, 2017). Furthermore, the age of the buds used in planting and their position on the stalk also affect germination indicators, which can be increased when using buds from the middle and upper part of the sugarcane (Samiullah *et al*., 2015), due to the greater availability of reserves in these parts. Temperature, humidity and soil conditions are also determinants of germination. Temperatures close to 35 °C and irrigation immediately after planting increase germination, as well as planting with a 6-10 cm layer of soil (CINCAE, 2004). In a study on integrated selection criteria in sugarcane breeding programs using discriminant function analysis (DFA), Abu-Ellail *et al*. (2020) determined that the most important attributes are stalk weight, stalk height, purity, °Brix and milling stalk yield.

In this study, there were significant differences ($p \leq 0.05$) among the hybrids evaluated for the characteristics plant height, stem diameter, SPAD index and °Brix (Table 2).

The greatest height was observed in the hybrids COLPOSCTMex 09-93, with 311.8 cm, and COLPOSCCMex 09-341, with 318.1 cm, while the lowest heights were obtained with COLPOSCCMex 09-222 and COLPOSCCMex 09-333 with values of 236.9 cm and 225.31 cm, respectively. In general, most hybrids responded significantly to this variable when compared to the control cultivars. The length of milling stalks is one

**Table 2.** Average performance with respect to stalk height, stalk diameter, SPAD index and °Brix in hybrids under selection and commercial cultivars of sugarcane (*Saccharum* spp.) in the Semi-commercial Stage, grown at the Experimental Field of the Colegio de Postgraduados Campus Córdoba, 2020-2021 and 2021-2022 growing seasons.

| Genotype | Stem height (cm) | Stem diameter (mm) | SPAD Index (ICC) | °Brix (%) |
|---|---|---|---|---|
| CP 72-2086 | 283.43±6.56$^{m}$ | 29.11±0.63$^{ghijk}$ | 29.43±1.14$^{hijk}$ | **22.42±0.17$^{a}$** |
| Mex 79-431 | 265.46±4.01$^{ghij}$ | 32.13±0.66$^{cdef}$ | 36.70±1.59$^{hijk}$ | 20.58±0.21$^{bcdefghi}$ |
| Mex 69-290 | 301.24±5.11$^{gh}$ | 34.95±0.56$^{cde}$ | 28.30±1.66$^{ghij}$ | 19.45±0.24$^{ghi}$ |
| Mex 05-204 | 272.31±4.61$^{cdef}$ | 26.7±0.56$^{l}$ | **45.52±2.86$^{def}$** | 16.64±0.56$^{j}$ |
| COLPOSCCMex 09-29 | 277.06±4.83$^{fgh}$ | 25.25±0.47$^{kl}$ | 29.05±1.96$^{jklm}$ | 19.21±0.27$^{i}$ |
| COLPOSCCMex 09-50 | 292.59±3.74$^{m}$ | 27.59±0.48$^{lm}$ | 12.96±0.69$^{m}$ | 19.79±0.32$^{fghi}$ |
| COLPOSCCMex 09-66 | 299.31±4.62$^{bcde}$ | 27.73±0.53$^{hijkl}$ | 18.66±1.48$^{klm}$ | 19.33±0.17$^{hi}$ |
| COLPOSCCMex 09-93 | **311.85±6.68$^{a}$** | 30.01±0.77$^{ijkl}$ | 36.51±1.79$^{bc}$ | 20.26±0.24$^{efghi}$ |
| COLPOSCCMex 09-95 | 285.63±5.68$^{kl}$ | 25.12±0.42$^{n}$ | 27.16±1.76$^{efgh}$ | 20.30±0.43$^{defghi}$ |
| COLPOSCCMex 09-97 | 292.31±4.58$^{jk}$ | 26.59±0.43$^{mn}$ | 22.96±1.15$^{klm}$ | **22.16±0.14$^{ab}$** |
| COLPOSCCMex 09-125 | 310.93±4.18$^{ghijk}$ | 28.8±0.47$^{jkl}$ | 22.92±1.34$^{lm}$ | 20.31±0.24$^{defghi}$ |
| COLPOSCCMex 09-132 | 293.96±5.67$^{ijk}$ | 30.24±0.40$^{jkl}$ | 32.0±1.27$^{ijkl}$ | 20.45±0.31$^{cdefghi}$ |
| **COLPOSCCMex 09-208** | 276.30±7.58$^{bcd}$ | **35.17±0.68$^{bc}$** | **40.90±1.83$^{cde}$** | **20.60±0.21$^{bcdefghi}$** |
| COLPOSCCMex 09-212 | 245.00±3.76$^{hijk}$ | 29.85±0.46$^{bcd}$ | **44.13±1.77$^{cd}$** | 20.20±0.28$^{efghi}$ |
| COLPOSCCMex 09-217 | 256.39±4.84$^{bcd}$ | 28.85±0.52$^{fghi}$ | 31.26±1.52$^{fghi}$ | 21.52±0.33$^{abcde}$ |
| COLPOSCCMex 09-222 | 236.94±6.19$^{ghijk}$ | 29.05±0.44$^{efgh}$ | 25.37±0.91$^{hijk}$ | 20.97±0.38$^{abcdefg}$ |
| COLPOSCCMex 09-273 | 282.22±4.24$^{lm}$ | 30.29±0.53$^{ghij}$ | 20.01±0.98$^{klm}$ | 20.98±0.38$^{abcdefg}$ |
| **COLPOSCCMex 09-289** | 268.59±4.37$^{efg}$ | **36.43±0.76$^{a}$** | 28.71±1.17$^{defg}$ | **21.89±0.15$^{abcd}$** |
| COLPOSCCMex 09-290 | 274.63±6.29$^{gh}$ | 30.29±0.71$^{bcde}$ | **41.12±2.07$^{def}$** | 20.09±0.26$^{efghi}$ |
| COLPOSCCMex 09-312 | 286.98±6.00$^{ghi}$ | 31.06±0.54$^{cdef}$ | **52.33±3.81$^{a}$** | 17.19±0.52$^{j}$ |
| COLPOSCCMex 09-321 | 298.06±6.44$^{bc}$ | 29.99±0.36$^{ghijk}$ | 51.76±2.06$^{b}$ | 20.93±0.26$^{abcdefgh}$ |
| COLPOSCCMex 09-333 | 225.31±5.35$^{m}$ | 29.43±0.39$^{defg}$ | 22.65±1.06$^{hijk}$ | **22.04**±0.42$^{abc}$ |
| COLPOSCCMex 09-341 | **318.09±6.77$^{b}$** | 33.45±0.56$^{cdef}$ | 22.54±1.09$^{lm}$ | 20.77±0.34$^{bcdefghi}$ |
| COLPOSCCMex 09-348 | 309.33±6.84$^{defg}$ | 32.98±0.88$^{b}$ | 39.69±2.29$^{cd}$ | 21.17±0.22$^{abcdef}$ |

Means± standard error. Means with different letters indicate statistical differences (Tukey, $p \leq 0.05$). Averages of measurements taken twelve months after planting are shown.

of the characteristics that can indicate the tolerance of sugarcane to drought stress, in addition to having a wide heritability, so it can be used as a selection criterion in breeding programs (Hartati and Yuniyati, 2022). In addition to the genotype factor, the significant differences found in stem height may be related to the climatic conditions and soil characteristics in the area where the study was conducted since the driest period coincides with the formative phase of sugarcane, a limiting factor for the normal development of the hybrids (Zhao *et al*., 2020).

The largest stem diameter was found in the hybrid COLPOSCCMex 09-289, with 36.43 mm, and COLPOSCCMex 09-208, with 35.17 mm. The latter genotype also showed high values for the SPAD and °Brix index traits, with values of 40.90 ICC and 20.60 %, respectively. Hybrids Mex 05 204, COLPOSCCMex 09-212 and COLPOSCCMex 09-290 showed the highest values for the SPAD index, with averages of 45.52, 44.13 and 41.12 ICC, respectively.

The hybrids showed significant differences in soluble solids content in the juice extracted from their stems. However, none exceeded the control cultivar CP 72-2086, which reached 22.42 °Brix. The hybrids that most closely resembled this value were COLPOSCCMEX 09-97, COLPOSCCMEX 09-333, COLPOSCCMEX 09-289, COLPOSCCMEX 09-217 and COLPOSCCMEX 09-348, with values of 22.2, 22.1, 21.9, 21.5 and 21.2 %, respectively (Table 2). The absence of significant differences observed among the hybrids evaluated with respect to the °Brix variable could be due to the uniform expression of genes controlling this attribute in the new sugarcane hybrids, rather than to environmental or management conditions (Muhammad *et al*., 2014).

Regarding the means of the variables leaf length, leaf width and number of leaves (Table 3), the hybrids Mex 79 431 and COLPOSCCMex 09-29 presented the longest leaf length, with 163.65 and 163.37 cm, respectively. However, leaf width was narrower for the hybrid COLPOSCCMex 09-29 (3.82 cm) compared to the other hybrids and control

**Table 3.** Agronomic response of phenotypic traits in control cultivars and hybrids of sugarcane in the Semi-commercial Stage, grown at the Experimental Field of the Colegio de Postgraduados Campus Córdoba, 2020-2021 and 2021-2022 growing seasons.

| Genotype | Leaf length (cm) | Leaf width (cm) | Number of leaves |
|---|---|---|---|
| CP 72-2086 | 149.28±2.52$^{jk}$ | 4.24±0.12$^{ijk}$ | **11.39±0.38$^{cdefg}$** |
| Mex 79-431 | **163.65±2.21$^{cde}$** | 4.46±0.12$^{fghij}$ | 11.0±0.31$^{bcd}$ |
| Mex 69-290 | **161.39±2.69$^{defgh}$** | **5.08±0.11$^{efghi}$** | 10.91±0.31$^{defg}$ |
| Mex 05-204 | 157.91±2.53$^{bcd}$ | 4.93±0.14$^{bcdef}$ | 10.15±0.31$^{i}$ |
| COLPOSCCMex 09-29 | **163.37±2.97$^{a}$** | 3.82±0.12$^{hijk}$ | 9.91±0.27$^{ab}$ |
| COLPOSCCMex 09-50 | 137.91±1.56$^{kl}$ | 4.58±0.11$^{ijk}$ | 10.56±0.29$^{bc}$ |
| COLPOSCCMex 09-66 | 139.04±2.92$^{fgh}$ | 4.57±0.14$^{ghij}$ | 9.21±0.28$^{efghi}$ |
| COLPOSCCMex 09-93 | 142.61±3.09$^{hij}$ | 4.64±0.11$^{ghijk}$ | 10.68±0.33$^{ab}$ |
| COLPOSCCMex 09-95 | 141.31±2.04$^{kl}$ | 4.68±0.13$^{jk}$ | **11.52±0.36$^{cde}$** |
| COLPOSCCMex 09-97 | 148.11±1.91$^{ijk}$ | 3.95±0.12$^{k}$ | 10.33±0.31$^{fghi}$ |
| COLPOSCCMex 09-125 | 132.50±2.55$^{l}$ | 4.94±0.15$^{cdefg}$ | **11.29±0.39$^{defg}$** |
| COLPOSCCMex 09-132 | **150.91±3.03$^{fgh}$** | 4.99±0.16$^{defgh}$ | 10.29±0.28$^{hi}$ |
| COLPOSCCMex 09-208 | 142.78±2.52$^{cdef}$ | **5.56±0.17$^{abcde}$** | 10.59±0.29$^{efgh}$ |
| COLPOSCCMex 09-212 | 139.98±2.12$^{efgh}$ | **5.85±0.14$^{a}$** | 10.37±0.29$^{ghi}$ |
| COLPOSCCMex 09-217 | 138.13±2.18$^{cdefg}$ | 4.87±0.12$^{defghi}$ | 10.67±0.35$^{defg}$ |
| COLPOSCCMex 09-222 | 135.63±1.62$^{ghi}$ | 4.73±0.13$^{abc}$ | 10.61±0.42$^{ab}$ |
| COLPOSCCMex 09-273 | 135.46±1.56$^{m}$ | 4.87±0.12$^{fghij}$ | 10.68±0.36$^{efgh}$ |
| COLPOSCCMex 09-289 | **149.33±2.39$^{a}$** | **5.36±0.15$^{abcd}$** | **11.15±0.34$^{a}$** |
| COLPOSCCMex 09-290 | 129.81±2.18$^{l}$ | **5.93±0.15$^{a}$** | **11.13±0.33$^{ab}$** |
| COLPOSCCMex 09-312 | 149.98±2.6$^{bc}$ | 5.23±0.13$^{abcde}$ | 9.71±0.31$^{ghi}$ |
| COLPOSCCMex 09-321 | 142.02±3.95$^{fgh}$ | **5.81±0.13$^{ab}$** | 10.24±0.42$^{cdefg}$ |
| COLPOSCCMex 09-333 | 127.80±3.08$^{m}$ | **5.53±0.14$^{a}$** | 10.52±0.33$^{ghi}$ |
| COLPOSCCMex 09-341 | **159.11±2.65$^{ab}$** | 4.92±0.12$^{hijk}$ | 10.15±0.31$^{defg}$ |
| COLPOSCCMex 09-348 | **151.06±2.67$^{cdef}$** | 4.65±0.12$^{fghij}$ | 10.96±0.34$^{cdef}$ |

Means± standard error. Means with different letters indicate statistical differences (Tukey, $p \leq 0.05$). Averages of measurements taken twelve months after planting are shown.

cultivars evaluated. The hybrid COLPOSCCMex 09-289 was the one that obtained high values for the variables stem diameter, °Brix, width and number of leaves. The hybrid COLPOSCCMex 09-290 showed significant values for leaf width (5.93 cm) and number of leaves (11.13).

For the leaf length variable, the control cultivar Mex 79-431 and the hybrid COLPOSCCMex 09-29 showed the highest averages, with 163.65 and 163.37 cm, respectively. The hybrid COLPOSCCMex 09-290 had the shortest leaf length (129.81 cm), although the value for leaf width was outstanding (5.93 cm). Furthermore, the latter genotype showed a higher number of leaves. The COLPOSCCMex 09-95 hybrid presented the highest mean for leaf number, which was 11.52 (Table 3). Leaf area is an important trait associated with plant growth rate and yield. Sugarcane stands out for being a C4 plant, which allows a high photosynthetic rate and a great capacity for carbohydrate synthesis (Rincón-Castillo and Becerra-Campiño, 2020).

## Morphological characterization

After agglomerative hierarchical grouping, the hybrids and control commercial cultivars were grouped into five clusters (Figure 2). The first one (cluster I) consisted of nine hybrids and two control cultivars (Mex 69-290 and Mex 05-204) based on their similarity. These genotypes were characterized by erect and semiprostrate growth habit, thick stems and long internodes, no bud canal, absence of pubescence on leaf structures, abundant stem wax and scarce sheath wax, large crown size and representative leaf length. The control commercial cultivar Mex 79-431 conformed to cluster II, with a more erect growth habit, medium height, yellowish-green nodes with abundant wax, a narrow bud canal and a tender green arched leaf blade and a brownish-green ligular collar.

Cluster III had five hybrids, which were characterized by an inclined growth habit and curved internodes of medium diameter, medium stem height, medium leaf length and width, and color variation from pale green to tender green. They had an open cup conformation, medium sheath adherence and lateral lalas. Cluster IV consisted of seven hybrids and the control cultivar CP 72-2086. These genotypes presented a semi-erect growth habit, medium height and stem diameter with zigzag internodes, stem color among yellow, green and purple with scarce wax, absence of bud canal, smooth bark and some with cracks in their stems, large buds of bulky and erect forms, with a curved apex of the leaf blade with a profuse inflorescence. Moreover, sheath adherence was medium and presented significant values for the number of leaves.

Cluster V was formed by the hybrids COLPOSCCMex 09-66 and COLPOSCCMex 09-222. The most representative features of these genotypes were their basket growth habit, medium stem diameter, long internodes and zigzag internode arrangement. The color of the nodes did not vary and presented a purplish-greenish coloration and a large number of stems in two linear meters, abundant wax on their stems, a very profuse inflorescence, lateral lalas on their stems and abundant pith.

Chidambaram and Sivasubramaniam (2017) found different morphological profiles of ten sugarcane cultivars, which help in the identification of different genotypes in the

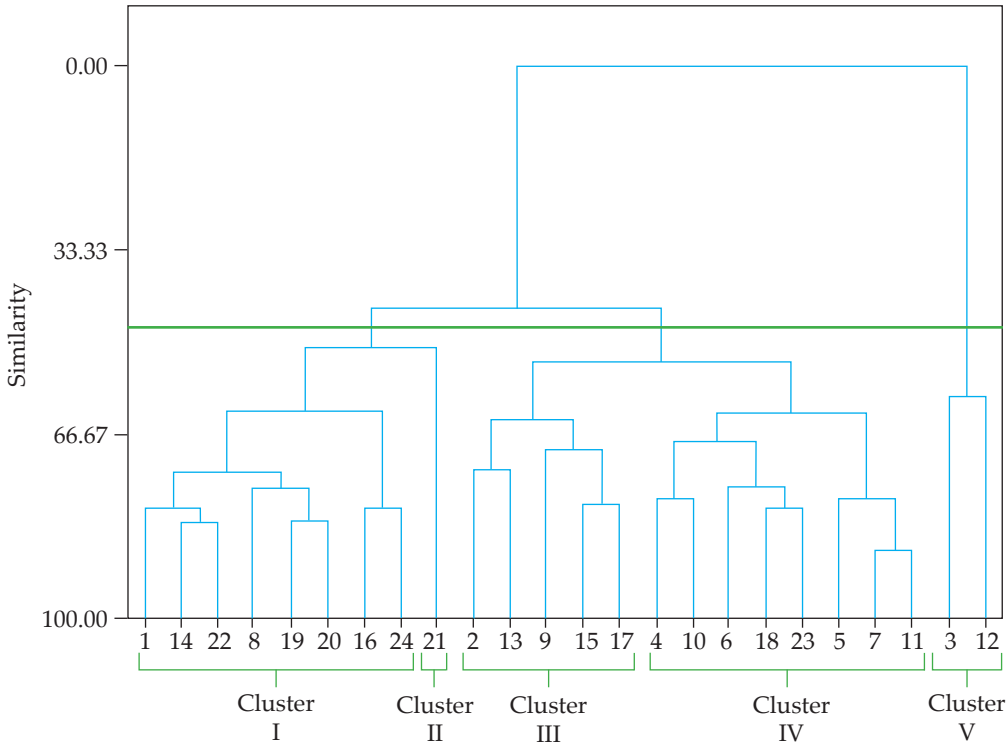


**Figure 2.** Dendrogram of genetic relationships among different sugarcane (*Saccharum* spp.) hybrids evaluated, based on morphological and agronomic traits. 1: COLPOSCCMex 09-29; 2: COLPOSCCMex 09-50; 3: COLPOSCCMex 09-66; 4: COLPOSCCMex 09-93; 5: COLPOSCCMex 09-95; 6: COLPOSCCMex 09-97; 7: COLPOSCCMex 09-125; 8: COLPOSCCMex 09-132; 9: COLPOSCCMex 09-208; 10: COLPOSCCMex 09-212; 11: COLPOSCCMex 09-217; 12: COLPOSCCMex 09-222; 13: COLPOSCCMex 09-273; 14: COLPOSCCMex 09-289; 15: COLPOSCCMex 09-290; 16: COLPOSCCMex 09-312; 17: COLPOSCCMex 09-321; 18: COLPOSCCMex 09-333; 19: COLPOSCCMex 09-341; 20: COLPOSCCMex 09-348; 21: Mex 79-431; 22: Mex 69-290; 23: CP 72-2086; 24: Mex 05-204.

field. Characteristics such as plant growth habit, stem bark surface, auricle shape, leaf sheath, internode wax and growth ring were considered for their work. Knowledge of morphology is of vital importance for a clear and precise identification of clones, cultivars and species in the field.

Principal component analysis (PCA) was used to differentiate genotypes into discrete groups associated with morphological and agronomic variables, and thus facilitate the identification of the traits most responsible for the variations observed among a set of genotypes. The first principal component (PC1) accounted for 12.4 % of the total variation, followed by 12.1 % for PC2. The most outstanding factors of PC1 based on their loadings were: growth ring thickness on the opposite side of the bud (0.33), presence of lalas (0.28), growth ring thickness on the bud side (0.21), leaf blade

conformation (0.24), inflorescence (0.22) and pith (0.23). For PC2, the factors of highest relevance were the number of water suckers (0.33), leaf length (0.26), ligule length (0.26) and ligule width (0.26) (Figure 3).

The principal component analysis (PCA) is a statistical method that simplifies the complexity of data, since a large number of variables can be reduced to just a couple of them. Nevertheless, this method has advantages and disadvantages. Among the pros, the PCA prevents overfitting, removes correlated features, speeds up other machine

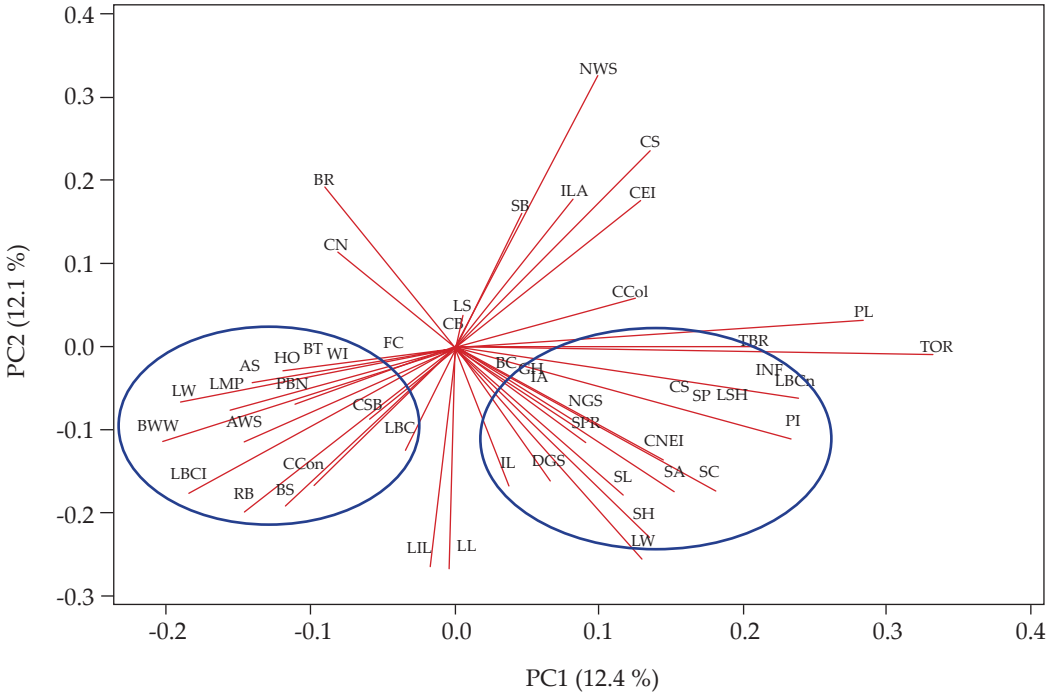


**Figure 3.** Loading biplot of 50 morphological and agronomic characteristics of 20 new hybrids and four control cultivars of sugarcane (*Saccharum* spp.) on principal components PC1 and PC2. GH: growth habit; DGS: diameter of ground stems (mm); IA: internode arrangement; SH: stem height (cm); ILA: internode longitudinal aspect; IL: internode length (cm); CEI: color of exposed internodes; CNEI: color of non-exposed internodes; NGS: number of ground stems; WI: wax on internodes; BC: bud canal; LBC: length of bud channel; FC: fissures corked; CSB: cracks in stem bark; TBR: thickness of bud side growth ring; TOR: thickness of opposite bud growth ring; RB: root band; PBN: position of bud at node; SB: shape of bud; CB: color of bud; CN: color of node; BS: bud size; BT: bud type; BWW: bud wing width; LL: leaf length (cm); LW: leaf width (cm); LBCn: leaf blade conformation; LBCl: leaf blade color; LMP: leaf margin pubescence; AWS: amount of wax in the sheath; SC: sheath color; SP: sheath pubescence; LSH: length of sheath hairs (mm); AS: auricle shape; LS: ligule shape; LW: ligule width (mm); LiL: ligule length (cm); CCol: collar color; CS: collar shape; SA: sheath adherence; SL: sheath length (cm); CCon: crown conformation; CS: crown size (cm); INF: inflorescence; PL: presence of lalas; NWS: number of water suckers; SPR: spreading; BR: °Brix; PI: pith; HO: hollowness.

learning algorithms, and improves visualization. On the other hand, using the PCA method can also have some disadvantages: all the variables should have a mean of 0 and a standard deviation of 1, which standardizes data; the PCA can lead to some loss of information, and therefore, interpretation of the outputs may result complicated. Indeed, Elhaik (2022) stated that PCA-based findings in population genetic studies are highly biased and must be reevaluated. Therefore, attention should be paid when implementing the PCA procedure and results must be deeply analyzed and correctly interpreted.

## CONCLUSION

Based on the results of the statistical analysis, the hybrids COLPOSCCMex 09-312 and COLPOSCCMex 09-321 presented desirable agronomic characteristics, such as the number of milling stems, with values of 162.33 and 120.67, respectively. The hybrids COLPOSCCMex 09-341 and COLPOSCCMex 09-93 showed the longest stem length, with means of 318.1 and 311.85 cm, respectively.

Thanks to multivariate analyses, and through the study of morphological traits, it was possible to learn more about the genetic profile of this population. The classification system concentrated the hybrids in clusters, relating the hybrids COLPOSCCMex 09-93, COLPOSCCMex 09-289, COLPOSCCMex 09-312, COLPOSCCMex 09-321 and COLPOSCCMex 09-341, which could be selected based on traits of interest, such as growth habit, stem height and diameter, internode size, amount of wax, leaf length and width, and leaf blade size. It is suggested that the most representative sugarcane genotypes in this work should be further tested in the different potential growing areas, in order to identify the best genotypes according to the agroecological zone where they are planted and grown.

## ACKNOWLEDGMENTS

The authors are grateful for the support granted by the National Council of Science and Technology of Mexico (CONACyT) for the GRM scholarship to pursue a Master's Degree in Sciences. We are also grateful for the support of the Central Motzorongo and San Nicolás sugar mills in the state of Veracruz and for their interest in evaluating these new sugarcane hybrids in their experimental fields.

## REFERENCES

Abu-Ellail FFB, Hussein EMA, El-Bakry A. 2020. Integrated selection criteria in sugarcane breeding programs using discriminant function analysis. Bulletin of the National Research Centre 44 (1): 161. https://doi.org/10.1186/s42269-020-00417-6

Baloch AW, Kumbhar MA, Mallano IA, Majeed Baloch A, Yasir TA, Sarki SM, Nizamani GS, Nizamani F, Baloch IA. 2017. Genetic diversity analysis in commercial sugarcane (*Saccharum officinarum* L.) genotypes. Pakistan Journal of Biotechnology 14 (2): 167–171.

Chidambaram K, Sivasubramaniam K. 2017. Morphological characterization and identification of morphological markers for selected sugarcane (*Saccharum* spp.) cultivars. International Journal of Current Microbiology and Applied Sciences 6 (12): 509–518. https://doi.org/10.20546/IJCMAS.2017.612.062

CINCAE (Centro de Investigación de la Caña de Azúcar del Ecuador). 2004. Fisiología, floración y mejoramiento genético de la caña de azúcar en Ecuador. Centro de Investigación de la Caña de Azúcar del Ecuador. Guayaquil, Ecuador. https://cincae.org/wp-content/uploads/2013/05/FISOLOGIA-Y-MEJORAMTO.pdf (Retrieved: September 2023).

CONABIO (Comisión Nacional para el Conocimiento y Uso de la Biodiversidad). 2011. La biodiversidad en Veracruz: estudio de Estado. Comisión Nacional para el Conocimiento y Uso de la Biodiversidad, Gobierno del Estado de Veracruz, Universidad Veracruzana, Instituto de Ecología: Xalapa, México. 541 p.

CONADESUCA (Comité Nacional para el Desarrollo Sustentable de la Caña de Azúcar). 2016. Nuevas variedades de Caña de Azúcar. Comité Nacional para el Desarrollo Sustentable de la Caña de Azúcar, Secretaría de Agricultura y Desarrollo Rural, Universidad Autónoma Chapingo. Mexico City, Mexico. https://www.gob.mx/cms/uploads/attachment/file/136406/NotaNuevasVariedadesd_Cana_deAzucar.compressed.pdf (Retrieved: September 2023).

CONADESUCA (Comité Nacional para el Desarrollo Sustentable de la Caña de Azúcar). 2021. Informe estadístico del sector agroindustrial de la caña de azúcar en México, zafras 2011-2012 / 2020-2021. Comité Nacional para el Desarrollo Sustentable de la Caña de Azúcar, Secretaría de Agricultura y Desarrollo Rural. Mexico City, Mexico. https://www.siiba.conadesuca.gob.mx/siiaca/docext/8vo_Informe_estadistico.pdf (Retrieved: September 2023)

Elhaik E. 2022. Principal component analyses (PCA)-based findings in population genetic studies are highly biased and must be reevaluated. Scientific Reports 12: 14683.https://doi.org/10.1038/s41598-022-14395-4

Emegha FE, Animasaun DA, Bankole F, Olaoye G. 2021. Analysis of genetic diversity in selected sugarcane (*Saccharum officinarum* L.) accessions using inter simple sequence repeat (ISSR) markers. Acta Agriculturae Slovenica 117 (4): 1–10. https://doi.org/10.14720/aas.2021.117.4.2015

FAO (Organización de las Naciones Unidas para la Alimentación y la Agricultura). 2023. FAOSTAT. Datos sobre alimentación y agricultura. Organización de las Naciones Unidas para la Alimentación y la Agricultura. Roma, Italia. https://www.fao.org/faostat/es/#data/QCL (Retrieved: August 2023).

Ganapathy S, Purushothaman RS. 2017. Performance of promising early maturing sugarcane clones for yield and quality traits during varietal development process. Electronic Journal of Plant Breeding 8 (1): 279–282. https://doi.org/10.5958/0975-928X.2017.00040.0

Gómez-Merino FC, Sentíes-Herrera HE. 2015. Manual para la identificación varietal de caña de azúcar. Colegio de Postgraduados: Texcoco, México. 40 p.

Gómez-Merino FC, Sentíes-Herrera HE, Trejo-Téllez LI, Pérez-Sato JA. 2014. El Campus Córdoba impulsa programa de mejoramiento de caña de azúcar. Agroentorno 2014: 13–15.

Gómez-Merino FC, Trejo-Téllez LI, Salazar-Ortiz J, Pérez-Sato JA, Sentíes-Herrera HE, Bello-Bello, Aguilar-Rivera N. 2017. Diversification of the sugar agroindustry as a strategy for Mexico. Agroproductividad 10 (11): 7–12.

Hartati RS, Yuniyati N. 2022. Field evaluation of the potential of drought-tolerant sugarcane (*Saccharum officinarum* L.) mutants based on morpho-agronomic characters. IOP Conference Series: Earth and Environmental Science 974 (1): 012005. https://doi.org/10.1088/1755-1315/974/1/012005

INEGI (Instituto Nacional de Estadística y Geografía). 2014. Subsistema de Información Económica. Encuesta Nacional Agropecuaria 2014. Instituto Nacional de Estadística y Geografía. Mexico City, Mexico. https://www.inegi.org.mx/programas/ena/2014/ (Retrieved: August 2023).

Junior CADK, Manechini JRV, Corrêa RX, Pinto ACR, da Costa JB, Favero TM, Pinto LR. 2020. Genetic structure analysis in sugarcane (*Saccharum* spp.) using Target Region Amplification Polymorphism (TRAP) markers based on sugar- and lignin-related genes and potential application in core collection development. Sugar Tech 22 (4): 641–654. https://doi.org/10.1007/S12355-019-00791-0

Lavín-Castañeda J, Sentíes-Herrera HE, Trejo-Téllez LI, Hidalgo-Contreras JV, Gómez-Merino FC. 2020. Advances in the selection program of sugarcane (*Saccharum* spp.) varieties in the Colegio de Postgraduados. Agroproductividad 13 (11): 123–129. https://doi.org/10.32854/agrop.v13i11.1776

Lesmes-Vesga RA, Odero CD, Sharma LK, Sandhu HS. 2023. Effects of planting pre-germinated buds on stand establishment in sugarcane. Agronomy 13: 1001. https:// doi.org/10.3390/agronomy13041001

Muhammad K, Rahman H, Ashiq Rabbani M, Khan A, Rahman H, Rabbani M, Khan A. 2014. Qualitative and quantitative assessment of newly selected sugarcane varieties. Sarhad Journal of Agriculture 30 (2): 187–191.

Patil PP, Patel DU. 2017. Study of genetic variability and heritability in sugarcane (*Saccharum* spp. complex). International Journal of Current Microbiology and Applied Sciences 6 (9): 3112–3117. https://doi.org/10.20546/ijcmas.2017.609.384

Rincón-Castillo A, Becerra-Campiño JJ. 2020. Respuesta agronómica de cuatro variedades de caña de azúcar en los Llanos Orientales de Colombia. Acta Agronómica 69 (2): 124–129. https://doi.org/10.15446/acag.v69n2.70649

Samiullah, Ehsanullah, Anjum SA, Raza M, Hussain N, Nadeem M, Ali N. 2015. Studies on productivity and performance of spring sugarcane sown in different planting configurations. American Journal of Plant Sciences 6 (19): 2984–2988. https://doi.org/10.4236/ajps.2015.619293

Seema N, Khan M, Khan I, Yasmeen S. 2017. Genetic itemization of exotic sugarcane clones on the basis of quantitative and qualitative parameters. Pakistan Journal of Botany 49 (4): 1471–1478.

Soto-Esparza M, García E. 1989. Atlas climático del estado de Veracruz. Instituto de Ecología: Xalapa, México. 125 p.

Torres-Torres F, Rojas-Martínez A. 2018. Suelo agrícola en México: retrospección y prospectiva para la seguridad alimentaria. Realidad, Datos y Espacio Revista Internacional de Estadística y Geografía 9 (3): 137–155.

UPOV (International Union for the Protection of New Varieties of Plants). 2005. Directrices para la ejecución del examen de la distinción, la homogeneidad y la estabilidad. Caña de azúcar. International Union for the Protection of New Varieties of Plants. Geneva, Switzerland. https://www.upov.int/edocs/tgdocs/en/tg186.pdf (Retrieved: September 2023).

Wu J, Wang Q, Pan YB, Xie J, Zhou F, Xu H, Qiu Y, Zhang C, Liu Z. 2021. Multivariate analysis of 31 phenotypic traits among major parental lines of sugarcane breeding programs in China. Journal of Animal and Plant Sciences 31 (3): 719–732. https://doi.org/10.36899/JAPS.2021.3.0262

Zhao D, Zhu K, Momotaz A, Gao X. 2020. Sugarcane plant growth and physiological responses to soil salinity during tillering and stalk elongation. Agriculture 10 (12): 608. https://doi.org/10.3390/agriculture10120608

Agrociencia

# AGRONOMIC RESPONSE OF FOUR *Dahlia pinnata* Cav. (Asteraceae) VARIETIES IN THREE PRODUCTION ENVIRONMENTS

Marco Antonio **Villegas-Olguín**[1], Rosalinda **Mendoza-Villarreal**[1], Adalberto **Benavides-Mendoza**[1], Hermila Trinidad **García-Osuna**[2], Marcelino **Cabrera-de la Fuente**[1], Valentín **Robledo-Torres**[1*]

[1] Universidad Autónoma Agraria Antonio Narro. Departamento de Horticultura. Calzada Antonio Narro 1923, Buenavista, Saltillo, Coahuila, Mexico. C. P. 25315.
[2] Universidad Autónoma Agraria Antonio Narro. Departamento de Fitomejoramiento. Calzada Antonio Narro 1923, Buenavista, Saltillo, Coahuila, Mexico. C. P. 25315.
* Author for correspondence: robledo3031@gmail.com

**Citation:** Villegas-Olguín MA, Mendoza-Villarreal R, Benavides-Mendoza A, García-Osuna HT, Cabrera-de la Fuente M, Robledo-Torres V. 2023. Agronomic response of four *Dahlia pinnata* Cav. (Asteraceae) varieties in three production environments. **Agrociencia** 57(8): 1696-1708. doi.org/ 10.47163/agrociencia.v57i8.2946

**Editor in Chief:**
Dr. Fernando C. Gómez Merino

Received: January 13, 2023.
Approved: November 11, 2023.
**Published in Agrociencia:** December 08, 2023.



## ABSTRACT

Flower cultivation has increased nationwide. Currently, species of the *Dahlia* genus (known colloquially as Dahlias) are grown for ornamental purposes, with central Mexico having the highest production rate. Due to its importance, we sought to evaluate the effect of three different methods of cultivation (shade net, greenhouse, and open field) on the growth and development of four dahlia varieties in Saltillo, Coahuila, Mexico. The experiment was carried out at the Horticulture Department of the Universidad Autónoma Agraria Antonio Narro. Tuberous roots of four *D. pinnata* varieties were sown directly into the soil and covered with mulch. The shade netting production environment proved to be the best in production, with the best results in plant height, stem diameter, number of leaves, and days to flowering. The highest-performing cultivar was the Antje variety. On the other hand, the Antje variety (cultivated under shade netting) had the longest flower stalks, the Boy Mick variety (cultivated in the greenhouse) had the heaviest flowers, and the Canby Centennial variety (cultivated in open field) had the flowers with the thickest stalks. The results show that Dahlias can be grown in northeastern Mexico because the area meets suitable conditions for crop development and production.

**Keywords**: Protected agriculture, production, Dahlias, flowers.

## INTRODUCTION

Mexico's diversity of climates provides ample opportunities for the development of first-rate floriculture (Tejeda-Sartorius *et al*., 2015). The cultivation of flowers has shown a growth rate of 9 %, while the cultivation of grain corn only increased by 1 % during 2016 (Orozco-Hernández *et al*., 2017). This demonstrates that this area of horticulture is booming and has a high economic potential (Soriano-Melgar *et al*., 2018). As an example, it is possible to cite the commercial success of lisianthus (*Eustoma grandiflorum* (Raf.) Shinners), a plant native to northern Mexico that has gained importance within the international market (Fernández-Pavía and Trejo-Téllez, 2018). Additionally, the case of pascuilla (*Euphorbia strigosa* Hook and Arn), which has ornamental potential

due to its red or crimson bracts and, because of its resemblance to the poinsettia (*Euphorbia pulcherrima* Willd. ex Klotzsch), it can be considered a dwarf version of the latter (Valdez-Hernández *et al*., 2018).

One of the most diverse botanical families native to Mexico is Asteraceae (Carrasco-Ortiz *et al*., 2019), which includes 417 genera and 3113 species (Villaseñor, 2018). Within this large number of genera is *Dahlia*, which is characterized by its peculiar inflorescences, or flower heads, with showy ligulate flowers located around the outside. *Dahlia* has been widely explored and diversified in terms of ornamental varieties abroad (Şekerci and Gülşen, 2016) and is a genus subject of diverse studies, both taxonomic (Castro-Castro *et al*., 2012), phylogenetic (Sánchez-Chávez *et al*., 2019), biogeographical (Carrasco-Ortiz *et al*., 2019), and biochemical (Hernández-Epigmenio *et al*., 2022). An example of the ornamental value of *Dahlia* is the more than 61 000 validated and accepted cultivars reported by the Royal Horticultural Society of the United Kingdom. In contrast, in Mexico there are only 25 cultivars reported as registered in the National Catalogue of Plant Varieties 2022 (SNICS, 2022).

The Dahlia was designated the national flower of Mexico in 1963 owing to its ornamental and economic value (DOF, 1963; Mera-Ovando *et al*., 2008). It is a symbol of Mexican floriculture due to its 38 species, all of which grow in Mexico (35 of which are endemic) (Carrasco-Ortiz *et al*., 2019). Currently, the Dahlia is mainly used as an ornamental plant, and its use has been promoted by utilizing its medicinal and nutritional benefits (Mera-Ovando *et al*., 2008).

Cultivation of these plants occurs primarily in central Mexico, in the states of Puebla, Mexico, and Mexico City, although there is production potential in other entities (Heredia-Hernández and Baltazar-Bernal, 2017), since their distribution includes most of the Mexican territory, with the exception of the Yucatán and Baja California peninsulas (Carrasco-Ortiz *et al*., 2019). The main propagation methods used in producing areas are seed and tuberous roots (Jiménez-Mariña, 2015; Mera-Ovando and Bye-Boettler, 2006), although methods by cuttings and *in vitro* culture have also been described (Jiménez-Mariña, 2015).

The temperature requirements for dahlia cultivation range from 18 to 23 °C (Jiménez-Mariña, 2015), although however some research studies manage to bring production even at temperatures of 45 °C (Heredia-Hernández and Baltazar-Bernal, 2017). This clearly demonstrates that the range of temperature tolerance is very broad. The city of Saltillo, Coahuila, is located at an altitude of 1600 m, has a dry, semi-warm climate with cool winter and summer rains (Molar-Orozco *et al*., 2020; Sánchez-Herrera *et al*., 2022), with annual average precipitation and temperature of 125 to 400 mm and 14 to 18 °C, respectively (Marroquín-Morales *et al*., 2018). These favorable conditions make Saltillo a good candidate for Dahlia production.

In this study, the growth and development of the plants and quality of the cut flowers of four dahlia varieties subjected to three varying production environments (open field, greenhouse, and shade net) for their cultivation in Saltillo, Coahuila, Mexico, were evaluated.

## MATERIALS AND METHODS

### Experiment site

The research was carried out in three production environments: open field (c), semi-automated greenhouse (i), and black shade net with 30 % shading (m). This took place at the Experimental Agricultural Field of the Horticulture Department of the Universidad Autónoma Agraria Antonio Narro in Saltillo, Coahuila, Mexico, located exactly at 25° 21′ 23″ N and 101° 01′ 54″ W, with an altitude of 1610 m and a mean annual temperature ranging between 12 and 18 °C, during the spring-summer 2020 agricultural cycle.

### Plant material

Tuberous roots of four varieties of *Dahlia pinnata*, obtained in the municipality of Huamantla, Tlaxcala, Mexico, were collected during the autumn of 2019. They were classified after being described (plant habit and growth habit, stem, leaf, flower head, and tuberous root), according to the Graphic Manual for Dahlia Varietal Description (Laguna-Cerda, 2007). For this purpose, 10 catalogs of varieties for this species were reviewed, identifying the presence of the four varieties used. The inflorescence's group, color, and size, as well as the curvature of the ligule, were all taken into account. As a result, the Dahlia Catalog Listing of Varieties (Crocoll *et al*., 2023) was chosen.

### Crop management

The tuberous roots of the four varieties were kept under greenhouse conditions until the day of planting. The planting of Dahlias was carried out directly in the soil on March 10, 2020, in 12 m long culture beds, which were covered with silver-colored mulch on the outside and black mulch on the inside. Eight tuberous roots were used per variety and per environment, resulting in a total of 96 roots, which were planted 60 cm apart in single rows, and the distance between planting lines between beds was 90 cm.

The crop was grown in three environments: open field (c), semi-automated greenhouse (i), and black shade net with 30 % shading (m). Prior to crop establishment, the ground was heavily irrigated with water only. After planting, the crops were irrigated every third day until the beginning of plant emergence, which occurred 7 days after planting (DDS). Then, the plants were fertilized with a Steiner nutrient solution (Steiner, 1961), which was adjusted based on the analysis of water used during the crop cycle. The nutrition was modified according to the phenological stage of the crop: during the post-emergence stage of the plant, the Steiner solution was used at 25 %, during vegetative development at 50 %, at the appearance of flower buds at 75 %, and during flowering at 100 %. Drip irrigation was applied every third day, for 45 to 60 min, depending on the already present soil moisture.

### Variables evaluated

The following variables were evaluated in each of the three environments: plant height (ADP) with a flexometer, basal stem diameter (DBT) with a Steren® HER-411 digital vernier, and number of leaves (NH) expressed in units. The variables listed above were evaluated weekly until the appearance of the first flower bud in all environments (72 DDS). The total number of inflorescences (NTI) was estimated at the end of the last harvest (143 DDS), and the number of days between sowing and the appearance of the first expanded inflorescence on each plant (DAF) was estimated for all varieties. The number of tuberous roots (NRT) was evaluated at the end of the production cycle, once they were removed from the experimental area (167 DDS).

The variables evaluated in the inflorescences were: length of floral stem (LTF) using a flexometer, fresh weight of inflorescence (PFF) with an OHAUS CS analytical balance with a capacity of 3000 g, diameter of inflorescence (DF), and floral stem (DTF) measured with a Steren® HER-411 digital vernier. These variables were evaluated on the day the flower stalk was cut.

### Statistical analysis

There were 12 treatments as a result of the combination of two factors: the dahlia variety (four varieties) and the production environment (greenhouse, shade net, and open field) (Table 1). A completely randomized experimental design (DCA) was used to distribute the treatments. Each treatment had four replicates, each with two experimental units. Each plant was considered an experimental unit. Analysis of variance (ANOVA) was performed with the variable mean values; for the comparison of means, a Tukey test was applied (Tukey, $\alpha \leq 0.05$). A data correlation analysis (Pearson's coefficient) was performed for the variables ADP, NH, NRT, and NTI, using the statistical software JMP Ver. 15 (Sall, 2020).

**Table 1**. Treatment description for four *Dahlia pinnata* Cav. varieties evaluated in three production environments in southeastern Coahuila de Zaragoza, Mexico.

| Environment | Variety | Treatment Key |
|---|---|---|
| Open Field | Antje | c-A |
| | Babylon | c-B |
| | Boy Mick | c-BM |
| | Canby Centennial | c-CC |
| Greenhouse | Antje | i-A |
| | Babylon | i-B |
| | Boy Mick | i-BM |
| | Canby Centennial | i-CC |
| Shade Net | Antje | m-A |
| | Babylon | m-B |
| | Boy Mick | m-BM |
| | Canby Centennial | m-CC |

## RESULTS AND DISCUSSION

The varieties used in the present work were classified as Antje, Babylon, Boy Mick, and Canby Centennial (Figure 1).

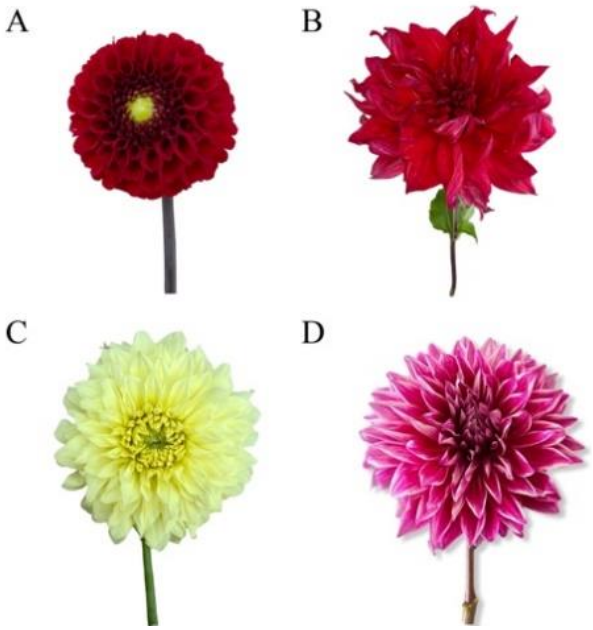


**Figure 1.** Photographs of four *Dahlia pinnata* Cav. varieties evaluated in three production environments in southeastern Coahuila de Zaragoza, Mexico. A: Antje; B: Babylon; C: Boy Mick; D: Canby Centennial.

The mean test performed on the agronomic variables evaluated showed significant differences ($p \leq 0.05$). For 6 out of 8 variables, better results were reflected in the shade net production environment (Table 2).

For the ADP variable, the Antje variety grown in the shade netting environment was the tallest, which could be the result of elongation caused by low exposure to light (Heredia-Hernández and Baltazar-Bernal, 2017), exceeding by 500 % the Canby Centennial variety, which presented the lowest value. Plants grown in shade netting were larger in size, showing significant differences with those obtained in open field and greenhouse. Plants with these characteristics represent an alternative for the producer, since a reduction in size can improve handling and presentation as potted plants (Laguna-Cerda *et al*., 2004). This variable is relevant for both crop management and inflorescence selection, since they are classified according to stem length (Flores-Ruvalcaba *et al*., 2005).

On the other hand, for the DBT variable, the Boy Mick variety grown in the shade net production environment had the thickest stems (27.13 mm), exceeding

**Table 2**. Test of means for the interactions between the two factors and the variables evaluated in plants and inflorescences of four varieties of *Dahlia pinnata* Cav.

| Treatment | ADP (cm) | DBT (mm) | NH | NTI | DAF (days) | NRT |
|---|---|---|---|---|---|---|
| c-A | 23.69 cd | 12.39 cd | 39.25 bcd | 5.50 de | 102.75 c | 10.04 ab |
| c-B | 31.92 cd | 16.13 bcd | 31.79 cd | 11.33 b-e | 86.00 ab | 15.00 a |
| c-BM | 39.19 bcd | 20.40 abc | 48.71 abc | 16.06 a-d | 80 a | 13.42 ab |
| c-CC | 24.28 cd | 11.84 cd | 49.86 abc | 5.58 de | 102.75 c | 10.92 ab |
| i-A | 35.25 cd | 10.80 d | 31.71 cd | 12.31 a-d | 87.50 abc | 8.25 ab |
| i-B | 20.23 cd | 13.86 cd | 19.33 d | 6.79 cde | 82.00 a | 9.92 ab |
| i-BM | 16.38 d | 11.71 cd | 17.19 d | 11.38 b-e | 101.25 bc | 10.44 ab |
| i-CC | 15.00 d | 7.19 d | 17.25 d | 3.22 e | 99.50 bc | 5.63 b |
| m-A | 91.31 a | 20.58 abc | 72.63 a | 17.79 abc | 76.75 a | 11.42 ab |
| m-B | 67.44 ab | 23.38 ab | 52.88 abc | 19.88 ab | 75.00 a | 11.94 ab |
| m-BM | 67.08 ab | 27.13 a | 65.23 ab | 27.67 a | 79.25 a | 10.04 ab |
| m-CC | 45.33 bc | 16.32 bcd | 62.61 ab | 14.94 b-e | 81.75 a | 7.42 ab |
| CV | 29.21 | 23.2 | 25.4 | 37.58 | 7.47 | 31.11 |

†Means with a common letter are not significantly different (Tukey, $p \leq 0.05$). CV: coefficient of variation; ADP: plant height; DBT: basal stem diameter; NH: number of leaves; NTI: total number of inflorescences; DAF: days to flowering; NRT: number of tuberous roots. c-A: Open field-Antje; c-B: Open field-Babylon; c-BM: Open field-Boy Mick; c-CC: Open field-Canby Centennial; i-A: Greenhouse-Antje; i-B: Greenhouse-Babylon; i-BM: Greenhouse-Boy Mick; i-CC: Greenhouse-Canby Centennial; m-A: Shade Netting-Antje; m-B: Shade Netting-Babylon; m-BM: Shade Netting-Boy Mick; m-CC: Shade Netting-Canby Centennial.

by 270 % the Canby Centennial variety grown in the greenhouse environment, which had the thinnest stems. Dahlia stems are hollow, which gives them a weak constitution (Jiménez-Mariña, 2015) when compared to other species; for example, *Tithonia diversifolia* (Hemsl.) A. Gray stems can measure 3.5 cm and have up to 36 vascular bundles, providing greater support (González-Castillo *et al*., 2014). Therefore, it is recommended that the Dahlia crop be protected from wind currents or rain. In contrast, Chrysanthemum stems show lower values (6 mm); however, their stems are not hollow (Gaytán-Acuña *et al*., 2006), giving greater consistency and support to the inflorescence (Flores-Ruvalcaba *et al*., 2005).

In terms of NH, the Antje variety had the highest values, with an average of 72.63 leaves for plants grown in the shade netting environment. This is consistent with the results obtained by Callejas-Chavero *et al.* (2020), who found a higher leaf production in closed sites than in open ones, which may be related to the absence of a canopy since they are exposed to environmental factors and, therefore, are vulnerable to various factors such as strong gusts of wind, rain, and hailstorms. On the other hand, the lowest values were expressed in plants grown in greenhouses, demonstrating that the high temperature in this environment induced stress on the plants, resulting in lower production of this organ (Heredia-Hernández and Baltazar-Bernal, 2017).

The most productive variety, regarding NTI, was the Boy Mick variety grown in shade netting, with an average of 27.67 inflorescences. The Canby Centennial variety, grown in greenhouses, produced 750 % less than the first. The Boy Mick variety was the second variety with the highest leaf production in the shade-mesh cover; since there was no thinning of this organ, the passage of light to the stems was limited, a factor that influences flowering (Sánchez-Vidaña *et al*., 2018). This also coincides with the fact that when grown under shade netting, this variety was the earliest in terms of the DAF variable. Fertilization is a factor that influences the flowering process, which was supplied under the same conditions in the three environments, inferring that the result could be due to other factors such as the temperature and humidity of the environments (Sánchez-Herrera *et al*., 2022).

The shade netting environment induced more precocity in DAF, since the four varieties had their first inflorescence before 82 days, with statistically significant differences ($p \leq 0.05$) when compared to the rest of the treatments. This demonstrates that this environment is ideal for producing inflorescences in a short period of time. Studies by Heredia-Hernández and Baltazar-Bernal (2017) report that Dahlias flowered 6 weeks after transplanting; however, the cultivation was carried out in 6" pots, whereas the present work was carried out in soil. Other species, such as sunflower (*Helianthus annuus* L.), may flower earlier (66 days after planting) (Carrillo-Criollo and Yumbla-Orbes, 2022), but the number of inflorescences varies from one for the latter and more than two for dahlias.

There were statistically significant differences ($p \leq 0.05$) in NRT. The Babylon variety produced the most units per plant in an open field environment, averaging 15 units per plant. Similar values were obtained by Lopera-Marín *et al*. (2020) in a study carried out on Yacon plants (*Smallanthus sonchifolius* (Poepp.) H. Rob.), which were established in similar conditions of distance between rows and between plants to those of the present study, and the high productivity may have been due to the generous distance during their development.

Pearson's correlation analysis applied to the variables showed a positive relationship ($p \leq 0.05$) between all of them (Figure 2), with the strongest relationship ($r = 0.82$) between ADP and NH, followed by ADP and NTI ($r = 0.75$). Previous studies have shown that when stems elongate, nodes appear, leading to an increase in the production of leaves and flower stems (Garzón-Solis *et al*., 2009). On the other hand, it could have been due to the use of shade netting, as it has been demonstrated that by reducing total radiation and photosynthetically active radiation, leaf area increases, resulting in a greater number of leaves (Ayala-Tafoya *et al*., 2011).

On the other hand, the variables LTF, PFF, and DTF showed significant differences ($p \leq 0.05$) (Figures 3, 4, and 5). The LTF presented by the Anje variety in the shade netting environment expressed the highest values (22.33 cm), significantly exceeding the behavior of the same variety produced in open field (Figure 3). The plants were not debudded, which was presumably the cause of the stem length, since doing so allows the main flower to reach stems of 60 to 70 cm long (Jiménez-Mariña, 2015), in addition to obtaining flowers with greater diameter (López *et al*., 2017).

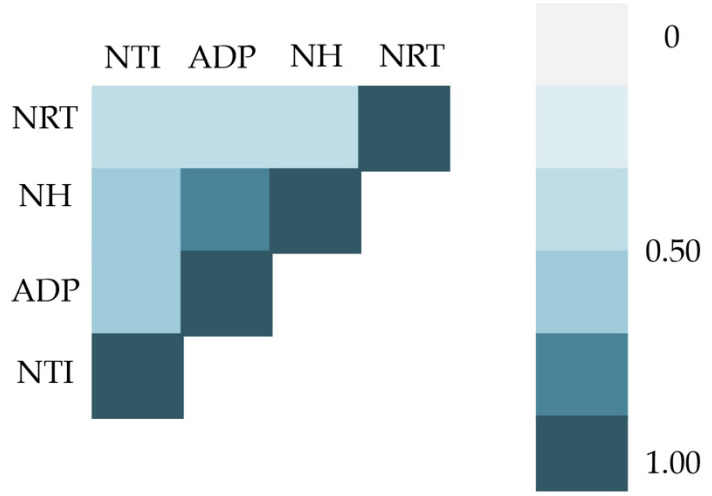


**Figure 2**. Pearson correlation matrix of the variables evaluated. Significant values ($p \leq 0.05$). NRT: number of tuberous roots; NH: number of leaves; ADP: plant height; NTI: total number of inflorescences.

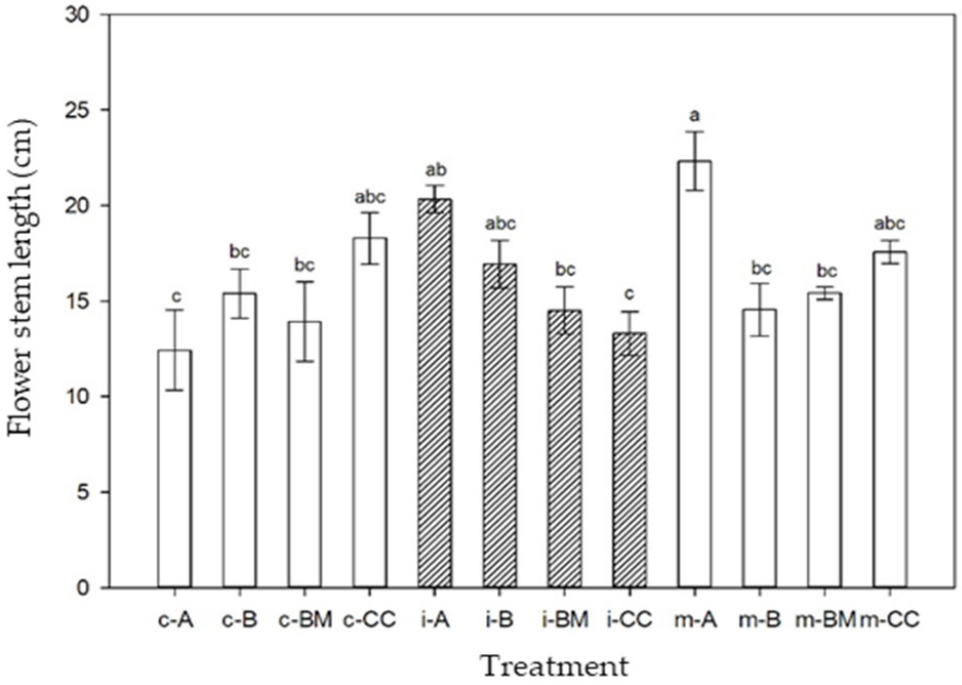


**Figure 3.** Differences in floral stem length of four varieties of *Dahlia pinnata* Cav. grown in three environments in southeastern Coahuila de Zaragoza, Mexico. Means with a common letter are not significantly different (Tukey, $p \leq 0.05$). c-A: Open field-Antje; c-B: Open field-Babylon; c-BM: Open field-Boy Mick; c-CC: Open field-Canby Centennial; i-A: Greenhouse-Antje; i-B: Greenhouse-Babylon; i-BM: Greenhouse-Boy Mick; i-CC: Greenhouse-Canby Centennial; m-A: Shade Netting-Antje; m-B: Shade Netting-Babylon; m-BM: Shade Netting-Boy Mick; m-CC: Shade Netting-Canby Centennial.

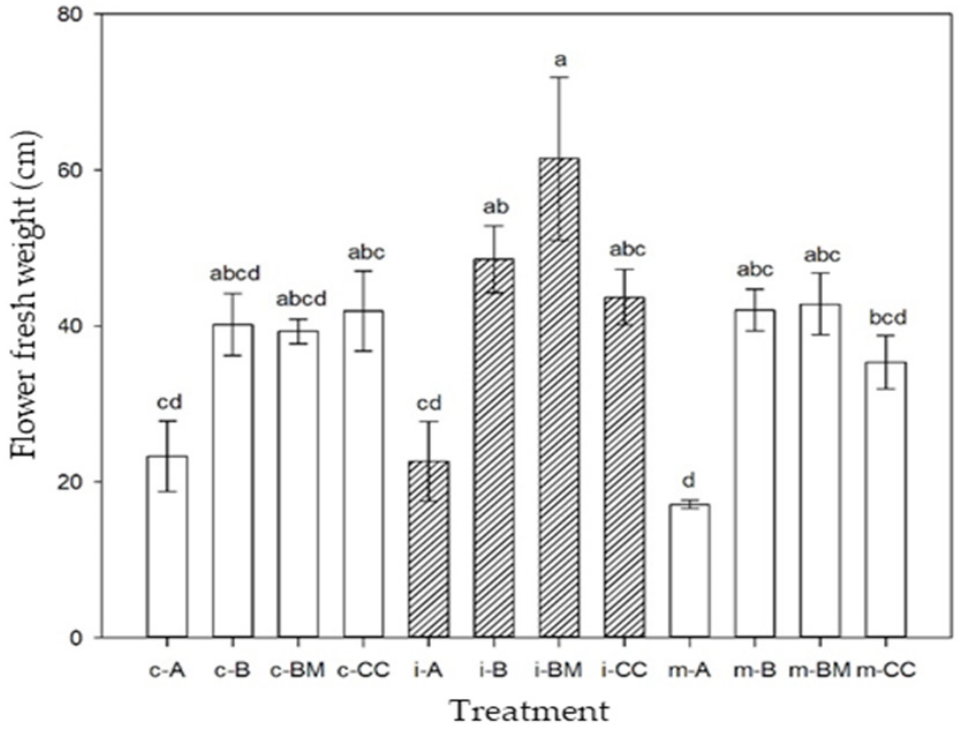


**Figure 4.** Influence of environment and variety of *Dahlia pinnata* Cav. on fresh weight of flowers produced in southeastern Coahuila de Zaragoza, Mexico. Means with a common letter are not significantly different (Tukey, $p \leq 0.05$). c-A: Open field-Antje; c-B: Open field-Babylon; c-BM: Open field-Boy Mick; c-CC: Open field-Canby Centennial; i-A: Greenhouse-Antje; i-B: Greenhouse-Babylon; i-BM: Greenhouse-Boy Mick; i-CC: Greenhouse-Canby Centennial; m-A: Shade Netting-Antje; m-B: Shade Netting-Babylon; m-BM: Shade Netting-Boy Mick; m-CC: Shade Netting-Canby Centennial.

The PFF was higher in flowers of the Boy Mick variety produced in the greenhouse, which increased by 250 % more than the variety with the lowest flower weight (Antje in shade netting) (Figure 4). The greenhouse had higher humidity than the open field and shade netting, promoting greater water absorption and resulting in higher fresh weight (Morales-Pérez *et al*., 2014).

There were no significant differences in the DF variable among the variables evaluated in the floral stems; however, the Antje variety grown in the greenhouse outgrew the same variety grown in the shade netting environment by more than 250 %, demonstrating that the supply or reduction of light does not affect the average diameter of the inflorescence (Chica-Toro and Correa-Londoño, 2005). Flores-Ruvalcaba *et al*. (2005) obtained a similar response, indicating that the genetic factor may be responsible for biomass accumulation in the flower.

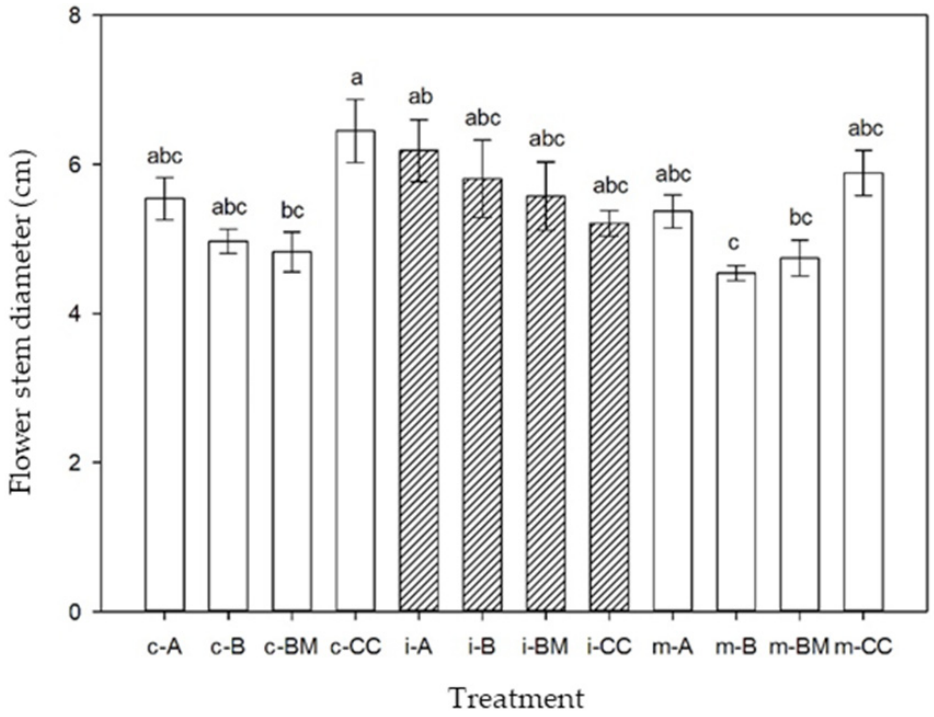


**Figure 5.** Difference in floral stem diameter of *Dahlia pinnata* Cav. flowers from three environments and four varieties of dahlias grown in southeastern Coahuila de Zaragoza, Mexico. Means with a common letter are not significantly different (Tukey, $p \leq 0.05$). c-A: Open field-Antje; c-B: Open field-Babylon; c-BM: Open field-Boy Mick; c-CC: Open field-Canby Centennial; i-A: Greenhouse-Antje; i-B: Greenhouse-Babylon; i-BM: Greenhouse-Boy Mick; i-CC: Greenhouse-Canby Centennial; m-A: Shade Netting-Antje; m-B: Shade Netting-Babylon; m-BM: Shade Netting-Boy Mick; m-CC: Shade Netting-Canby Centennial.

The thinnest DTF was shown by the inflorescences of the Babylon variety produced in the shade netting environment (4.54 mm). In contrast, the Canby Centennial variety grown in open field had 40 % thicker stems (Figure 5). Studies on flowering stems of *Freesia* × *hybrida* (Miranda-Villagómez *et al*., 2014) showed similar values to those in this experiment, indicating that even when the stems are hollow, their thickness is superior to other species, promoting greater support to the flower. On the other hand, the flower stalk of sunflower (*Helianthus annuus*) is a relevant parameter since it serves as a food reservoir for the formation of future organs (Carrillo-Criollo and Yumbla-Orbes, 2022).

## CONCLUSIONS

Dahlia cultivation in northeastern Mexico produces better results when using a shade netting production environment since it promotes plant productive development,

flowering in less time, and flowers with longer stems. However, the open field and greenhouse environments favor a higher production of tuberous roots and a higher fresh flower weight (in the BM variety), respectively. It is worth mentioning that this information represents an important turn in Dahlia production due to the economic and social significance it represents, in addition to the little information available on the same crop in southeastern Coahuila de Zaragoza, Mexico.

## REFERENCES

Ayala-Tafoya F, Zatarain-López DM, Valenzuela-López M, Partida-Ruvalcaba L, Velázquez-Alcaraz T de J, Díaz-Valdés T, Osuna-Sánchez JA. 2011. Crecimiento y rendimiento de tomate en respuesta a radiación solar transmitida por mallas sombra. Terra Latinoamericana 29 (4): 403–410.

Callejas-Chavero A, Pérez-Velázquez D, Palacios-Vargas JG, Castaño-Meneses G. 2020. Growth and leaves production of *Pittocaulon praecox* (Asteraceae) from two contrasting sites in a xerophytic shrubland in Mexico. Caldasia 42 (2): 330–332. https://doi.org/10.15446/caldasia.v42n2.73059

Carrasco-Ortiz M, Munguía-Lino G, Castro-Castro A, Vargas-Amado G, Harker M, Rodríguez A. 2019. Riqueza, distribución geográfica y estado de conservación del género *Dahlia* (Asteraceae) en México. Acta Botanica Mexicana 126 (e1354): 1–24. https://doi.org/10.21829/abm126.2019.1354

Carrillo-Criollo JF, Yumbla-Orbes M. 2022. Caracterización morfológica y análisis de crecimiento de tres cultivares de *Helianthus annuus* L. para flor de corte. Siembra 9 (1): e3323. https://doi.org/10.29166/siembra.v9i1.3323

Castro-Castro A, Rodríguez A, Vargas-Amado G, Harker M. 2012. Diversidad del género *Dahlia* (Asteraceae: Coreopsideae) en Jalisco, México y descripción de una especie nueva. Revista Mexicana de Biodiversidad 83 (2): 347–358.

Chica-Toro FJ, Correa-Londoño GA. 2005. Evaluación de dos tratamientos fotoperiódicos en crisantemo (*Dendranthema grandiflorum* (Ramat.) Kitam.), bajo condiciones del intertrópico andino alto. Revista Facultad Nacional Agronomía - Medellín 58 (2): 2859–2881.

Crocoll E, Verbeek B, Krausse F, Auinger H. 2023. Dahlienverzeichnis. Dahlia Catalog Listing of the Varieties. Stutensee, Germany. http://www.dahlie.net/de/Impressum.html (Retrieved: March 2023).

Şekerci AD, Gülşen O. 2016. Overview of Dahlia breeding. Horticulture 60: 199–204.

DOF (Diario Oficial de la Federación). 1963. Decreto por el que se declara símbolo de la floricultura nacional la flor de la dalia en todas sus especies y variedades. Secretaría de Agricultura y Ganadería. Ciudad de México, México. https://dof.gob.mx/nota_to_imagen_fs.php?codnota=4720563&fecha=13/05/1963&cod_diardi=203468 (Retrieved: March 2023).

Fernández-Pavía YL, Trejo-Téllez LI. 2018. Biología, importancia económica y principales líneas de investigación en Lisianthus: una especie ornamental nativa de México. Agro Productividad 11 (8): 177–182. https://doi.org/10.32854/agrop.v11i8.1115

Flores-Ruvalcaba JS, Becerril-Román AE, González-Hernández VA, Tijerina-Chávez L, Vásquez-Rojas T. 2005. Crecimiento vegetativo y floral del crisantemo [*Dendranthema x grandiflorum* (Ramat) Kitamura] en respuesta a la presión osmótica de la solución nutritiva. Revista Chapingo Serie Horticultura 11 (2): 241–249.

Garzón-Solis C, Mejía-Muñoz JM, Trejo-Calzada R, Gómez-Lorence F, Espinosa-Flores A, Sánchez-Abarca C. 2009. Fenología de dalia campanulata (*Dahlia campanulata* Saar.): nueva especie para la horticultura ornamental. Revista Chapingo Serie Zonas Áridas 8 (1): 19–24.

Gaytán-Acuña EA, Ochoa-Martínez DL, García-Velasco R, Zavaleta-Mejía E, Mora-Aguilera G. 2006. Producción y calidad comercial de flor de crisantemo. Terra Latinoamericana 24 (4): 541–548.

González-Castillo JC, Hahn von-Hessberg CM, Narváez-Solarte W. 2014. Características botánicas de *Tithonia diversifolia* (Asterales: Asteraceae) y su uso en la alimentación animal. Boletín Científico Centro de Museos Museo de Historia Natural de la Universidad de Caldas 18 (2): 45–58.

Heredia-Hernández D, Baltazar-Bernal O. 2017. Producción y comercialización de *Dahlia variabilis* Cav., en maceta en las altas montañas de Veracruz, México. Agroproductividad 10 (6): 84–90.

Hernández-Epigmenio F, García-Mateos MR, Sosa-Montes E, Mejía-Muñoz JM, Fernández-Pavia YL, Cruz-Álvarez O, Martínez-Damián MT. 2022. Perfil fenólico y valor nutricional de flores de *Dahlia x hortorum*. Revista Chapingo Serie Horticultura 28 (3): 161–174. https://doi.org/10.5154/r.rchsh.2022.03.004

Jiménez-Mariña L. 2015. El cultivo de la dalia. Cultivos Tropicales 36 (1): 107–115.

Laguna-Cerda A. 2007. Manual gráfico para la descripción varietal de dalia. Servicio Nacional de Inspección y Certificación de Semillas: Tlanepantla, México. 116 p.

Laguna-Cerda A, Martínez JV, Guadarrama-Guadarrama ME. 2004. Reducción de la altura en plantas de dalia [*Dahlia variabilis* (Willd.) Desf.] con Unicozole-P (Sumagic). Ciencia Ergo Sum 11 (1): 59–64.

Lopera-Marín JJ, Angulo-Arizala J, Murgueitio-Restrepo E, Mahecha-Ledesma L. 2020. Production of tubers and aerial biomass of yacón *Smallanthus sonchifolius* (Poepp.) H. Rob. (Asteraceae) for animal feed in the tropical highlands of Colombia. Livestock Research for Rural Development 32 (8): 1–6.

López L, Barrios N, Sarubbi H, González V, Vázquez V. 2017. Manual de floricultura Producción y manejo fitosanitario. Instituto Interamericano de Cooperación para la Agricultura: Asunción, Paraguay. 63 p.

Marroquín-Morales P, Méndez-González J, Jiménez-Pérez J, Aguirre-Calderón OA, Yerena-Yamallel JI. 2018. Estimación de biomasa aérea en *Pinus cembroides* Zucc. y *Pinus halepensis* Mill. en Saltillo, Coahuila. Revista Mexicana de Ciencias Forestales 9 (47): 94–110. https://doi.org/10.29298/rmcf.v9i47.172

Mera-Ovando LM, Bye Boettler R. 2006. La Dahlia una belleza originaria de México. Revista Digital Universitaria 7 (11): 1–11.

Mera-Ovando LM, Mejía-Muñoz JM, Bye-Boettler RA, Laguna-Cerda A, Espinosa-Flores A, Treviño de Castro G. 2008. Diversidad de dalias cultivadas. Secretaría de Agricultura, Ganadería, Desarrollo Rural, Pesca y Alimentación; Servicio Nacional de Inspección y Certificación de Semillas; Sistema Nacional de Recursos Fitogenéticos para la Alimentación; La Agricultura Red de Ornamentales: Tlalnepantla, México. 49 p.

Miranda-Villagómez É, Carrillo-Salazar JA, Rodríguez-Mendoza MN, Colinas-León MT, Livera-Muñoz M, Gaytán-Acuña EA. 2014. Crecimiento y calidad del tallo floral de *Freesia x hybrida* en hidroponía. Revista Fitotecnia Mexicana 37 (1): 31–39.

Molar-Orozco ME, Velázquez-Lozano J, Vázquez-Jiménez MG. 2020. Comportamiento térmico de tres prototipos en Saltillo, Coahuila (bloques de tierra, concreto y tapa de huevo). Revista Hábitat Sustentable 10 (1): 22–31. https://doi.org/10.22320/07190700.2020.10.01.02

Morales-Pérez E, Morales-Rosales EJ, Franco-Mora O, Pérez-López DJ, González-Huerta A, Urbina-Sánchez E. 2014. Producción de flores de *Gerbera jamesonii* cv. 'Dream' en función de los ácidos giberélico y salicílico. Phyton 83 (2): 333–340.

Orozco-Hernández ME, García-Fajardo B, Álvarez-Arteaga G, Mireles-Lezama P. 2017. Tendencias del sector agrícola, Estado de México. Quivera 19 (1): 99–121.

Sall J. 2020. JMP Statistical Discovery. Cary, NC, USA.

Sánchez-Chávez E, Rodríguez A, Castro-Castro A, Pérez-Farrera MA, Sosa V. 2019. Spatio-temporal evolution of climbing habit in the *Dahlia-Hidalgoa* group (Coreopsidae, Asteraceae). Molecular Phylogenetics and Evolution 135: 166–176. https://doi.org/10.1016/j.ympev.2019.03.012

Sánchez-Herrera JH, Oliva M, Collazos R, Meléndez-Mori JB. 2022. Efecto de la fertilización y aplicación de fitohormonas sobre la floración y rendimiento de *Hylocereus megalanthus* (K. Schum. ex Vaupel). Revista de Investigaciones Agropecuarias 48 (2): 155–159.

Sánchez-Vidaña MR, Tejeda-Sartorius O, Hernández-Anguiano AM, Trejo-Téllez LI, Soto-Hernández RM, Gaytán-Acuña EA. 2018. Ambiente y antecedentes de floración en el crecimiento, inducción y desarrollo floral de *Laelia anceps* subesp. *anceps* (Orchidaceae). Agrociencia 52 (1): 35–54.

SNICS (Servicio Nacional de Inspección y Certificación de Semillas). 2022. Catálogo nacional de variedades vegetales 2022. Servicio Nacional de Inspección y Certificación de Semillas, Ciudad de México, México. https://www.gob.mx/snics/articulos/catalogo-nacional-de-variedades-vegetales-cnvv-2022 (Retrieved: January 2023).

Soriano-Melgar LAA, López-Guerrero AG, Córtez-Mazatan G, Mendoza-Mendoza E, Peralta-Rodríguez RD. 2018. Nanopartículas de óxido de zinc y óxido de zinc/grafeno empleadas en soluciones florero durante la vida poscosecha de lisianthus (*Eustoma grandiflorum*). Agroproductividad 11 (8): 137–144. https://doi.org/10.32854/agrop.v11i8.1109

Steiner A. 1961. A universal method for preparing nutrient solutions of a certain desired composition. Plant and Soil 15 (2): 134–154. https://doi.org/10.1007/BF01347224

Tejeda-Sartorius O, Ríos-Barreto Y, Trejo-Téllez LI, Vaquera-Huerta H. 2015. Caracterización de la producción y comercialización de flor de corte en Texcoco, México. Revista Mexicana de Ciencias Agrícolas 6 (5): 1105–1118. https://doi.org/10.29312/remexca.v6i5.602

Valdez-Hernández EF, Flores-Vilchez F, Pedraza-Santos ME, Colinas-León MT, Ramírez-Guerrero LG, Martínez-Cárdenas L, García-Díaz RF. 2018. Distribution of *Euphorbia strigosa* Hook and Arn: a Mexico native plant with ornamental potential. Revista Bio Ciencias 5 (1): e303.

Villaseñor JL. 2018. Diversity and distribution of the Asteraceae family in Mexico. Botanical Sciences 96 (2): 332–358. https://doi.org/10.17129/botsci.1872

Agrociencia

# FEMUR CHARACTERISTICS AND FECAL NITROGEN IN HEALTHY AND CANCER-AFFECTED WISTAR RATS SUPPLEMENTED WITH INULIN AND AGAVE FRUCTANS

Evelyn **Regalado-Rentería**[1], Bertha Irene **Juárez-Flores**[1], Juan Carlos **García-López**[1], César Iván **Godínez-Hernández**[1], Miguel Ángel **Ruiz-Cabrera**[2], Juan Rogelio **Aguirre-Rivera**[1]*

[1] Universidad Autónoma de San Luis Potosí. Instituto de Investigación de Zonas Desérticas. Altair 200, Fracc. del Llano, San Luis Potosí, San Luis Potosí, Mexico. C. P. 78377.
[2] Universidad Autónoma de San Luis Potosí. Facultad de Ciencias Químicas. Av. Dr. Manuel Nava Martínez 6, Zona Universitaria, San Luis Potosí, San Luis Potosí, Mexico. C. P. 7821.
* Author for correspondence: rogelio.aguirre@uaslp.mx

**Citation:** Regalado-Rentería E, Juárez-Flores BI, García-López JC, Godínez-Hernández CI, Ruiz-Cabrera MA, Aguirre-Rivera JR. 2023. Femur characteristics and fecal nitrogen in healthy and cancer-affected Wistar rats supplemented with inulin and agave fructans. **Agrociencia** 57(8): 1709-1717. doi.org/ 10.47163/agrociencia.v57i8.2716

**Editor in Chief:**
Dr. Fernando C. Gómez Merino

Received: March 15, 2022.
Approved: July 04, 2023.
**Published in Agrociencia:** October 30, 2023.



## ABSTRACT

The aim of this study was to evaluate the effect of 10 % supplementation with commercial chicory fructans (I), commercial *Agave tequilana* fructans (ATC), experimental *A. tequilana* fructans (ATE), experimental *A. salmiana* fructans (AS), rice starch (RS), and a control diet (C) on Wistar rats, both healthy and carcinogen-induced to colorectal cancer. It was hypothesized that agave and chicory fructans have similar effects. The supplements evaluated in both experiments maintained the dry weight and length of rat femurs in both groups without producing significant changes. Only healthy rats supplemented with chicory and both *A. tequilana* fructans showed higher fecal nitrogen levels. The femur ash content in rats that were carcinogen-induced to develop colorectal cancer was significantly lower ($p \leq 0.05$) than the content in healthy rats. Minerals in the femurs of both groups of rats were similar. The hypothesis of this work was rejected.

**Keywords**: prebiotics, colorectal cancer, femur mineral content, fecal nitrogen.

## INTRODUCTION

Prebiotic consumption has been related to increased intestinal absorption and bioavailability of some macro minerals such as calcium, magnesium, and phosphorus, as well as micro minerals such as iron and zinc (Kruger *et al.*, 2003; Scholz-Ahrens *et al.*, 2007; Weaver *et al.*, 2011). The potential mechanisms of prebiotics' influence on calcium absorption in the large intestine are related to the increase in calcium solubility as a result of a pH reduction induced by the increase in bacterial synthesis of short-chain fatty acids (SCFA), an increase in the dynamic trans-epithelial interchange of cellular $H^+$ and $Ca^{+2}$ triggered by the SCFA, or an increase in the absorption area growth and levels of calbindin-D in the large intestine due to cellular proliferation promoted by metabolites produced by the resident microbiota, such as butyrate or polyamines (Whisner and Castillo, 2018).

Prebiotics can increase the intestinal absorption of other minerals such as magnesium and zinc, given that several of their effects are not specific to calcium, such as the microstructure change of intestinal tissue and mineral availability (Raschka and Daniel, 2005). Phytic acid, naturally present and abundant in insoluble fiber, is considered to be responsible for the absorption and retention of some minerals (calcium, magnesium, and zinc) due to its chelation property. In contrast, soluble fiber consumption, such as pectin, gum, resistant starch, lactulose, fructooligosaccharides (FOS), and inulin, has been demonstrated to increase mineral absorption and bioavailability (López *et al*., 2000). This is due to intake and fermentation increasing SCFA concentrations, decreasing pH, hypertrophying cecal tissue, and promoting phytic acid dissociation and its negative effects on mineral homeostasis (López *et al*., 2000).

Soluble fiber improves mineral solubility, permeability, and absorption in the gut (Raschka and Daniel, 2005; Scholz-Ahrens and Schrezenmeir, 2007), as well as mineral bioavailability for bones (Scholz-Ahrens *et al*., 2007). Moreover, diets with high soluble fiber reduce protein utilization while increasing fecal nitrogen excretion (Falcón *et al*., 2011). Fecal nitrogen originates from dietary protein that escapes digestion, endogenous protein from pancreatic and intestinal secretions, detached epithelial cells, blood urea after diffusing through the intestinal tract, and increased bacterial mass (Beynen *et al*., 2002; Delzenne *et al*., 2011).

The aim of this study was to compare the effects of commercial chicory, *A. tequilana* fructans, and standardized stem fructans from *A. salmiana* and *A. tequilana* on femur mineral absorption and nitrogen content in the feces of healthy and carcinogen-induced colorectal cancer Wistar rats. It was hypothesized that agave and chicory fructans have similar effects in this regard.

## MATERIALS AND METHODS

### Tested polysaccharides

Chicory fructans (*Cichorium intybus* L.), known as inulin (Orafti® Synergy 1, Tienen, Belgium), *A. tequilana* fructans F.A.C. Weber (Inufib™, Jalisco, Mexico), and rice starch (Tres Estrellas®, Toluca, Mexico) were the commercial polysaccharides used. In addition, *A. salmiana* and *A. tequilana* fructans extracted from the stems of six individuals in optimum physiological maturity (Aguirre-Rivera *et al*., 2001) from the Charcas (San Luis Potosí) and Arandas (Jalisco) regions were included as noncommercial polysaccharides, both extracted according to the process developed in our laboratory (Godínez-Hernández *et al*., 2016).

### Animals and diets

A total of 36 male, two-month-old Wistar rats with an average body weight of 200−250 g were used for each experiment. The animals were provided by the Centro de Biociencias of the Universidad Autónoma de San Luis Potosí. The experimental unit was regarded as each individual rat, which were housed in separate polypropylene

cages in a climate-controlled environment with a temperature between 20 and 25 °C, relative humidity between 30 and 60 %, and an inverted circadian cycle of 12 h of light and 12 h of darkness. Animals were kept in accordance with the local ethical guidelines for cautions and proper maintenance (NOM 062-ZOO-1999). Protocols were approved by the institutional ethics committee (CONBIOÉTICA-24-CEI-003-20160830).

The animals were given a one-week adaptation period with a *per capita* portion of 25 g of standard rodent feed (Chow® 5008, Brentwood, MO, USA) and *ad libitum* water. Moreover, six treatments were assigned at random (n = 6): standard commercial feed (C) or 90 % same feed plus 10 % of the following polysaccharides: commercial inulin (I), commercial fructans from *A. tequilana* (ATC), experimental fructans from *A. tequilana* (ATE), experimental fructans from *A. salmiana* (AS), and commercial rice starch (RS). Commercial fructans contain a higher proportion of FOS, whereas AS fructans have a lower polymerization degree (Regalado-Rentería *et al*., 2020).

During the 20-week experimental trial, each feed portion for all treatments, with or without supplementation, was administered every day at the start of the dark period. Standard composition of the feed was 12 % moisture, 23 % protein, 6.5 % fat, 4 % fiber, 8 % ash, and 46.5 % nitrogen free extract: with an energy content of 84.12 Kcal per 25 g. At the end of the experiments, all animals were sacrificed with pentobarbital sodium (0.063 g $mL^{-1}$) (SEDALPHARMA®, Pet´s Pharma, Mexico) at an intraperitoneal dose of 40 mg $kg^{-1}$ live weight.

### Inducement of incipient colorectal carcinogenesis

After eight weeks of treatment, the colon cancer preneoplastic stage was induced by administering two intraperitoneal doses of 15 mg of the carcinogenic drug azoxymethane (AOM) (Sigma-Aldrich®, San Louis Missouri, USA, A2853) by kg of body weight, dissolved in sterile solution saline (0.85 %) (Dávila-Céspedes *et al*., 2014), one at the end of the eighth week and the other at the end of the ninth week of the experimental period.

### Mineral content and femur characterization

At the end of the experimental period, both femurs per animal were dried and immersed in a 0.85 % saline solution. The muscular tissue was removed and the femurs were dried (at 40 °C for 36 h) (Shel-Lab FX-14, USA) until constant weight (Sartorius BPAA1S, Germany) and their length was measured with a digital vernier (Digital Cadena® Model A020, China).

Ash content was estimated using the left femur (550 °C after 6 h) (LINDBERG SB, 51844, Mexico). The macro and micro mineral content of the pulverized right femur was estimated after the organic matter was removed with concentrated $H_2NO_3$. Calcium, magnesium, phosphorus, and potassium content were determined using an optical emission spectrometer (Thermo Scientific iCAP 7000 Series, USA) and atomic emission spectrometry with plasm coupled inductively (ICP-OES); sodium, iron, zinc,

and sulfur were determined using mass plasma spectrometry coupled inductively (ICP-MS) with a quadrupole system in a spectrophotometer of optical emission coupled to a mass spectrometer.

### Nitrogen content in feces

At the end of the experiment, sample feces were collected and dried to constant weight 15 (40 °C for 36 h) (Shel-Lab FX-14, USA); then, 100 mg of dry feces were used to estimate the 16 nitrogen content, according to AOAC 993.13 methodology using a FLASH 2000 17 N/Protein analyzer (Thermo Scientific™, Series No. 2015FO106).

### Experimental design and statistical analysis

A completely randomized design was used in both groups of rats, healthy and carcinogen-induced colorectal cancer. One-way analysis of variance (ANOVA) and the Tukey test ($p \leq 0.05$) were used. SAS 9.2 (SAS Institute Inc., 2019) was used for statistical analysis. The Student's *t*-test was used to compare all variables between the two experiments: healthy rats and carcinogen-induced colorectal cancer rats; the error probability was set at 5 % ($p \leq 0.05$).

## RESULTS AND DISCUSSION

### Femur mineral content and characterization

There were no differences ($p > 0.05$) in dry weight and femur length in both experiments, in contrast to the results found by Lobo *et al*. (2006) and Rivera-Huerta *et al*. (2017), who observed an increase in femur mass, density, and volume in response to FOS supplementation, attributing this to fructan consumption decreasing bone turnover through suppression of osteoclast resorption.

There were no differences ($p > 0.05$) among treatments for K, Zn, and Fe in healthy rats (Table 1) or colorectal cancer rats (Table 2). In contrast, there were some differences ($p \leq 0.05$) in healthy rats and colorectal cancer rats for Ca, P, Na. and Mg (Tables 1 and 2).

**Table 1**. Mineral content (mg $g^{-1}$ dry matter) in femurs of healthy Wistar rats.

| Treatment | Ca | P | Na | S | Mg | K | Zn | Fe |
|---|---|---|---|---|---|---|---|---|
| C | 644.83± 5.65a | 294.34± 4.76b | 29.09±0.89b | 17.60±0.22a | 11.47±0.60a | 1.54±0.14a | 0.95±0.17a | 0.21±0.11a |
| I | 611.17±29.94ab | 322.71±31.00ab | 34.72±2.31a | 17.88±0.36a | 10.55±0.65ab | 1.86±0.31a | 0.91±0.10a | 0.20±0.03a |
| CAT | 599.94±23.76ab | 343.97±24.10ab | 25.56±0.78b | 17.89±0.07a | 9.71±0.81ab | 1.55±0.07a | 1.13±0.04a | 0.25±0.06a |
| EAT | 607.01±20.14ab | 335.17±20.18ab | 27.74±1.39b | 17.94±0.65a | 9.41±0.82b | 1.67±0.28a | 0.77±0.03a | 0.28±0.07a |
| AS | 600.85±5.65ab | 343.77±5.21ab | 25.32±0.88b | 17.56±0.36a | 9.60±1.02ab | 1.52±0.32a | 1.07±0.25a | 0.31±0.09a |
| RS | 586.37±12.60b | 356.14±2.14a | 27.04±2.14b | 17.95±0.26a | 9.77±0.07ab | 1.65±0.21a | 0.83±0.13a | 0.25±0.04a |
| *p-value* | 0.0484 | 0.0393 | <0.0001 | 0.8391 | 0.0311 | 0.4359 | 0.3316 | 0.2807 |

C: control; I: commercial inulin; CAT: commercial fructans from *A. tequilana*; EAT: experimental fructans from *A. tequilana*; AS: fructans from *A. salmiana*; RS: rice starch. a,b: Means with different letters in the same column are statistically different ($p \leq 0.05$).

**Table 2.** Mineral content (mg $g^{-1}$ dry matter) in femurs of carcinogen-induced colorectal cancer Wistar rats.

| Treatment | Ca | P | Na | S | Mg | K | Zn | Fe |
|---|---|---|---|---|---|---|---|---|
| C | 648.42± 5.79a | 290.62±4.56b | 29.14±0.66ab | 17.41±0.46a | 11.52±0.04a | 1.64±0.25a | 0.95 ±0.02a | 0.30±0.12a |
| I | 610.75±24.09ab | 332.21±39.17ab | 26.66±0.76b | 17.61±0.75a | 10.65±0.98a | 1.13± 0.13a | 0.82±0.03a | 0.17±0.01a |
| CAT | 607.86±10.89ab | 337.40±11.02a | 25.59±0.58b | 17.53±0.15a | 9.02 ±0.36b | 1.30±0.19a | 1.00±0.22a | 0.28±0.01a |
| EAT | 616.81±12.29ab | 324.68±9.53ab | 27.66±1.76ab | 17.74±0.66a | 10.59±0.49a | 1.45±0.22a | 0.83±0.17a | 0.21±0.06a |
| AS | 589.46± 7.39b | 354.15±6.72a | 26.18±1.31b | 17.59±0.51a | 10.09±0.45ab | 1.18±0.24a | 1.11±0.17a | 0.22±0.05a |
| RS | 627.69± 2.88ab | 309.22±3.21ab | 30.79±0.52a | 18.15±0.17a | 11.24±0.18a | 1.58±0.24a | 1.11±0.41a | 0.24±0.05a |
| *p-value* | 0.0167 | 0.0074 | 0.0049 | 0.7307 | 0.0021 | 0.1376 | 0.4292 | 0.2645 |

C: control; I: commercial inulin; CAT: commercial fructans from *A. tequilana*; EAT: experimental fructans from *A. tequilana*; AS: fructans from *A. salmiana;* RS: rice starch. a,b: Means with different letters in the same column are statistically different ($p \leq 0.05$).

In both healthy and colorectal cancer rats, the highest Ca concentrations were found in the control treatment. Thus, the increased intestinal absorption and bioavailability of Ca and P assumed for the fructans (Kruger *et al*., 2003; Raschka and Daniel, 2005) was not reflected in a higher concentration in the femur, as reported by García-Vieyra *et al.* (2014). However, it is likely that this occurred for the P concentration in rats that were carcinogen-induced to colorectal cancer for the AS treatment (Table 2), corresponding to *A. salmiana* fructans. For all treatments with fructans, the Ca-P ratio changed from 1.6:1 to 1.9:1, which is less than the normal 2:1 ratio (Rivera-Huerta *et al*., 2017).

In general, supplementation with fructans has little effect on femur mineral concentration. It should be noted that inulin (I) induced the highest Na content in healthy rats, but one of the lowest values in colorectal cancer rats; in addition, in the experiment with colorectal cancer rats, *A. salmiana* (AS) fructans induced the lowest Ca content and the highest P content, in a 1.6:1 ratio.

### Nitrogen content in feces

The experiment with healthy rats revealed a significant ($p \leq 0.05$) increase in nitrogen content in feces for three out of the four fructan treatments (Table 3). In contrast, in the experiment with unhealthy rats, all treatments had similar nitrogen fecal content.

In general, high levels of nutritional fiber increase N excretion in feces. Moreover, diets high in soluble fiber reduce protein utilization while increasing fecal nitrogen excretion (Falcón *et al*., 2011). Feces nitrogen is derived from dietary protein that escapes digestion and endogenous proteins such as pancreatic and intestinal secretions, detached epithelial cells, and blood urea after diffusion through the intestinal gut (Beynen *et al*., 2002).

Fructans, in addition to interfering with protein digestion because they are indigestible, are a basic substrate for a variety of intestinal acidophilous bacteria (Rendón-Huerta *et al*., 2011); therefore, supplementation with these prebiotics significantly increases

**Table 3.** Effect of supplementation on fecal nitrogen content (mg $g^{-1}$ dry matter).

| Treatment | Healthy | Colorectal cancer |
|---|---|---|
| C | 36.0 ± 3.3b | 38.3 ± 2.2a |
| I | 43.8 ± 1.8a | 44.4 ± 1.7a |
| CAT | 43.6 ± 2.6a | 41.8 ± 5.5a |
| EAT | 44.3 ± 3.3a | 37.7 ± 4.1a |
| AS | 40.5 ± 4.6ab | 37.7 ± 5.7a |
| RS | 34.9 ± 2.5b | 38.7 ± 3.9a |
| *p-value* | 0.0014 | 0.3756 |

C: control; I: commercial inulin; CAT: commercial fructans from *A. tequilana*; EAT: experimental fructans from *A. tequilana*; AS: fructans from *A. salmiana*; RS: rice starch. a,b: Means with different letters in the same column are statistically different ($p \leq 0.05$).

the quantity of these bacteria in the cecum, gut, and feces, which in turn incorporate a significant portion of residual N, lower the pH, and thus reduce ammoniacal absorption in the colon (Cani and Delzenne, 2011; Delzenne *et al.*, 2011). Reduced intestinal ammonia absorption reduces urea generation in the liver, causing N excretion to shift from urine to feces. As a result, fructans favor the extra renal route of N excretion while increasing N elimination via the feces (Younes *et al.*, 1999).

## Contrast between experiments

Aspects probably involved in the prebiotics-mediated stimulation of mineral absorption, solubility, and bone mineralization are due to the decrease in pH in the intestinal lumen caused by the production of short-chain fatty acids, aside from indirectly stimulating passive calcium absorption by increasing its solubility via lowering the pH with the exchange of cellular proton ($H^+$) for luminal cation ($Ca^{++}$) (Scholz-Ahrens *et al*., 2007).

The dry weight, length, ashes, and main minerals in the bones were compared in both experiments on healthy and carcinogen-induced colorectal cancer patients (Table 4). There were differences ($p \leq 0.05$) in ashes percentage with the lowest value for the unhealthy rats, possibly due to the bone demineralization presented by cancer patients due to their pathological and degenerative physiological processes (Rivera-Huerta *et al*., 2017). There were statistical similarity ($p > 0.05$) for the rest of the variables evaluated.

**Table 4.** Femur parameters and minerals (mg $g^{-1}$) by state of health.

| Item | Healthy | Colorectal cancer | *p-value* |
|---|---|---|---|
| Ashes (%) | 67.28 ± 8.91a | 57.78 ± 3.23b | 0.001 |
| Dry weigth (g) | 0.88 ± 0.02a | 0.92 ± 0.11a | NS |
| Length (mm) | 42.42 ± 2.21a | 41.48 ± 2.23a | NS |
| Ca | 609.67 ± 33.92a | 612.82 ± 22.31a | NS |
| P | 331.62 ± 25.51a | 329.12 ± 24.42a | NS |
| Na | 28.4 ± 3.62a | 27.3 ± 1.92a | NS |
| S | 17.8 ± 1.14a | 17.6 ± 1.49a | NS |
| Mg | 10.0 ± 0.92a | 10.3 ± 0.77a | NS |
| K | 1.64 ± 0.21a | 1.35 ± 0.11a | NS |
| Zn | 0.94 ± 0.11a | 0.98 ± 0.12a | NS |
| Fe | 0.25 ± 0.03a | 0.23 ± 0.04a | NS |

a,b: Means with different letters between rows are statistically different ($p \leq 0.05$).

## CONCLUSIONS

The supplements tested in both experiments resulted in no significant changes in femur dry weight or length. Only healthy rats supplemented with chicory and *Agave tequilana* fructans had higher fecal nitrogen.

The femur ash content in rats affected by colorectal cancer was notably lower than in healthy rats. The minerals in the femurs of rats in both experiments were similar.

## ACKNOWLEDGMENTS

To the Consejo Nacional de Humanidades Ciencias y Tecnologías (CONAHCyT) for the PhD scholarship granted to first author E. Regalado. To Dr. María Elena García Arreola for the technical assistance of the mineral analysis.To Dr. Manuel Núñez Muñoz (Nutrición y Genética Saludable, S.A. de C.V.) for the financial support for this study, through the grant "Programa de Estímulos a la Innovación PEI-CONACYT", No. 251911. To Megafarma S.A. de C.V. for chicory inulin donation. Authors disclose that financiers did not have any participation or access into the experimental design, data collection and analysis; nor on the decision for publishing this manuscript.

## REFERENCES

Aguirre-Rivera JR, Charcas-Salazar HF, Flores-Flores JL. 2001. El maguey mezcalero potosino. Universidad Autónoma de San Luis Potosí, Consejo Potosino de Ciencia y Tecnología: San Luis Potosí, México. 87 p.

Beynen AC, Baas JC, Hoekemeijer PE, Kappert HJ, Bakker MH, Koopman JP, Lemmens AG. 2002. Faecal bacterial profile, nitrogen excretion and mineral absorption in healthy dogs fed supplemental oligofructose. Journal of Animal Physiology and Animal Nutrition 86 (9–10): 298–305. https://doi.org/10.1046/j.1439-0396.2002.00386.x

Cani PD, Delzenne NM. 2011. The gut microbiome as therapeutic target. Pharmacology and therapeutics 130 (2): 202–212. https://doi.org/10.1016/j.pharmthera.2011.01.012

Dávila-Céspedes A, Juárez-Flores BI, Pinos-Rodríguez JM, Aguirre-Rivera JR, Oros-Ovalle AC, Loyola-Martínez ED, Andrade-Zaldívar H. 2014. Protective effect of Agave salmiana fructans in azoxymethane-induced colon cancer in Wistar rats. Natural Product Communications 9 (10): 1503–1506. https://doi.org/10.1177/1934578X1400901025

Delzenne NM, Neyrinck AM, Cani PD. 2011. Modulation of the gut microbiota by nutrients with prebiotic properties: Consequences for host health in the context of obesity and metabolic syndrome. Microbial Cell Factories 10 (1): S10. https://doi.org/10.1186/1475-2859-10-S1-S10

Falcón VM del R, Barrón HJM, Romero BAL, Domínguez SMF. 2011. Efecto adverso en la calidad proteica de los alimentos de dietas con alto contenido de fibra dietaria. Revista Chilena de Nutrición 38 (3): 369–375. https://doi.org/10.4067/s0717-75182011000300012

García-Vieyra MI, Del Real A, López MG. 2014. Agave fructans: their effect on mineral absorption and bone mineral content. Journal of Medicine Food 17 (11): 1247–1255. https://doi.org/10.1089/jmf.2013.0137

Godínez-Hernández CI, Aguirre-Rivera JR, Juárez-Flores BI, Ortiz-Pérez MD, Becerra-Jiménez J. 2016. Extracción y caracterización de fructanos de *Agave salmiana* Otto ex Salm-Dyck. Revista Chapingo Serie Ciencias Forestales y del Ambiente 22 (1): 59–72. https://doi.org/10.5154/r.rchscfa.2015.02.007

Kruger MC, Brown KE, Collett G, Layton L, Schollum LM. 2003. The effect of fructooligosaccharides with various degrees of polymerization on calcium bioavailability in the growing rat. Experimental Biology and Medicine 228 (6): 683–688. https://doi.org/10.1177/153537020322800606

Lobo AR, Colli C, Filisetti TM. 2006. Fructooligosaccharides improve bone mass and biomechanical properties in rats. Nutrition Research 26 (8): 413–420. https://doi.org/10.1016/j.nutres.2006.06.019

López HW, Coudray C, Levrat-Verny MA, Feillet-Coudray C, Demigné C, Rémésy C. 2000. Fructooligosaccharides enhance mineral apparent absorption and counteract the deleterious effects of phytic acid on mineral homeostasis in rats. The Journal of Nutritional Biochemistry 11 (10): 500–508. https://doi.org/10.1016/S0955-2863(00)00109-1

Raschka L, Daniel H. 2005. Mechanisms underlying the effects of inulin-type fructans on calcium absorption in the large intestine of rats. Bone 37 (5): 728–735. https://doi.org/10.1016/j.bone.2005.05.015

Regalado-Rentería E, Aguirre-Rivera JR, Godínez-Hernández CI, García-López JC, Oros-Ovalle AC, Martínez-Gutiérrez F, Martinez-Martinez M, Ratering S, Schnell S, Ruíz-Cabrera MÁ, Juárez-Flores BI. 2020. Effects of agave fructans, inulin and starch on metabolic syndrome aspects in healthy Wistar rats. ACS Omega 5 (19): 10740–10749. https://doi.org/10.1021/acsomega.0c00272

Rendón-Huerta JA, Juárez-Flores BI, Pinos-Rodríguez JM, Aguirre-Rivera JR, Delgado-Portales RE. 2011. Effects of different kind of fructans on *in vitro* growth of *Lactobacillus acidophilus*, *Lactobacillus casei*, and *Bifidobacterium lactis*. African Journal of Microbiology Research 5 (21): 2706–2710. https://doi.org/10.5897/ajmr11.455

Rivera-Huerta M, Lizárraga-Grimes VL, Castro-Torres IG, Tinoco-Méndez M, Macías-Rosales L, Sánchez-Bartéz F, Tapia-Pérez GG, Romero-Romero L, Gracia-Mora MI. 2017. Functional effects of prebiotic fructans in colon cancer and calcium metabolism in animal models. BioMed Research International 2017: 9758982. https://doi.org/10.1155/2017/9758982

SAS Institute Inc. 2019. Statistical Analysis System version 9.4. Windows. SAS Institute, Inc., Cary, NC, USA. 1028 p.

Scholz-Ahrens KE, Ade P, Marten B, Weber P, Timm W, Asil Y, Glüer CC, Schrezenmeir J. 2007. Prebiotics, probiotics, and synbiotics affect mineral absorption, bone mineral content, and bone structure. The Journal of Nutrition 137 (3): 838S–846S. https://doi.org/10.1093/jn/137.3.838s

Scholz-Ahrens KE, Schrezenmeir J. 2007. Inulin and oligofructose and mineral metabolism: The evidence from animal trials. The Journal of Nutrition 137 (11): 2513S–2523S. https://doi.org/10.1093/jn/137.11.2513s

Weaver CM, Martin BR, Nakatsu CH, Armstrong AP, Clavijo A, McCabe LD., McCabe GP, Duignan S, Schoterman MHC, van den Heuvel EGHM. 2011. Galactooligosaccharides improve mineral absorption and bone properties in growing rats through gut fermentation. Journal of Agricultural and Food Chemistry 59 (12): 6501–6510. https://doi.org/10.1021/jf2009777

Whisner CM, Castillo LF. 2018. Prebiotics, bone and mineral metabolism. Calcified Tissue International 102 (4): 443–479. https://doi.org/10.1007/s00223-017-0339-3

Younes H, Alphonse JC, Behr SR, Demigné C, Rémésy C. 1999. Role of fermentable carbohydrate supplements with a low-protein diet in the course of chronic renal failure: experimental bases. American Journal of Kidney Diseases 33 (4): 633–646. https://doi.org/10.1016/S0272-6386(99)70213-1

Agrociencia

# IMPORTANCE OF PINEAPPLE (*Ananas comosus* L.) WASTE AS A POSSIBLE SOURCE OF INDUSTRIAL PROTEASES

Nelda Xanath **Martínez-Galero**[1*], Rosa Elia **Agüero-Padilla**[2], Alejandro **Hernández-López**[1], Alma Xochil **Avila-Alejandre**[1], Jeiry **Toribio-Jiménez**[3], Héctor **López-Arjona**[1]

[1] Universidad del Papaloapan. Centro de Investigaciones Científicas. Circuito Central 200, Col. Parque Industrial, San Juan Bautista Tuxtepec, Oaxaca, Mexico. C.P. 68301.
[2] Universidad del Papaloapan. Ingeniería en Biotecnología. Circuito Central 200, Col. Parque Industrial, San Juan Bautista Tuxtepec, Oaxaca, Mexico. C.P. 68301.
[3] Universidad Autónoma de Guerrero. Facultad de Ciencias Químico-Biológicas, Laboratorio de Microbiología Molecular y Biotecnología Ambiental. Av. Lázaro Cárdenas s/n, Col. El Centenario, Chilpancingo de los Bravo, Guerrero, Mexico. C.P. 39086.
* Author for correspondence: nmartinez@unpa.edu.mx

**Citation:** Martínez-Galero NX, Agüero-Padilla RE, Hernández-López A, Avila-Alejandre AX, Toribio-Jiménez J, López-Arjona H. 2023. Importance of pineapple (*Ananas comosus* L.) waste as a possible source of industrial proteases. **Agrociencia** 57(8): 1718-1729. doi.org/ 10.47163/agrociencia.v57i8.2973

**Editor in Chief:**
Dr. Fernando C. Gómez Merino

Received: February 18, 2023.
Approved: August 08, 2023.
**Published in Agrociencia:** November 16, 2023.



## ABSTRACT

Pineapple (*Ananas comosus* L.) is a tropical fruit highly valued for its flavor, sweetness, aroma, and nutraceutical properties. The 'Cayena Lisa' cultivar is the most widely used for both fresh consumption and industrial purposes in Mexico. The municipalities of Tuxtepec and Loma Bonita, in the state of Oaxaca, produce around 582 thousand Mg of solid waste per year from fruit processing, to which the waste from plantations attacked by pests and diseases must be added. Consequently, these wastes must be processed in order to generate added value. Isolation of cysteine proteases from industrial residues is one possibility. In the present study, the parameters of the Mexican Official Standard for measuring pH (NOM-F-317-S-1978), total soluble solids (SST) (NMX-F-103-1982), and cysteine-protease activity in pineapple fruit processing residues at two stages of ripening over four months of harvest were used to determine whether there is a factor of quality attributes that correlates with the activity of this protein. In both ripening stages, cysteine-protease activity is higher in August. Regardless of the degree of ripening, peel and core are the best sources of cysteine-proteases. SST and pH values have no correlation with cysteine-protease activity, so they cannot be used as indicators of such activity. The findings show that 'Cayena Lisa' pineapple residues grown in Loma Bonita, Oaxaca, could be a good source of cysteine-proteases.

**Keywords**: agro-industrial wastes, peptidases, revalorization of agricultural wastes.

## INTRODUCTION

Pineapple (*Ananas comosus* L.) is a tropical plant highly valued for the flavor, sweetness, aroma, and nutraceutical properties of its fruit (Mohd *et al.*, 2020). In Mexico, the 'Cayena Lisa' variety accounts for nearly 80 % of pineapple production, both for fresh consumption and for industrialization of pulp, juices, and peptidases, due to its size, weight, pale yellow color, pulp softness, and reducing sugar content (Uriza-Ávila *et*

*al*., 2018). Pineapple harvesting generates two types of waste: harvesting and canning waste, both of which produce a large amount of solid waste. Some authors mention that waste production from pineapple processing can constitute 25 to 35 %, or even up to 50 %, of the total weight of the fruit (Seleni *et al*., 2014; Conesa *et al*., 2015), depending on the commercial form of the product. It is worth mentioning that waste derived by food processing generates solid waste management and pollution problems (Hikal *et al*., 2021).

Banerjee *et al*. (2018) pointed out that the low valorization of pineapple residues is due to the lack of knowledge of their potential economic value. Pineapple residues represent raw materials that can be converted into high-value products, such as silage, paper, fabrics, biopolymers, cellulose and hemicellulose, fertilizers, methane, ethanol, citric acid, antioxidant compounds, and proteolytic enzymes. Pineapple proteases are proteins that have applications in the food industry as a meat tenderizer, in the hydrolysis of soluble proteins, beer and wine production, cosmetic, and pharmaceutical industries. In the clinical area, they have been successfully employed as phytotherapeutics (Arshad *et al*., 2014; Banerjee *et al*., 2018; Santos *et al*., 2021). Bromelain is the most well-known pineapple cysteine endopeptidase, with a global market worth $2 956 120 000 USD and a compound annual growth rate (CAGR) of 4.72 % from 2022 to 2027 (Market Reports World, 2022). The 'Cayena Lisa' variety's potential utility for this purpose needs to be confirmed.

The Mexican state of Oaxaca contributes 13 % of national pineapple production, and the municipalities of Loma Bonita and San Juan Bautista Tuxtepec generate 80 % of state production (SIAP, 2022). Pineapple pulp and juice are the most commonly used in industrial processing; the rest of the plant material (crown, peel, core, stem, and trimmings) is discarded. In the Papaloapan Basin region, 582 thousand Mg of solid waste are generated annually, to which the waste from plantations whose fruits are attacked by pests and diseases must be added. There is a clear need to seek a biotechnological solution for processing and generating added value from these agroindustrial wastes (Hikal *et al*., 2021).

The objectives of this study were to determine: the cysteine-protease activity in the pulp and in the different parts that make up the pineapple fruit residues (peel, core, and crown); the changes in cysteine-protease activity during the harvest period (from May to August); and the relationship between this activity and quality attributes (total soluble solids (SST) and pH), in order to decide on the destination of the harvest and its residues.

## MATERIALS AND METHODS

Sigma-Aldrich reagents were used. Plant material was provided by the Unión Estatal de Productores de Piña (State Union of Pineapple Producers) in Loma Bonita, Oaxaca, during the period May-August 2019, in a commercial plantation (18° 4' 0.4'' N, 95° 53' 32.4'' W). Each month, fruits were selected from *Ananas comosus* (L). Merr, cultivar 'Cayena Lisa', without disease or pest symptoms, at two stages of physiological

maturity, based on color criteria corresponding to Code 2 (C2) and Code 5 (C5) according to NMX-FF-028-SCFI-2008 (Garcia-Tain *et al*., 2011).

The experimental unit consisted of five randomly selected fruits from each ripening stage, in each sampling month. The fruits were transported to the Food Workshop of the Universidad del Papaloapan (UNPA) in Tuxtepec, Oaxaca, where they were washed with a water jet to remove soil and air-dried. The fruits were cut, and the pulp and residues (peel, crown, and core) were separated. The pulp was used to evaluate enzyme activity. Each type of residue from the five fruits was mixed to have a composite sample.

To prepare the homogeneous fresh extract, 100 g of each composite mixture were taken; they were ground in a centrifugal juice extractor (Oster) to obtain the crude extracts. The resulting mixture was filtered using gauze, and 2 mL aliquots of each crude extract were taken in triplicate and centrifuged at 10 000 xg for 20 min at 4 °C. The supernatant was kept at 4 °C until enzymatic evaluation, which was performed the same day upon completion of sample extraction of each residue and pulp.

Subsequently, the solid portion of each extract was removed by centrifugation at 5000 xg for 8 min at room temperature. The pH was measured according to Mexican Official Standard NOM-F-317-S-1978 in a HI 2211 ORP Meter (Hanna® Instruments, Mexico). SST was quantified as indicated in NMX-F-103-1982. Zero calibration of the optical refractometer (Atago Master-M, Bellevue, WA, USA) was performed by adding 40 μL of distilled water at room temperature through the prism; for the experimental samples, 40 μL of the supernatant of the centrifuged crude extract were used, waiting one minute to obtain the sample result. The results were expressed in °Brix. Readings were taken in triplicate for each crude extract.

For the calculation of the specific activity, total proteins were quantified by the Bradford method, using bovine serum albumin (BSA) as a standard (Bradford, 1976). From the crude extracts of each residue, 2 mL were taken in triplicate, centrifuged at 10 000 xg for 20 min at 4 °C; 25 μL of the supernatant of each sample were used and mixed with 1 mL of Bradford's reagent; absorbance was recorded at 595 nm in a UV-Vis spectrophotometer (Thermo Scientific™ Waltham, MA, USA).

The proteolytic activity of cysteine endopeptidases in crude enzyme extracts was determined by the method modified by Ketnawa *et al*. (2012): the assay is based on the proteolytic hydrolysis of casein by cysteine endopeptidases to release L-tyrosine. The peptidase activity calibration curve was performed with six concentrations of L-tyrosine (0, 100, 200, 300, 400, and 500 μg $mL^{-1}$) in reaction buffer (casein 1 % w/v, cysteine 0.03 M, EDTA 0.006 M, potassium phosphate 0.05 M, pH 7.0).

For the samples, 1 mL of the supernatant of the crude extracts and 1 mL of the reaction buffer were mixed. The reaction was carried out at 37 °C for 10 min and stopped by adding 3 mL of 5 % w/v trichloroacetic acid (TCA) to precipitate the casein. The reaction mixture was centrifuged at 8000 xg for 10 min and the supernatant with L-tyrosine was measured at 275 nm. The reactions were carried out in triplicate. A unit of enzyme activity was defined as the amount of enzyme releasing a product

equivalent to 1 µg tyrosine $min^{-1}$ $mL^{-1}$ under standard assay conditions and was expressed as casein digesting units (CDU $mL^{-1}$ $mg\ protein^{-1}$).

### Statistical analysis

Statistical analyses were performed in Minitab Statistical Software (19) and Microsoft Excel (2019). Differences between samples for pH, SST, protein concentration, and enzyme activity were determined by analysis of variance; comparison of means was performed by Tukey's test ($p < 0.05$).

## RESULTS AND DISCUSSION

Representative images of the samples used in the study are shown below (Figure 1). The average weight of the peel, core, and pulp of the four monthly samplings was higher in the fruit at the most advanced ripening stage (C5, 88 % w/w) than in the fruit at the C2 stage (80.2 % w/w). For the crowns, the highest weight corresponded to C2 (19.8 % w/w) (Table 1). The higher crown weight in C2 may be because the fruit filling process had not yet been completed, so this structure was not yet entering senescence (Uriza-Ávila *et al*., 2018).

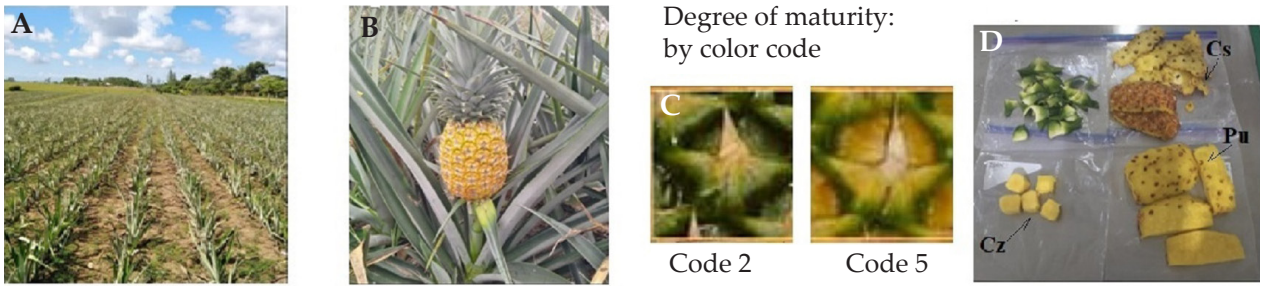


**Figure 1**. Representative images of the *Ananas comosus* L. plantation and fruits used in the study. A: plantation in Loma Bonita, Oaxaca; B: ripe fruit (C5); C: maturity degree classification; D: material used to obtain the fresh pulp extract (Pu) and the peel (Cs), crown (Co), and core (Cz) residues.

**Table 1.** Average weight of pulp and residue of pineapple (*Ananas comosus* L.) fruits at two ripening stages. Averages of four monthly samplings, May to August 2019.

| Part of the fruit | Maturity stage | | | |
|---|---|---|---|---|
| | C2 | | C5 | |
| | kg | % w/w* | kg | % w/w* |
| Peel | 0.843 | 30.7 | 0.978 | 32.1 |
| Crown | 0.543 | 19.8 | 0.358 | 11.8 |
| Core | 0.462 | 16.8 | 0.586 | 19.2 |
| Pulp | 0.899 | 32.7 | 1.124 | 36.9 |
| Total: | 2.747 | 100 | 3.046 | 100 |

*Weight proportion of residues compared to the whole fruit.

At both ripening stages, pulp accounted for 33 and 37 % (w/w) of the average total fruit weight, while the total sum of residue weight (peel, core, and crown) accounted for 67 and 63 % (w/w) in C2 and C5 pineapples, respectively. These data were similar to those obtained by Ketnawa *et al*. (2012) and Conesa *et al*. (2015) for 'Nang Lea' and 'Phu Lea' varieties, where the residues (peel, core, stem, and crown) produced during processing represented approximately 50 % (w/w) of the total fruit weight. These authors indicate that peel and core constituted the main residues, which was confirmed in the present study as peel and core represented 47.5 and 51.3 % w/w of the residues in pineapples at C2 and C5 stages, respectively. The municipality of Loma Bonita produced approximately 123 038 Mg of pineapple in 2021, of which 74 901 were of the 'Cayena Lisa' variety (SIAP, 2022). The usable industrial waste in the process of extracting by-products, including cysteine-proteases, is approximately 37 450 Mg per season; therefore, the potential for useful raw material is enormous.

Regarding the physicochemical characterization (Table 2), at the C2 ripening stage, the pH values of the peel were the lowest compared to the other residues, and did not show significant variations in any of the four months of harvest (Figure 2A).

**Table 2**. pH values of various parts of the fruit of pineapple (*Ananas comosus* L.) varieties.

| Variety | Part of the fruit | | | |
|---|---|---|---|---|
| | Peel | Core | Other | Reference |
| Morris | 4.04 ± 0.02 | 3.89 ± 0.01 | 3.92 ± 0.01 (pulp) | Misran *et al.* (2019) |
| N36 | 3.94 ± 0.01 | -- | -- | Nadzirah *et al.* (2012) |
| Phu Lea | 4.01± 0.13 | 4.09± 0.22 | 4.64± 0.22 (stem) | Ketnawa *et al.* (2012) |
| Nang Lea | 4.02 ± 0.30 | 4.27 ± 0.24 | 4.76 ± 0.16 (stem) | |
| **Cayena Lisa C2** | **3.91 ± 0.17** | **4.98 ± 0.22** | **4.61± 0.97 (pulp)** | **This study** |
| **Cayena Lisa C5** | **4.20 ± 0.49** | **4.48± 0.47** | **5.26 ± 0.84 (pulp)** | **This study** |

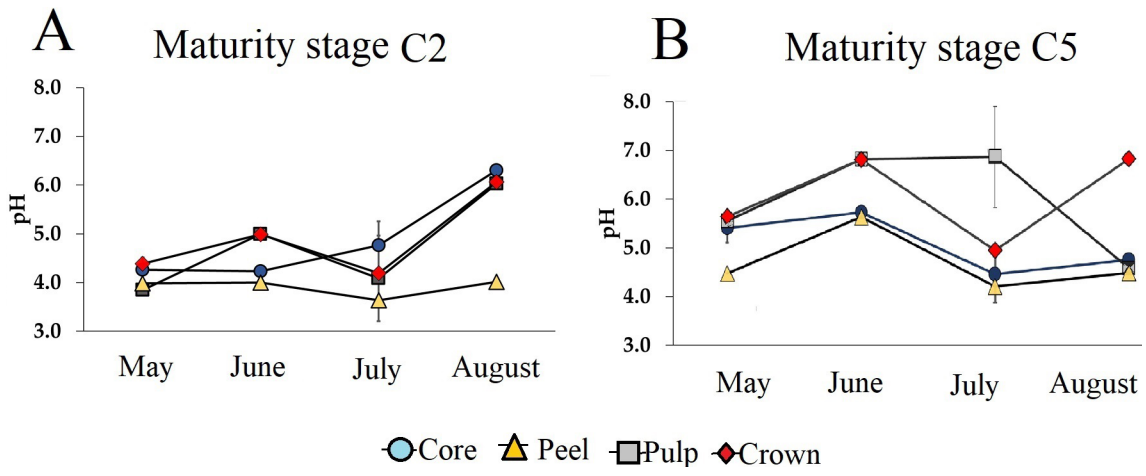


**Figure 2**. pH values in pineapple (*Ananas comosus* L.) from different parts of the fruit at two maturity stages, during the months of harvest (n = 3).

The pH values of the core, pulp, and crown remained at around 4 to 5 for the first three months and increased significantly ($p \geq 0.05$) in August with comparison to the peel values, showing no differences between them. The final pH value of the fruit components, except the peel at this stage of ripening, was close to 6 (Figure 2A).

In the case of samples at the C5 ripening stage, the pH values of each fruit component varied throughout the months (Figure 2B). In the month of May, the pH of the peel was 4.01±0.01, which was significantly lower than that of the other residues (around 5, on average). In June, the pH of the pulp, peel, and crown increased; the core showed no significant changes. In July, except for pulp, pH decreased in all residues. In August, the pH values of the crown (6±0.01) were significantly higher than those of the peel, core, and pulp (around 4).

The average pH of the residues during the period analyzed was 4.64±0.69 and 4.82±0.45 for C2 and C5, respectively, which are higher than the values described for 'Cayena Lisa' grown in China, which ranged from 3.58 to 3.86 (Lu *et al*., 2014), or for 'Cayena Sarawak' at maturity stage 5 (maximum maturity). Soloman *et al*. (2016) observed that the mean pH value was around 3.88±0.18, and suggested that it is an internal indicator of maturity that can be used to determine the best harvesting period. The pH of a fruit is the result of the mixture of various compounds; Truc *et al*. (2008) observed that the acid composition of unripe pineapple includes mainly citric acid, malic acid, and succinic acid, which decrease during fruit ripening following a conversion of organic acids to reducing sugars (Siti Rashima *et al*., 2021). These physicochemical changes give pineapple its characteristic flavor and odor.

Another important parameter in the physicochemical characterization of fruit is SST, which is usually expressed as a percentage or °Brix. At ripening stage C2 (Figure 3A),

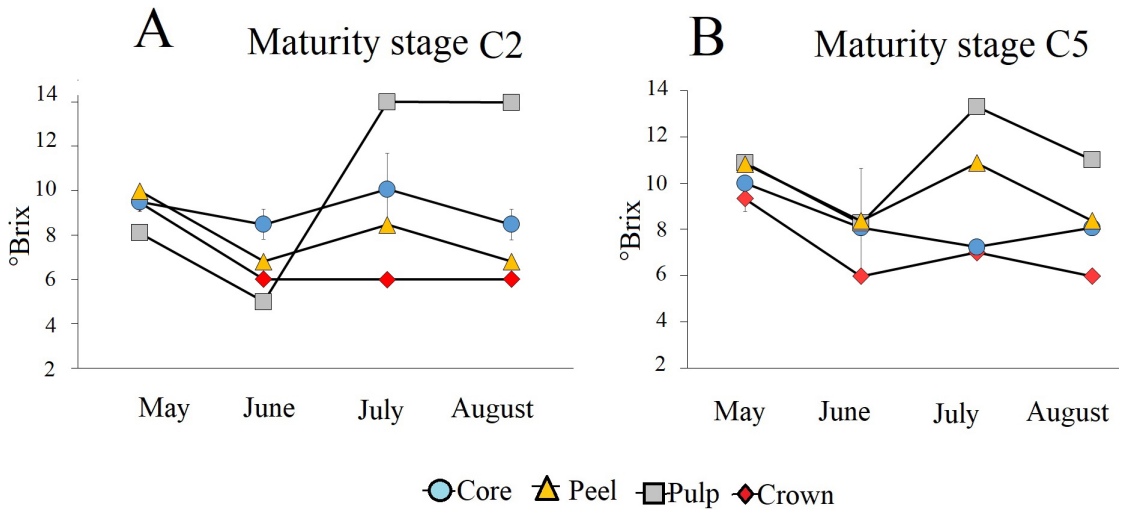


**Figure 3.** Average total soluble solids content (°Brix) of pineapple (*Ananas comosus* L.) pulp and residues at two maturity stages, during the harvest months (n = 3).

core SST values did not show significant differences in any of the months and remained between 8.3 and 10 °Brix, while those of the pulp and peel decreased significantly in July and August compared to May (Figure 3A). This indicates that from May and June onwards, the concentration of soluble solids, probably sugars, increases. The residue with the lowest SST was the peel, while the pulp showed the highest SST values (around 13) and these remained stable over time. On the other hand, at the C5 ripening stage, the pulp had the highest SST values, followed by the peel, core, and crown; this trend repeated itself in all harvesting months. Pineapple 'Cayena' is described as one of the cultivars with high SST values compared to other varieties. The results of this study for *A. comosus* cv. 'Cayena Lisa' (8 to 14 °Brix) are higher than the cultivars 'Nang Lae', 'Phu Lae', 'N36', and the 'Morris' variety, where the °Brix range from 2.55 for peel to 6.27 for crown (Ketnawa *et al*., 2012; Misran *et al*., 2019).

Finally, the results indicated the presence of cysteine protease activity in the pulp and in all pineapple residues (Figure 4). The CDU activity was very similar, regardless of residue type or ripening stage. Proteolytic activity was minimal in the period from May to July in all parts analyzed, except the crown in May. In August, activity increased significantly in the pulp and in all residues.

Regardless of maturity stage, the maximum activity for all tissues occurred in August, though the parts showed differential proteolytic activity in this month. This could be due to the functions of proteases within the plant, as explained below. At stage C5, the peel had the highest activity and the crown had the lowest (Figure 5). The activity of cysteine proteases at the C2 ripening stage in the pulp and peel (20.48 and 17.39 $mL^{-1}$ $mg^{-1}$) was significantly higher than that in the core and crown (16 and 2.84 CDU $mL^{-1}$ $mg^{-1}$, respectively). In the case of C5 samples core and peel (15.73 and 21.85 CDU $mL^{-1}$ $mg^{-1}$, respectively) had significantly higher activity compared to pulp and crown.

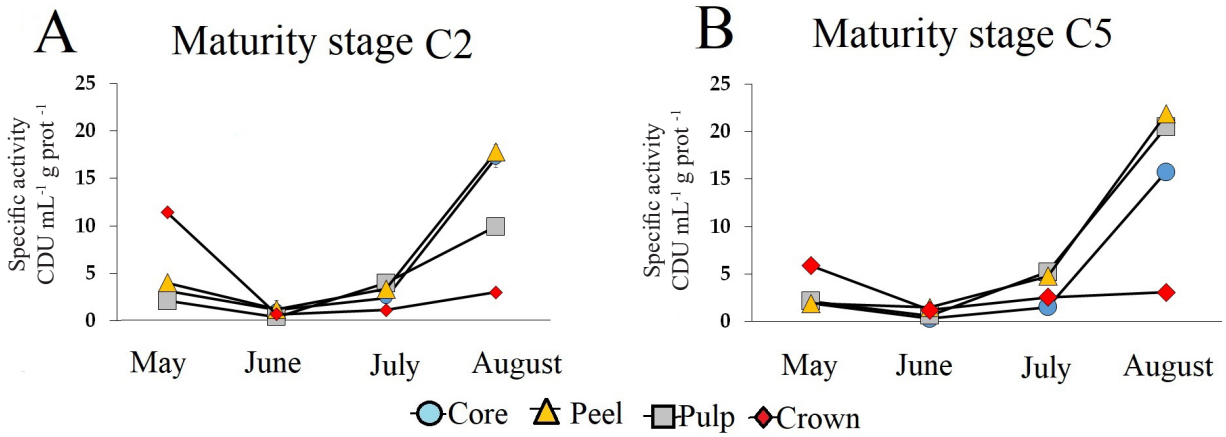


**Figure 4**. Cysteine protease activity in pulp and residues of pineapple (*Ananas comosus* L.) of two ripening stages, during the months of harvest (n = 3).

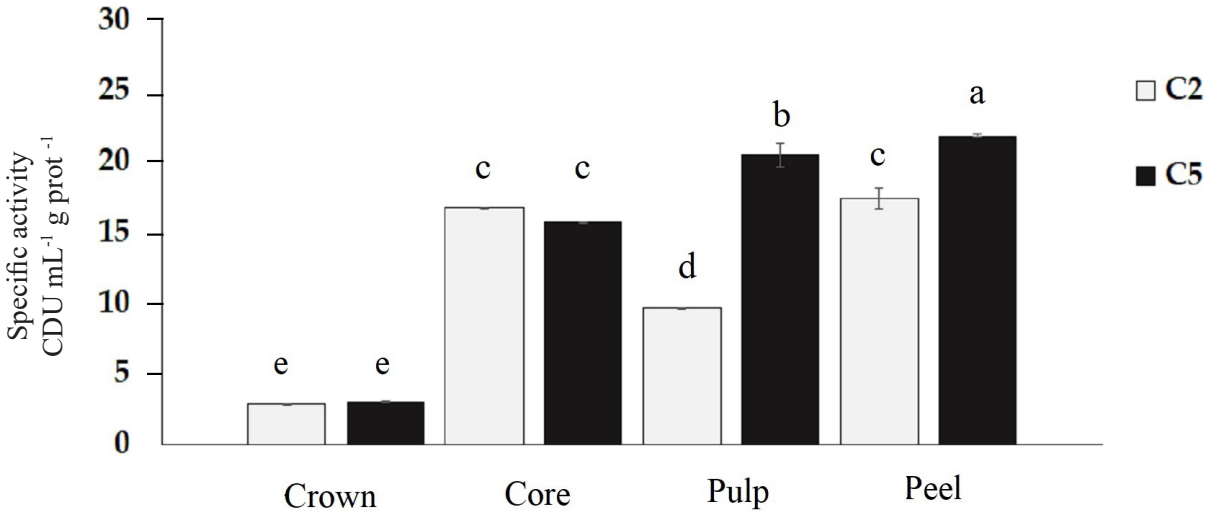


**Figure 5.** Proteolytic activity of different pineapple parts corresponding to the month of August for two ripening stages (n = 3; different letters indicate significant differences, Tukey $p \leq 0.05$).

This behavior is similar to that described by other authors; for example, in cultivars 'Nang Lae' and 'Phu Lae', it was observed that the extract from each type of residue exhibited different proteolytic activity and protein content: the highest value was from the crown, while the extract from the stem had the lowest value in both cultivars (Vasiljevic, 2019). On the other hand, pineapple core extracts have greater effect on meat tenderizing than peel and pulp extracts; this may indicate that pineapple core contains bromelain with higher enzymatic activity than that of any other part of the fruit (Clavijo *et al*., 2012).

Cysteine-proteases are involved in the control of apoptosis, the hypersensitive response (HR), senescence, embryogenesis, floral development, several types of environmental stress, and pathogen resistance in various plant species (Grudkowska and Zagdańska, 2004; López-García *et al.*, 2012). Hydric stress is one of the most common stresses in plants; although studies of its effect on pineapple are scarce, drought is known to delay flowering and affects fruit morphology and quality (Ortiz, 2022).

One of the mechanisms of stress response includes protein degradation by proteases, which is closely related to the synthesis of new proteins. On the other hand, although the effect of excess moisture on protease activity has been less studied, it is known to affect fruit morphology (water core) and increase susceptibility to pathogen attack, particularly fungi (Shu, 2019). The above suggests that seasonal environmental factors could influence protease activity. From May to August, in the Loma Bonita area, rainfall gradually increases; the month with the most rainfall is August (CONAGUA, 2022) which coincides with the maximum peak of cysteine protease activity (Figure 6). Temperature is another environmental factor to consider.

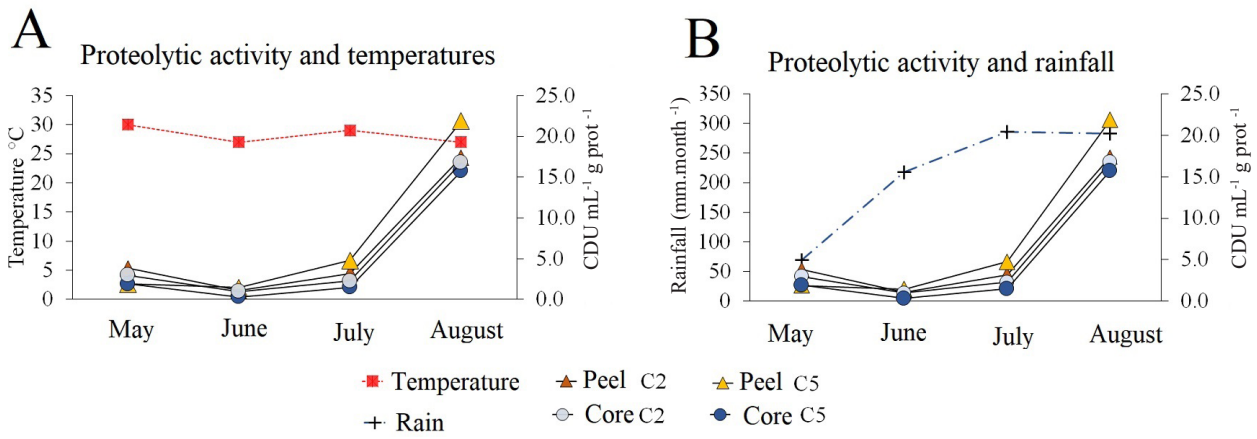


**Figure 6.** Relationship of proteolytic activity of pineapple fruit parts with environmental conditions of temperature and rainfall during the harvest months.

The record does not show significant differences in temperature during the sampling months; however, such months correspond to the hottest time of the year in Mexico (CONAGUA, 2022). In particular, the period of highest temperature during the year is known as "canícula", which in 2019 lasted 40 days and officially ended on August 20 of that year.

As indicated, the edible portion of pineapple fruit is about 35 %. Waste in the canning industry ranges between 45 and 65 %, and includes, among others, peel and trimmings (Difonzo *et al*., 2019), which, due to their large volume, can become a focus of microbiological and environmental infection. Therefore, revaluing waste by obtaining by-products is an attractive alternative; in particular, obtaining enzymes is interesting, as there is a market for them. Extracts obtained from *A. comosus* residues can also be a source of phosphatases, glucosidases, peroxidases, cellulases, glycoproteins, and carbohydrates, in addition to cysteine-endopeptidases.

## CONCLUSIONS

Two stages of pineapple fruit ripening (C2 and C5) were evaluated, and both showed different behaviors for pH and SST. The pH of fruit increased during the C2 stage and peaked in August; on the contrary, in the C5 stage, pH increased in June and decreased again in August. On the other hand, SST decreased compared to May and remained stable until August. As for cysteine protease activity, the maximum values occurred in August in all parts of the fruit. In particular, the peel and core sections had a significantly higher activity than the pulp and crown in both ripening stages, which represents an advantage since proteases can be obtained from these residues, remaining as an element to be considered in the value chain of the commercialization of the 'Cayena Lisa' pineapple in the Papaloapan Basin region.

## ACKNOWLEDGEMENTS

We thank the Unión Estatal de Productores de Piña (State Union of Pineapple Producers) in Loma Bonita, Oaxaca, for providing the biological material used in this study.

## REFERENCES

Arshad ZIM, Amid A, Yusof F, Jaswir I, Ahmad K, Loke SP. 2014. Bromelain: An overview of industrial application and purification strategies. Applied Microbiology and Biotechnology 98 (17): 7283–7297. https://doi.org/10.1007/s00253-014-5889-y

Banerjee S, Ranganathan V, Patti A, Arora A. 2018. Valorisation of pineapple wastes for food and therapeutic applications. Trends in Food Science & Technology 82 (1): 60–70. https://doi.org/10.1016/j.tifs.2018.09.024

Bradford MM. 1976. A rapid and sensitive method for the quantification of microgram quantities of protein utilizing the principle of Protein-Dye binding. Analytical Biochemistry 72 (1–2): 248–254. https://doi.org/10.1016/0003-2697(76)90527-3

Clavijo D, Portilla-Martinez MC, Quijano-Parra A. 2012. Cinética de la bromelina obtenida a partir de la piña perolera (*Ananas comosus*) de Lebrija-Santander. Bistua: Revista de la Facultad de Ciencias Básicas 10(2): 41–49.

CONAGUA (Comisión Nacional de Agua). 2022. Información estadística climatológica. Estación Loma Bonita 20063. Gobierno de México, Comisión Nacional de Agua. Ciudad de México, México. https://smn.conagua.gob.mx/es/climatologia/informacion-climatologica/informacion-estadistica-climatologica (Retrieved: June 2023).

Conesa C, García-Breijo E, Loeff E, Seguí L, Fito P, Laguarda-Miró N. 2015. An electro chemical impedance spectroscopy-based technique to identify and quantify fermentable sugars in pineapple waste valorization for bio-ethanol production. Sensors 15 (9): 22941–22955. https://doi.org/10.3390/s150922941

Difonzo G, Vollmer K, Caponio F, Pasqualone A, Carle R, Steingass CB. 2019. Characterisation and classification of pineapple (*Ananas comosus* [L.] Merr.) juice from pulp and peel. Food Control 96: 260–270. https://doi.org/10.1016/j.foodcont.2018.09.015

García-Tain Y, Pérez-Padrón J, García-Pererira A, Hernández-Gómez A. 2011. Determinación de las propiedades de calidad de la piña (*Ananas Comosus*) variedad Cayena Lisa almacenada a temperatura ambiente. Ciencias Técnicas Agropecuarias 20 (1): 62–65.

Grudkowska M, Zagdańska B. 2004. Multifunctional role of plant cysteine proteinases. Acta Biochimica Polonica 51 (3): 609–624. https://doi.org/10.18388/abp.2004_3547

Hikal WM, Mahmoud AA, Said-Al Ahl HAH, Bratovcic A, Tkachenko KG, Kačániová M, Rodriguez RM. 2021. Pineapple (*Ananas comosus* L. Merr.), waste streams, characterisation and valorisation: an overview. Open Journal of Ecology 11 (9): 610–634. https://doi.org/10.4236/oje.2021.119039

Ketnawa S, Chaiwut P, Rawdkuen S. 2012. Pineapple wastes: A potential source for bromelain extraction. Food and Bioproducts Processing 90 (3): 385–391. https://doi.org/10.1016/j.fbp.2011.12.006

López-García B, Hernández M, Segundo BS. 2012. Bromelain, a cysteine protease from pineapple (*Ananas comosus*) stem, is an inhibitor of fungal plant pathogens. Letters in Applied Microbiology 55 (1): 62–67. https://doi.org/10.1111/j.1472-765x.2012.03258.x

Lu XH, Sun DQ, Wu QS, Liu SH, Sun GM. 2014. Physico-chemical properties, antioxidant activity and mineral contents of pineapple genotypes grown in China. Molecules 19 (6): 8518–8532. https://doi:10.3390/molecules19068518

Market Reports World. 2022. Global bromelain market 2022 by manufacturers, regions, type and application, forecast to 2028. Pune, India. https://www.marketreportsworld.com/global-bromelain-market-19899147 (Retrieved: July 2023).

Misran E, Idris A, Mat Sarip SH, Ya'akob H. 2019. Properties of bromelain extract from different parts of the pineapple variety Morris. Biocatalysis and Agricultural Biotechnology 18: 101095. https://doi.org/10.1016/j.bcab.2019.101095

Mohd Ali M, Hashim N, Abd Aziz S, Lasekan O. 2020. Pineapple (*Ananas comosus*): A comprehensive review of nutritional values, volatile compounds, health benefits, and potential food products. Food Research International 137 (1): 109675. https://doi.org/10.1016/j.foodres.2020.109675

Nadzirah KZ, Zainal S, Noriham A, Normah I, Siti AM. 2012. Physico-chemical properties of pineapple crown extract variety N36 and bromelain activity in different forms. APCBEE Procedia 4: 130–134. https://doi.org/10.1016/j.apcbee.2012.11.022

NMX-F-103-1982 (Norma Mexicana). 1982. Alimentos-determinación de grados Brix en alimentos y bebidas método de ensayo http://diariooficial.gob.mx/nota_detalle.php?codigo=5075420&fecha=23/12/2008#gsc.tab=0 (Retrieved: July 2023).

NMX-FF-028-SCFI-2008 (Norma Mexicana). 2008. Productos alimenticios no industrializados para consumo humano —fruta fresca—Piña (*Ananas comosus* var. *comosus*)–especificaciones. http://www.economia-nmx.gob.mx/normas/nmx/2009/nmx-ff-028-scfi-2008.pdf (Retrieved: July 2023).

NOM-F-137-S-1978 (Norma Oficial Mexicana). 1978. Determinación de pH en alimentos". Secretaría de Patrimonio y Fomento Industrial. https://dof.gob.mx/nota_detalle.php?codigo=4704689&fecha=23/05/1978&print=true (Retrieved: July 2023).

Ortiz RA. 2022. Abiotic stress factors influencing calcium nutrition of export bananas (*Musa* sp.) and pineapples (*Ananas comosus*) in Central America. Acta Horticulturae 1333: 99–106. https://doi.org/10.17660/ActaHortic.2022.1333.14

Santos DI, Martins CF, Amaral RA, Brito L, Saraiva JA, Vicente AA, Moldão-Martins M. 2021. Pineapple (*Ananas comosus* L.) by-products valorization: novel bio ingredients for functional foods. Molecules 26 (11): 3216. https://doi.org/10.3390/molecules26113216

Seleni MM, Canniatti SG, dos Santos CT, Ratnayake WS, Flores RA, Bianchini A. 2014 Characterization and potential application of pineapple pomace in an extruded product for fiber enhancement. Food Chemistry 163: 23–30. https://doi.org/10.1016/j.foodchem.2014.04.076

Shu HY, Sun W, Li KM, Xu GY, Zhan RL, Chang SH. 2019. The cause for water-heart fruit of pineapple and protective measurements. American Journal of Plant Sciences 10 (6): 885–892. https://doi.org/10.4236/ajps.2019.106063

SIAP (Servicio de Información Agroalimentaria y Pesquera). 2022. Anuario Estadístico de la Producción Agrícola. Gobierno de México, Servicio de Información Agroalimentaria y Pesquera. Ciudad de México, México. https://nube.siap.gob.mx/cierreagricola (Retrieved: June 2023).

Siti Rashima R, Azhar ME, Maizura, M. 2021. Influence of post-harvest physiology on sensory perception, physical properties, and chemical compositions of Morris pineapples (*Ananas comosus* L.). Journal of Food Sciences 86 (9): 4159–4171. https://doi.org/10.1111/1750-3841.15877

Soloman DG, Razali Z, Somasundram C. 2016. Physiochemical changes during growth and development of pineapple (*Ananas comosus* L. Merr. cv. Sarawak). Journal Agricultural Sciences and Technology 18: 491–503.

Truc TT, Binh LN, Muoi NV. 2008. Physico-chemical properties of pineapple at different maturity levels. The First International Conference on Food Science and Technology, Can Tho, Vietnam, 130–134.

Uriza-Ávila DE, Torres-Ávila A, Aguilar-Ávila J, Santoyo-Cortés VH, Zetina-Lezama R, Rebolledo-Martínez A. 2018. La piña mexicana frente al reto de la innovación. Avances y retos en la gestión de la innovación. Colección Trópico Húmedo. Universidad Autónoma Chapingo: Texcoco, México. 479 p.

Vasiljevic T. 2019. Chapter 10 – Pineapple. *In* Charis M. Galanakis. (ed.), Valorization of fruit processing by-products. Academic Press: Cambridge, MA, USA. pp: 203–225.

Agrociencia

# FLORISTIC INVENTORY AND ANNUAL AVAILABILITY OF MELLIFEROUS FLORA IN CERVANTES Y LOZADA, CORDOBA MUNICIPALITY, VERACRUZ, MEXICO

Natalia **Real-Luna**[1,2], Jaime Ernesto **Rivera-Hernández**[1,3*], Graciela **Alcántara-Salinas**[1], Juan Antonio **Pérez-Sato**[1], Edgardo **Zalazar-Marcial**[1], Miguel Ignacio **Delgado-Blancas**[4], Amauri **Díaz-Solís**[3]

[1] Colegio de Postgraduados Campus Córdoba. Carretera Federal Córdoba-Veracruz km 348, Congregación Manuel León, Amatlán de los Reyes, Veracruz, Mexico. C. P. 94953.
[2] Doctorado en Ciencias Naturales para el Desarrollo (DOCINADE), Instituto Tecnológico de Costa Rica, Universidad Nacional, Universidad Estatal a Distancia, Costa Rica.
[3] Centro de Estudios Geográficos, Biológicos y Comunitarios, S. C. Calle Santa María No. 13, Unidad Habitacional San Román, Córdoba, Veracruz, Mexico. C. P. 94542.
[4] Tecnológico Nacional de México- Instituto Tecnológico Superior de Tierra Blanca. Avenida Veracruz S/N, esq. C. Héroes de Puebla y Pemex, Tierra Blanca, Veracruz, Mexico. C. P. 95180.
* Author for correspondence: jriverah@geobicom.org

**Citation:** Real-Luna N, Rivera-Hernández JE, Alcántara-Salinas G, Pérez-Sato JA, Zalazar-Marcial E, Delgado-Blancas MI, Díaz-Solís A. 2023. Floristic inventory and anual availability of melliferous flora in Cervantes y Lozada, Cordoba municipality, Veracruz, Mexico. **Agrociencia** 57(8): 1730-1745. doi.org/ 10.47163/agrociencia.v57i8.3028

**Editor in Chief:**
Dr. Fernando C. Gómez Merino

Received: June 09, 2023.
Approved: September 10, 2023.
**Published in Agrociencia:** December 12, 2023.



## ABSTRACT

Pollinators depend on the melliferous flora for food, in return, flowers are pollinated, which contributes for the maintenance of ecosystems and conservation of biodiversity, increasing food production and ensuring food security. This research aims to provide an inventory of melliferous flora and its annual availability in Cervantes y Lozada, Córdoba, Veracruz, Mexico. During 26 months, the plants interacting with bees were collected on defined rural roads; we also documented the resource provided by the flowers (pollen, honey, etc.), their origin (native or exotic), life form and flowering periods. From 122 collections, 76 melliferous species were inventoried, grouped in 74 genera and 35 botanical families, being Asteraceae (25 %) the family with more species, followed by Malvaceae (9.21 %) and Lamiaceae (7.89 %); 67.11 % are polliniferous, 7.86 % nectariferous, and 25 % provide both; 82.89 % are native and 17.11 % exotic; 15.79 % are trees, 28.95 % shrubs and 55.26 % herbs. Seven species provided resources for bees all year round, two for 10 months and the rest for shorter periods. The flora species that were inventoried have different uses, so it is important to protect and promote the sustainable management of the melliferous flora, which is essential for the conservation of the pollination service, which in turn is essential for agriculture and ecosystems, in addition to protecting species of social, ecological, and economic importance.

**Keywords**: bee flora, pollinators, nectar, pollen, flowering season.

## INTRODUCTION

Bees depend on the melliferous flora for food and to obtain nesting sites; in return, flowers are pollinated for succeeding in reproduction that provides seeds and fruits for humans and other animals, thus contributing to food security and the ecological balance of ecosystems (Bonet and Vergara, 2016; Montoya-Bonilla *et al*., 2017).

Despite its importance, melliferous flora is under threat, mainly due to deforestation. In this regard, Mexico suffered an average annual gross deforestation of 212834 ha in 2021, caused primarily by changes in land use for agriculture, livestock, mining, tourism developments and/or real estate projects (CONAFOR, 2022). Other factors affecting the melliferous flora are the use of agrochemicals, the presence of invasive exotic species, diseases, pests, transgenic varieties, and climate change (Quezada-Euán and Ayala-Barajas, 2010). Climate change causes loss of biological corridors for pollinators, as it promotes habitat fragmentation, soil erosion, loss of biodiversity, and reduction of environmental services. All these problems result in small and isolated populations, increasing their probability of extinction (Aguilar *et al*., 2019; Ramírez-Bravo and Hernández-Santín, 2016; Von *et al*., 2021).

In Mexico, the state of Veracruz has an inventory of 63 families, 176 genera and 216 species of honey plants. Of that, Asteraceae and Fabaceae families have the largest number of species (Real-Luna *et al*., 2021). In Mexico, the Asteraceae is the most diverse botanical family, with approximately 3000 species, that means 14 % of Mexico´s flora as a whole (Villaseñor-Ríos *et al*., 2013). Thus, Mexico has 147 species of Asteraceae reported as significant for beekeeping (Cadena *et al*., 2019; Castellanos-Potenciano *et al*., 2012; Quiroz and Arreguín-Sánchez, 2008). Additionally, the families Fabaceae, Convolvulaceae, Combretaceae, Bignoniaceae, and Verbenaceae are also considered important sources of pollen and nectar (González *et al*., 2016). This research aims to provide an inventory of melliferous flora and its annual availability in Cervantes y Lozada, Córdoba, Veracruz. We expect to provide fundamental contribution of scientific knowledge for the implementation of effective and viable conservation strategies, both for pollinators and for the regional honey flora.

## MATERIALS AND METHODS

### Description of the study area

The study was carried out in the rural locality of Cervantes y Lozada located to the northeast of the municipality of Córdoba, in the "Sierra del Gallego" region; at 18° 57′ 14.4" N and 96° 55′ 35.04" W with an altitude average of 1214 m (Figure 1). It has a semi-warm humid climate with abundant rainfall in summer, and a temperature ranging from 18 to 24°C, and precipitation of 1900-2100 mm (Sistema de Información Estadística y Geográfica del Estado de Veracruz de la Llave, 2021).

There are two types of vegetation in the area, according to Rzedowski's classification (1978): Cloud forest (deciduous forest or medium or low evergreen forest, according to Miranda and Hernández-X., 1963), and tropical evergreen forest (or medium sub evergreen forest, according to Miranda and Hernández-X., 1963), as well as a transition strip between these two vegetal communities and patches of secondary vegetation derived from these types of vegetation.

The location is considered highly marginalized with a population of 173 inhabitants provided of essential needs (drinking water, basic schools, electricity, etc.); the main

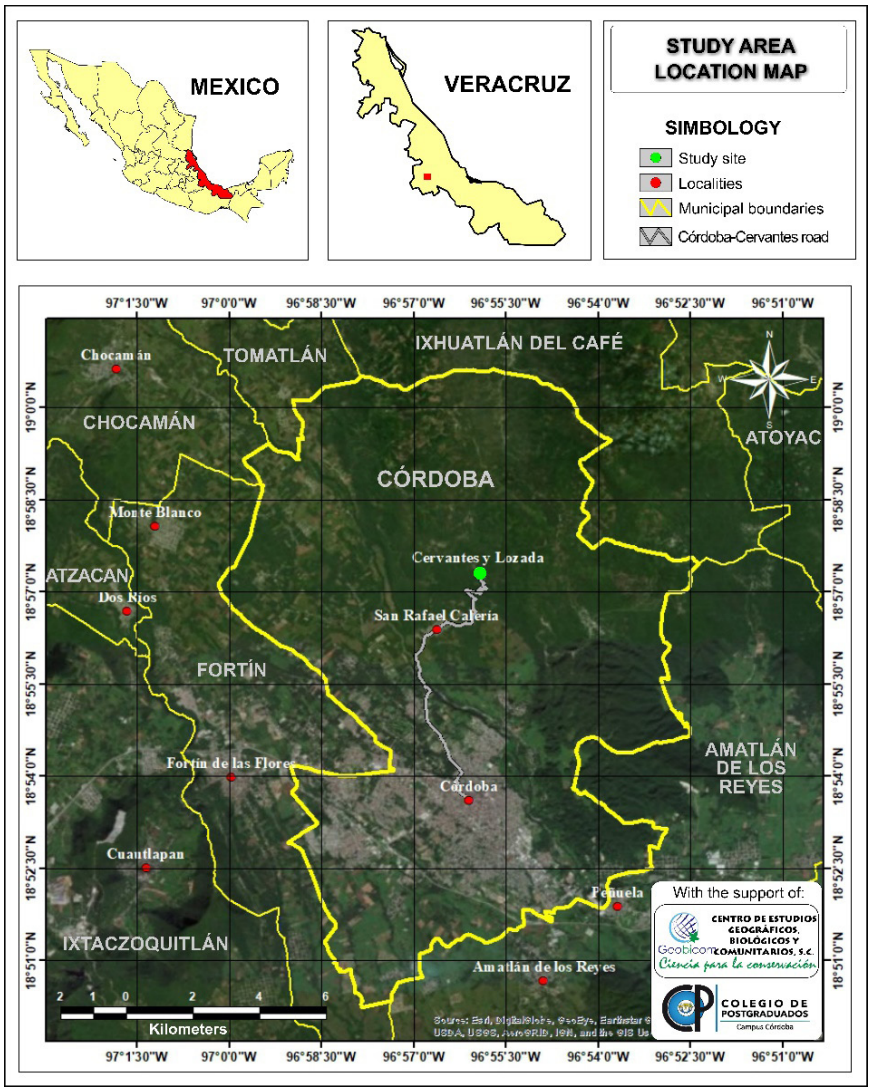


**Figure 1.** Location of Cervantes y Lozada, Córdoba, Veracruz, Mexico.

productive activity is agriculture, with coffee, banana, beans, corn, chili, and squash (Sistema de Información Estadística y Geográfica del Estado de Veracruz de la Llave, 2021). The inhabitants conduct an agroecological production system combining different kinds of crops in their plots, such as coffee (*Coffea arabica* L.), different varieties of banana (*Musa* x *paradisiaca* L.) and other ornamental species as the parlour palms (*Chamaedorea elegans* Mart. and *Ch. metallica* O.F. Cook ex H.E. Moore), cornstalk dracaena (*Dracaena fragrans* (L.) Ker Gawl.) and ti plant (*Cordyline fruticosa* (L.) A. Chev.).

**Inventory of melliferous flora**

We established a weekly collection of plants on the community roads for 26 months, following the periods of March to December 2020, January to December 2021 and January to April 2022, from 10:00-16:00 h, when bees present greater activity. All the species that were visited by bees were collected. The plants were herborized using traditional techniques of pressing, drying, and disinfecting (Lot and Chiang, 1986). Subsequently, they were taxonomically determined through the use of specialized literature (dichotomous keys), as well as by comparison of herbarium vouchers. Plant taxonomy was based on the Missouri Botanical Garden Tropics database proposal (Tropicos.org, 2023) and the International System established by the Angiosperm Phylogeny Group IV (Chase *et al*., 2016). Taxon authors were abbreviated according to the Tropicos database of the Missouri Botanical Garden (Tropicos.org, 2023). On the other hand, the resources provided by the plants to the bees (pollen, nectar, or both), its origin (native or exotic), the life form (tree, shrub, or grass) were documented through a bibliographic review of scientific articles published in databases such as Scopus, Web of Science Group, Academic Google, Elsevier and Springer Link, and the flowering periods were recorded through observations made during the field work.

Botanical specimens were deposited in the following herbaria: Herbarium of the Colegio de Postgraduados Campus Córdoba (CPC) (in Manuel León, Amatlán de los Reyes, Veracruz), Herbarium "Jerzy Rzedowski Rotter" of the Facultad de Ciencias Biológicas y Agropecuarias de la Universidad Veracruzana, Zona Córdoba-Orizaba (CORU) (in Peñuela, Amatlán de los Reyes, Veracruz), and Herbarium of the Instituto de Ecología (XAL) (in Xalapa, Veracruz).

## RESULTS AND DISCUSSION

**Inventory of melliferous flora**

A total of 122 plant collections were made for a total of 76 species, distributed in 74 genera and 35 families. The most important family was Asteraceae with 19 species (25 %), coinciding with those reported by Granados-Argüello *et al.* (2020), González-Suárez *et al.* (2020) and Real-Luna *et al*. (2021). They are followed in order of importance by Malvaceae with seven (9.21 %), Lamiaceae with six (7.89 %), Fabaceae and Verbenaceae with three species each (3.95 %) and Acanthaceae, Amaryllidaceae, Cucurbitaceae, Euphorbiaceae, Ranunculaceae, Rubiaceae and Solanaceae with two species each (2.63 %) (Table 1).

The species of the Asteraceae family were the most visited by bees, since they have flowers that provide them with nectar and pollen, as well as being easily accessible, thus have the function of shelter sites. Asteraceae is one of the families with the largest number of species on the planet, being common and sometimes even dominating different regeneration sites, such as the edges of crops and roads. The importance of the Asteraceae family for bee foraging has been recorded in Argentina, Brazil, Colombia, and Mexico (Araujo-Mondragón and Redonda-Martínez, 2019; Chamorro-García *et al*., 2013).

**Table 1.** Botanical families that make up the melliferous flora of the Cervantes y Lozada location, in Córdoba, Veracruz, Mexico.

| Families | Genus | % | Species | % | Families | Genus | % | Species | % |
|---|---|---|---|---|---|---|---|---|---|
| ANGIOSPERMS | | | | | Fabaceae | 3 | 4.05 | 3 | 3.95 |
| MONOCOTYLEDONS | | | | | Heliotropiaceae | 1 | 1.35 | 1 | 1.32 |
| Amaryllidaceae | 2 | 2.70 | **2** | 2.63 | Lamiaceae | 5 | 6.76 | 6 | 7.89 |
| Arecaceae | 1 | 1.35 | 1 | 1.32 | Loranthaceae | 1 | 1.35 | 1 | 1.32 |
| Asparagaceae | 1 | 1.35 | 1 | 1.32 | Lythraceae | 1 | 1.35 | 1 | 1.32 |
| Hypoxidaceae | 1 | 1.35 | 1 | 1.32 | Malpighiaceae | 1 | 1.35 | 1 | 1.32 |
| Iridaceae | 1 | 1.35 | 1 | 1.32 | Malvaceae | 7 | 9.46 | 7 | 9.21 |
| Orchidaceae | 1 | 1.35 | 1 | 1.32 | Meliaceae | 1 | 1.35 | 1 | 1.32 |
| EUDICOTYLEDONS | | | | | Myrsinaceae | 1 | 1.35 | 1 | 1.32 |
| Acanthaceae | 2 | 2.70 | 2 | 2.63 | Myrtaceae | 1 | 1.35 | 1 | 1.32 |
| Adoxaceae | 1 | 1.35 | 1 | 1.32 | Nyctaginaceae | 1 | 1.35 | 1 | 1.32 |
| Amaranthaceae | 1 | 1.35 | 1 | 1.32 | Onagraceae | 1 | 1.35 | 1 | 1.32 |
| Asteraceae | 19 | 25.68 | 19 | 25 | Petiveriaceae | 1 | 1.35 | 1 | 1.32 |
| Bignoniaceae | 1 | 1.35 | 1 | 1.32 | Polygalaceae | 1 | 1.35 | 1 | 1.32 |
| Bixaceae | 1 | 1.35 | 1 | 1.32 | Ranunculaceae | 2 | 2.70 | 2 | 2.63 |
| Campanulaceae | 1 | 1.35 | 1 | 1.32 | Rosaceae | 1 | 1.35 | 1 | 1.32 |
| Convolvulaceae | 1 | 1.35 | 2 | 2.63 | Rubiaceae | 2 | 2.70 | 2 | 2.63 |
| Cucurbitaceae | 2 | 2.70 | 2 | 2.63 | Solanaceae | 2 | 2.70 | 2 | 2.63 |
| Euphorbiaceae | 2 | 2.70 | 2 | 2.63 | Verbenaceae | 3 | 4.05 | 3 | 3.95 |
| | | | | | **TOTAL** | **74** | **100** | **76** | **100** |

Of the total number of species recorded, 67.11 % are polliniferous, 7.86 % nectariferous and 25 % nectariferous-polliniferous. Regarding the origin, 82.89 % are native species and 17.11 % exotic. Indeed, we have expected such results, since Mexico has a lower number of exotic species than in other regions of the Americas. However, it is important to conduct more studies on exotic species, which are mostly herbaceous and can become invasive (Espinosa-García and Villaseñor-Ríos, 2017; Pérez-Postigo *et al*., 2021). Regarding the life forms of the melliferous flora, 15.79 % are trees, 28.95 % shrubs, and 55.26 % herbs. Similar results were reported for Tamaulipas, with 42.32 % herbaceous species identified (González-Suárez *et al*., 2020) (Table 2).

Species that were found in bloom throughout the year represent 7.89 % (*Bidens alba*, *Cuphea hyssopifolia*, *Holmskioldia sanguinea*, *Eriobotrya japonica*, *Malvaviscus arboreus*, *Melampodium divaricatum* and *Thunbergia alata*); those that were in bloom for 10 months were 2.63 % (*Teucrium vesicarium* and *Aldama dentata*); eight months, 3.95 % (*Bougainvillea glabra*, *Salvia xalapensis* and *Anoda cristata*); seven months, 6.58 % (*Ageratum houstonianum*, *Salvia lasiocephala*, *Melanthera nivea*, *Solidago altissima* and *Hamelia patens*); six months, 7.89 %; five months, 5.26 %; four months, 3.95 %; three months, 6.58 %; two months, 18%; and one month, 36.84 %.

During fieldwork, January had the lowest number of flowering species (15) and the months with the most floral resources were May (32), July (29), November (28), and December (29) (Figure 2).

**Table 2**. List of melliferous plant species from the community of Cervantes y Lozada, Córdoba, Veracruz, Mexico. Origin: N = Native, E = Exotic. Life form: H = Herb, S = Shrub, T = Tree. Product for pollinator: P = Pollen, N = Nectar, P/N = Pollen/Nectar. Flowering Period: JA = January, FB = February, MC = March, AP = April, MY = May, JN = June, JL = July, AG = August, SP = September, OC = October, NV = November, DC = December, AY = all year. Collectors: NRL = Natalia Real-Luna, JERH = Jaime Ernesto Rivera-Hernández and MAJC = Marco Antonio Juárez-Calderón. Herbaria: CPC = Herbarium of the melliferous flora of Veracruz, Colegio de Postgraduados Campus Córdoba, Manuel León, Veracruz; CORU = Jerzy Rzedowski Rotter Herbarium of the Facultad de Ciencias Biológicas y Agropecuarias, Zona Orizaba-Córdoba, Peñuela, Veracruz; and XAL = Herbarium of the Instituto de Ecología, Xalapa, Veracruz.

| Family/ Scientific name | Local common name | Origin | Life form | Product for pollinator | Flowering period | Collector (herbarium) |
|---|---|---|---|---|---|---|
| AMARYLLIDACEAE | | | | | | |
| *Agapanthus africanus* (L.) Hoffmanss | "ciento en uno", "agapando africano" | E | H | P | MY-JL | NRL 55 (CPC, CORU) |
| *Zephyranthes miradorensis* (Kraenzl.) Espejo y López-Ferrari | "mañanitas", "mañanitas veracruzanas" | N | H | P | MY | NRL 61 (CPC) NRL 66 (CPC) |
| ARECACEAE | | | | | | |
| *Syagrus romanzoffiana* (Cham.) Glassman | "palma coyolera", "palmera pindó" | E | H | P | AP-AG | JERH 6329 (CPC, CORU) |
| ASPARAGACEAE | | | | | | |
| *Cordyline fruticosa* (L.) A. Chev. | "gracena morada", "banderilla" | E | S | P | JA | JERH 6330 (CPC, CORU) |
| HYPOXIDACEAE | | | | | | |
| *Molineria capitulata* (Lour.) Herb. | "palma acordeón" | E | H | P | MY | NRL 60 (CPC, CORU) |
| IRIDACEAE | | | | | | |
| *Trimezia steyermarkii* R.C. Foster | "íris ojo de tigre" | N | H | P | MY-JL | NRL 53 (CPC, CORU) |
| ORCHIDACEAE | | | | | | |
| *Oncidium sphacelatum* Lindl. | "flor de mayo", "orquídea dama amarilla" | E | H | P | MY | NRL 54 (CPC, CORU) |
| EUDICOTYLEDONS | | | | | | |
| ACANTHACEAE | | | | | | |
| *Odontonema callistachyum* (Schltdl. & Cham.) Kuntze | "vara babosa", "canutillo" | N | H | P | DC-MC | NRL 1 (CPC, CORU, XAL) NRL 34 (CORU) |
| *Thunbergia alata* Bojer ex Sims | "manto", "hierba africana del susto" | E | H | N | AY | NRL 27 (CORU) NRL 87 (CPC, CORU) |
| ADOXACEAE | | | | | | |
| *Sambucus nigra* L. | "sauco", "sauco negro" | N | T | P | JL-AG | NRL 79 (CPC, CORU) |
| AMARANTHACEAE | | | | | | |
| *Chamissoa altissima* (Jacq.) Kunth | "bejuco de agua" | N | H | N | DC | NRL 29 (CPC, CORU) |
| ASTERACEAE | | | | | | |
| *Ageratum houstonianum* Mill. | "chichán", "yerba del zopilote" | N | H | P | OC-AP | NRL 18 (CORU) NRL 30 (CORU) NRL 90 (CPC, CORU) |

**Table 2**. Continue.

| Family/ Scientific name | Local common name | Origin | Life form | Product for pollinator | Flowering period | Collector (herbarium) |
|---|---|---|---|---|---|---|
| *Aldama dentata* La Llave | "acahual" | N | H | P | MC-DC | NRL 8 (CPC, CORU) NRL 11 (CPC, CORU) NRL 85 (CPC, CORU) |
| *Baccharis trinervis* Pers. | "cortadillo" | N | S | P/N | FB-AP | NRL 5 (CPC, CORU) NRL 38 (CORU) NRL 44 (CORU) |
| *Bidens alba* (L.) DC. | "amor seco", "amozote", "acahual blanco" | N | H | P/N | AY | NRL 3 (CORU) NRL 14 (CORU) NRL 16 (CORU) NRL 86 (CPC, CORU) |
| *Chromolaena odorata* (L.) R.M. King & H. Rob. | "albahaquilla" | N | S | P/N | MC-AP | NRL 4 (CPC, CORU) |
| *Critonia morifolia* (Mill.) R.M. King & H. Rob. | "hoja de San Nicolás", "árbol de Santa María" | N | S | P | JA-JN | NRL 114 (CPC) MAJC 4 (CPC) |
| *Fleischmannia pycnocephala* (Less.) R.M. King & H. Rob. | "cruz dulce chica" | N | H | P | MC-AP | NRL 2 (CPC, CORU) NRL 42 (CPC) |
| *Heliopsis buphtalmoides* (Jacq.) Dunal | "botoncillo" | N | H | P | AP-JL | NRL 9 (CORU) NRL 41 (CPC) NRL 68 (CPC, CORU XAL) NRL 84 (CPC, CORU) MAJC 5 (CPC) |
| *Melampodium divaricatum* (Rich.) DC. | "cabezona", "acahual amarillo" | N | H | P/N | AY | NRL 10 (CPC, CORU) NRL 43 (CORU) NRL 83 (CPC, CORU, XAL) NRL 99 (CPC, CORU, XAL) |
| *Melanthera nivea* (L.) Small | "capitaneja", "totolquelite" | N | H | P | MY-NV | NRL 59 (CPC, CORU) NRL 95 (CPC, CORU) |

**Table 2**. Continue.

| Family/ Scientific name | Local common name | Origin | Life form | Product for pollinator | Flowering period | Collector (herbarium) |
|---|---|---|---|---|---|---|
| *Montanoa grandiflora* (DC.) Sch. Bip. ex Hemsl. | "cecilia", "acahual" | N | S | P/N | NV-DC | NRL 15 (CPC, CORU, XAL) NRL 100 (CPC, CORU, XAL) NRL 103 (CPC, CORU, XAL) NRL 109 (CPC, CORU, XAL) NRL 104 (CPC) |
| *Schistocarpha bicolor* Less | "polocote", "margarita" | N | S | P | FB-MC | NRL 7 (CORU) NRL 37 (CORU) |
| *Smallanthus maculatus* (Cav.) H. Rob. | "polocote morado", "conquelite" | N | H | P | JL-DC | NRL 71 (CPC, CORU) NRL 81 (CPC, CORU) |
| *Solidago altissima* L. | "vara de oro" | E | H | P/N | MY-NV | NRL 63 (CPC, CORU) NRL 98 (CPC, CORU, XAL) |
| *Tithonia diversifolia* (Hemsl.) A. Gray | "gigantón", "acahual", "árnica" | N | H | P | NV | NRL 102 (CPC, CORU, XAL) |
| *Verbesina turbacensis* Kunth | "lengua de vaca", "capitaneja" | N | H | P | NV | NRL 106 (CPC) |
| *Vernonanthura patens* (Kunth) H. Rob. | "chiquite", "flor de cuaresma" | N | S | P/N | MC | NRL 6 (CPC, CORU) NRL 45 (CPC, CORU) NRL 46 (CORU) |
| *Viguiera cordata* (Hook. & Arn.) D'Arcy | "jabalí", "mozote amarillo" | N | H | P | DC-JA | NRL 20 (CPC) |
| *Zinnia elegans* Jacq. | "viuda", "flor de San Miguel" | N | H | P/N | JL-NV | NRL 93 (CPC, CORU, XAL) |
| BIGNONIACEAE | | | | | | |
| *Podranea ricasoliana* (Tanfani) Sprague | "campana rey sudafricana" | E | S | P | FB-JL | NRL 111 (CPC) MAJC 3 (CPC) |
| BIXACEAE | | | | | | |
| *Bixa orellana* L. | "achiote" | N | S | P | JL-AG | NRL 22 (CORU) NRL 78 (CPC, CORU) |
| CAMPANULACEAE | | | | | | |
| *Lobelia xalapensis* Kunth | "berros", "barba de guajolote" | N | H | P | OC-DC | NRL 13 (CPC, CORU) NRL 97 (CPC, CORU, XAL) |
| CONVOLVULACEAE | | | | | | |
| *Ipomoea hastigera* Kunth | "bejuco", "campanillas" | N | H | N | AP | NRL 49 (CPC, CORU) |

**Table 2**. Continue.

| Family/ Scientific name | Local common name | Origin | Life form | Product for pollinator | Flowering period | Collector (herbarium) |
|---|---|---|---|---|---|---|
| *I. indica* (Burm.) Merr. | "quiebra platos", "bejuco blanco" | N | H | N | AG-DC | NRL 32 (CPC, CORU) NRL 82 (CPC, CORU) |
| CUCURBITACEAE | | | | | | |
| *Polyclathra cucumerina* Bertol. | "calabacilla", "chilacayotillo" | N | H | P | NV-DC | NRL 105 (CPC, CORU, XAL) NRL 107 (CPC) NRL 108 (CPC) |
| *Sechium edule* (Jacq.) Sw. | "chayote", "erizo" | N | H | P | JL-DC | NRL 75 (CPC, CORU) |
| EUPHORBIACEAE | | | | | | |
| *Croton draco* Schltdl. & Cham. | "sangregado", "sangre de grado", "drago" | N | T | N | MC-AP | NRL 40 (CPC) |
| *Jatropha podagrica* Hook. | "botella", "tártago" | N | S | P | MY | NRL 62 (CPC, CORU) |
| FABACEAE | | | | | | |
| *Inga vera* Willd. | "vainillo", "jinicuil", "aguatope" | N | T | P/N | AP-MY | NRL 47 (CORU, XAL) |
| *Leucaena leucocephala* (Lam.) de Wit | "guaje", "Tepehuaje dormilón" | N | T | P | MC | NRL 115 (CPC) |
| *Mimosa albida* Humb. & Bonpl. ex Willd. | "chomapique", "dormilona grande" | N | S | P | NV-JA | NRL 101 (CPC, CORU, XAL) |
| HELIOTROPIACEAE | | | | | | |
| *Tournefortia hirsutissima* L. | "tlachichinole", "hierba rasposa" | N | S | P | AP | NRL 50 (CPC, CORU) |
| LAMIACEAE | | | | | | |
| *Holmskioldia sanguinea* Retz. | "bugambilia extranjera", "sombrilla china" | E | S | P/N | AY | JERH 6331 (CPC, CORU) |
| *Hyptis capitata* Jacq. | "botoncillo" | N | H | P | DC-JA | NRL 24 (CORU) |
| *Leonurus sibiricus* L. | "mariguana cimarrona", "altamisa" | E | H | P | OC | NRL 91 (CPC, CORU, XAL) |
| *Salvia lasiocephala* Hook. & Arn. | | N | H | P | SP-AP | JERH 6340 (CPC, CORU, XAL) |
| *S. xalapensis* Benth. | "salvia jalapeña" | N | H | P | MY-DC | NRL 72 (CPC, CORU, XAL) |
| *Teucrium vesicarium* Mill. | "mozote", "pega pega" | N | H | P | JA-OC | NRL 36 (CORU) NRL 51 (CPC, CORU) |
| LORANTHACEAE | | | | | | |
| *Struthanthus quercicola* (Schltdl. & Cham.) Blume | "hiedra", "correhuela" | N | H | P | JL | NRL 73 (CPC, CORU, XAL) |
| LYTHRACEAE | | | | | | |
| *Cuphea hyssopifolia* Kunth | "falso brezo mexicano" | N | S | P | AY | NRL 69 (CPC, CORU, XAL) |

**Table 2**. Continue.

| Family/ Scientific name | Local common name | Origin | Life form | Product for pollinator | Flowering period | Collector (herbarium) |
|---|---|---|---|---|---|---|
| MALPIGHIACEAE | | | | | | |
| *Byrsonima crassifolia* (L.) Kunth | "nanche", "nananche" | N | T | P/N | MY | MAJC 2 (CPC); NRL 56 (CPC, CORU, XAL) |
| MALVACEAE | | | | | | |
| *Anoda cristata* (L.) Schltdl. | "violeta de campo", "alache" | N | H | P | MY-DC | NRL 17 (CORU, XAL) NRL 21 (CORU, XAL) NRL 92 (CPC, CORU, XAL) |
| *Bernoullia flammea* Oliv. | "platanillo", "amapola" | N | T | P | AP | JERH 6332 (CPC, CORU) |
| *Heliocarpus americanus* L. | "jonote" | N | T | P | FB | NRL 39 (CORU) |
| *Malvaviscus arboreus* Cav. | "chochito", "tulipán corriente", "altea" | N | S | P/N | AY | NRL 77 (CPC, CORU); NRL 112 (CPC) |
| *Pseudobombax ellipticum* (Kunth) Dugand | "lele", "coquito" | N | T | P/N | AP | JERH 6333 (CPC, CORU) |
| *Robinsonella lindeniana* (Turcz.) Rose & Baker | "manzanillo", "jocorró" | N | T | P | NV-DC | NRL 19 (CORU, XAL) NRL 31 (CORU, XAL) |
| *Triumfetta semitriloba* Jacq. | "cadillo", "mozote" | N | S | P | DC | NRL 28 (CORU) |
| MELIACEAE | | | | | | |
| *Trichilia havanensis* Jacq. | "rama tinaja", "palo de cuchara" | N | T | P | JA | NRL 113 (CPC) |
| MYRTACEAE | | | | | | |
| *Psidium guajava* L. | "guayaba", "guayaba dulce" | N | T | P/N | AP-MY | NRL 48 (CORU, XAL) |
| NYCTAGINACEAE | | | | | | |
| *Bougainvillea glabra* Choisy | "bugambilia" | E | S | P | AP-NV | NRL 58 (CPC, CORU) |
| ONAGRACEAE | | | | | | |
| *Oenothera rosea* L'Hér. ex Ait. | "hierba del golpe" | N | H | P/N | OC | NRL 89 (CPC, CORU, XAL) |
| PETIVERIACEAE | | | | | | |
| *Rivina humilis* L. | "bajatripa" | N | H | N | MY-AG | NRL 65 (CPC, CORU) NRL 70 (CPC, CORU) |
| POLYGALACEAE | | | | | | |
| *Polygala berlandieri* S. Watson | "hierba de yódex" | N | H | P | OC-NV | NRL 96 (CPC, CORU, XAL) |
| PRIMULACEAE | | | | | | |
| *Ardisia compressa* Kunth | "capulín", "capulín negro" | N | S | P | DC | NRL 110 (CPC, CORU) |

**Table 2**. Continue.

| Family/ Scientific name | Local common name | Origin | Life form | Product for pollinator | Flowering period | Collector (herbarium) |
|---|---|---|---|---|---|---|
| RANUNCULACEAE | | | | | | |
| *Clematis dioica* L. | "barba de chivo" | N | H | P | DC | NRL 35 (CPC, CORU, XAL) |
| *Ranunculus petiolaris* Humb., Bonpl. & Kunth ex DC. subsp. *Petiolaris* | "aceitilla" | N | H | P | MY-OC | NRL 67 (CPC, CORU, XAL) NRL 94 (CPC, CORU, XAL) |
| ROSACEAE | | | | | | |
| *Eriobotrya japonica* (Thunb.) Lindl. | "níspero", "níspero chino" | E | S | P | JL | NRL 76 (CPC) |
| RUBIACEAE | | | | | | |
| *Coffea arabica* L. | "café", "cafeto" | E | S | P | MY | NRL 64 (CPC, CORU, XAL) |
| *Hamelia patens* Jacq. | "coralillo" | N | S | P/N | MY-NV | NRL 52 (CPC, CORU) NRL 74 (CPC) NRL 88 (CPC) |
| SOLANACEAE | | | | | | |
| *Brugmansia arborea* (L.) Lagerh. | "florifundio", "florifundio sudamericano" | E | S | P/N | JL-DC | NRL 33 (CPC) |
| *Capsicum annuum* L. | "chile tabaquero", "chile" | N | H | P | MY | NRL 57 (CPC, CORU) |
| VERBENACEAE | | | | | | |
| *Lippia myriocephala* Schltdl. & Cham. | "popotoca", "colpanchi blanco" | N | T | P/N | DC | NRL 26 (CORU) |
| *Petrea volubilis* L. | "rasca petate", "raspa sombrero", "bejuco de ajo" | N | H | P | FB-JN | JERH 6334 (CPC, CORU) |
| *Verbena carolina* L. | "verbena de perro" | N | H | P/N | DC | NRL 25 (CORU) |

However, further studies on the availability of floral resources are needed, as climate change may affect plant phenology by bringing forward flowering and affecting plant-pollinator interaction, as there is no synchronization with pollinator emergence. Plants may also alter their nectar composition and pollen protein concentration, which may affect pollinator longevity. Another aspect that can be affected is foraging activity, since if temperatures increase, they can be critical and lethal for insects, which will impede foraging, resulting in a lack of pollination (Farias-Silva and Freitas, 2020).

During the fieldwork we could observe that the species with the greatest number of floral visitors were: *Heliopsis buphthalmoides*, *Aldama dentata*, *Bidens alba*, *Byrsonima crassifolia*, *Eriobotrya japonica*, *Hamelia patens*, *Melampodium divaricatum*, *Montanoa*

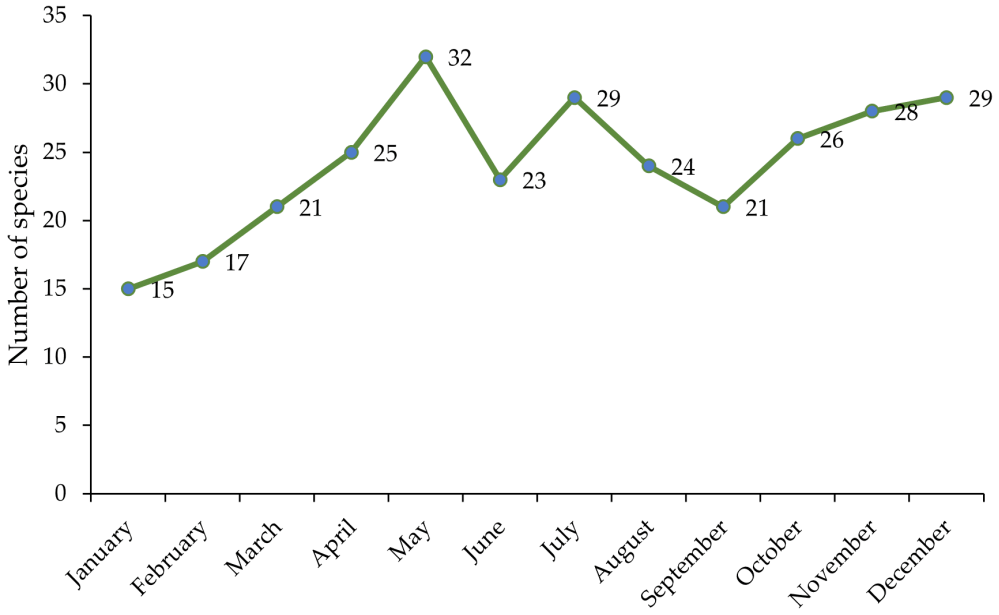


**Figure 2.** Number of flowering species during the year in Cervantes y Lozada, Córdoba, Veracruz, Mexico.

*grandiflora* and *Sechium edule*. Those that presented a regular number of visiting species were *Smallanthus maculatus*, *Odontonema callistachyum*, *Tithonia diversifolia* and *Viguiera cordata*, which coincides with the data reported by Araujo-Mondragón and Redonda-Martínez (2019).

In Cervantes y Lozada the main agricultural products obtained during the rainfed period are: coffee, banana, chili, beans, corn, and squash; as well as chayote, nanche, guava and loquat. Most of these crops require pollination by external agents for fruit production, so the presence of pollinators is important in this place. However, these crops have short flowering periods, thus, it is crucial to maintain pollinators for its ecological importance.

We observed in Cervantes y Lozada a great diversity of pollinator species such as those belonging to the orders Hymenoptera, Lepidoptera and Apodiformes. Regarding bees, there are different species, including nine species of meliponines (*Partamona bilineata* (Say, 1837), *Plebeia pulchra* Ayala, 1999, *Scaptotrigona mexicana* (Guérin, 1845), *Scaptotrigona pectoralis* (Dalla Torre, 1896), *Scaura argyrea* (Cockerell, 1912), *Trigona corvina* Cockerell, 1913, *Trigona fulviventris* Guérin, 1845, *Trigona fuscipennis* Friese, 1900, and *Trigona nigerrima* Cresson, 1878). In addition, there are some *Apis mellifera* L. hives brought to Cervantes y Lozada by people outside this place, as they found a perfect place with a high quantity of melliferous flora to assure honey production. The

Cervantes y Lozada inhabitants only rent their land to this foreign people, but do not produce their own honey.

We suggest further research studies on bees' biology as their flight capacity, which is a function of body size, for instance, small bees as *Plebeia droryana* (1.35 mm maximum forewing length) could become isolated in case of the distance between vegetation fragments are greater than 600 m. Species such as *Melipona compressipes* (3.25 mm) and *Melipona quadrifasciata* (2.90 mm), could be isolated if the forest fragments are more than 2 km apart (Meléndez *et al*., 2013). Therefore, the risk of extinction is greater in smaller species.

Another aspect worth considering is their behavior for dispersion within the research area; to do this, bees depend on the parental nest to provide the new nest with food and material for the construction of the new nest. In this sense, Cervantes y Lozada is immersed in the forest, supplying all the resources needed, and bees would not have to travel long distances to find the resources needed for their survival.

It is also important to emphasize that the melliferous flora supports ecosystem services, as the provisions for insects, birds, bats, etc., pollination, soil conservation, availability of food and habitat for the natural enemies of pests, as well as for the contribution of aesthetic and social services. On the other hand, these species have uses by humans, whether medicinal, food, coloring, ornamental, timber, fodder, agroforestry, fungicide, for restoration, ceremonies, fuel, construction, biofuel and/or handicrafts, which highlights the importance of the conservation of this flora, mainly composed of herbaceous plants (Albrecht *et al*., 2016; Hernández-Villa *et al*., 2020).

## CONCLUSIONS

The melliferous flora of Cervantes y Lozada provided scientific knowledge of 76 species, distributed in 74 genera and 35 families. The most important families were Asteraceae, Malvaceae, Lamiaceae, Fabaceae, and Verbenaceae. Most species provide pollen as the principal resource for pollinators, 82.89 % are native and 55.26 % are herbaceous. Seven species provided resources for bees all year round, two for 10 months and the rest for shorter periods. The months with the most flowering species were May, July, November, and December.

The present study seeks to provide enough information about the melliferous flora; thus people would be able to promote their conservation, especially those that are generally considered weeds and normally grow in gardens, roadsides, and crops. Many of these plants are eliminated or prevented from growing, because we do not know how important they are for the ecosystem and indirectly to produce our food.

The species of melliferous flora have different uses, so this information will allow the development of strategies to protect and promote sustainable management for the conservation of the pollination service, which is essential for agriculture and ecosystems, as well as strategies to protect species that have social, ecological, and economic importance.

Based on the results and the knowledge that the inhabitants have about bees, an awareness campaign can be proposed to reduce the use of agrochemicals and avoid

the elimination of vegetation on roadsides and crop edges, which will contribute to a greater availability of resources for pollinators, favoring their conservation.

## ACKNOWLEDGEMENTS

The valuable and active participation of the inhabitants of Cervantes y Lozada is gratefully acknowledged. The first author is grateful to the Doctoral Program in Natural Sciences for Development, coordinated by the Instituto Tecnológico de Costa Rica, the Universidad Nacional and the Universidad Estatal a Distancia. The second author thanks to the National Council of Humanities, Science and Technology (CONAHCyT) for the postdoctoral scholarship granted. Special thanks to the institutions that supported this work: Colegio de Postgraduados Campus Córdoba, and Centro de Estudios Geográficos, Biológicos y Comunitarios, S. C. (GEOBICOM). Finally, thanks to the anonymous reviewers who helped improve the manuscript.

## REFERENCES

Aguilar R, Cristóbal-Pérez EJ, Balvino-Olvera FJ, Aguilar-Aguilar MJ, Aguirre-Acosta N, Ashworth L, Lobo JA, Martén-Rodríguez S, Fuchs EJ, Sánchez-Montoya G, Bernardello G, Quesada M. 2019. Habitat fragmentation reduces plant progeny quality: a global synthesis. Ecology Letters 22 (7): 1163–1173. https://doi.org/ 10.1111/ele.13272

Albrecht H, Cambecèdes J, Lang M, Wagner M. 2016. Management options for the conservation of rare arable plants in Europe. Botany Letters 163 (4): 389–415. https://doi.org/10.1080/23818107.2016.1237886

Araujo-Mondragón F, Redonda-Martínez R. 2019. Flora melífera de la región centro-este del municipio de Pátzcuaro, Michoacán, México. Acta Botanica Mexicana 126 (e1444): 1–20. https://doi.org/10.21829/abm126.2019.1444

Bonet FM, Vergara CH. 2016. Abejas silvestres de un cafetal orgánico en Veracruz, México. Universidad de las Américas Puebla. Escuela de Ciencias. Colección Sapientias. San Andrés Cholula, Puebla, México. 517 p.

Cadena RYJ, Vázquez-Sánchez M, Cruz-Cárdenas G, Villaseñor JL. 2019. Use of ecological niche models of plant species to optimize placement of apiaries. Journal of Apicultural Science 63 (2): 243–265. https://doi.org/10.2478/jas-2019-0017

Castellanos-Potenciano BP, Ramírez-Arriaga E, Zaldivar-Cruz JM. 2012. Análisis del contenido polínico de mieles producidas por *Apis mellifera* L. (Hymenoptera: Apidae) en el Estado de Tabasco, México. Acta Zoológica Mexicana 28 (1): 13–36. https://www.scielo.org.mx/pdf/azm/v28n1/v28n1a2.pdf

Chamorro-García FJ, León-Bonilla D, Nates-Parra G. 2013. El polen apícola como producto forestal no maderable en la Cordillera Oriental de Colombia. Colombia Forestal 16 (1): 53-66. https://doi.org/10.14483/udistrital. jour.colomb.for.2013.1.a04

Chase MW, Christenhusz MJM, Fay MF, Byng JW, Judd WS, Soltis DE, Mabberley DJ, Sennikov AN, Soltis PS, Stevens PF, et al. 2016. An update of the angiosperm phylogeny group classification for the orders and families of flowering plants: APG IV. Botanical Journal of the Linnean Society 181 (1): 1–20. https://doi.org/10.1111/ boj.12385

CONAFOR (Comisión Nacional Forestal). 2022. Programa Anual de Trabajo 2022. Secretaría de Medio Ambiente y Comisión Nacional Forestal. Ciudad de México, México. https://

www.conafor.gob.mx/transparencia/docs/2022/Programa_Anual_de _Trabajo_2022.pdf (Retrieved: December 2022).

Espinosa-García FJ, Villaseñor-Ríos JL. 2017. Biodiversity, distribution, ecology, and management of non-native weeds in México: a review. Revista Mexicana de Biodiversidad 88: 76–96.

Farías-Silva FJ, Freitas BM. 2021. Thermoregulation in the large carpenter bee *Xylopa frontalis* in the face of climate change in the Neotropics. Apidologie 52: 341-357. https://doi.org/ 10.1007/ s13592-020-00824-8

González-Suárez M, Mora-Olivo A, Villanueva-Gutiérrez R, Lara-Villalón M, Vanoye-Eligio V, Guerra-Pérez A. 2020. Diversidad de la flora de interés apícola en el estado de Tamaulipas, México. Revista Mexicana de Ciencias Pecuarias 11 (3): 914–932. https://doi.org/10.22319/ rmcp.v11i3.4717

González SR, Catalán HC, Domínguez MVM, Luna LC, Hernández CE, Damián NA, Cruz LB, Palemón FA. 2016. Análisis palinológico de los recursos florales utilizados por *Apis mellifera* L. (Hymenoptera: Apidae) en cuatro municipios del Estado de Guerrero, México. Tropical and Subtropical Agroecosystems 19 (1): 19–28.

Granados-Argüello RI, Villanueva-Gutiérrez R, Martínez-Hernández E, García MLE, González TJE. 2020. Análisis melisopalinológico de mieles de *Apis mellifera* L. en la zona centro de Veracruz, México. Polibotánica 50: 147–163. https://doi.org/ 10.18387/polibotanica.50.11

Hernández-Villa V, Vibrans H, Uscanga-Mortera E, Aguirre-Jaimes A. 2020. Floral visitors and pollinator dependence are related to floral display size and plant height in native weeds of central Mexico. Flora 262: 1-9. https://doi.org/10.1016/j.flora.2019.151505

Lot A, Chiang F. 1986. Manual de herbario. Administración y manejo de colecciones, técnicas de recolección y preparación de ejemplares botánicos. Consejo Nacional de la Flora de México, A. C. https://itvolivre.wordpress.com/2013/09/28/manual-de-herbario-lot-antonio-chiang-fernando-1986/

Meléndez RV, Meneses CL, Kevan PG. 2013. Chapter 19. Effects of human disturbance and habitat fragmentation on stingless bees. *In* Vit P, Pedro SRM, Roubik DW. (ed.), Pot-Honey. Springer New York. pp. 269-282 https://doi.org/10.1007/978-1-4614-4960-7_19 (Retrieved: August 2022).

Miranda F, Hernández-X E. 1963. Los tipos de vegetación de México y su clasificación. Boletín de la Sociedad Botánica de México 28: 29–179. https://www. botanicalsciences.com.mx/ index.php/botanicalSciences/article/view/1084/776

Montoya-Bonilla BP, Baca-Gamboa AE, Bonilla BL. 2017. Flora melífera y su oferta de recursos en cinco veredas del municipio de Piendamó, Cauca. Biotecnología en el Sector Agropecuario y Agroindustrial 1: 20–28. https://doi.org/10.18684/BSAA

Pérez-Postigo I, Bendix J, Vibrans H, Cuevas-Guzmán R. 2021. Diversity of alien roadside herbs along an elevational gradient in western Mexico. NeoBiota 65: 71–91. https://doi.org/10.3897/ neobiota.65.67192

Quezada-Euán JJ, Ayala-Barajas R. 2010. Abejas nativas de México. La importancia de su conservación. Ciencia y desarrollo 36 (247): 8-13. https://www.researchgate.net/ publication/306012956_Abejas_nativas_de_Mexico_La_importancia_de_su_conservacion

Quiroz GD, Arreguín SM. 2008. Determinación palinológica de los recursos florales utilizados por *Apis mellifera* L. (Hymenoptera: Apidae) en el estado de Morelos, México. Polibotánica 26: 159–173. https://polibotanica.mx/index.php/polibotanica/ article/view/889/ 1111

Ramírez-Bravo OE, Hernández-Santin L. 2016. Plant diversity along a disturbance gradient in a semi-arid ecosystem in Central Mexico. Acta Botanica Mexicana 117: 11–25. https://doi.org/10.21829/abm117.2016.1164

Real-Luna N, Rivera-Hernández JE, Alcántara-Salinas G, Zalazar-Marcial E, Pérez-Sato JA. 2021. The melliferous flora of Veracruz, Mexico. Agroproductividad 14 (4): 65–80. https://doi.org/10.32854/agrop.v14i4.1932

Rzedowski J. 1978. Vegetación de México. Limusa. https://www.biodiversidad.gob.mx/publicaciones/librosDig/pdf/ VegetacionMx_Cont.pdf

Sistema de Información Estadística y Geográfica del Estado de Veracruz de la Llave. 2021. Cuadernillos Municipales 2021 Córdoba. http://ceieg.veracruz.gob.mx/wp-content/uploads/sites/21/2021/06/CÓRDOBA_2021.pdf (Retrieved: June 2022).

Tropicos.org. 2023. Tropicos.org. Missouri Botanical Garden. http://www.tropicos.org. (Retrieved: August 2023).

Villaseñor-Ríos JL, Ortiz E, Beutelspacher CR, Gómez-López JA. 2013. La familia Asteraceae en el municipio de San Cristóbal de Las Casas, Chiapas, México. Lacandonia 7 (1): 31–55.

Von TJ, Manson RH, Congalton RG, López-Barrera F, Jones KW. 2021. Evaluating the environmental effectiveness of payments for hydrological services in Veracruz, Mexico: A landscape approach. Land Use Policy 100: 1-13. https://doi.org/ 10.1016/j.landusepol.2020.105055

Agrociencia

# PERCEPTION OF GREEN INFRASTRUCTURE SYSTEMS: GREEN WALLS AND GREEN ROOFS

María Magdalena **Nevárez-Favela**[1], J. Cruz **García-Albarado**[2*], Abel **Quevedo-Nolasco**[1], Adolfo **López-Pérez**[1], Martin Alejandro **Bolaños-González**[1]

[1] Colegio de Postgraduados. Campus Montecillo. Carretera Federal México-Texcoco km. 36.5, Montecillo,Texcoco, State of Mexico, Mexico. C. P. 56264
[2] Colegio de Postgraduados. Campus Córdoba. Carretera Córdoba-Veracruz km. 348, Manuel León, Amatlán de los Reyes, Veracruz, Mexico. C. P. 94953.
* Author for correspondence: jcruz@colpos.mx

**Citation:** Nevárez-Favela MM, García-Albarado JC, Quevedo-Nolasco A, López-Pérez A, Bolaños-González MA. 2023. Perception of green infrastructure systems: green walls and green roofs. **Agrociencia** 57(8): 1746-1759. doi.org/ 10.47163/agrociencia.v57i8.3077

**Editor in Chief:**
Dr. Fernando C. Gómez Merino

Received: August 02, 2023.
Approved: November 20, 2023.
**Published in Agrociencia:** December 04, 2023.



## ABSTRACT

Integrating green walls (GWs) and green roofs (GRs) into urban areas enables several sustainable development objectives to be met. However, there is little research on the aesthetic perception and environmental and psychological benefits that users assign to these greening systems. Therefore, this paper evaluated the perception towards these two green infrastructures, GWs and GRs. The research was conducted via the Internet through a semi-structured survey with Likert scale questions, with a total of 243 participants. The results revealed that approximately 90 % of the participants have a positive perception of GWs and GRs. The psychological and environmental benefits of greening in urban environments are recognized, such as creating habitats for small species, reducing stress, and improving mood, among others. Some significant differences were seen in some socioeconomic aspects, such as age, gender and educational level. Women showed a tendency to find calm when in contact with plants, while the tendency for men is more neutral. Participants with a lower educational level, secondary school and a technical career, do not fully agree that nature positively affects their mood. In general, green walls were found to be preferred to green roofs; however, it is suggested to consider incorporating more colors, flowers and a greater variety of plants to improve the aesthetics of these structures.

**Keywords:** Aesthetic perception, green walls, vertical gardens, green roofs, psychological and environmental benefits.

## INTRODUCTION

Perception allows people to interpret, differentiate and analyze the environment around them according to their values. Landscape perception is influenced by an individual's memory and experiences, cultural background, beliefs and preferences (Rahman *et al.*, 2015). The study of landscape perception, also called environmental assessment, is a transdisciplinary methodological tool, necessary in the territorial planning process, in which users actively participate by responding to the perceived needs of the environment (Bruno-Rivera *et al.*, 2014).

In cities, vegetated areas have decreased and with it the quality of life of the inhabitants. Despite the changes and evolution of the human habitat, man still perceives the environment as a source of comfort and pleasure that plays a pivotal role in his emotional and psychological state (Rosley *et al.*, 2014). The World Health Organization (WHO) recommends 9 to 12 square meters of green area per inhabitant (Thaiutsa *et al*., 2008); however, there are few places in the world that comply with this recommendation. For example, in Mexico City the average is 12.75 square meters of green area per inhabitant, since in some areas such as in the south of the city the index is higher, but in the north and east it is much lower (Checa-Artasu, 2016).

In recent decades, greening elements have been incorporated into urban infrastructure as conservation tools (Manso *et al*., 2021). Greening systems in buildings are established both vertically and horizontally and are called green walls (vertical gardens, green facades, living walls) and green roofs (naturalized roofs), respectively. These two systems contain a set of layers that may vary with the complexity of the design, but the essential ones are vegetation, substrate, irrigation system (may not include it, especially on roofs), a waterproof membrane (green roofs and living walls), and a support system (Perini and Ottelé, 2012; Abass *et al*., 2020).

Green infrastructures, such as green walls and green roofs, are highly visual implementations that contribute to several sustainable development goals, such as 3 (health and well-being), 10 (reduced inequalities), 11 (sustainable cities and communities), 13 (climate action) and 15 (life on land) (Nguyen-Dang *et al*., 2023). Liberalesso *et al.* (2020) emphasize that these greening systems bring various economic, social and environmental benefits, such as supplying food and ornamentals through urban agriculture, improving aesthetics, regulating microclimates, and significantly improving air quality, among others. This is why researchers encourage stakeholders and the public to adopt greening infrastructures, such as green roofs and green walls, as a climate change mitigation strategy (Shafique *et al*., 2020).

Many cities promote the installation of green roofs and green walls, such as Mexico City, Tokyo, Chicago, Toronto, Copenhagen, and Lisbon, among others. However, globally, few studies have evaluated public perception regarding the benefits and potential problems of these greening systems, as well as the policies for promoting them (Loder, 2014; Ávila-Hernández *et al*., 2023). García-Albarado *et al.* (2021) show that infrastructure in good condition, cleanliness and evident maintenance (signs of care) are necessary to improve the visual attractiveness of green areas in cities, as could apply to greening systems.

There are several studies on the perception of urban greening, carried out mainly from the aesthetic, economic, social and environmental points of view. Aesthetically, differences in perception have been found. On the one hand, Butler *et al.* (2012) found that, among green roof experts, architects are the most likely to promote native species while engineers are on the opposite end of the spectrume, and landscape architects and biologists are in the middle. On the other hand, Nagase and Koyama (2020) found that Japanese people prefer green roofs with turf because they are "neat and

tidy" and they like biodiverse meadow roofs less, totally contrary to what was found by (Jungels *et al.* (2013) who indicate that Americans had more positive reactions to mixed perennial roofs than to grass ones. In Copenhagen, Denmark, Danuta-Lausen *et al.* (2022) found that 70 % of their interviewees have a positive opinion of the aesthetics of wild vegetation.

Zhang *et al.* (2020) found that residents of Guangzhou, China value environmental services related to their daily life such as air pollution, high temperatures and noise pollution, and care less about biodiversity protection services. Jim *et al*. (2022) note that Tokyo residents agree with the contribution of green roofs and green walls to improving air quality, thermal comfort and the aesthetics of the urban landscape, but they find the costs high and consider the presence of mosquitoes and the accumulation of plant waste a problem.

From an economic point of view, studies show that not all users of these greening systems are willing to pay for them. At a train station in Lisbon, Portugal, Benoliel *et al.* (2021) found that users attributed value to greening systems, but are willing to pay only a little and prefer more seats or better waiting areas. In Guangzhou, China, 80 % of 409 participants were willing to pay to use and maintain greening systems, especially young people (Zhang *et al*., 2020). For their part, Tokyo residents, according to Jim *et al.* (2022), are mostly unwilling to pay to improve neighborhood vegetation (40.2 %), and of those who are willing to pay, 29.4 % would not pay more than $ 300 MXN (2000 JPY).

The objective of this study was to analyze the perception of green roofs and green walls from an aesthetic, psychological and environmental point of view in order to recommend design criteria to landscaping professionals.

## MATERIALS AND METHODS

A semi-structured survey was conducted to ascertain people's perceptions. This was prepared in Google Forms and was executed via the Internet during the month of November 2022. The instrument consisted of three sections; in the first, the socioeconomic characteristics of the respondents were collected: age, sex, place where they lived, place where they currently live, monthly income (MXN), occupation and educational level. The importance of these characteristics lies in the fact that they usually constitute the independent variables used in experimental research. The second included two photographs, an extensive green roof and an outdoor green wall (Figure 1) that respondents evaluated aesthetically: liking, color, design, and plant selection, as well as their affinity to the existence of these greening systems. In the third section, participants chose their degree of agreement (strongly disagree (1), disagree (2), neutral (3), agree (4) and strongly agree (5)) with statements indicating the psychological and environmental benefits associated with nature and greening systems.

The survey consisted of 30 questions divided into 3 sections. Sections 2 and 3 used 4- and 5-level Likert scales, as shown in Table 1. The survey items are long sentences,


**Figure 1**. A: Extensive green roof; B: Outdoor green wall.

**Table 1.** Perception survey applied via the Internet.

| Variable | Code | Values entered in R |
|---|---|---|
| **Section 1. General data** | | |
| Age | Age | 16 to 64 (years) |
| Gender | Gen | Female (F), Male (M) |
| Place where you grew up | Lived | Rural area (RA), Urban area (UA) |
| Place where you live | Live | Rural area (RA), Urban area (UA) |
| Educational level | Educa | Elementary, Secondary, High School, Technical career, University, Postgraduate |
| Occupation | Occup | Student, Employed, Unemployed, Retired, Other |
| ¿What is your monthly income ($MXN)? | Income | < 5,000; 5,000 – 10,000 ; 10,000 – 15,000; 15,000 – 20,000; 20,000 – 30,000; > 30,000 |
| **Section 2. Design of greening systems** (Photos of a green roof and a green wall are evaluated) | | |
| How much do you like this green roof? ǂ | GRliking | Not at all (1), a little (2), somewhat (3) and a lot (4) |
| How attractive do you find the green roof design? ǂ | GRdesign | |
| How attractive do you find the plant selection? ǂ | GRplants | Not at all (1), a little (2), somewhat (3) and very attractive (4) |
| How attractive do you find the color selection? ǂ | GRcolors | |
| What would you like to add or remove to make the green roof to your total liking? ǂ | GRadd | NA (Keywords were identified in the respondents' comments in Excel®). |
| How much would you agree that there should be more green roof spaces in the city? ǂ | MoreGRs | Strongly disagree (1), disagree (2), agree (3) and strongly agree (4). |
| How much do you like this green wall? ǂ | GWliking | Not at all (1), a little (2), somewhat (3) and a lot (4) |
| How attractive do you find the design? ǂ | GWdesign | |
| How attractive do you find the plant selection? ǂ | GWplants | Not at all (1), a little (2), somewhat (3) and very attractive (4) |
| How attractive do you find the color selection? ǂ | GWcolors | |

**Table 1.** Continue.

| Variable | Code | Values entered in R |
|---|---|---|
| What would you like to add or remove to make the green wall to your total liking? † | GWadd | NA (Keywords were identified in the respondents' comments in Excel®). |
| How much would you agree that there should be more green wall spaces in the city? | MoreGWs | Strongly disagree (1), disagree (2), agree (3), and strongly agree (4) |
| Which do you prefer, a green roof or a green wall? † | GRvsGW | A green roof (1), a green wall (2), both (3) and neither (4) |
| **Section 3. Benefits of greening systems** | | |
| Green roofs and walls provide a space for the development of small animal species (bees, butterflies, and other insects). ††† | SmallAni | Strongly disagree (1), disagree (2), neutral (3), agree (4), and strongly agree (5). |
| I like the aesthetics of a building with greening (green walls and roofs) more than a concrete one. † | GreenBuild | |
| It is important to integrate nature into urban areas. †† | NatUA | |
| Integrating vegetation into urban areas represents an opportunity to manifest Mexican culture. ††† | Culture | |
| I consider that the presence of nature positively affects my mood. ††† | PosMood | |
| I consider that being in contact with nature reduces my stress level. ††† | LessStr | |
| I associate nature with pleasant memories. ††† | PleasMem | |
| Being in contact with plants makes me calm. ††† | PlantCalm | |
| I seek more contact with plants after the COVID confinement. ††† | PlantCOV | |
| I would like to have a green wall or roof in my home † | HomeGWGR | |

†Aesthetic, ††environmental and †††psychological criteria.

so they were coded for handling in the Rstudio software and for the creation of the graphs.

The statistical analysis was performed in the free software Rstudio and Excel®. Cronbach's alpha was applied to the items to evaluate the reliability of the questions. The Kolmogorov-Smirnov test was used to evaluate the normality (p-value > 0.05) of the variables. Graphs were made of the distribution of responses (percentage of agreement, disagreement, etc.) for sections 2 and 3. Because of the type of variables in the survey, the non-parametric Kruskal Wallis test was performed, with the dependent variable being one of the items and the independent variable being some socioeconomic data (age, gender, lived, live, education, occupation, income). The non-parametric Kruskal Wallis test was also included, in which the evaluation of the aesthetics of the green roof and the green wall was considered to depend on the design, colors and plant selection. In addition, manually, with the help of Excel®

filters, keywords were identified for open-ended questions 5 and 11, which sought the essential characteristics of green roofs and walls.

## RESULTS AND DISCUSSION

### Socioeconomic characteristics of respondents

A total of 243 participants were obtained, of which 125 were women and 118 were men, 51.4 % and 48.6 %, respectively. Of these, 53.1 % grew up in rural areas; however, 82.7 % currently live in urban areas, which is consistent with the phenomenon of rural-to-urban population change in Mexico. Ages ranged from 16 to 64 years, with most of the participants being between 16 and 40 years old (83.6 % of the sample). The educational level of the respondents is high: 49.8 % have a university degree, 40.3 % have a postgraduate degree, 7.4 % have a high school diploma, 1.2 % have a technical diploma and 1.2 % have a secondary school diploma, and more than half of them are students (51.9 %). It should be noted that, like age, educational level does not represent the reality of the Mexican population and this could impact the results since people with higher levels of education are more aware of current environmental damage and the need to make changes.

### Statistical analysis of the survey

The tool used in this research was the survey, in which sections 2 and 3 contain closed questions using the Likert scale with 4 and 5 categories. Some researchers, who have also applied surveys using a Likert scale, have carried out parametric analyses such as ANOVA and Tukey's test, as in the case of Jungels *et al.* (2013) and Nagase and Koyama (2020). However, in the present research, the Kolmogorov-Smirnov normality test was performed on the survey variables (p-value > 0.05, normal), and the data did not present normality, so they were analyzed with non-parametric tests as was done by Lee *et al.* (2014) and Liberalesso *et al.* (2020) who also found their variables to be non-normal. Jamieson (2004) is of the opinion that Likert scale data are ordinal, that is, they can be ordered, so they should be treated as interval data since the intervals between Likert scales are not equal.

### Reliability and distribution of perception responses

Cronbach's alpha internal consistency test was used to check the reliability of the survey. It was applied to the items with a Likert scale and an alpha of 0.891 was obtained, indicating that the internal consistency of the data is good (Taber, 2018). Subsequently, response distribution plots of all respondents were made with the "Likert" package in R.

Participants had a positive response towards green infrastructures, with green roofs receiving 94 % and green walls 96 % (Figure 2), which is consistent with the biophilia effect, which describes the human drive to connect with nature (García-Albarado *et al.*, 2021; Rosley *et al.*, 2014). It is noteworthy that green walls received more of the "I like it a lot" response than green roofs with 76.5 % and 55.1 %, respectively.


**Figure 2.** Distribution of preferences for green walls and green roofs (n=243). GW: green wall, GR: green roof. GWliking: How much do you like this green wall, GRliking: How much do you like this green roof?

Green walls obtained higher positive percentages and within positive appreciation they received more "very attractive" responses for design, plant selection and color selection than green roofs. In this study, participants tended to express greater liking for the outdoor green wall (Figure 3). Even with the differences in aesthetic perception between green roofs and green walls, the participants showed similar behavior in acceptance towards the establishment of these greening systems (94 % GR, 95 % GW). Respondents generally gave positive responses about the psychological and environmental benefits of green structures (Figure 4). Of the 10 items, 6 had more than a 90 % positive response ("agree" and "strongly agree"). Likewise, 3 other items exceeded 85 % positive response. The item "I seek more contact with plants after the

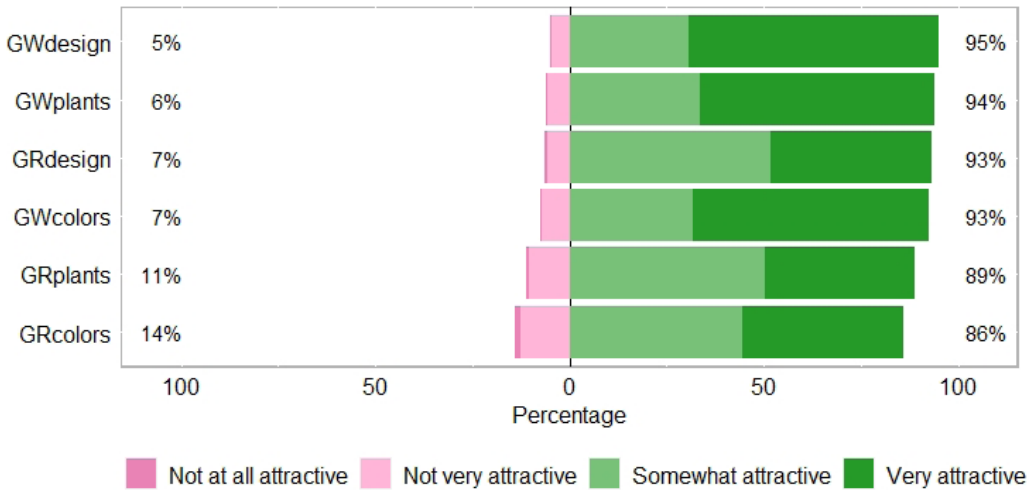


**Figure 3**. Perception of green roofs and green walls (n=243). GW: green wall, GR: green roof, Design: How attractive do you find the design?, Colors: How attractive do you find the color selection?, and Plants: How attractive do you find the plant selection?

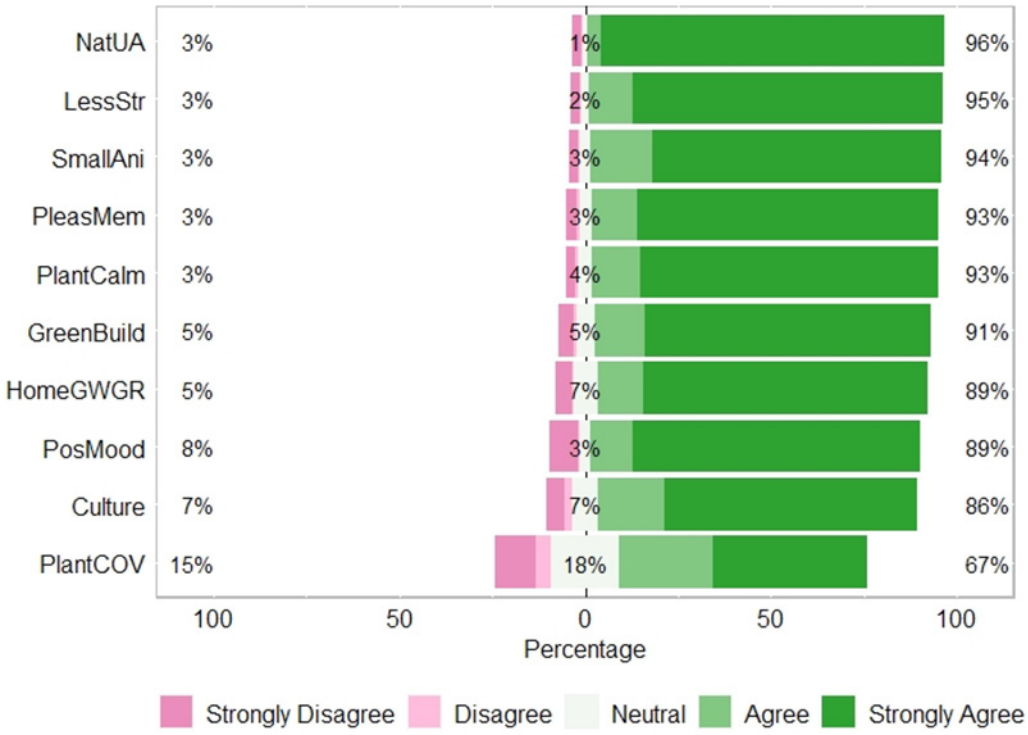


**Figure 4.** Benefits that respondents associate with greening systems (n=243). NatUA: it is important to integrate nature into urban areas, LessStr: I consider that being in contact with nature reduces my stress level, SmallAni: green roofs and walls provide a space for the development of small animal species (bees, butterflies and other insects), PleasMem: I associate nature with pleasant memories, PlantCalm: being in contact with plants makes me calm, GreenBuild: I like the aesthetics of a building with greening (green walls and roofs) more than a concrete one, HomeGWGR: I would like to have a green wall or roof in my home, PosMood: I consider that the presence of nature positively affects my mood, Culture: integrating vegetation into urban areas represents an opportunity to manifest Mexican culture, and PlantCOV: I seek more contact with plants after the COVID confinement.

COVID confinement" was the most varied, with 11.1 % answering "strongly disagree," 4.1 % "disagree," 18.1 % "neutral," 25.5 % "agree" and 41.2 % "strongly agree."

The results show a trend indicating that 9 out of 10 participants considered integrating nature into urban areas, due to the benefits of less stress, calm and pleasant moments in these spaces (Arvay, 2016). This also agrees with Benoliel *et al.* (2021), who suggest that integrating vegetation into the urban environment provides several environmental, economic and social benefits.

According to descriptive statistics, the results indicate that participants positively valued the psychological and environmental benefits attributed to the presence of

greening systems presented in the survey. A study that agrees with what was found here is that of Zhang *et al.* (2020), who stated that the inhabitants of Canton, China value the environmental services of greening systems that are related to their daily life, such as the reduction in noise and air pollution. Moreover, the findings of Williams *et al.* (2019) give evidence that green roofs can provide greater aesthetic enjoyment, attention control, and restorative experiences.

Respondents indicated that they really like green roofs and green walls, and they also agree on the benefits they bring. However, there was a lack of research on how much they are willing to pay for these greening systems, so it is suggested that future work should include this variable, as other authors have done (Benoliel *et al.*, 2021; Jim *et al.*, 2022).

### Differences in aesthetic perception, and psychological and environmental benefits by socioeconomic variables

The non-parametric Kruskal Wallis test ($\alpha = 0.05$) was applied to determine whether there are significant differences in the aesthetic, psychological and environmental perceptions of the respondents. Most of the items showed no significant differences, with a few exceptions (Table 2). Similarly, Nguyen-Dang *et al.* (2023) found, at a Sydney university, that user perception did not differ by sociodemographic characteristics, although students perceived social benefits more than administrative staff. It should be noted that in this study 51.9 % of the participants were students; however, there were no differences by occupation.

The age group of 49-56 years old unanimously mentioned that they like the green wall "a lot" and the youngest group, 16-24 years, responded similarly. In their research, Liberalesso *et al*. (2020) found no significant differences (Kruskal Wallis test) between the age ranges and the dependent variable "green infrastructure as a decision point for choosing a hosting location." On the other hand, Zhang *et al.* (2020) found that age had

**Table 2.** Kruskal Wallis test for all items.

| Independent variable | Dependent variable | Chi-square ($X^2$) | p-value | Significance level |
|---|---|---|---|---|
| Age (6 intervals) | GWliking | 11.749 | 0.038 | * |
| Gender | PlantCalm | 4.139 | 0.041 | * |
| Like | GRvsGW | 4.051 | 0.044 | *¿1 |
| Education | NatUA | 13.510 | 0.009 | ** |
| Education | PosMood | 10.248 | 0.036 | * |

Significance levels: NS (Not significant), * ($P < 0.05$), ** ($P < 0.01$). GWliking: How much do you like this green wall?, PlantCalm: Being in contact with plants makes me calm, GRvs GW: Which do you prefer, a green roof or a green wall?, NatUA: It is important to integrate nature into urban areas and PosMood: I consider that the presence of nature positively affects my mood.

a significant effect on willingness to pay for the maintenance of green roofs and green walls, with young Cantonese people (18-35 years old) being the most willing to pay.
In terms of gender, the results also show that there is a greater tendency for women to "totally agree" with the statement "Being in contact with plants makes me calm," while the tendency for men is more "neutral." Given this, Liberalesso *et al.* (2020) indicated that women have a moderately stronger environmental concern and sensitivity than men since the "urban men" group frequently responded with lower ratings to questions about possible benefits, disadvantages and their perception of the installation of green roofs and green walls than the "urban women" group (significant differences). García and Dunnett (2009) suggest in their study that these differences between men and women, as well as by age, could be due to cultural factors or evolutionary theories of landscape perception. They also found a tendency for women to have a more favorable perception of naturalistic plantings compared to those with a more formal appearance.
Education also influenced the items "It is important to integrate nature into urban areas" and "Nature positively affects my mood," as respondents with a technical diploma, unlike the other levels of education, only "agreed" and not "strongly agreed". However, it is very likely that this difference occurred because this group did not have a representative number.
Allard-Poesi *et al.* (2022) proposed a model that measures how the individual's perception and the characteristics of nature influence the sense of well-being. In this study, the respondents, 2500 French citizens, indicated that small spaces with nature (a balcony, a patio, or a roof garden) contribute to well-being, but to a lesser extent than less domesticated natural areas (forests, fields, and scrubland).

**Differences in aesthetic perception between green roofs and green walls**

There was a difference between the aesthetic perception of green roofs and green walls (Table 3). The green wall shown in this survey was consistently rated more positively in terms of overall liking, design, plant selection, and color scheme compared to green roofs. This indicates a widespread preference for green walls over green roofs among

**Table 3**. Kruskal Wallis test for aesthetic perception of green roofs and walls.

| Variable | Chi-square ($X^2$) | p-value | Significance level |
|---|---|---|---|
| Liking | 23.076 | 1.557E-06 | ** |
| Design | 22.779 | 1.82E-06 | ** |
| Plants | 21.976 | 2.76E-06 | ** |
| Colors | 18.918 | 1.37E-05 | ** |
| More | 0.600 | 0.4385 | NS |

Significant levels: NS (Not significant), * (P <0.05), ** (P <0.01).

participants. The inclination towards green walls may be associated with properties that characterize the aesthetics of a landscape, such as colors, textures, and shapes, and how these relate to each other, as noted by López-Contreras *et al.* (2019) in their research.

Liberalesso *et al.* (2020) had similar results, where respondents, hostel users in Lisbon, Portugal, showed a preference for five types of greening structure in the following order: 1) Indoor living wall, 2) Accessible green roof, 3) Outdoor living wall, 4) Green façade and 5) Inaccessible green roof. Teotónio *et al*. (2020) found that users prefer and are willing to pay more for accessible greening systems. In their research, users valued the additional space of an accessible green roof for recreational activities more than the aesthetic improvement obtained through the greening of the building.

The work of Ávila-Hernández *et al.* (2023) shows that in Mexico there is more research on green roofs than on green walls; however, it is necessary to increase the research and legislation on green walls, since they are of interest to potential users.

### Respondents' proposals for aesthetic improvement

From the main responses to the questions "What would you like to add or remove to make the green roof/green wall to your total liking," it is indicated that for both greening systems, more needs to be added in terms of colors, flowers and plant variety. Among others, it was mentioned to include plants for pollinators and plants with low water consumption (Table 4).

The design of greening systems and their attractiveness are correlated with the selection of plants and their colors. That is, they are more attractive if they integrate a diversity of colors, flowers and plant species. In addition to these characteristics, García-Albarado *et al.* (2021) state that infrastructure in good condition, cleanliness and evident maintenance (signs of care) are necessary to improve the visual appeal of green spaces where greening systems can be included.

Lee *et al.* (2014) found the following preferences of employees in Melbourne, Australia: herbaceous plants over succulents, green foliage over gray and red foliage, and taller vegetation over lower-growing vegetation on green roofs. They also found that flowers

**Table 4.** What respondents would add to the green roof and green wall to improve its aesthetics.

| Green roof | | Green wall | |
|---|---|---|---|
| **Characteristic** | **Frequency** | **Characteristic** | **Frequency** |
| More colors | 44 | More colors | 38 |
| More flowers | 32 | More flowers | 19 |
| Edible plants | 20 | Creeper plants | 7 |
| Design (improve) | 16 | Red color | 6 |
| Shade plants | 13 | Symmetrical shapes | 5 |
| Greater plant variety | 10 | Greater plant variety | 4 |

make any arrangement of vegetation on a green roof more attractive. On the other hand, Nagase and Koyama (2020) found that Japanese people prefer green roofs with turf because they are "neat and tidy" and like biodiverse meadow roofs less, contrary to Jungels *et al.* (2013) who indicate that Americans prefer green roofs with mixed perennial or Sedum-dominated species over those with grasses. Likewise, Garcia and Dunnett (2009) found that women tend to prefer plantings with a greater diversity of colors and flowers. They attribute this in part to the fact that, evolutionarily speaking, women, in charge of the fruit-gathering process, have specialized their sense of selection, unlike men.

## CONCLUSIONS

In Mexico, little has been studied about the perception of urban greening systems, green roofs and green walls, although it is important since this type of work provides a guide for the characteristics and types of greening systems that users are willing to adopt and therefore maintain in order to improve their quality of life.

In this study, in general, no significant differences were found in the perception of the participants based on the socioeconomic variables, although some differences were observed by age, gender and educational level. Within the scope of this research we found a positive tendency of the participants towards green walls and green roofs; in addition, they attribute psychological and environmental benefits to these greening systems such as the creation of habitats for small species, stress reduction, mood improvement and evocation of pleasant memories. This suggests that greening is perceived as beneficial to the quality of life. From the results of this research, it can be suggested that greening systems, green roofs and green walls, should include a greater diversity of plants, colors and flowers to make them more aesthetically appealing. This finding is consistent with previous studies and can help in the design and creation of these green infrastructures in cities.

Furthermore, and given that perception is affected by all the sensory senses, namely touch, smell, hearing, taste and not just vision, it is suggested that future research include *in situ* perception surveys applied in the greening systems.

## ACKNOWLEDGMENTS

The authors thank the College of Postgraduates for its support through the Hydro-sciences (Montecillo Campus) and Landscape and Rural Tourism (Córdoba Campus) postgraduate programs, as well as the National Council of Humanities, Sciences and Technologies (CONAHCYT) of Mexico.

## REFERENCES

Abass F, Ismail LH, Wahab IA, Elgadi AA. 2020. A review of green roof: definition, history, evolution and functions. IOP Conference Series: Materials Science and Engineering 713 (1): 012048. https://doi.org/10.1088/1757-899X/713/1/012048

Allard-Poesi F, Matos LBS, Massu J. 2022. Not all types of nature have an equal effect on urban residents' well-being: a structural equation model approach. Health and Place 74: 102759. https://doi.org/10.1016/j.healthplace.2022.102759

Arvay CG. 2016. El efecto biofilia: el poder curativo de los árboles y las plantas. Ediciones Urano, S. A. U. Barcelona, España. 251 p.

Ávila-Hernández A, Simá E, Ché-Pan M. 2023. Research and development of green roofs and green walls in Mexico: a review. The Science of The Total Environment 856: 158978. https://doi.org/10.1016/j.scitotenv.2022.158978

Benoliel MA, Manso M, Dinis-Ferreira P, Matos-Silva C, Oliveira-Cruz C. 2021. "Greening" and comfort conditions in transport infrastructure systems: Understanding users' preferences. Building and Environment 195: 107759. https://doi.org/10.1016/j.buildenv.2021.107759

Bruno-Rivera A, García-Albarado JC, Pérez-Vázquez A, Gallardo-López F, Vargas-Mendoza MC. 2014. La percepción en la evaluación del paisaje. Revista Mexicana de Ciencias Agrícolas 9: 1811–1817. https://doi.org/10.29312/remexca.v0i9.1068

Butler C, Butler E, Orians CM. 2012. Native plant enthusiasm reaches new heights: Perceptions, evidence, and the future of green roofs. Urban Forestry and Urban Greening 11 (1): 1–10. https://doi.org/10.1016/j.ufug.2011.11.002

Checa-Artasu MM. 2016. Las áreas verdes en la Ciudad de México. Biblio3W, Revista bibliográfica de geografía y ciencias sociales 21: 22. http://www.ub.edu/geocrit/b3w-1159.pdf

Danuta-Lausen E, Backhaus A, Bergen-Jensen M. 2022. Urbanites' perception of vegetation in landscape-based stormwater management elements (LSM). Urban Ecosystems 25 (5): 1577–1588. https://doi.org/10.1007/s11252-022-01250-7

García-Albarado JC, Dunnett N. 2009. Percepción del público hacia plantaciones de herbáceas ornamentales. Revista Chapingo Serie Horticultura 15 (2): 49–55. https://www.scielo.org.mx/pdf/rcsh/v15nspe/v15nspea8.pdf

García-Albarado JC, Rivera-Bruno A, Rodríguez-Lozano LA. 2021. Percepción de áreas verdes. *En* Olivares E. (ed.), Diseño de paisajes para ciudades biodiversas. Sistema de Apoyos a la Creación y Proyectos Culturales (FONCA): México, pp: 158–173.

Jamieson S. 2004. Likert scales: how to (ab)use them. Medical Education 38 (12): 1217–1218. https://doi.org/10.1111/j.1365-2929.2004.02012.x

Jim CY, Hui LC, Rupprecht CDD. 2022. Public perceptions of green roofs and green walls in Tokyo, Japan: a call to heighten awareness. Environmental Management 70 (1): 35–53. https://doi.org/10.1007/s00267-022-01625-8

Jungels J, Rakow DA, Allred SB, Skelly SM. 2013. Attitudes and aesthetic reactions toward green roofs in the Northeastern United States. Landscape and Urban Planning 117: 13–21. https://doi.org/10.1016/j.landurbplan.2013.04.013

Lee KE, Williams KJH, Sargent LD, Farrell C, Williams NS. 2014. Living roof preference is influenced by plant characteristics and diversity. Landscape and Urban Planning, 122: 152–159. https://doi.org/10.1016/j.landurbplan.2013.09.011

Liberalesso T, Mutevuie-Júnior R, Oliviera-Cruz C, Matos-Silva C, Manso M. 2020. Users' perceptions of green roofs and green walls: an analysis of youth hostels in Lisbon, Portugal. Sustainability, 12 (23): 1–25. https://doi.org/10.3390/su122310136

Loder A. 2014. "There's a meadow outside my workplace": a phenomenological exploration of aesthetics and green roofs in Chicago and Toronto. Landscape and Urban Planning 126: 94–106. https://doi.org/10.1016/j.landurbplan.2014.01.008

López-Contreras C, Collantes-Chávez-Costa AL, Barrasa-García S, Alanís-Rodríguez E. 2019. Bases conceptuales y métodos para la evaluación visual del paisaje. Agrociencia 53 (7): 1085–1104.

Manso M, Teotónio I, Matos-Silva C, Oliveira Cruz C. 2021. Green roof and green wall benefits and costs: a review of the quantitative evidence. Renewable and Sustainable Energy Reviews 135: 110111. https://doi.org/10.1016/j.rser.2020.110111

Nagase A, Koyama S. 2020. Attractiveness and preference of extensive green roofs depend on vegetation types and past experience with plants in Japan. Urban Forestry and Urban Greening 51: 126658. https://doi.org/10.1016/j.ufug.2020.126658

Nguyen-Dang HA, Legg R, Khan A, Wilkinson S, Ibbett N, Doan AT. 2023. Users' perceptions of the contribution of a university green roof to sustainable development. Sustainability 15 (8): 1–11. https://doi.org/10.3390/su15086772

Perini K, Ottelé M. 2012. Vertical greening systems: contribution to thermal behaviour on the building envelope and environmental sustainability. WIT Transactions on Ecology and the Environment 165: 239–250. https://doi.org/10.2495/ARC120221

Rahman SRA, Ahmad H, Mohammad S, Rosley MSF. 2015. Perception of green roof as a tool for urban regeneration in a commercial environment: the secret garden, Malaysia. Procedia170: 128–136. https://doi.org/10.1016/j.sbspro.2015.01.022

Rosley MSF, Rahman SRA, Lamit H. 2014. Biophilia theory revisited: experts and non-experts perception on aesthetic quality of ecological landscape. Procedia - Social and Behavioral Sciences 153: 349–362. https://doi.org/10.1016/j.sbspro.2014.10.068

Shafique M, Xue X, Luo X. 2020. An overview of carbon sequestration of green roofs in urban areas. Urban Forestry and Urban Greening 47: 126515. https://doi.org/10.1016/j.ufug.2019.126515

Taber KS. 2018. The use of cronbach's alpha when developing and reporting research instruments in science education. Research in Science Education 48 (6): 1273–1296. https://doi.org/10.1007/s11165-016-9602-2

Teotónio I, Oliveira-Cruz C, Matos-Silva C, Morais J. 2020. Investing in sustainable built environments: the willingness to pay for green roofs and green walls. Sustainability 12 (8). https://doi.org/10.3390/SU12083210

Thaiutsa B, Puangchit L, Kjelgren R, Arunpraparut W. 2008. Urban green space, street tree and heritage large tree assessment in Bangkok, Thailand. Urban Forestry and Urban Greening 7 (3): 219–229. https://doi.org/10.1016/j.ufug.2008.03.002

Williams KJH, Lee KE, Sargent L, Johnson KA, Rayner J, Farrell C, Miller RE, Williams NSG. 2019. Appraising the psychological benefits of green roofs for city residents and workers. Urban Forestry and Urban Greening, 44: 126399. https://doi.org/10.1016/j.ufug.2019.126399

Zhang X, Ni Z, Wang Y, Chen S, Xia B. 2020. Public perception and preferences of small urban green infrastructures: a case study in Guangzhou, China. Urban Forestry and Urban Greening 53: 126700. https://doi.org/10.1016/j.ufug.2020.126700

Agrociencia

# *Trichoderma erinaceum* AND *Trichoderma virens* IN THE CONTROL OF *Meloidogyne incognita* IN *Solanum lycopersicum*

Orlando **Martínez-Canto**[1], Jairo **Cristóbal-Alejo**[1], José María **Tun-Suárez**[1], Arturo **Reyes-Ramírez**[1]*

[1] Tecnológico Nacional de México. Instituto Tecnológico de Conkal. Avenida Tecnológico s/n, Conkal, Yucatán, Mexico. C. P. 97345.
* Author for correspondence: arturo.rr@conkal.tecnm.mx

**Citation:** Martínez-Canto O, Cristóbal-Alejo J, Tun-Suárez JM, Reyes-Ramírez A. 2023. *Trichoderma erinaceum* and *Trichoderma virens* in the control of *Meloidogyne incognita* in *Solanum lycopersicum*. **Agrociencia** 57(8): 1760-1772. doi.org/ 10.47163/agrociencia.v57i8.2784

**Editor in Chief:**
Dr. Fernando C. Gómez Merino

Received: May 04, 2022.
Approved: June 29, 2023.
**Published in Agrociencia:** December 05, 2023.



## ABSTRACT

In this study, the antagonistic potential of *Trichoderma erinaceum* 10-15 and *T. virens* 32-09 against the nematode *Meloidogyne incognita* was evaluated in tomato (*Solanum lycopersicum* L.) plants. A solution of $10^6$ conidia $mL^{-1}$ of each strain was inoculated on tomato plants, and the variables of nematode control, galling index, eggs per gram of root, and females per gram of root were determined. The *in vitro* antagonism of *Trichoderma* filtrates on the hatching of eggs and J2 juveniles of *M. incognita* was evaluated. The results were used for analysis of variance and comparison of means using the Tukey method ($p \leq 0.05$). Control variables of the phytopathogen on *S. lycopersicum* were determined by measuring the area under the disease progress curve (AUDPC), the Weibull parameter, the coefficient of determination, and the final severity of root damage. *T. erinaceum* 10-15 showed a greater inhibitory effect on *M. incognita*, relative to *T. virens* 32-09. Both strains evaluated showed significant differences in comparison to the uninoculated control, resulting in a 60 % reduction in juvenile stage mobility and egg hatching, as well as greater control of the phytonematode in the AUDPC variables, Weibull parameter, and final severity under controlled conditions. The strain *T. erinaceum* 10-15 showed a better antagonistic effect on egg formation at 68 days, at 60.3 %, and on reducing the number of *M. incognita* females with at 60 days, at 80.6 %. Both *T. erinaceum* 10-15 and *T. virens* 32-09 were found to be potential biocontrol agents of *M. incognita* in *S. lycopersicum*.

**Key words:** galling, filtering, nematode, severity, tomato.

## INTRODUCTION

Tomato (*Solanum lycopersicum* L.) is one of the vegetables with the highest demand worldwide, where Mexico is the main supplier of exports. However, in recent years, the total area of the crop has decreased (SIAP, 2020) due to production losses from diseases caused by fungi, viruses, bacteria, and nematodes, the latter with a wide geographical distribution and host range (Mukhtar *et al*., 2018).

Parasitism caused by nematodes is a devastating and difficult-to-manage problem, as in the case of root-knot nematodes of the genus *Meloidogyne*, which are the most destructive and cause significant crop yield losses (Khan *et al*., 2020). *Meloidogyne incognita* is a polyphagous, obligate endoparasitic, gill-forming nematode on plant

roots and is considered one of the most damaging agents for crops worldwide (Fan *et al*., 2020) because it reduces plant growth, quality, and yield, and has reduced host resistance to biotic and abiotic stresses. In its juvenile stage, this organism penetrates the root through the cortex, near the elongation zone, and migrates towards the root tips, where it establishes its feeding site, which generates hypertrophy and hyperplasia of the surrounding cells (Temitope *et al*., 2020), which causes weakening of the tips, inhibition or excessive root stimulation, and also induces the formation of knots or galls in the root system (Martínez-Medina *et al*., 2017).

Several strategies have been developed to control *M. incognita*, the most common of which is the use of chemical nematicides, which are sometimes ineffective (Cristóbal-Alejo *et al*., 2018), as they affect human health and generate resistance. Because of this, it is necessary to implement safe and sustainable alternatives, such as the use of biological controllers through microorganisms, which offer a safe and economically feasible alternative for the control of nematodes (Pocurull *et al*., 2020). Herrera-Parra *et al*. (2017) demonstrated a greater nematicidal effect of *T. atroviride* compared to the chemical Oxamyl 24 % at a dose of 1 mL $L^{-1}$. *Trichoderma* spp. can be an alternative biocontrol against *M. incognita* by reducing the number of galls, eggs, females, and galling index in *S. lycopersicum* (Candelero *et al*., 2015). In *Capsicum chinense,* it showed similar effects from the nematicide Oxamyl at the same dose. (Herrera-Parra *et al.*, 2018). Moo-Koh *et al.* (2018) evaluated incompatible combinations of *T. citrinoviride* 33-58 and *T. harzianum* 33-59 that, when interacted, showed promising results in reducing *M. incognita*, in addition to improving the growth of *S. lycopersicum*.

The objective of the present study was to evaluate the *in vitro* antagonistic effect of two native species, *T. erinaceum* 10-15 and *T. virens* 32-09 against *M. incognita*, under controlled conditions on *S. lycopersicum* L. plants.

## MATERIALS AND METHODS

### *Trichoderma* strains used

The strains *T. erinaceum* 10-15 and *T. virens* 32-09, previously identified (Martinez-Canto *et al.*, 2021; Moo-Koh *et al*., 2018), were seeded on potato dextrose agar medium PDA (BD BIOXON, Mexico) (4 g potato infusion, 20 g dextrose, and 15 g agar per L, pH 5.6) for 8 days (d). Then, 5 mm diameter mycelial discs were extracted and deposited in 250 mL Bosch bottles (PYREX®, Czech Republic) with the potato-dextrose broth culture medium CPD (SIGMA-ALDRICH, Saint Louis, MO, USA) (300 g potato and 20 g dextrose per L, pH 6.8). Cultures were maintained at 30 °C without shaking for 27 d. The culture supernatant was filtered with sterile gauze and centrifuged (SOLBAT C600, Mexico) at 3000 rpm for 10 min, subsequently filtered with Whatman No. 1 paper and finished with a 0.45 μm millipore filter (Fisherbrand, Ireland); filtrates were deposited in sterile 50 mL Falcon tubes and stored at 4 °C until use (Candelero *et al*., 2015).

### Obtaining of *Meloidogyne incognita*

Egg masses were obtained from galled roots of *S. lycopersicum* that were disinfected with 1 % sodium hypochlorite (NaClO) for 2 min before being washed with potable water in sieves with 300 and 400 mesh numbers (FIIC S. A. de C. V., Mexico) to remove excess NaClO and incubated at 30 °C until J2 hatching (Cristóbal-Alejo *et al*., 2018). The *M. incognita* species was confirmed through perineal patterns of females and morphotaxonomic characterization (Jepson, 1987), for which a compound microscope (LABOMED Lx500, USA) was used.

### Antagonistic effects of *Trichoderma* on the immobility of J2 of *Meloidogyne incognita*

The assay was carried out using a siracusae, 2.5 cm wide by 3 cm high, with 100 µL of the filtrate of the cultures of *T. erinaceum* 10-15 and *T. virens* 32-09, and 900 µL of esteril distilled water, to which 20 viable J2 nematodes of *M. incognita* were added. The nematostatic effect was determined at 72 h under laboratory conditions with an environmental temperature of 30 °C. Sterile distilled water was used as a negative control, and the commercial product Oxamyl 24 % (Vydate®, Dupont, Mexico) was used as a positive control at a concentration of 1 mL $L^{-1}$. Using a stereoscopic microscope (Leica ZOOM 2000, Buffalo, NY, USA) and with the help of a brush, the immobility of the nematode was corroborated when stimulated in the cephalic region, and, when no response to the stimulus was presented, it was considered immobile (Cristóbal-Alejo *et al*., 2018), the percentage of immobility was calculated according to the formula proposed by Abbott (1925).

### *In vitro* effect of *Trichoderma* on hatching inhibition of *M. incognita* eggs

In this assay, 100 µL of the filtrates of *T. erinaceum* 10-15 and *T. virens* 32-09 were added to the siracusae. Five egg masses of *M. incognita* were placed in each egg mass, and the ability to inhibit egg hatching was evaluated with the aid of a stereoscopic microscope. Hatched juveniles were counted at 7, 14, and 21 days after hatching (dah) to fungal filtrates. Sterile distilled water was used as a negative control and the commercial product Oxamyl 24 % at a concentration of 1 mL $L^{-1}$ was used as a positive control (Moo-Koh *et al*., 2018), the percentage of hatching inhibition was calculated according to the formula of Abbott (1925).

### Effect of *Trichoderma* spp. on *M. incognita* in *S. lycopersicum*

To evaluate the level of antagonism of *Trichoderma* strains on *M. incognita* on *S. lycopersicum*, a suspension of $10^6$ conidia $mL^{-1}$ of *T. erinaceum* 10-15 and *T. virens* 32-09, obtained from mycelium grown in Petri dishes on potato dextrose agar medium PDA (BD BIOXON, Mexico) for 8 d, was prepared. At the time of transplanting *S. lycopersicum* plants from the seedbed to plastic pots (capacity 8 kg) with previously homogenized soil, inoculations of $10^6$ conidia $mL^{-1}$ of each strain were made directly at the base of the stem, which was maintained with daily irrigation. The commercial

product Oxamyl 24 % was used as a positive control, dosed at 1 mL $L^{-1}$ at the time of transplanting, and sterile distilled water was used as a negative control, without the application of conidia. Two more applications of the same concentration ($10^6$ conidia $mL^{-1}$) of *Trichoderma* were made at 15 and 30 days after transplanting (dat). Each treatment included 10 replicates, homogeneously distributed in a completely randomized design under protected conditions (Moo-Koh *et al*., 2018).

## Estimation variables in the control of nematodes

### Galling index

The galling index was determined at 68 dat, estimated using the severity scale proposed by Taylor and Sasser (1978), where root damage was evaluated: 0 = healthy root system, 1 = 1 to 10 % small galls present in the root system, 2 = 11 to 25 % severely galled root system, 3 = 26 to 50 % severely galled root system, 4 = 51 to 75 % severely galled root system, and 5 = 76 to 100 % severely galled root system with sparse healthy roots (Moo-Koh *et al*., 2018). The galling index test was defined by an analysis of variance that determined the area under the disease progress curve (AUDPC), the distribution parameter of the Weibull model, the coefficient of determination ($r^2$) and the final disease severity ($Y_f$).

### Eggs per gram of root

To determine the number of eggs per g of root, 2 g of fragmented galled roots were cut, homogenized, and one gram of the sample was taken and liquefied in 30 mL of 2 % NaClO for 10 s. In order to recover the eggs, the mix was sieved successively in sieves of 50, 100, 200, 325, and 500, respectively. They were rinsed in running water and counted using compound microscopy with the aid of a nematode counting chamber (Cristóbal-Alejo *et al*., 2018).

### Females per gram of root

To determine the variable of the number of adult females per root, 1 g of root was stained with 4 mL of acid fuchsin (Analytyka, Mexico) in 50 mL of distilled water until boiling point for 10 min. The mix was left to cool at room temperature. A series of washes with running water were made, and these were deposited in flasks with 78 % glycerin (Golden Bell, Mexico). Using stereoscopic microscopy, roots were dissected and adult females were counted (Moo-Koh *et al*., 2018).

## Statistical analysis

For the analysis of the effect of *Trichoderma* spp. on J2 immobility and inhibition of *M. incognita* egg hatching, each treatment consisted of five replicates (five siracuses). With the data obtained, analysis of variance and comparison of means were performed using Tukey's test ($p \leq 0.05$) with the help of the InfoStat 2019 program.

To determine the estimation variables in nematode control, each treatment (*T. erinaceum* 10-15, *T. virens* 32-09, Oxamyl, and distilled water) consisted of 10 replicates, distributed in a completely randomized design. The data obtained were analyzed in SAS version 9.0 software for analysis of variance (ANOVA) and the separation of means was performed using Tukey's test ($p \leq 0.05$). The measurements of the variables recorded were determined in triplicate and calculated separately. Using SAS software, the galling index test was defined using an analysis of variance ($p \leq 0.05$) that determined the area under the disease progress curve (AUDPC), the distribution parameter of the Weibull model, the coefficient of determination ($r^2$), and the final disease severity ($Y_f$).

## RESULTS AND DISCUSSION

### Antagonistic effect of *Trichoderma* on the immobility of J2 of *M. incognita*

Differences were observed in the mobility of J2 at 72 h of exposure to the filtrates of the *Trichoderma* strains compared to the control; however, they were lower than those shown by the commercial product Oxamyl. Between the two *Trichoderma* strains, no significant differences were found, since *T. erinaceum* 10-15 showed an efficiency of 76 % of immobility and *T. virens* 32-09 had 64 %, while the chemical product (Oxamyl) showed a total capacity in the percentage of immobility of the J2 of *M. incognita*, while the control indicated a value of 1.6 % (Table 1).

**Table 1.** *In vitro* antagonistic effect of *Trichoderma* spp. filtrates on *M. incognita.*

| Treatment | J2 immobility at 72 h (%) | Inhibition of egg hatching at day 7 (%) |
|---|---|---|
| Oxamyl | 100.0 a | 100.0 a |
| *T. erinaceum* 10-15 | 76.0 ab | 84.2 a |
| *T. virens* 32-09 | 64.0 b | 63.3 a |
| Control | 1.6 c | 0.0 b |

a,b,c Means with different letters are statistically different (Tukey, $p \leq 0.05$).

In similar assays against second instar larvae of *Meloidogyne* sp., Xalxo *et al*. (2013) reported that *T. viride* filtrates, isolated from agriculturally active soil, had an immobilization capacity on juveniles of 65 % at 48 h, and 93.7 % at 72 h. Similarly, *T. harzianum* has been reported to possess nematicidal activity from the first 24 h of exposure as it showed significant antagonistic effects on *M. incognita* juveniles (Pinzón-Espinoza *et al*., 2015); these results match with those reported by Sellami *et al*. (2017), who showed that *T. harzianum* Th.6 and *T. atroviride* Ta.13 possess significant mortality rates of juveniles at three different concentrations evaluated, where the

most effective was *T. harzianum* (71.9 %) with 100 % filtrate, while *T. atroviridae* had an effectiveness of 56.94 %. Zhang *et al*. (2015) determined the antagonistic capacity of different concentrations of *T. longibrachiatum* on J2 of *M. incognita*, demonstrating a linear relationship between the lethal effects of this antagonist and the juvenile stage of the phytoparasite, as higher concentrations of *T. longibrachiatum* increased the mortality rate of J2 of *M. incognita.*

It is known that the antagonistic capacity of filtrates, more than the species itself evaluated, is associated with the type of strain, the element composition of the substrate used for its growth, and the exposure time of the J2 of *M. incognita* to the volatile and non-volatile secondary metabolites contained in *Trichoderma* filtrates, such as peptaibols, siderophores, policetides, and terpenoids (Fan *et al*., 2020). In the working group, previous trials have been conducted with the strain *T. virens* 32-09, where the antagonistic effect against *M. incognita* in tomato was determined (Pinzón-Espinoza *et al*., 2015; Moo-Koh *et al*., 2018). It has also been shown that residual filtrate fractions of *T. virens* 32-09, at a concentration of 100 %, presented a mortality of 83 % on *M. incognita* juveniles at 72 h, while the antagonistic effect of ethyl acetate fractions from this same strain registered a mortality of 100 % against *M. javanica* juveniles, also at 72 h (Moo-Koh *et al*., 2022). These differences in sensitivity in the behavior of different nematode species, or even between different populations of the same species, are attributed to various exposure conditions, both in their habitat and the environment in which they develop (Nourani *et al*., 2015). No studies were found evaluating the antagonism of *T. erinaceum*, so the use of this species as a potential biological controller of *M. incognita* was considered.

***In vitro* inhibitory effect of *Trichoderma* on hatching of *M. incognita* eggs.**

The egg hatch inhibition parameter indicates the ability to reproduce and could be interpreted as a decrease of the phytonematode in the field (Cristóbal-Alejo *et al*., 2018). At 7 d, a significant difference between treatments was observed because the filtrate of strain *T. erinaceum* 10-15 had a percentage inhibition of egg hatching of 84.1 %, followed by strain *T. virens* 32-09 with 63.3 %. The commercial nematicide Oxamyl showed 100 % hatch suppression (Table 1). Sellami *et al.* (2017) determined that *T. harzianum* Th.6 filtrate was the most effective in suppressing *M. incognita* egg hatching after 8 d of exposure, comparable to those used in the present study. Hernández-Ochandía *et al.* (2015) demonstrated the parasitic capacity of *T. asperellum Ta*. 90 on eggs of *M. incognita* race 2 using microscopy, indicating that the fungus is capable of penetrating and damaging the egg contents, generating dark spots characteristic of parasitism, as well as emerging hyphae, which caused the embryos to die.

Similar percentages to those obtained in this study were reported by Fan *et al.* (2020) when evaluating the ovicidal capacity of *T. citrinoviride* Snef1910, indicating that it had an inhibition in the hatching of *M. incognita* eggs higher than 90.2 % at 48 h, since it maintained its ovicidal potential on *M. incognita* eggs for approximately 96 h. An increase in enzymes (chitinases and proteases) prevented hatching by parasitizing the

different layers that protect the embryo inside the egg, such as vitellin and chitin, which, together with primary, secondary metabolites and various active compounds, give *Trichoderma* its antimicrobial and biocontrol properties (Zhang *et al*., 2015; Benttoumi *et al*., 2020).

## Variables in nematode control

### Galling index

To evaluate the galling index, a comparison was made between the roots of the different treatments by analysis of variance ($p \leq 0.05$). Differences between treatments were observed, as well as a correlation between the different parameters of epidemic intensity. The AUDPC values fluctuated between 817.1 of the negative control and 310.4 of the positive control (Oxamyl). The two *Trichoderma* strains did not show significant differences in this value; however, *T. erinaceum* 10-15 showed the greatest effect with a value of 539.0 (Table 2). As for the Weibull parameter, Oxamyl recorded the lowest value (0.0100), followed by *T. erinaceum* strain 10-15, with 0.0109. A relationship

**Table 2.** Variables in the control of the severity of *M. incognita* in tomato plants inoculated with *Trichoderma* spp.

| Treatment | AUDPC (% unit day$^{-1}$) | Weibull | $r^2$ | $Y_f$(%) |
|---|---|---|---|---|
| Oxamyl | 310.4 a | 0.0100 a | 0.9983 | 16.6 a |
| *T. erinaceum* 10-15 | 539.1 b | 0.0109 a | 0.9675 | 27.7 ab |
| *T. virens* 32-09 | 581.4 b | 0.0123 ab | 0.9960 | 35.8 b |
| Control | 817.1 c | 0.0145 b | 0.8363 | 60.2 c |

a,b,c Means with different letters are statistically different (Tukey, $p \leq 0.05$). $r^2$: coefficient of determination; $Y_f$: final disease severity.

between $r^2$ and $Y_f$ was also observed in the *Trichoderma* treatments, where *T. erinaceum* 10-15 was the strain that achieved a decrease in the galling index with a coefficient of determination of 0.9675 and a final severity of 27.7 (Table 2).

The variability of the results obtained in this work could be due to the interaction of the different *Trichoderma* strains with the pathogenic capacity of the nematodes, the origin of the isolates, genetic variability, or efficiency of the antagonists to parasitize the nematodes. These results are in agreement with those reported by Al-Hazmi and TariqJaveed (2015), who indicated that higher concentrations of *T. harzianum* and *T. viride* persistently and significantly suppressed the gilling index of *M. javanica* in tomato, in addition to the number of eggs and juveniles, where it was found that *T. harzianum* was able to suppress the reproductive characteristics of the nematode.

Some *Trichoderma* species have been shown to have the ability to induce systemic resistance in plants through an early increase in transcript levels of jasmonic acid marker genes (Babu and Kamra, 2021). Martínez-Medina *et al*. (2017) pointed out that *T. harzianum* T78 could limit the infection cycle of *M. incognita*, as it affected galling, fecundity, and invasion in tomato roots. Temitope *et al.* (2020) reported that the higher the application rate of *T. asperellum*, the lower the population of *M. incognita* on *Celosia argentea*. This was due to the fact that *Trichoderma* conidia can adhere to and parasitize the eggs and prevent the mobilization of the juveniles. As they are not present, galling does not occur; therefore, the number of nematodes is directly proportional to the galling index. The antagonism exerted by *Trichoderma* varies according to species and isolate, as different strains show variable controlling activity on *M. incognita* (Moo-Koh *et al*., 2018).

**Number of *M. incognita* eggs**

At 60 d, strain *T. virens* 32-09 showed a mean egg number of 1756, which represented 67.55 % relative to the control, which had a mean of 5412, while strain *T. erinaceum* 10-15 recorded a mean of 4065, equivalent to 24.88 % (Figure 1). However, at 68 d, the strain *T. erinaceum* 10-15, with a mean of 5808.67, showed a greater suppressive effect on the hatching of *M. incognita* eggs per gram of root with 60.27 %, while the strain *T. virens* 32-09 recorded a suppression of hatching of 20.62 % compared to the control, which had a mean average number of eggs of 14621.33 (Figure 1). On both days, Oxamyl recorded higher hatch suppression. Zhang *et al.* (2015) reported that *T. harzianum* has the ability to decrease both the number of eggs and the galling rate per gram of root of *M. incognita* in a short time; however, such effects tend to decrease in the long term, a result that matches what was observed in the present work with strain *T. virens* 32-09, which up to day 60 showed an ascending effect, but at the conclusion of day 68, a decrease in its ability to suppress egg production was observed.

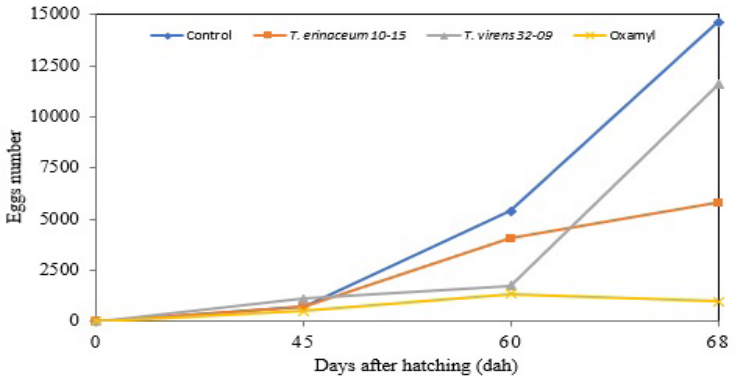


**Figure 1.** Temporal dynamics of the antagonistic effect of *Trichoderma* inoculum on the number of *M. incognita* eggs in *S. lycopersicum* roots.

On the other hand, strain *T. erinaceum* 10-15 decreased its suppressive capacity, but with a significant difference from the results obtained with strain *T. virens* 32-09. The literature indicates that many factors can contribute to the different levels of efficiency among *Trichoderma* species, such as contact time between antagonist and pathogen, pathogenicity of the fungus, species and origin of the nematodes, climatic adaptability, and crop type influence, among other unknown factors (Zhang *et al*., 2015). Kiriga *et al.* (2018) evaluated the efficacy of three *Trichoderma* species against *M. javanica* on commercial pineapple, *Ananas comosus*, and reported that *T. asperellum* $M_2RT_4t$ reduced the number of galls by 81.8 %, number of egg masses by 78.5 %, and the number of eggs by 88.4 %.

These results suggest that the aggressiveness possessed by each *Trichoderma* species may be influenced by the origin and interaction of various biotic and abiotic factors during its development, as well as the dependent dose of the inoculum, since it has been shown that results obtained in biological control depend on the amount of inoculum applied and the time of exposure to it (Saikia *et al*., 2013). Similarly, when evaluating the antagonistic effectiveness of *T. viride* against *M. incognita* in tomato, it was reported that it is able to reduce the number of galls per plant, egg masses per gall, number of eggs per egg mass, and reproductive factors of the nematode when treating the crop soil with this fungus (Sonkar *et al*., 2018). Previous reports indicated that, although there is no reduction in the nematode galling index and number of galls, a decrease in the number of females and eggs per female is possible, suggesting a better behavior of plants still parasitized by nematodes (Hernández-Ochandía *et al.*, 2015). There is evidence that *Trichoderma* is able to activate systemic defense in plants triggered by pests or pathogen attacks, which reduces the possibility of infections as well as the impact of a pest (Martínez-Canto *et al*., 2021; Poveda *et al*., 2021).

**Number of *M. incognita* females**

Regarding the number of females per gram of root, the analysis of variance showed significant reductions ($p \leq 0.05$) in this variable. At 45 d, no significant differences were observed between the treatments of the two *Trichoderma* strains, but significant differences were observed in relation to the negative control, which recorded an average of 471 females. *T. erinaceum* 10-15 recorded an average of 311.67 eggs, equivalent to 33.82 %, and *T. virens* 32-09 recorded a percentage of 48.05 %, with an average of 244.67 eggs per gram of root; Oxamyl obtained the best effect with 84 % inhibition in hatching (Figure 2). However, at 60 d, the treatment with the best results was strain *T. erinaceum* 10-15 with an average number of females of 43, which corresponds to 80.60 % with respect to the control, which had an average of 221.67 females per gram of root, while *T. virens* 32-09 and Oxamyl obtained percentages of 26.76 and 36.39 %, respectively (Figure 2).

These results agree with Herrera-Parra *et al*. (2017), who reported that *T. atroviride* and *T. harzianum* C1 and C2 performed better against *M. incognita* on *Capsicum annuun* with reductions of 21.90, 14.52, and 8.80 %, respectively, in relation to Oxamyl at 24 % in doses of 1 mL $L^{-1}$ of water. Also, Herrera-Parra *et al*. (2018) demonstrated the ability to

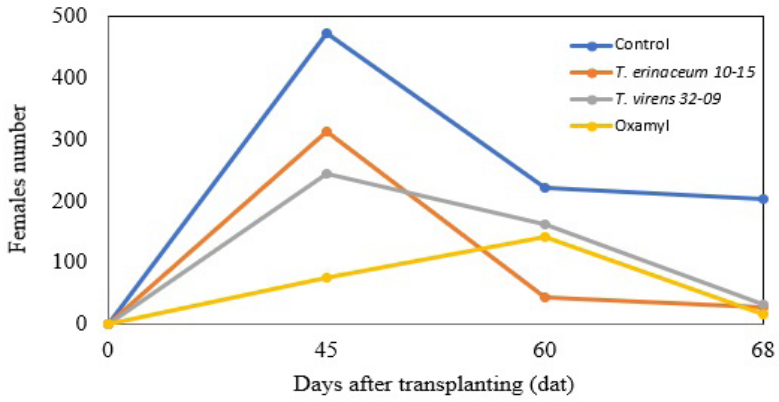


**Figure 2.** Antagonistic effect of *Trichoderma* on the number of *M. incognita* females at 45, 60 and 68 d on *S. lycopersicum* roots.

reduce the number of females per gram of *M. incognita* in *C. chinense*, indicating that *T. atroviride* and *T. harzianum* C1 and C2 were able to reduce the number of females above 50 % compared to the control, but without exceeding the product Oxamyl at 24 % in doses of 1 mL $L^{-1}$ of water. At the end of 68 d, all treatments achieved a reduction of females greater than 80 % compared to the control, where the best result was Oxamyl with 92.47 %, although among the two strains evaluated, *T. erinaceum* was the best performer with 86.74 % (Figure 2).

Applications with *T. harzianum* and *T. virens* also achieved a decrease in the number of *M. incognita* females in tomato crops, with a percentage higher than 80 % (Pinzón-Espinoza *et al*., 2015; Cetz-Chi *et al*., 2018). Medeiros *et al.* (2017) reported that *T. atroviride* is able to activate a defense system in response to the attack of *M. javanica* on tomato plants, where the number of adults and galls was significantly reduced, even without establishing direct contact with the nematode. These results coincide with those obtained in this work, where a reduction of the nematode was observed before the inoculum of *Trichoderma* due to the effect exerted by this fungus against phytonematodes. This could be explained as the result of the production of diverse non-volatile metabolic compounds of enzymatic type, which are capable of exerting a defense response by hydrolyzing the main component of the nematode walls, besides increasing the production of phenolic compounds that intervene in the systemic resistance.

## CONCLUSIONS

The *Trichoderma* species evaluated in this work, *T. erinaceum* 10-15 and *T. virens* 32-09, were able to reduce juvenile mobility at 72 h and egg hatching at day seven by more than 60 %. *T. erinaceum* 10-15 stood out in both variables, with values of 76 and 84.17 %, respectively. Regarding the results obtained in the galling index, both

strains achieved similar performances in terms of ABCPE, Weibull parameter, and final severity; however, the antagonistic effect on egg formation at 68 d was better for *T. erinaceum* 10-15 (60.27 %) than *T. virens* 32-09 (20.62 %). *T. erinaceum* 10-15 had a similar performance, reducing the number of *M. incognita* females by 80.60 % at 60 d, surpassing the commercial control Oxamyl and which led to the conclusion that under optimal conditions, the *Trichoderma* strains used in this research could have better results than the commercial chemical products.

## REFERENCES

Abbott WS. 1925. A method of computing the effectiveness of an insecticide. Journal of Economic Entomoly 18 (2): 265–267. https://doi.org/10.1093/jee/18.2.265a

Al-Hazmi AS, TariqJaveed M. 2015. Effects of different inoculum densities of *Trichoderma harzianum* and *Trichoderma viride* against *Meloidogyne incognita* on tomato. Saudi Journal of Biological Sciences 23 (2): 288–292. https://doi.org/10.1016/j.sjbs.2015.04.007

Babu BV, Kamra A. 2021. Biocontrol potential and rhizosphere competence of *Trichoderma harzianum* against *Meloidogyne incognita* infecting tomato cv. Pusa ruby. Journal of Entomology and Zoology Studies 9 (2): 587–592.

Benttoumi N, Colagiero M, Sellami S, Boureghda H, Keddad A, Cicacio A. 2020. Diversity of nematode microbial antagonists from Algeria shows occurrence of nematotoxic *Trichoderma* spp. Plants 9: 941. https://doi.org/10.3390/plants9080941

Candelero J, Cristóbal J, Reyes A, Tun J, Gamboa M, Ruíz E. 2015. *Trichoderma* spp. promotoras del crecimiento en plántulas de *Capsicum chinense* Jacq. y antagónicas contra *Meloidogyne incognita*. Phyton 84: 113–119.

Cetz-Chi JI, Cristóbal-Alejo J, Tún-Suárez JM, Peraza-Luna FA, Candelero-de la Cruz J. 2018. Especies nativas de *Trichoderma* spp. y su actividad antagónica contra *Meloidogyne incognita* en *Solanum lycopersicum* L. Investigación y Ciencia de la Unievrsidad Autónoma de Aguascalientes 73: 5–12. https://doi.org/10.33064/iycuaa201873136

Cristóbal-Alejo J, Cetz-Chi J, Tun-Suárez J, Moo-Koh F, Peraza-Luna F, Candelero-de la Cruz J. 2018. Filtrados fúngicos de *Trichoderma* con actividad nematicida contra *Meloidogyne incognita* (Kofoid & White) Chitwood. Revista de Protección Vegetal 33: 1–8.

Fan H, Yao M, Wang H, Zhao D, Zhu X, Wang Y, Liu X, Duan Y, Chen L. 2020. Isolation and effect of *Trichoderma citrinoviride* Snef1910 for the biological control of root-knot nematode, *Meloidogyne incognita*. BMC Microbiology 20 (1): 299. https://doi.org/10.1186/s12866-020-01984-4

Hernández-Ochandía D, Rodríguez MG, Peteira B, Miranda I, Arias Y, Martínez B. 2015. Efecto de cepas de *Trichoderma asperellum* Samuels, Lieckfeldt y Niremberg sobre el desarrollo del tomate *y Meloidogyne incognita* (Kofoid y White) Chitwood. Revista de Protección Vegetal 30 (2): 139–147.

Herrera-Parra E, Cristóbal-Alejo J, Ramos-Zapata J. 2017. *Trichoderma* strains as growth promoters in *Capsicum annum* and as biocontrol agents in *Meloidogyne incognita*. Chilean Journal of Agricultural Research 77 (4): 318–324. https://doi.org/10.4067/s0718-58392017000400318

Herrera-Parra E, Ramos-Zapata J, Cristóbal-Alejo J, Tun-Suárez J, Reyes-Ramírez A. 2018. Species of *Trichoderma* antagonistic to the root knot nematode (*Meloidogyne incognita*) in habanero pepper. Phyton 87 (1): 7–13. https://doi.org/10.32604/phyton.2018.87.007

Khan R, Naz I, Hussain S, Khan RA, Ullah S, Rashid MU, Siddique I. 2020. Phytochemical management of root knot nematode (*Meloidogyne incognita*) kofoid and white chitwood by *Artemisia spp*. in tomato (*Lycopersicum esculetum* L.). Brazilian Journal of Biology 80 (4): 829–838. https://doi.org/10.1590/1519-6984.222040

Jepson SB. 1987. Identification of Root-Knot Nematodes (*Meloidogyne* Species). CAB International: Wallingford, UK. 265 p.

Kiriga AW, Haukeland S, Kariuki GM, Coyne DL, Beek NV. 2018. Effect of *Trichoderma* spp. and *Purpureocillium lilacinum* and *Meloidogyne javanica* in commercial pineapple production in Kenya. Biological Control 119: 27–32. https://doi.org/10.1016/j.biocontrol.2018.01.005

Martínez-Canto OJ, Cristóbal-Alejo J, Tun-Suárez JM, Reyes-Ramírez A. 2021. Detección de genes *Epl1* y *Sm1* en *Trichoderma* spp. antagonistas contra hongos fitopatógenos. Ecosistemas y Recursos Agropecuarios 8 (2): e2791. https://doi.org/10.19136/era.a8n2.2791

Martínez-Medina A, Fernandez I, Lok G, Pozo M, Pieterse C, Van Wees S. 2017. Shifting from priming of salicylic acid - to jasmonic acid - regulated defenses by *Trichoderma* protects tomato against the root knot nematode *Meloidogyne incognita*. New Phytologist 213: 1363–1377. https://doi.org/10.1111/nph.14251

Medeiros H, Araújo J, Freitas L, Castillo P, Rubio M, Hermosa R, Monte E. 2017. Tomato progeny inherit resistance to the nematode *Meloidogyne javanica* linked to plant growth induced by the biocontrol fungus *Trichoderma atroviride*. Scientific Reports 7 (1): 40216. https://doi.org/10.1038/srep40216

Moo-Koh F, Cristóbal-Alejo J, Reyes-Ramírez A, Tun-Suárez J, Gamboa-Angulo M, Islas-Flores I. 2018. Incompatibilidad interespecífica de especies de *Trichoderma* contra *Meloidogyne incognita* en *Solanum lycopersicum*. Scientia Fungorum 47: 37–45. https://doi.org/10.33885/sf.2018.47.1191

Moo-Koh F, Cristóbal-Alejo J, Fé M, Martín J, Reyes F, Tun-Suárez J, Gamboa-Angulo M. 2022. In vitro assessment of organic and residual fractions of nematicidal culture filtrates from thirteen tropical *Trichoderma* strains and metabolic profiles of most-active. Journal of Fungi 8 (1): 82. https://doi.org/10.3390/jof8010082

Mukhtar T, Hussain MA, Kayani MZ. 2018. Yield responses of 12 okra cultivars to southern root-knot nematode (*Meloidogyne incognita*). Bragantia 76 (1): 108–112. https://doi.org/10.1590/1678-4499.005

Nourani SL, Mohammadi-Goltapeh E, Safaie N, Jalali-Javaran M, Pourjam E, Shams- Bakhsh M, Jahanshahi-Afshar F. 2015. The effects of *Arthrobotrys oligospora* and *Arthrobotrys conoides* culture filtrates on second stage juvenile mortality and egg hatching of *Meloidogyne incognita* and *Meloidogyne javanica*. Journal of Crop Protection. 4 (5): 667-674. URL: http://jcp.modares.ac.ir/article-3-1286-en.html

Pinzón-Espinoza L, Candelero-de la Cruz J, Tun-Suárez J, Reyes-Oregel V, Cristóbal J. 2015. Control de *Meloidogyne incognita* en tomate (*Solanum lycopersicum* L.) con la aplicación de *Trichoderma harzianum*. Fitosanidad 19 (1): 5–11.

Pocurull M, Fullana AM, Ferro M, Valero P, Escudero N, Saus E, Gabaldón T, Sorribas FJ. 2020. Comercial formulates of *Trichoderma* induce systemic plant resistance to *Meloidogyne incognita* in tomato and the effect es addictive to that of the *Mi*-1.2 resistance gene. Frontiers in Microbiology 10: 3042. https://doi.org/10.3389/fmicb.2019.03042

Poveda J. 2021. *Trichoderma* as biocontrol agent against pests: New uses for a mycoparasite. Biological Control 159: 104634. https://doi.org/10.1016/j.biocontrol.2021.104634

SIAP (Servicio de Información Agroalimentaria y Pesquera). 2020. Boletín mensual de avance de la producción de tomate rojo (jitomate) febrero 2020. Servicio de Información Agroalimentaria y Pesquera. Ciudad de México, México. https//www.gob.mx/cms/uploads/Attachment/file/539942/Bolet_n_avance_producci_n_tomate_rojo_enero_2020 (Retrieved: December 2020).

Saikia SK, Tiwari S, Pandey R. 2013. Rhizospheric biological weapons for growth enhancement and *Meloidogyne incognita* management in *Withania somnífera* cv. Poshita. Biological Control 65 (2): 225–234. https://doi.org/10.1016/j.biocontrol.2013.01.014

Sellami S, Benttoumi N, Berrahia S, Boureghda H. 2017. Evaluation of antagonistic activity of *Trichoderma* spp. against *Meloidogyne incognita*. Acta Phytopathologica et Entomologica Hungarica 52 (2): 177–184. https://doi.org/10.1556/038.52.2017.023

Sonkar SS, Bhatt J, Meher J, Kashyap P. 2018. Bio-efficacy of *Trichoderma viride* against the root-knot nematode (*Meloidogyne incognita*) in tomato plant. Journal of Pfarmacognosy and Phytochemistry 7 (6): 2010–2014

Taylor AL, Sasser JN. 1978. Biology, identification and control of root-knot nematodes (*Meloidogyne* species). North Carolina State University: Raleigh, NC, USA. 111 p.

Temitope A, Patrick A, Abiodum J, Olasekan A, Onye A, Vincent A, Abondunde A, Wutem E, Elliseus R. 2020. *Trichoderma asperellum* affects *Meloidogyne incognita* infestation and development in *Celosia argentea*. Open Agriculture 5: 778–784. https://doi.org/10.1515/opag-2020-0075

Xalxo PC, Karkun D, Poddar AN. 2013. Rhizospheric fungal associations of root knot nematode infested cucurbits: *in vitro* assessment of their nematicidal potential. Research Journal of Microbiology 8 (2): 81–91. https://doi.org/10.3923/jm.2013.81.91

Zhang S, Gan Y, Xu B. 2015. Biocontrol potential of a native species of *Trichoderma longibrachiatum* against *Meloidogyne incognita*. Applied Soil Ecology 94: 21–29. https://doi.org/10.1016/j.apsoil.2015.04.010

Agrociencia

# EVALUATION OF THE SUSTAINABILITY OF TWO TYPES OF *Agave tequilana* Weber var. blue AGROECOSYSTEMS IN TEQUILA, JALISCO

Lusmila **Herrera-Pérez**[1], Esteban **Valtierra-Pacheco**[2*], Ignacio **Ocampo-Fletes**[3], Mario Alberto **Tornero-Campante**[3], Jorge Antonio **Hernández-Plascencia**[3], Ramón **Rodríguez-Macías**[4]

[1] Universidad Popular Autónoma del Estado de Puebla. Facultad de Ingeniería Ambiental. 21 Sur No. 1103, Barrio Santiago, Puebla, Puebla. Mexico. C. P. 72410.
[2] Colegio de Postgraduados Campus Montecillo. Programa de Posgrado en Estudios del Desarrollo Rural. Carretera Mexico-Texcoco km 36.5, Montecillo, Texcoco, State of Mexico, Mexico. C. P. 56264.
[3] Colegio de Postgraduados Campus Puebla. Boulevard Forjadores No. 205, Santiago Momoxpan, San Pedro Cholula, Puebla, Mexico. C. P. 72760.
[4] Universidad de Guadalajara. Centro Universitario de Ciencias Biológicas y Agropecuarias. Cam. Ramón Padilla Sánchez No. 2100, Las Agujas, Zapopan, Jalisco, Mexico. C. P. 44600.
* Author for correspondence: evaltier@colpos.mx

**Citation:** Herrera-Pérez L, Valtierra-Pacheco E, Ocampo-Fletes I, Tornero-Campante MA, Hernández-Placencia JA, Rodríguez-Macías R. 2023. Evaluation of the sustainability of two types of *Agave tequilana* Weber var. blue agroecosystems in Tequila, Jalisco. **Agrociencia** 57(8): 1773-1788. doi.org/ 10.47163/agrociencia.v57i8.2638

**Editor in Chief:**
Dr. Fernando C. Gómez Merino

Received: December 18, 2021.
Approved: May 18, 2023.
**Published in Agrociencia:** December 18, 2023.



## ABSTRACT

Tequila is an alcoholic beverage that must be produced exclusively from the species *Agave tequilana* Weber var. azul (blue) and only in regions with certification of origin within Mexico. The "Tequila Boom" began in 1992, making it a popular beverage in several countries, including Mexico. This boosted exports, production, and the expansion of blue agave plantation areas, which had negative social, economic, and environmental consequences in producing regions and for agave farmers. The aim of the study was to evaluate the degree of sustainability of the *Agave tequilana* crop in two types of agroecosystems: monoculture and polyculture. The research hypothesis was that the *A. tequilana* polyculture agroecosystem is more sustainable than monoculture. A random sample of agave farmers from the municipality of Tequila, Jalisco, was surveyed and distributed equally: 25 agave farmers who practice monoculture and 25 who practice polyculture. The methodology was based on and adapted from the Framework for the Evaluation of the Natural Resource Management Systems incorporating Sustainability Indices (MESMIS), which was used to create a Composite Sustainability Indicator for *A. tequilana* (ICSAT) to compare both agroecosystems. The results show that polyculture is more sustainable than monoculture in 13 of the 15 indicators evaluated. Polyculture displayed a sustainability level of 77.06 % in the Composite Sustainability Indicator, whereas monoculture had 58.43 %. Our conclusion is that the evaluation of sustainability helped to determine that the *Agave tequilana* polyculture agroecosystem is more sustainable than monoculture.

**Keywords:** Composite Sustainability Indicator, monoculture, polyculture, tequila industry, agroecological practices.

## INTRODUCTION

Tequila is an alcoholic beverage produced from the fermentation of sugars extracted from the *piñas* (hearts) of the *Agave tequilana* Weber var. azul (blue). Tequila was named after the region of Tequila, Jalisco, Mexico, the place where the drink originated in the 16th century (CRT, 2019).

Tequila must be produced exclusively from the species *Agave tequilana* Weber var. blue, and the name "tequila" can only be given to an alcoholic beverage that meets the Official Mexican Standard (NOM-006-SCFI-2012, Alcoholic Beverages, Tequila-Specifications) (Secretaría de Economía, 2012). The resolution of the Secretariat of Industry and Trade (1974), published on December 9th, 1974, in the Official Journal of the Federation, protects the Certificate of Origin of the plantation of *A. tequilana* and the production of the beverage known as tequila for production in municipal areas of five Mexican states: the entire state of Jalisco, eight municipalities of Nayarit, 30 in Michoacán, 11 in Tamaulipas, and seven in Guanajuato. When the beverage is obtained from other agave species or varieties, it is known as mezcal or other local names (IMPI, 2023).

In 1992, the "Tequila Boom" began, making the beverage fashionable in several countries. This resulted in an increase in exports, increased production, and the expansion of the species *A. tequilana*. Between 2009 and 2018, tequila production increased 24.1 %, exports increased 64.3 %, and agave demand grew by 23.1 %. From 2017 to 2018, tequila production increased by 13.9 %, while exports increased by 5.1 % (CRT, 2019).

Because the tequila industry forces farmers to grow agave in monoculture, the "Tequila Boom" has created environmental problems in the production areas. Some of the problems affecting the biophysical environment as a result of agave monoculture include soil deterioration, inefficient nutrient recycling, pest susceptibility, displacement of traditional crops, and biodiversity loss (Gerritsen *et al.*, 2011).

Valenzuela-Zapata (2003) and Gómez-Arriola (2012) found that blue agave is produced in polyculture associated with beans, maize, and peanuts. These authors indicate that there are benefits to producing agave in polyculture, such as increased plant coverage, which reduces erosion, retains moisture, and improves soil fertility. When associated with legumes, it helps to reduce pest attacks while also increasing nitrogen fixation in the soil.

Evaluating the sustainability of productive agroecosystems is a complex process since they are dynamic and multidimensional systems. In addition, it must consider farmers' perspectives since agroecosystem management is the result of an evolutionary process that has frequently been passed down from one generation to the next and has adapted to the biophysical, social, and economic circumstances (Astier and Arnés, 2018).

Moreno-Hernández *et al.* (2011) carried out eminently agronomic evaluations of the sustainability of the agave crop and developed a composite indicator known as the Agronomic Management Index (IMA) with five crop practices. Evaluating agroecosystems with productivity and economic yield indicators is crucial for designing sustainable agricultural and food systems (Bolívar, 2011). This vision,

however, is not always sufficient to evaluate sustainability since the social and cultural factors of farmers are decisive to the functioning of agroecosystems.

The goal of this study was to evaluate and compare the degree of sustainability of the *Agave tequilana* Weber agroecosystem in two types of agroecosystems: monoculture and polyculture. A Composite Sustainability Indicator for *Agave tequilana* (ICSAT) was developed to help determine which agroecosystem is the most sustainable in the municipality of Tequila, Jalisco, Mexico, based on specific social, economic, productive, agronomic, and cultural indicators. The research hypothesis was that the *Agave tequilana* polyculture agroecosystem is more sustainable and has less negative environmental impact than monoculture.

## MATERIALS AND METHODS

### Area of study

This investigation was carried out in the municipality of Tequila, in the state of Jalisco, Mexico, which is located between the coordinates 20° 25′ 00″ and 21° 12′ 30″ N, 103° 36′ 00″ and 104° 03′ 30″ W. The altitude of the municipal area ranges between 700 and 2900 m, and the main climates are warm subhumid and semiwarm. Temperatures range between 14 and 26 °C, annual rainfall varies between 700 and 1100 mm, and the predominant soils are Leptosol and Luvisol (Gobierno del Estado de Jalisco, 2023).

### Sampling techniques

A survey was conducted among a general sample of 50 *A. tequilana* farmers from the municipality of Tequila, which was subdivided into 2 subsamples: a) 25 farmers that grow agave in monoculture, and b) 25 that grow agave in polyculture.

The general sample was calculated using a maximum variance formula, modified from Martínez-García and Martínez-Caro (2008), with a reliability of 95 % and an accuracy of 10 %, with a universe of 101 agave farmers. The estimated sample size was 49.23 ≈ 50 farmers.

$$n = \frac{NZ^2_{\alpha/2}\, pq}{Nd^2 + Z^2_{\alpha/2}\, pq}$$

where: $n$ = sample size = 50, $N$ = population size = 101, $p$ = *a priori* proportion of the binomial variable = 0.5, $q$ = *a priori* proportion of the other binomial variable = 1-p = 0.5, $Z$ = value of normal distribution tables ($Z_{\alpha/2}$) with a reliability of 95 % = 1.96, and $d^2$ = error or accuracy at 10 % = 0.1.

### Sustainability Evaluation Methodology

The assessment of agroecosystem sustainability for monoculture and polyculture was based on and adapted from the methodology developed by Masera *et al.* (1999)

in the Framework for the Evaluation of the Natural Resource Management Systems Incorporating Sustainability Indices (MESMIS). The methodological approach is based on the comparison of an alternative agroecosystem with another reference agroecosystem. The sustainability assessment compared two types of agroecosystems managed by different farmers: monoculture (reference agroecosystem), linked to the farmers who work in the tequila industry, and polyculture, linked to annual crops (alternative agroecosystem), generally composed of independent farmers, linked to the *tabernas* (distilleries) where the tequila is handcrafted. The information was gathered between 2014 and 2015.

## Sustainability indicators

The 15 sustainability indicators and their weighting values were selected based on the diagnosis of the current problem faced by the production of agave in the municipality of Tequila, Jalisco.

The sustainability evaluation used the creation of a Composite Indicator, which is a simplified representation that attempts to summarize a multidimensional concept in a simple index (unidimensional) based on an underlying conceptual model (CEPAL, 2009). The sustainability data for each of the 15 specific indicators (both numerical and categorical) were transformed into percentages. The proposed Composite Sustainability Indicator for *A. tequilana* (ICSAT) is the average of the percentages of the 15 specific indicators, with each indicator receiving the same pondered weight.

### Index for Agroecological Practice in *Agave tequilana* (IPAAT)

This was obtained by identifying the number of agroecological practices in the agronomic management of the agave agroecosystem: 1) alternating crops (polyculture); 2) incorporation of organic matter into the soil by cattle grazing; 3) plantation of agave in level curves; 4) soil and water conservation works; 5) crop rotation; 6) lands in fallow; 7) staggering agave plantation; and 8) reduction in the use of herbicides.

The IPAAT values are: null = 0 practices; low= 1-2 practices; medium = 3–4 practices; high= 5 practices; very high = 6–7 practices; and excellent = 8 practices.

### Cost-benefit ratio (R B/C)

This was calculated in the monoculture from the estimation of the gross incomes and the costs of the agave in a six-year cycle. The R B/C of the polyculture included the gross incomes and the costs of agave, added to the costs of the perennial crops (lemon and cacti) in a six-year cycle and the annual cycles (maize, bean, and peanut) associated with the first four years.

### Agroecosystem Yield (RAG)

Yield in Mg $ha^{-1}$ was obtained: a) in monoculture, the number of plants $ha^{-1}$ was multiplied by the average weight of the agave *piñas;* and b) in polyculture, the production in Mg of agave was added to the production in Mg of the alternate crops,

such as maize, bean, and peanut (during the first four years of the total of the agave cycle). The optimum reference yield was 140 Mg of agave *piñas* with a plant density of 4000 $ha^{-1}$ (SAGARPA, 2015).

**Percentage of Organic Matter (% MO)**

Soil samples were collected in both agroecosystems based on the proposal of Uvalle-Bueno *et al*. (2007). A total of eight samples were analyzed in the Plant Nutrition Laboratory of the Soil Science Program of the Colegio de Postgraduados Campus Montecillo. The optimal percentage of MO was calculated using mean ($\chi$) of the reference value of the Integrated Differential Diagnosis methodology by Uvalle-Bueno *et al*. (2007): $\boldsymbol{X}$ = High 4.39 %. According to these authors, the following strata were determined based on the percentage of MO in agave fields: deficient (less than 0.65 %); low (0.65 to 1.29 %); moderately low (1.29 a 2.13 %); sufficient (2.13 to 3.02 %); moderately high (3.03 to 3.64 %); high (3.64 to 5.16 %); and excessive (more than 5.16 %).

**Agricultural Diversification Index (IDA)**

This index, modified from the indicator proposed by Moreno-Hernández *et al*. (2011), considers the agricultural and livestock species that coexist in a plot of land for a given amount of time. A higher diversification of crops and livestock leads to more products and income. The parameters obtained were as follows: a) number of crops in the system; b) number of crops in rotation; and c) number of livestock species that graze in the fields.

$$IDA = \frac{\sum \text{number of crops and livestock species}}{\sum \text{maximum number of crops and livestock species}} \times 100$$

**Adaptation and Alternatives Index (IAA)**

The adaptation and alternative processes of farmers in the face of variations in the prices of agave were identified as follows: 1) added value of the production through the production of tequila (*taberna* owners); 2) alternating crops; and 3) planting other crops. Percentages were assigned depending on the number of alternatives, i.e., if the three were performed = 100 %; 2 = 80 %; and 1 = 50 %.

**Intergenerational Relay (RIG)**

A lack of intergenerational relay is considered a risk for the continuity of the agroecosystem. This indicator was obtained from the percentage of farmers who believe that their children take over the production of agave in both agroecosystems.

**Family Participation in Agricultural Chores (PFLA)**

The percentage of the production units in which family members participate in the agave-planting tasks was taken.

**Agroecosystem Knowledge Index (ICA)**

This integrates the farmer's experience with agave plantation and alternating crops. The variables are: a) average age of the farmer; and b) the number of years they have grown their own agave. This was estimated using the formula proposed by Moreno-Hernández *et al*. (2011).

$$ICA = \left(\frac{ACP}{EA}\right) \Big/ \left(\frac{ACP\ \max.}{EA\ \max.}\right) \times 100$$

where *EA* = average age of agave farmers, *ACP* = average of years of farmers planting their own agave, *ACP* max. = maximum number of years of farmers planting their own agave, and *EA* max. = maximum age of agave farmers.

**Control of the Planting Process through Leasing (CPCA)**

The three main forms of agricultural contracts identified in the municipality of Tequila were: 1) leasing; 2) sharecropping; and 3) 50-50 harvest sharing. The index represents a percentage assigned to each restriction imposed on agave farmers by lease contracts. Two forms were considered: a) farmers under contract and b) farmers under restrictive conditions of alternating crops and grazing livestock.

**Land Occupancy Index (IOT)**

This indicator estimates the efficiency of land use. The number of months in which each crop uses the land was calculated by dividing a) the months of occupancy of the soil by alternate crops, by b) the months of occupation by monocultures. The formula is as follows:

$$IOT = \left(\frac{\sum \text{months of intercrop occupation per year (agave + other crops)}}{\sum \text{months of monoculture occupation}}\right) \Big/ 2$$

**Dependency on Technical Assistance (DAT)**

This indicator is divided into three categories: 1) farmers who do not receive technical assistance; 2) institutions that provide technical assistance; and 3) the number of service-providing technicians. Farmers in the two agroecosystems who had not received assistance were counted, and institutions and technicians who provided assistance were identified using categories 2 and 3.

**Organization of Farmers (OP)**

Comprises two aspects: 1) the number of farmers who belong to an organization; and 2) the type of organization. This indicator was calculated using the number of farmers who are members of an organization in each ecosystem, and the percentage was used as the calculated value.

**Dependency on External Capital for Production (DCEP)**

This indicator considered the percentage of farmers who self-fund their plantations and the percentage of farmers who received external investment funds (such as a credit or crop funding through a buy and sell contract) during the production cycle.

**Dependency on Agrochemicals (DAQ)**

Three cultural practices were included that reduce or eliminate dependence on agrochemicals such as fertilizers and pesticides: 1) manual weed control; 2) free grazing of animals amongst the agave; and 3) producing and applying organic inputs in the plantations. The indicator was calculated by assigning a percentage to the number of the three agricultural practices used by agave farmers (3 = 100 %; 2 = 80 %; and 1 = 50 %).

## RESULTS AND DISCUSSION

The Composite Sustainability Indicator for *Agave Tequilana* (ICSAT) combines the 15 indicators into a single scale and was calculated by taking the simple average of the unweighted values (all variables have the same percentage weight) to compare two types of agroecosystems: monoculture and polyculture.

### Index for Agroecological Practice in *Agave tequilana* (IPAAT)

Farmers working in monoculture carried out an average of 3.32 practices out of the eight practices considered, placing the IPAAT at a middle level, while farmers working in polyculture carried out 5.52 practices, ranking it in a very high category. Farmers with polycultures used more agroecological practices, which are crucial components of sustainable agriculture, and agroecological principles based on the use of natural products and local knowledge. Moreno-Hernández *et al*. (2011) evaluated the performance of polyculture and monoculture practices for agave and found that more than 60 % of the polyculture plots had a medium-to-high level of practices carried out, whereas all monoculture plots had a low level.

### Cost-benefit ratio (R B/C)

The cost-benefit ratio (R B/C) is 7.91. Both agroecosystems are profitable because the net incomes exceed costs (B/C > 1), with polyculture being 1.05 times more profitable than monoculture (Table 1). When a field is planted following the technical recommendation by SAGARPA (2015) of 4000 plants $ha^{-1}$, an average yield of 140 Mg $ha^{-1}$ is obtained, leading to a total production cost of MXN 106 197 $ha^{-1}$ and a gross total income of MXN 840 000 $ha^{-1}$ in a six-year cycle (at 2015 prices).

**Table 1.** Cost-benefit ratio of planting the *Agave tequilana* under monoculture and polyculture in Tequila, Jalisco, Mexico.

| Agroecosystem | Costs (MXN) | Income (MXN) | Cost-benefit ratio |
|---|---|---|---|
| Monoculture | 88 420.00 | 665 910.00 | 7.53 |
| Polyculture | 90 208.00 | 773 780.00 | 8.58 |

### Agroecosystem Yield (RAG)

Monoculture yield was 110.98 Mg ha$^{-1}$ with an average of 3171 plants ha$^{-1}$, while polyculture yield was 129.43 Mg ha$^{-1}$ with an average of 3698 plants ha$^{-1}$. At the end of the six-year agave cycle, the yields of the maize, bean, or peanut crops were added for the first four years. According to the results of the farmers surveyed, the agave density per hectare is low according to the technical recommendations for the Tequila region (4000 plants ha$^{-1}$) (SAGARPA, 2015).

The average agave yield in the municipality of Tequila ranges from 96.04 to 122.5 Mg ha$^{-1}$ (SIAP, 2016). This confirms the findings of Ebel *et al*. (2017), who state that yield in polyculture increases due to synergies established among the different crops that grow in the same field, resulting in maize, in association with bean and squash, having a yield 1.2 times higher per plant in comparison to maize in monoculture, whereas bean and squash were almost equal.

### Percentage of Organic Matter (% MO)

The analysis of the eight soil samples revealed that monoculture had a sufficient percentage of MO with 2.31 %; while polyculture had a moderately high MO level with 3.07 %, according to the reference values on the fertility of soils in *Agave tequilana* proposed by Uvalle-Bueno *et al*. (2007).

The practice of incorporating the annual crop residues that are alternated (maize, bean, and peanut) into the soil is linked to a higher percentage of MO in polyculture plantations. Meanwhile, soils in monoculture have less MO because the residues are not incorporated into the soil due to the absence of other crops. Incorporating residues in the soil is an important component in the maize alternated with fruit trees (MIAF) agroecosystem for recovering soil fertility and generating carbon capture processes in the soil (Cortés-Flores and Turrent-Fernández, 2018)

### Agricultural Diversification Index (IDA)

In the reference system, the optimal number of crops and livestock in a plot is ten species (100 %). The distinction between both agroecosystems is substantial. According to the farmers, the average number of crops and livestock species in polyculture is two (20 %) and nine (90 %). Diversification is crucial in sustainability, as pointed out by Spiaggi *et al*. (2016), who claim it is necessary to opt for diversified agroecosystems, such as polycultures, to obtain economically viable and environmentally sustainable products in small-scale fields.

### Adaptation and Alternatives Index (IAA)

Agave *piñas* prices fluctuate from year to year, so agave farmers use a variety of strategies to minimize and mitigate the negative consequences of market variations. Three alternatives were identified: 1) the farmers who own *tabernas* allocate the production of agave *piñas* to produce tequila or receive income through contract manufacturing to produce tequila; 2) they alternate crops for selfconsumption and

livestock; and 3) in extreme cases, they carry out crop conversion, primarily planting maize instead of agave.

The percentage of IAA found in the monoculture agroecosystem was 80 %, while in polyculture it was 100 %. Agave farmers who practice polyculture face better in terms of agave price volatility than monoculture farmers, because diversifying production and agricultural activities leads to the production of edible crops, which mitigates the risk posed by agave price volatility.

**Intergenerational Relay (RIG)**

In the survey, some of the agave farmers indicated that many of their married elder sons and daughters do not work in the production of agave. Most farmers believe that even the children who live at home will probably work in other activities unrelated to the agave agroecosystem (60 % of those who produce in polyculture and 15 % in monoculture). This is regardless of whether agave farmers incorporate their children in plantation work or in *tabernas* for the production of tequila, starting at an early age and passing their knowledge down to them throughout the years. This is due to three main reasons: 1) work in agave plantations is "tough"; 2) the economic benefits of agave farming are not very attractive; and 3) there is a growing number of children that have jobs in other production sectors.

**Family Participation in Agricultural Chores (PFLA)**

The persistence of traditional agroecosystems is a positive factor in sustainability because development is aided by field management and family bonds (Castelán-Vega *et al*., 2014). Family involvement is essential in agricultural activities. There were no differences in the proportion of family members who supported labor in agave monoculture versus polyculture (72 %).

**Agroecosystem Knowledge Index (ICA)**

The experience gained by farmers through the years favors the knowledge required for the management of the agroecosystem. A farmer with many years of dedication is considered to have a better understanding of agave sustainability than one who has planted it for only a few years (Moreno-Hernández *et al*., 2011). The estimated ICA was 54.7 % for farmers with monoculture and 63.5 % with polyculture.

**Control of the Planting Process through Leasing (CPCA)**

Out of all the farmers surveyed, 38 % have formal or informal contracts. Out of those with informal contracts, 24 % are under a sharecropping scheme, and 12 % are under 50-50 harvest sharing. In monoculture, nine farmers (seven lessees and three sharecroppers), corresponding to 47.37 %, have production contracts, which impose restrictions on the agave production process management and allow them to only perform the duties authorized by the tequila companies (Orozco-Martínez, 2010).

The tequila industry dictates what they must do, how and when, even if it goes against the agave farmer's criteria (for example, the number of herbicide applications). Polyculture farmers, on the other hand, are not bound by rules or regulations when it comes to managing and controlling their agave plantations, even if they have sharecropping or 50-50 harvest sharing arrangements.

**Land Occupancy Index (IOT)**

This index calculates the efficiency of arable land surface use. Agave is a semipermanent crop that remains on the ground 12 months a year for six years. In polycultures, the soil between rows of agaves is used for annual crops to be planted. The optimum IOT level (100 %) is 24 months per crop, which is equal to the agave plus another crop, occupying the same surface of land for the 12 months of the year, times the six years that the cycle lasts. In the municipality of Tequila, rainfed maize (*Zea mays*) lasts an average of five months on the soil, bean (*Phaseolus vulgaris*) lasts three months, peanut (*Arachis hypogaea*) lasts five months, and perennial crops such as cacti (*Opuntia albicarpa*) and lemon (*Citrus aurantifolia*) last 12 months.

The IOT for agave monoculture resulted in 50 % because it occupies the ground for 12 months a year for six years. In polyculture, IOT was 78 %, indicating that alternated annual or perennial crops added 3.36 months (28 %) of occupation per year per six-year cycle. Results indicate that polyculture is more efficient in terms of land use than monoculture. This advantage translates into the minimization of production costs because two or more crops benefit from the same cultivation work; more produce is obtained in Mg $ha^{-1}$, and the soil has greater plant coverage in the year, reducing soil erosion problems (Nicholls *et al*., 2015).

**Dependency on Technical Assistance (DAT)**

In monoculture, 80 % of farmers pointed out that they do not depend on technical assistance due to the experience they have gained over the years. However, farmers under contract must adhere to the crop practices specified in their contracts, and should they require support, tequila companies have technicians who can assist them. In polyculture, 68 % of farmers have received no technical assistance. They occasionally seek the advice of agrochemical company owners and employees. This information is similar to that found in the study by Sánchez-Soto (2016) in the municipality of Tequila, which states that when farmers require technical assistance, they turn to fellow farmers, agrochemical distributors, or agencies selling machinery to answer questions. This is the only indicator value in which monoculture surpasses polyculture, since 68 % of polyculture farmers receive no technical assistance and 80 % of monoculture farmers do not.

**Organization of Farmers (OP)**

The Agave Association is the representative state organization in the agave-tequila chain, although few of the interviewees are members. Only 32 % of the farmers of

the monoculture agroecosystem belong to the association, along with 36 % of the polyculture agroecosystem.

Farmers affiliated with agricultural organizations such as the Agave Association have greater possibilities of acquiring inputs, machinery, tools, and technical assistance, achieving scale economies. In addition, they have the possibility of accessing better market conditions for marketing: they are eligible for funding and access to government programs. This is an advantage over farmers who are not affiliated.

### Dependency on External Capital for Production (DCEP)

This indicator considers the proportion of farmers who fund their own plantations with financial, material, and human resources for agave cropping. Survey results indicate that 18 monoculture farmers (72 %) have covered the expenses for their crops out of pocket, and seven farmers have contracts with distilleries. Polyculture farmers (88 %) have funded the costs of plantations with their own funds, and only three of them have formal contracts for buying and selling produce. Results show that farmers using polyculture depend less on external capital for planting and production maintenance.

### Dependency on Agrochemicals (DAQ)

Three practices were evaluated in order to know the level of dependence of agave farmers on the use of phytosanitary products: 1) the manual control of weeds helps reduce or eliminate the use of herbicides, a practice that was carried out by seven farmers in monoculture and another seven in polyculture; 2) livestock grazing also contributes to the control of weeds and was carried out by four farmers in monoculture and eight in polyculture; 3) agave farmers that produce and apply compost were three in polyculture and only one in monoculture. The total percentage that applied one or more of these three practices in monoculture was 48 %, and 72 % in polyculture.

The optimization of farming systems with the aim of generating sustainable farming systems is achieved when external inputs, mainly industrial ones, are replaced with inputs generated in the agroecosystem itself (Nicholls *et al*., 2015). When properly managed, agroecosystems, which include crop and livestock integration, contribute to a higher self-sufficiency of nutrients in the soil and their conservation (Boincean and Francis, 2017).

### Joint analysis of the Composite Sustainability Indicator of *A. tequilana* (ICSAT) for the monoculture and polyculture agroecosystems in Tequila, Jalisco

The joint analysis displays the values clustered on the same scale as the evaluation of the 15 indicators, with the values calculated with regard to the optimum values (Table 2) used to calculate the ICSAT for each type of agroecosystem. The result of the calculation was a total difference of 18.64 % between monoculture (58.43 %) and polyculture (77.07 %).

When compared to monoculture, polyculture has higher values in 13 of the 15 sustainability indicators evaluated (Table 2). Polyculture only has lower DAT values and equal PFLA Index values. The indicators for productivity could be considered

**Table 2.** Composite Sustainability Indicator for A. tequilana (ICSAT) and optimum and calculated values of the specific indicators for two types of agroecosystems: monoculture and polyculture in Tequila, Jalisco, Mexico.

| Attribute | Diagnosis criteria | Specific indicators | Optimum | Monoculture (reference) | Polyculture (alternative) |
|---|---|---|---|---|---|
| Productivity | Efficiency | Index for Agroecological Practice in *Agave tequilana* (IPAAT) | 8 practices (100 %) | 3.32 (41.5 %) | 5.52 (69 %) |
| | Crop economy efficiency | Cost-benefit ratio (R B/C) | 7.91 (100 %) | 7.53 (95.2 %) | 8.58 (100 %) |
| | Productive yield | Agroecosystem yield (RAG) | 140 Mg ha $^{-1}$ (100 %) | 110.08 Mg ha$^{-1}$ (78.6 %) | 129.43 Mg ha $^{-1}$ (92.5 %) |
| | Organic efficiency | Organic Matter Percentage (% MO) | High 3.637–5.158 % $\bar{X}$ = 3.49 % | $\bar{X}$ = 2.31 sufficient (53 %) | $\bar{X}$ = 3.07 medium-high (70 %) |
| Stability, resilience, and reliability | Crop diversification | Agricultural Diversification Index (IDA) | 10 crops and species (100 %) | 2 (20 %) | 9 (90 %) |
| Adaptability | Ability of adaptation under pressure from price fluctuation | Adaptation and Alternatives Index (IAA) | 3 alternatives (100 %) | 2 (80 %) | 3 (100 %) |
| | Continuity of the system | Intergenerational relay (RIG) | 25 farmers (100 %) | 13 (52 %) | 15 (60 %) |
| | Family participation | Family participation in agricultural chores | 25 farmers (100 %) | 18 (72 %) | 18 (72 %) |
| Equidad | Farmer's knowledge | Agroecosystem Knowledge Index (ICA) | 100 % experience | 54.7 % | 63.5 % |
| | Degree of control over the process | Control of the Planting Process through Leasing (CPCA) | Zero restrictions by the farmer (100 %) | 9 (47.4 %) | 0 (100 %) |
| Autogestión | Efficiency of land occupancy | Land Occupancy Index (IOT) | 24 months year$^{-1}$ (100 %) | 12 (50 %) | 18.8 (78 %) |
| | Dependency on technical assistance | Dependency on Technical Assistance (DAT) | 25 farmers (100 %) | 20 (80 %) | 17 (68 %) |
| | Degree of self-management of the production process | Organization of Farmers (OP) | 25 farmers (100 %) | 8 (32 %) | 9 (36 %) |
| | Funding sources and conditions | Dependency on External Capital for Production (DCEP) | 25 farmers (100 %) | 18 (72 %) | 22 (85 %) |
| | Use of industrial inputs | Dependency on Agrochemicals (DAQ) | 25 farmers (100 %) | 12 (48 %) | 18 (72 %) |
| **Composite Sustainability Indicator** | | | **100 %** | **58.43 %** | **77.06 %** |

the most traditional and important in sustainability evaluations, and in all of them, polyculture is the most sustainable: the IPAAT, the R B/C, RAG, and the percentage of MO. No agroecosystem is totally sustainable or totally unsustainable, since sustainability is a goal that is achieved through the addition of diverse, adequate attributes that maintain a balance of all agroecosystem components (Astier and Arnés, 2018; Nicholls *et al*., 2015; Castelán-Vega *et al*., 2014).

Below, the resulting percentages of each indicator appear with their optimum value (100 %) in the same plain (Figure 1), along with the values calculated for monoculture (reference agroecosystem) and polyculture (alternative ecosystem).

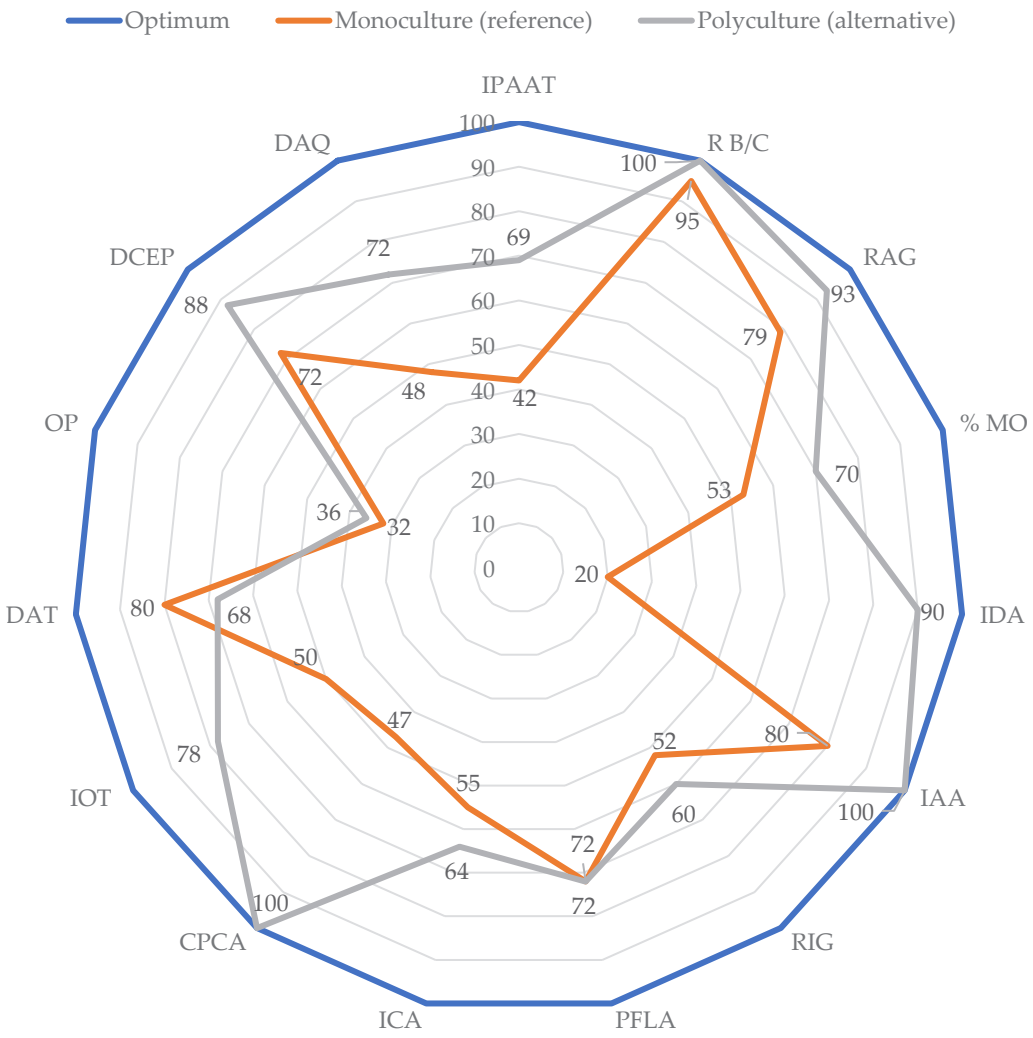


**Figure 1.** Comparison of the Composite Sustainability Indicator for *A. tequilana* (ICSAT) in monoculture and polyculture.

## CONCLUSIONS

Sustainability evaluation, based on the methodological proposal of the Framework for the Evaluation of the Natural Resource Management Systems incorporating Sustainability Indices (MESMIS), helped determine that the polyculture agroecosystem is more sustainable than the monoculture because it had a higher value in the Composite Sustainability Indicator for *Agave tequilana* (ICSAT) and higher calculated sustainability values in 13 out of 15 indicators. Polyculture outperformed monoculture in all traditional agroecosystem productivity evaluation indicators (IPAAT, R B/C, RAG, and % MO).

Research shows the environmental irrationality of maintaining monoculture as the predominant method of agave production. It is not even profitable for agave farmers. Monoculture prevails because it is advantageous for the tequila industry to have a supply of agave *piñas*, even if it implies disadvantages for agave farmers. This study proved that the evaluation of the sustainability of the agave agroecosystem must have a holistic focus, considering social, economic, cultural, and institutional factors that affect, limit, or strengthen sustainability. These results may be useful in helping the government, the Tequila Regulation Council, and the tequila industry in promoting more sustainable development through polyculture and working on the indicators with a greater difference in values between polyculture and monoculture.

## REFERENCES

Astier M, Arnés E. 2018. Introducción: Sistemas campesinos y desarrollo sostenible en países andinos. *In* Sostenibilidad en sistemas de manejo de recursos naturales en países andinos. Organización de las Naciones Unidas para la Educación, la Ciencia y la Cultura, Centro de Investigaciones en Geografía Ambiental de la Universidad Nacional Autónoma de Mexico: Ciudad de México, Mexico, pp: 15–31. https://www.ciga.unam.mx/publicaciones/images/abook_file/MESMIS.pdf (Retrieved: August 2020).

Boincean B, Francis C. 2017. Agroecological rotation designs reduce dependence on industrial inputs. Agroecology and Sustainable Food Systems 41 (9–10): 1068–1080. https://doi.org/10.1080/21683565.2017.1358682

Bolívar H. 2011. Metodologías e indicadores de evaluación de sistemas agrícolas hacia el desarrollo sostenible. Revista del Centro de Investigación de Ciencias Administrativas y Gerenciales 8 (1): 1–18.

Castelán-Vega R, Tamaris-Flores V, Ruiz-Careaga J, Linares-Fleites G. 2014. Evaluación de la sustentabilidad de la actividad agrícola de tres localidades campesinas en Pahuatlán, Puebla. Ecosistemas y Recursos Agropecuarios 1 (3): 219–231.

CEPAL (Comisión Económica para América Latina). 2009. Guía metodológica - Diseño de indicadores compuestos de desarrollo sostenible. Agencia Alemana de Cooperación Técnica. Organización de las Naciones Unidas. Comisión Económica para América Latina. Santiago, Chile, 109 p. https://www.cepal.org/es/publicaciones/3661-guia-metodologica-diseno-indicadores-compuestos-desarrollo-sostenible (Retrieved: November 2019).

Cortés-Flores J, Turrent-Fernández A. 2018. MIAF: una tecnología multiobjetivo sustentable para la agricultura tradicional. *In* Calva JL. (ed.), Soberanía alimentaria para el desarrollo del campo. Nueva Estrategia de Desarrollo 9. Consejo Nacional de Universitarios: Ciudad de México, Mexico, pp: 189–206.

CRT (Consejo Regulador del Tequila). 2019. ¿Qué es el Tequila? Información estadística. Consejo Regulador del Tequila. Zapopan, Mexico. https://www.crt.org.mx/index.php/es/ (Retrieved: July 2019).

Ebel R, Pozas-Cárdenas JG, Soria-Miranda F, Cruz-González J. 2017. Manejo orgánico de la milpa: rendimiento de maíz, frijol y calabaza en monocultivo y policultivo. Terra Latinoamericana 35 (2): 149–16.

Gerritsen PRW, Rosales-Adame JJ, Moreno-Hernández A, Martínez-Rivera LM. 2011. Agave azul y el desarrollo sustentable en la cuenca baja del río Ayuquila, Costa Sur de Jalisco (1994-2004). Región y Sociedad 23 (51): 161–192. https://doi.org/10.22198/rys.2011.51.a53

Gobierno del Estado de Jalisco. 2023. Tequila. Gobierno del Estado de Jalisco. Guadalajara, Mexico. https://www.jalisco.gob.mx/wx/jalisco/municipios/tequila (Retrieved: April 2023)

Gómez-Arriola L. 2012. Tequila, de la antigua taberna artesanal a una industria de alcance global. Editorial Quid Media Services: Guadalajara, Mexico. 168 p.

IMPI (Instituto Mexicano de la Propiedad Industrial). 2023. Actualmente la Denominación de Origen Mezcal comprende los estados de Guerrero, Oaxaca, Durango, San Luis Potosí y Zacatecas. Secretaría de Economía. Instituto Mexicano de la Propiedad Industrial. Ciudad de México, Mexico. https://www.gob.mx/impi/articulos/conoce-las-modificaciones-a-la-declaracion-general-de-proteccion-a-la-denominacion-de-origen-mezcal (Retrieved: April 2023)

Martínez-García JA, Martínez-Caro L. 2008. Determinación de la máxima varianza para el cálculo del factor de imprecisión sobre la escala de medida, y extensión a diferentes tipos de muestreo. Psicothema 20 (2) 311–316.

Masera O, Astier M, López-Ridaura S. 1999. Sustentabilidad y manejo de recursos naturales: El marco de evaluación MESMIS. Mundiprensa: Ciudad de México, Mexico. 82 p.

Moreno-Hernández A, Estrella-Chulin N, Escobedo-Garrido S, Bustamante-González Á, Gerritsen PW. 2011. Prácticas de manejo agronómico para la sustentabilidad: características y medición en *Agave tequilana* weber en la región Sierra de Amula, Jalisco. Tropical and Subtropical Agroecosystems 4: 159–169.

Nicholls CI, Altieri MA, Vázquez LL. 2015. Agroecología: principios para la conversión y el rediseño de sistemas agrícolas. Agroecología 10 (1): 61–72.

Orozco-Martínez JL. 2010. La globalización y su relación con la competitividad de la industria del Tequila. *In* Gómez-Gómez CV, Miguel-Cruz F, Orozco-Martínez JL, Alanís-Pérez ME. (eds.), Propiedad industrial como herramienta competitiva frente a la globalización: el caso del tequila y el Consejo Regulador Tequila en México. Universidad de Guadalajara: Ocotlán, Mexico, pp: 143–167.

SAGARPA (Secretaría de Agricultura, Ganadería, Desarrollo Rural, Pesca y Alimentación). 2015. Agenda Técnica Agrícola de Jalisco (Segunda edición). Secretaría de Agricultura, Ganadería, Desarrollo Rural, Pesca y Alimentación. Servicio Nacional de Sanidad, Inocuidad y Calidad Agroalimentaria. Instituto Nacional de Investigaciones Forestales, Agrícolas y Pecuarias. Ciudad de México, Mexico. 179 p. https://vun.inifap.gob.mx/VUN_MEDIA/BibliotecaWeb/_media/_agendas/3093_4798_Agenda_Tecnol%c3%b3gica_Jalisco_2015.pdf (Retrieved: May 2023).

Sánchez-Soto A. 2016. Las necesidades de información en los agricultores de Agave azul de Tequila, Jalisco: Un estudio de caso. Investigación Bibliotecológica 30 (69): 143–178. https://doi.org/10.1016/j.ibbai.2016.04.016

Secretaría de Economía. 2012. NORMA Oficial Mexicana NOM-006-SCFI-2012, bebidas alcohólicas-Tequila-especificaciones. Secretaría de Gobernación. Diario Oficial de la Federación. Ciudad de México, Mexico. https://www.dof.gob.mx/nota_detalle.php?codigo=5282165&fecha=13/12/2012#gsc.tab=0 (Retrieved: May 2023).

Secretaría de Industria y Comercio (1974). RESOLUCIÓN por la que se otorga la protección prevista por el capítulo X de la Ley de la Propiedad Industrial vigente, a la denominación de origen "Tequila", para aplicarse a la bebida alcohólica del mismo nombre. Secretaría de Gobernación. Diario Oficial de la Federación. Ciudad de México, Mexico. https://www.dof.gob.mx/nota_to_imagen_fs.php?codnota=4731635&fecha=09/12/1974&cod_diario=203903 (Retrieved: June 2019).

SIAP (Servicio de Información Agroalimentaria y Pesquera). 2016. Cierre de la producción agrícola por estado. Anuario Estadístico de la Producción Agrícola. Agave. Servicio de Información Agroalimentaria y Pesquera. Ciudad de México, Mexico. http://infosiap.siap.gob.mx/aagricola_siap_gb/icultivo/index.jsp (Retrieved: December 2019).

Spiaggi E, Ottmann G, Miretti A, Alesio C, Frattin M. 2016. Agroecología en la región pampeana argentina: indicadores para la evaluación y sistematización. La medición del impacto de la agroecología. LEISA Revista de Agroecología 32 (3): 26–28.

Uvalle-Bueno JX, Vélez-Gutiérrez C, Ramírez-Figueroa A. 2007. Muestreo y análisis de suelo en plantaciones de agave. *In* Pérez-Domínguez JF, del Real-Laborde JI. (eds.), Conocimiento y prácticas agronómicas para la producción de *Agave tequilana* Weber en la zona de denominación de origen del tequila. Instituto Nacional de Investigaciones Forestales, Agrícolas y Pecuarias. Centro de Investigación Regional del Pacífico Centro. Tepatitlán de Morelos, Mexico, pp: 37–55. http://www.inifapcirne.gob.mx/Revistas/Archivos/agave_final_baja%20resolucion.pdf (Retrieved: May 2023).

Valenzuela-Zapata A. 2003. El agave tequilero: Cultivo e industria en México (Tercera edición). Mundiprensa: Ciudad de México, Mexico. 215 p.

VOLUMEN 57, NÚMERO 8 | 16 DE NOVIEMBRE - 31 DE DICIEMBRE, 2023 | MÉXICO